NASA CR-165,219

NASA CR-165219

NASA-CR-165219
1982 0005554

NASA

LOW-THRUST CHEMICAL PROPULSION SYSTEM PUMP TECHNOLOGY

by R. L. Sabiers
A. Siebenhaar

AEROJET LIQUID ROCKET COMPANY

Prepared for

NATIONAL AERONAUTICS AND SPACE ADMINISTRATION

NASA/Lewis Research Center

Contract NAS 3-21960

1. Report No.
NASA CR-165219

2. Government Accession No.

3. Recipient's Catalog No.

4. Title and Subtitle
Low-Thrust Chemical Propulsion System Pump Technology

5. Report Date
March 1981

6. Performing Organization Code

7. Author(s)
R. L. Sabiers; A. Siebenhaar

8. Performing Organization Report No.

10. Work Unit No.

9. Performing Organization Name and Address
Aerojet Liquid Rocket Company
Post Office Box 13222
Sacramento, CA 95813

11. Contract or Grant No.
NAS 3-21960

13. Type of Report and Period Covered
Contractor Report, Final

12. Sponsoring Agency Name and Address
National Aeronautics and Space Administration
Washington, D.C. 20546

14. Sponsoring Agency Code

15. Supplementary Notes
Project Managers: R. E. Connelly and J.P. Wanhainen,
Space Propulsion and Power Division, NASA/Lewis Research Center
Cleveland, OH 44135

16. Abstract

This program provides a complete review and analysis of candidate pump and driver systems for low-thrust cargo orbit-transfer vehicle engines which would deliver large space structures to geosynchronous equatorial orbit and beyond. The pumps surveyed operate to 68 atmospheres (1000 psi) discharge pressure and flowrates suited to cryogenic engines using either LOX/methane or LOX/hydrogen propellants in thrust ranges from 445 to 8900 N (100 to 2000 lbF).

In all, 116 references on types of pumps and pump drives were consulted. Three types of drives, six dynamic pumps (including one jet pump), and five positive-displacement pumps were reviewed in depth.

The general survey indicated that to date only three pumps had been built in the size (flow and pressure) range of interest.

Analysis of the various pumps and drivers indicated that the low specific speed requirement, i.e., less than

$$9.69 \frac{(\mathrm{RPM})(\mathrm{m}^3/\mathrm{s})^{1/2}}{\mathrm{m}^{3/4}} \left(500 \frac{(\mathrm{RPM})(\mathrm{GPM})^{1/2}}{\mathrm{ft}^{3/4}}\right)$$

will make high fluid efficiencies difficult to achieve. As such, multiple stages would be required. In addition, all pumps required inducer stages, the most

17. Key Words (Suggested by Author(s))
Low-Thrust
Cargo Orbit-Transfer Vehicle
Chemical Rocket Engines
H_2/O_2, CH_4/O_2, Propellant Combinations
Centrifugal, Gear, Tesla, Vane Pumps
Gas Turbines and Electric Motor Drives

18. Distribution Statement
Unclassified-Unlimited

19. Security Classif. (of this report)
Unclassified

20. Security Classif. (of this page)
Unclassified

21. No. of Pages
193

22. Price*

N82-13427#

16. Abstract (cont.)

attractive being a centrifugal stage. The Tesla (shear) pump indicated excellent suction performance; however, a data base is clearly lacking. The most attractive main pumps were the multistage centrifugal pumps. The piston positive-displacement pumps appear to have definite life limitations which may restrict their usefulness. They are also subject to propellant carry-over which degrades suction performance.

The gas turbine driver showed the best overall operation, with the electric motor drives being very attractive at both moderate speed and low horsepower.

This report also includes a rating analysis of the various pump/driver combinations, together with an identification of the most significant current technologies.

FOREWORD

This report is the final report for the Low-Thrust Chemical Propulsion System Pump Technology study program performed by the Aerojet Liquid Rocket Company (ALRC) for the National Aeronautics and Space Administration/Lewis Research Center (NASA/LeRC) under Contract NAS 3-21960. The period of performance was 1 October 1979 to 15 April 1981.

The major objective of this contract was to review and analyze the capabilities of pump designs, both dynamic and positive-displacement types, that can meet the pressure and flow requirements of a rocket engine having a thrust level between 445 to 8900 N (100 to 2000 lbF) and a maximum chamber pressure of 3447 kPa (500 psi).

The NASA/LeRC project managers were Mr. R. E. Connelly and Mr. J. P. Wanhainen. The ALRC program manager was Mr. L. B. Bassham, and the project engineer was Mr. R. L. Sabiers. Major technical contributions were provided by Mr. P. S. Buckman and Mr. B. K. Lindley. The overall effort was performed under the supervision of Dr. A. Siebenhaar, manager, Turbomachinery System Design.

TABLE OF CONTENTS

LIST OF TABLES

LIST OF FIGURES

LIST OF FIGURES (cont.)

LIST OF FIGURES (cont.)

LIST OF FIGURES (cont.)

I. SUMMARY

Low-thrust chemical propulsion is being considered for missions transferring acceleration-limited large space structures from low earth-orbit to geosynchronous or other high earth-orbits. Recent engine/vehicle studies have indicated that the propellants of interest for this mission are LOX/hydrogen, LOX/methane, or LOX/kerosene (RP-1). The very long burn times for these engines exclude the potential of pressure-fed systems and drive the designs toward pump-fed rocket engines. To date, very little information has been compiled for pumps that must operate at these low flowrates and moderate pressure levels. Both dynamic and positive-displacement type pumps need to be evaluated in terms these requirements and the most promising concepts, along with the attendant technologies for developing the design base for these systems, must be identifed. For this reason, and to evaluate this need, the Aerojet Liquid Rocket Company (ALRC) was contracted by the National Aeronautics and Space Administration/Lewis Research Center (NASA-LeRC) to perform the Low-Thrust Chemical Propulsion System Pump Technology study (NAS 3-21960) presented in this report.

The stated objectives of the contract were to evaluate the state of the art of rocket propellant feed pumps and drives, define the characteristics of ideal pumps for this application, and identify the technical programs necessary to develop these pumps. Particular elements of the contract included analyzing various types of pumps and drivers, performing tradeoff studies, selecting the best designs, and making in-depth technical assessments of the systems.

This is the final report of this effort. It consists of the data obtained from a literature search, selection of candidate pumps, generation of data on fourteen selected pumps (including data on hydrodynamic characteristics and performance), and the selection of the most promising pump concepts for further evaluation.

In all, 116 relevant references were consulted for information on types of pumps and three types of drives, and extensive studies were made on five (5) different rotodynamic pumps, five (5) different positive-displacement pumps, one (1) jet pump, and three (3) different pump drives (see Table I).

The literature search conducted revealed that only three pumps had been built and tested under conditions similar to those required for the Low-Thrust Chemical Propulsion Technology study. These pumps were:

- Aerojet Titan I Auxiliary Pump, LO_2 (low flow)
- Goddard Pump, LO_2 (high flow)
- NASA Piston Pump, LH_2 (low pressure)

TABLE I. TYPES OF PUMPS AND DRIVES REVIEWED AND ANALYZED

	Reviewed in References	Analyzed
PUMPS		
Dynamic		
Centrifugal, Conventional	√	√
Centrifugal, Barske	√	
Centrifugal, Idling Shroud	√	
Axial, Conventional	√	√
Axial, "Impulse"	√	
Axial, Supercavitating	√	√
Multiple Disk (Tesla)	√	√
Roto-Jet (Pitot)	√	
Vapor Core	√	√
Regenerative (Drag)	√	
Positive Displacement		
Vane, Conventional	√	√
Vane, Pivoting Pad Vane	√	
Piston	√	√
Roots/Lobe	√	√
Gear	√	√
Diaphragm	√	√
Other		
Jet	√	√
PUMP DRIVES		
Gas Turbine	√	√
Electrical Motors	√	√
Hot-Gas Positive-Displacement Motors	√	√

Analysis of the various pump types yielded the data listed in Table II for the requested flow regimes. In particular, the analyses established the following findings:

- Dynamic pumps have long life potential, but their efficiencies are low (<55%).
- Positive-displacement pumps have high efficiencies (up to 90%), but produce unsteady flow and may be subject to life-limiting wear or fatigue.
- Jet pumps are suitable only for pumping LO_2, not LH_2 or LCH_4.

Analysis of the various pump drives yielded the following data (shown in Table III):

- Turbines are good for centrifugal pumps, but their efficiencies are low for low-speed positive-displacement pumps.
- Electric motors are suitable for all pumps, especially in a turbine/alternator/motor combination for low-power, lower-speed pumps.
- Positive-displacement hot-gas motors have low efficiency and may have only limited life.

Careful analysis leads to the conclusion that, of the types studied, the following three basic pump/driver combinations have the best potential for satisfying the pressurization needs of future rocket engines in the 445 to 8900 N (100 to 2000 lbF) thrust range using hydrogen or methane fuels with oxygen as the oxidizer. These systems are:

- Centrifugal pump, driven by a gas turbine or electric motor
- Piston pump, driven by an electric motor
- Gear pump, driven by an electric motor

All of these combinations will satisfy the needs of hydrogen and methane propellant systems for at least the high-thrust portion of the engine pressure flow map. Since the liquid oxygen pumping power is significantly lower than that of the fuel and has the lowest pump speeds for the three propellants, it is the only propellant pump for which an electric-motor-driven centrifugal pump appears practical. Considering the system probabilities, a turbine-driven fuel pump and alternator running on one shaft and an electric-motor-driven oxygen pump running on a separate shaft and bearing system provide the added

TABLE II. PUMP STUDY RESULTS

Pump Type	Efficiency, %	No. of Stages Required	Limitation
Dynamic			
Centrifugal	40-55	1-6	
Axial	50-60	5-62	May be impractical above 3360 N (750 lbF)
Tesla	20-35	1	Limited use
Drag	<40	1	
Pitot	40-55	1	
Jet	<30		Not suitable with hydrogen and methane
Positive Displacement			
Vane	50-80	1	Life
Gear	50-90	1	Life
Piston	80-85	1	Life
Lobe	60-80	1	Life
Diaphragm	30-40	1	Life

TABLE III. PUMP DRIVE STUDY RESULTS

Pump Drive	Efficiency, %	Speed	Weight
Gas Turbines	51-80	High only	50.3 to 1696 N/W (0.3 to 10.0 lb/HP) power source
Electric Motors	85-90	Moderate to high	251 to 2179 N/W (1.5 to 13 lb/HP) power source
Hot-Gas Positive-Displacement Motor	35-45	Moderate	168 to 335 N/W (1 to 2 lb/HP) power source

benefit of eliminating the interpropellant seal between a fuel-powered driver and the liquid oxygen pump. Although this study is not directed to consider engine system capabilities, this combination does appear to offer the best potential.

The study also yielded the following data:

- Very low-thrust (less than 2224 N (500 lbF), high-pressure systems present the most difficult design problem.
- Axial flow pumps require too many stages to be practical.
- Liquid methane does not present a severe pumping problem.

It is recommended that further study concentrate on pumps for a 890 N (200 lbF) thrust, high-pressure engine. For use with LO_2, only centrifugal pumps should be evaluated, whereas for use with LH_2, centrifugal as well as piston and gear pumps should be evaluated.

II. INTRODUCTION

Low-thrust chemical propulsion (using either pump-fed or pressure-fed engines) is a candidate being considered for transferring acceleration-limited large space structures from low earth-orbit to geosynchronous or other high earth-orbits. For these rocket systems, conventional dynamic-type pumps (centrifugal) appear to be capable of meeting the maximum anticipated life requirements of up to 18,000 seconds (50 hours) but may not be capable of providing the pressure flow requirements of the entire thrust ranges. Positive-displacement-type pumps have a well-developed technology base for conventional fluids but, due to the poor lubricating properties of the candidate rocket propellants (cryogenic fluids) considered for use, may have problems meeting the engine service life requirements. To provide insight into the feasibility of dynamic pumps, the National Aeronautics and Space Administration, Lewis Research Center (NASA/LeRC) initiated a study contract with the Aerojet Liquid Rocket Company (ALRC) to conduct the Low-Thrust Chemical Propulsion System Pump Technology program presented in this final report.

The purpose of this study was to review and analyze the capabilities of pumps, both dynamic and positive-displacement types, that can meet the pressure/flow requirements of a rocket engine having a thrust level between 445 to 8900 N (100 to 2000 lbF) and a maximum chamber pressure of 3447 kPa (500 psi). This study was also structured to provide the propulsion system designer with information on the current state of the art of candidate pumps, pump characteristics data, and performance information for making propulsion system trades. In addition, this study was to provide a base from which to start future pump technology programs.

The objective of the program was to select prospective candidate pumps and drives and assess their potential for application to low-thrust rocket propulsion systems. Specific study objectives were as follows:

- Establish the state of the art of pumps suitable for use as feed pumps for a 445 to 8900 N (100 to 2000 lbF) thrust range rocket with a chamber pressure of less than 3447 kPa (500 psia).
- Devise a list of candidate pumps and drivers suitable for the application.
- Generate parametric performance, weight, and envelope data for various pump/driver candidates based upon historical data and conceptual evaluations.
- Devise a system for ranking candidate pumps and then determine the best pumps for the application.
- Identify the technology issues that should be addressed for the most promising concepts.

Eleven pump types were assessed for their applicability to the pressure-flow range of hydrogen, methane, and oxygen propellants at the contract minimum net positive suction heads (NPSH).

III. CONCLUSIONS

As a result of this investigation, it was determined that the following three pump/driver configurations have the best potential of meeting the requirements set forth for the low-thrust propulsion system:

- Centrifugal pump, driven by a gas turbine
- Piston pump, driven by an electric motor
- Gear pump, driven by an electric motor

The principal criteria that governed the selection of the candidate pump were as follows:

- Dimensional/machining characteristics
- Minimum level of performance
- Suction performance
- Wear/life characteristics

Driver selection typically is limited by the following:

- Power requirements
- Power at a particular speed level
- Operating speed
- Driver fluid

The following conclusions have been developed from the study:

Dynamic Pumps

1. Centrifugal pumps are the most promising candidates.

2. Centrifugal hydrogen pumps require two to six stages.

3. Centrifugal methane pumps require two to five stages.

4. Centrifugal oxygen pumps require one to three stages.

5. All centrifugal pumps require inducer stages.

6. The low-flow centrifugal pumps have large frictional losses.

7. Centrifugal pumps can be designed for engines with thrust levels greater than 890 N (200 lbF for a LH_2/LO_2 system and 1779 N (400 lbF) for a LCH_4/LO_2 system.

8. Hydraulic efficiencies of centrifugal pumps can be expected to be in the 40 to 55% range.

9. Drag pump efficiencies are low (less than 50%).

10. The suction performance of drag pumps is lower than that of gear and vane pumps.

11. Pitot pump efficiencies in hydrogen would typically be less than 40%.

12. The large size of Pitot pumps is undesirable but their life is almost unlimited.

13. Tesla pumps look quite attractive from a life and suction performance perspective and may make desirable inducer pumps. However, their hydraulic performance is poor and little empirical data have been developed for that type of pump.

14. Axial pumps develop quite high hydrodynamic efficiencies, however, the number of stages required for the low-thrust requirements makes them impractical.

15. Jet pumps do not appear attractive for the low-thrust requirements. Their large NPSH requirements, coupled with high drive fluid pressure, render them undesirable.

<u>Positive Displacement Pumps</u>

1. These pumps can meet the entire flow/pressure requirement.

2. Pump life is a severe limitation, especially for the vane pump.

3. All pumps require centrifugal or axial inducer stages.

4. Performance is low due to high internal leakage rates.

5. High efficiencies are required to avoid "vapor lock" in suction porting.

6. Vane positive-displacement pumps are the lightest of those considered.

7. Vane pumps are the least expensive.

8. High-pressure gear pumps have low efficiencies due to internal leakage.

9. High tooth loading is the primary life limitation on gear pumps.

10. Positive-displacement pumps will most likely produce undesirable pressure oscillations.

11. Piston pumps are superior for low-flow, high head-rise applications. Vane pumps are better for high flow/low head, and gear pumps are most desirable in between.

12. The NASA LH_2 piston pump design is highly desirable where size is not an important criterion.

13. Flow/pressure pulsations and weight are the major limitations of Lobe and Roots pumps.

14. Diaphragm pumps appear attractive for low-flow/low-pressure requirements. Their efficiencies are low (in the 30-40% range).

Drivers

1. Three types of drivers were evaluated: 1) gas turbines, 2) electrical motors (polyphase induction, permanent magnet (PM) induction, and DC brush) and alternators/generators, and 3) positive-displacement drive motors.

2. Gas turbines can meet the speed/power requirements of all candidate pumps.

3. Gas turbine efficiencies can be obtained at levels from 30 to 55%.

4. Both bipropellant and hydrogen expander-cycle drive fluids are suitable for gas-turbine designs.

5. Hydrogen pumps for thrusts greater than 1779 N (400 lbF) and less than 4481 kPa (650 psi) can be driven by PM induction motors.

6. Motor efficiencies are in the 60 to 80% range.

7. Weight of electrical drive systems is the primary drawback.

8. Positive-displacement motors will only meet the Pitot and drag pump requirements without speed change between motor and pump.

9. Positive-displacement motors operate with efficiencies from to 35 to 45%.

10. Due to limited data, life of these motors has not been fully assessed.

Pump/Drive Matching

1. Pump/drive matching was accomplished by using both a numerical rating (13 elements) and a sorting technique (4 categories). Both produced the same result.

2. Rotodynamic pumps with either gas turbine or electric motor drive were the most promising combinations.

3. Pumps with efficiencies below 40% were difficult to match with drivers.

4. Confidence in meeting predicted performance was the primary discriminator.

5. The most promising hydrogen pumping systems, listed in order of merit, were:

   Multistage centrifugal pump/gas turbine
   Piston/electric motor
   Gear/electric motor

6. The most promising pumping system for both oxygen and methane was a centrifugal pump driven by a gas turbine.

General

1. Detailed turbomachinery designs should be conducted for a multi-stage centrifugal pump and an electric-motor-driven gear or positive-displacement pump.

2. These activities should focus on "size-oriented" mechanical design issues which will influence weight/life and performance projections.

III, Conclusions (cont.)

3. Sealing, leakage, and bearing performance appear to be the most significant transmission system issues.

4. Hardware investigations should be initiated on turbo-alternator drive configurations and hydrostatic bearings and seals.

IV. CANDIDATE PUMPS AND DRIVERS

The low-thrust propulsor requires feed pumps that are basically on the outer limits of the state of the art. The flows are low, the pressures are relatively high for the pump speed, and the fluids have poor lubricating qualities. Centrifugal pumps, the most prevalent type of pumps used in existing rocket applications, can produce the pressure at the required flow-rates but at a lower efficiency than larger pumps. Positive-displacement pumps may be capable of achieving higher efficiencies, but they may have problems with life limitations due to wear which, in turn, will degrade efficiencies.

One alternative to meeting the low flow requirements is to throttle a centrifugal pump or to recirculate part of the flow via a jet pump. However, this system will result in an unacceptably low pump efficiency of less than 40 percent. Since a typical expander-cycle engine needs a combined efficiency of 25 to 30% for pump and driver, such systems have little utility for this application.

Candidate pumps selected for their potential of satisfying the requirements of rocket engines at thrust levels from 445 to 8900 N (100 to 2000 lbF) were studied during Task I. They are listed in the order of merit for the prescribed duty cycle:

1. Centrifugal
2. Drag
3. Pitot
4. Tesla
5. Axial
6. Jet
7. Vane
8. Gear
9. Piston
10. Lobe or Roots
11. Diaphragm

V. DESIGN LIMITS AND OPERATING REQUIREMENTS

Design operating conditions for all pump types studied involved three propellants (hydrogen, methane, and oxygen) over the pressure/flow ranges depicted in Figure 1. Service life for all pumps is to vary inversely with thrust, as shown in Figure 2. Tables IV, V, and VI summarizes some of the design criteria for all pumping systems.

The design criteria used in this study originate from three sources: 1) contractual requirements given in Exhibit "A" of the contract Statement of Work (SOW); 2) limits mutually agreed upon between the NASA/LeRC project manager and ALRC; and 3) ALRC and NASA design criteria monographs. Design flowrate/pressure rise values for hydrogen, methane, and oxygen were taken from Exhibit "A" of the SOW, reproduced herein as Figure 1. Numbered points around the map identify the pressure flowrate values used in the analysis of all pumps reported herein. All pumps analyzed for performance or size utilized one or more of these numbered conditions. Unless specifically stated otherwise, all pumps analyzed were assumed to be capable of operating at the minimum NPSH values shown in Figure 1.

Mutually agreed-upon design limits were selected to denote when values of significant influence on performance or fabrication are obtained. Categories and their limit values are given in Table IV.

Miscellaneous design limits not covered by the contract or mutually agreed-upon are noted in Tables V, VI, and VII for bearings, shafting, and seals, respectively.

The following descriptions, review of pump types, and conclusions of applicability to the study requirements were conducted during Task I for each of the previously noted pump types.

Candidate drivers to match the speed/power requirements of the pumps are as follows:

Gas Turbines
Electric Motors
Positive-Displacement Motors

It was assumed that no speed changer would be used between the pump and its driver. The small size of these machines, plus the additional environmental problem of accommodating a lubricating system for the traditional gear box, prompted this position. The use of an alternator/electric motor does, in effect, allow for controlling the speed ratio between the two. This would allow for designing an alternator into the fuel turbopump and using an electric motor to drive the oxidizer pump at a lower speed.

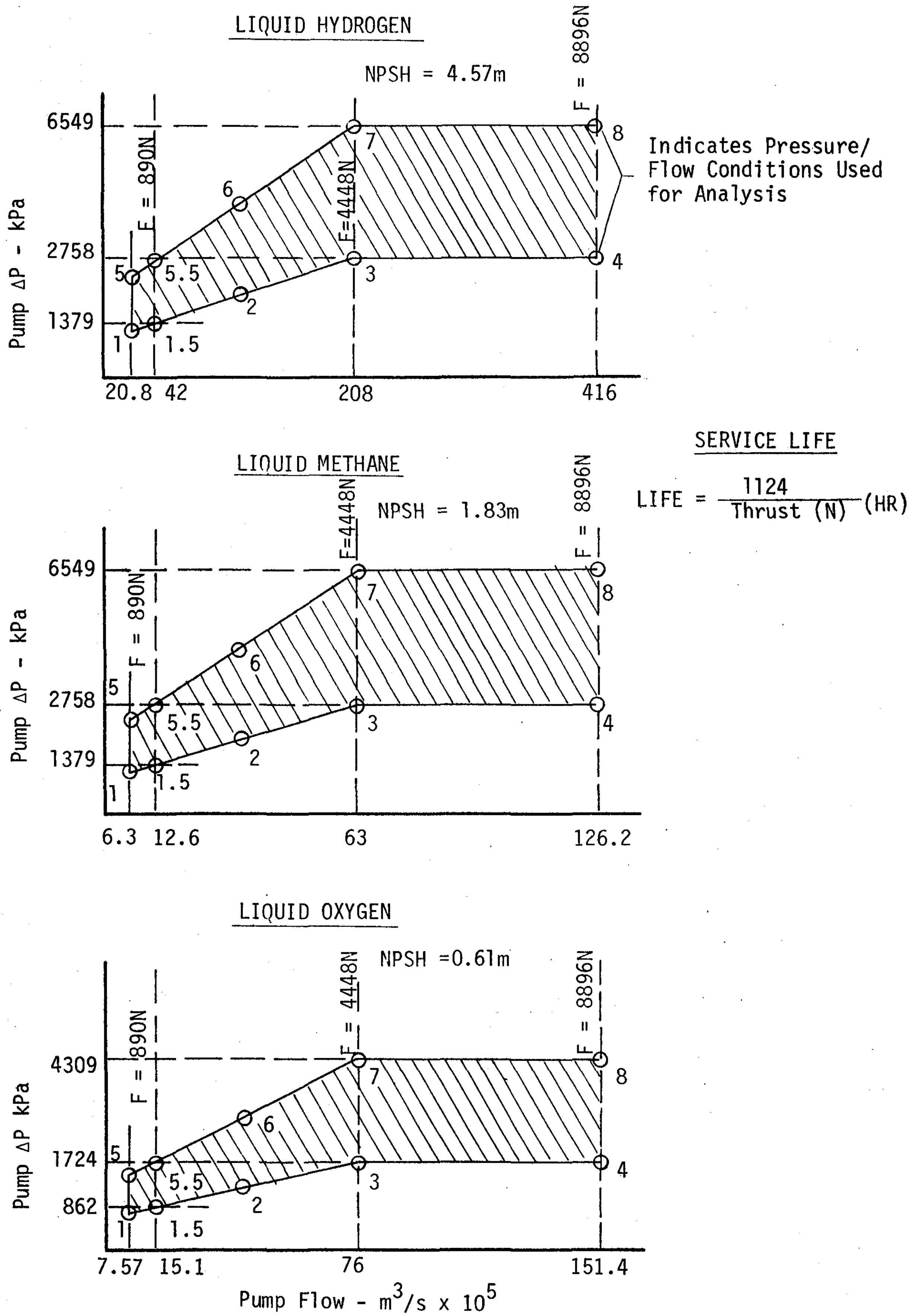

Figure 1. Design Pressure/Flow Map for Propellant Feed Pumps

SI UNITS

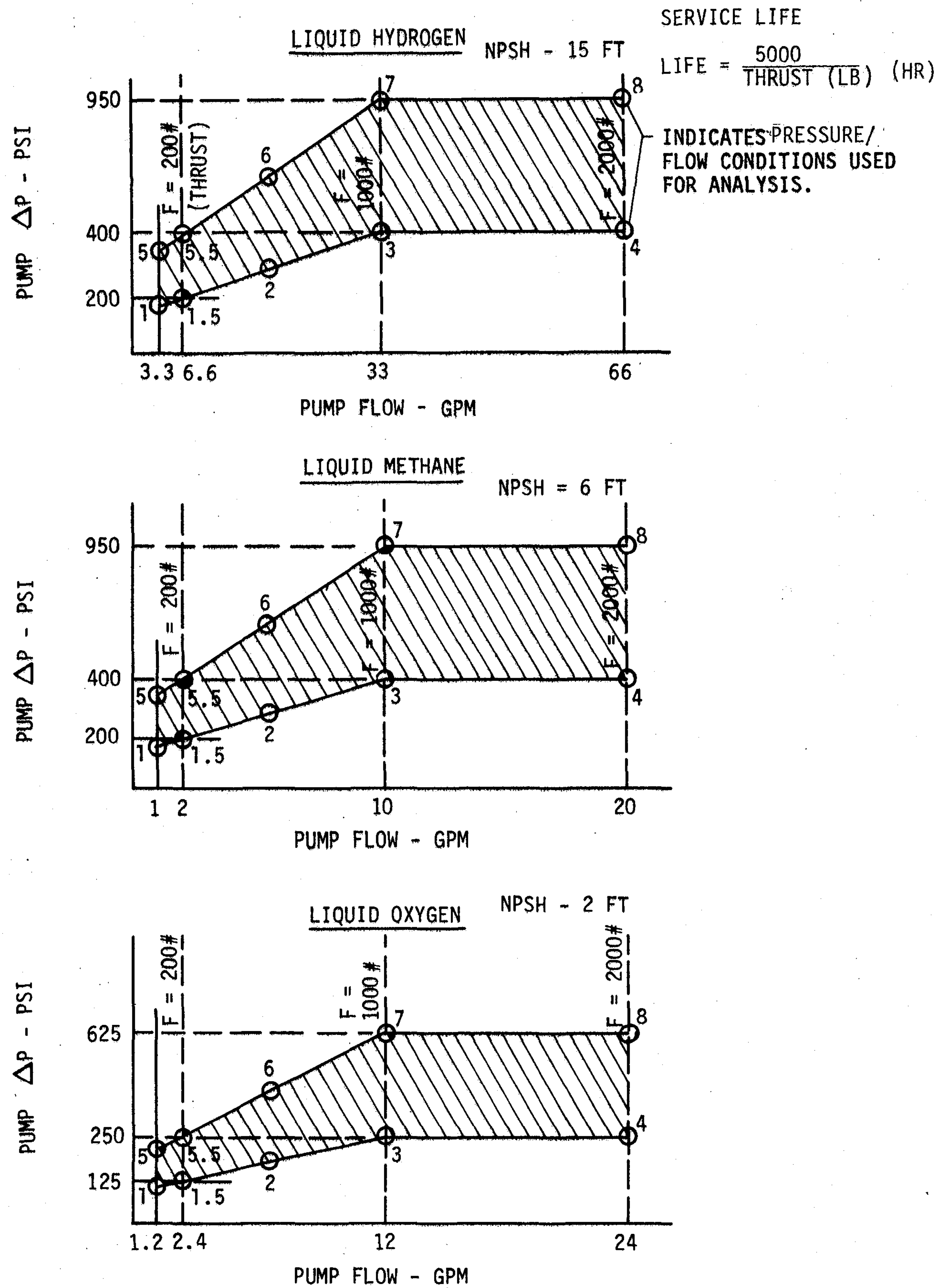

Figure 1 (cont.) Design Pressure/Flow Map for Propellant Feed Pumps

ENGLISH UNITS

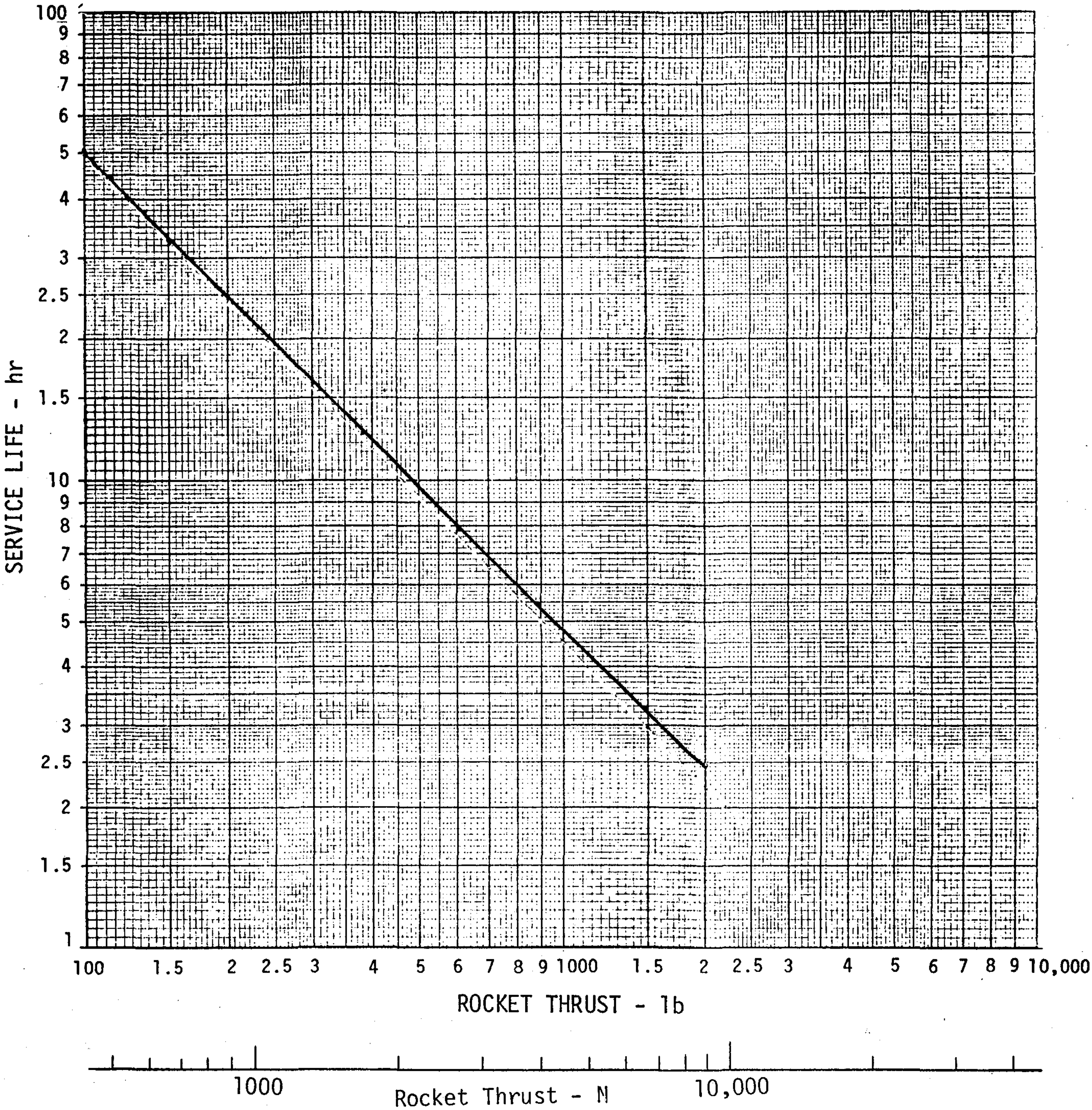

Figure 2. Service Life

TABLE IV. MUTUALLY AGREED-UPON DESIGN LIMITS

Centrifugal impeller diameter (min.) 1.78 cm (0.7 in.)

Centrifugal impeller exit blade height (min.) (0.0762 cm (0.03 in.)

Centrifugal pump stage specific speed (min.) $9.69 \frac{(\mathrm{RPM})(\mathrm{m}^3/\mathrm{s})^{1/2}}{\mathrm{m}^{3/4}}$

$$\left(500 \frac{(\mathrm{RPM})(\mathrm{GPM})^{1/2}}{\mathrm{ft}^{3/4}}\right)$$

Minimum rolling contact bearing size 10 mm (0.394 in.)

Fuel oxidizer pumps use separate drivers

Include "carry-over" volume of leakage flows

Use "Wilson" positive-displacement pump cavitation criteria (Ref. 72)

Suction specific speed maximum value for centrifugal pumps

Hydrogen = $775.2 \frac{(\mathrm{RPM})(\mathrm{m}^3/\mathrm{s})^{1/2}}{\mathrm{m}^{3/4}} \left(40{,}000 \frac{(\mathrm{RPM})(\mathrm{GPM})^{1/2}}{\mathrm{ft}^{3/4}}\right)$

Methane = 620 (32,000)

Oxygen = 581 (30,000)

Suction inlet velocity coefficient, $\frac{2g\ \mathrm{NPSH}^*}{C_m^{\ 2}}$, for centrifugal pumps

Hydrogen = 1.3

Methane = 2.08

Oxygen = 2.3

Minimum inducer inlet blade for centrifugal pumps

Flow coefficient = 0.06

*where C_m is the meridional velocity in m/s (ft/sec). NPSH is in m(ft) and 9 is 9.8 m/s (32.16 ft/sec).

TABLE V. BEARING DESIGN LIMITS

Bearings

Loading (Rolling Contact and Hydrostatic)

Dynamic Unbalance

$$W_V = \frac{W_s N}{984} \text{ (N)} \quad \left(W_V = \frac{W_s N}{4377} \text{ (lb)} \right)$$

where: W_s = Shafting weight, N (lb)

N = Shaft speed (RPM)

Impeller Radial Load

$$W_I = \frac{P\ d\ w}{11.24} \text{ (N)} \quad \left(W_I = \frac{P\ d\ w}{50} \text{ (lb)} \right)$$

where: P = Pump discharge pressure, N/m^2 (psi)

d = Impeller diameter, m (in.)

w = Impeller width, m (in.)

Shafting Design Load

$$W_{SD} = 14.81\ (W_V + W_I)\text{(N)} \quad \left(W_{SD} = 3.33\ (W_V + W_I)\text{(lb} \right)$$

Rolling Element Load = 95% of Total

Bearing Total Design Load

$$W_{BD} = 89 \times W_{SD} \text{ (N)} \quad \left(W_{BD} = 20 \times W_{SD} \text{ (lb)} \right)$$

Maximum DN Value (Rolling Contact)

Hydrogen = 2.0×10^6 (mm x RPM)

Methane = 1.9×10^6

Oxygen = 1.5×10^6

Life

Design Life = 10 x service life

Service Life = (function of thrust)

Reliability = 90.0% (90% will meet or exceed rated life before first sign of fatigue sets in)

Load Capability = Catalog fatigue life load as a function of speed and size

Bearing Sizes = 15, 17, 20, 25, 30, and 35 mm

Life = Unlimited

Clearance = 2 micron minimum

TABLE VI. SHAFT DESIGN LIMITS

Critical Speed of Shaft Assembly

First bending critical speed is at least 125% of the design speed.
First torsional critical speed is at least 125% of the design speed.

TABLE VII. SEAL DESIGN LIMITS

Seals

Face contact seal maximum PV, FV, and P_fV factors:

	LH_2	LO_2	LCH_4
PV	105 (50,000)	52.5 (25,000)	73.55 (35,000)
FV	213,500 (4000)	106,750 (2000)	170,803 (3200)
P_fV	420 (200,000)	126.1 (60,000)	252 (120,000)

where: PV = Unit load times rubbing velocity - MPa x m/s (psi x ft/s)

FV = Face load per unit length times rubbing velocity - N/s (psi x ft/s)

P_fV = Fluid pressure differential times rubbing velocity - MPa x m/s (psi x ft/s)

VI. ANALYSIS OF CANDIDATE PUMPS

The pumps considered consisted of both dynamic and positive-displacement types. The dynamic-type pumps included centrifugal, drag or regenerative, Pitot, Tesla, axial and jet pumps. The centrifugal, drag, Pitot, and axial pumps have vanes or blades which transport the fluid from low to high pressure. The Tesla has a series of disks which, through viscous shearing action, move the flow to a higher pressure. The jet pump uses a portion of the returned engine flow of high-energy fluid to drive the pumped fluid from tank to engine.

The positive-displacement pumps include the vane, gear, piston, lobe or Roots, and diaphragm. The vane, gear, and lobe or Roots pumps trap fluid between rotor vanes, gear teeth and lobes, respectively, to displace the fluid to a higher pressure. The piston and diaphragm pumps employ reciprocating elements which alternately increase and decrease a volume between two valves or ports.

A. DYNAMIC PUMPS

1. Centrifugal Pumps

a. Description

In a typical centrifugal pump, the pumped fluid enters the impeller axially and leaves the impeller after acquiring radial and tangential velocity components (kinetic energy). The impeller stage adds kinetic energy to the fluid through a set of rotating vanes. After leaving the impeller, the pumped fluid enters a volute in which the flow is diffused and static pressure is recovered. In many cases, it becomes necessary to arrange several pump stages in series in order to obtain the required pump pressure at an acceptable efficiency level. Centrifugal pumps are very sensitive to the available net positive suction pressure. In order to increase the suction performance, centrifugal pumps are often equipped with an inducer stage which runs at the same speed as the impeller. Variations of the basic centrifugal pump concept include the following:

- open or shrouded impeller
- vaned or vaneless diffuser
- full or partial emission

Typical examples of centrifugal pumps are the liquid oxygen and kerosine rocket engine pumps used on Titan I second-stage engines, shown in Figure 3, and the fuel pump designed for Picatinny Arsenal's 22,240 N (5,000 lbF) rocket engine shown in Figure 4.

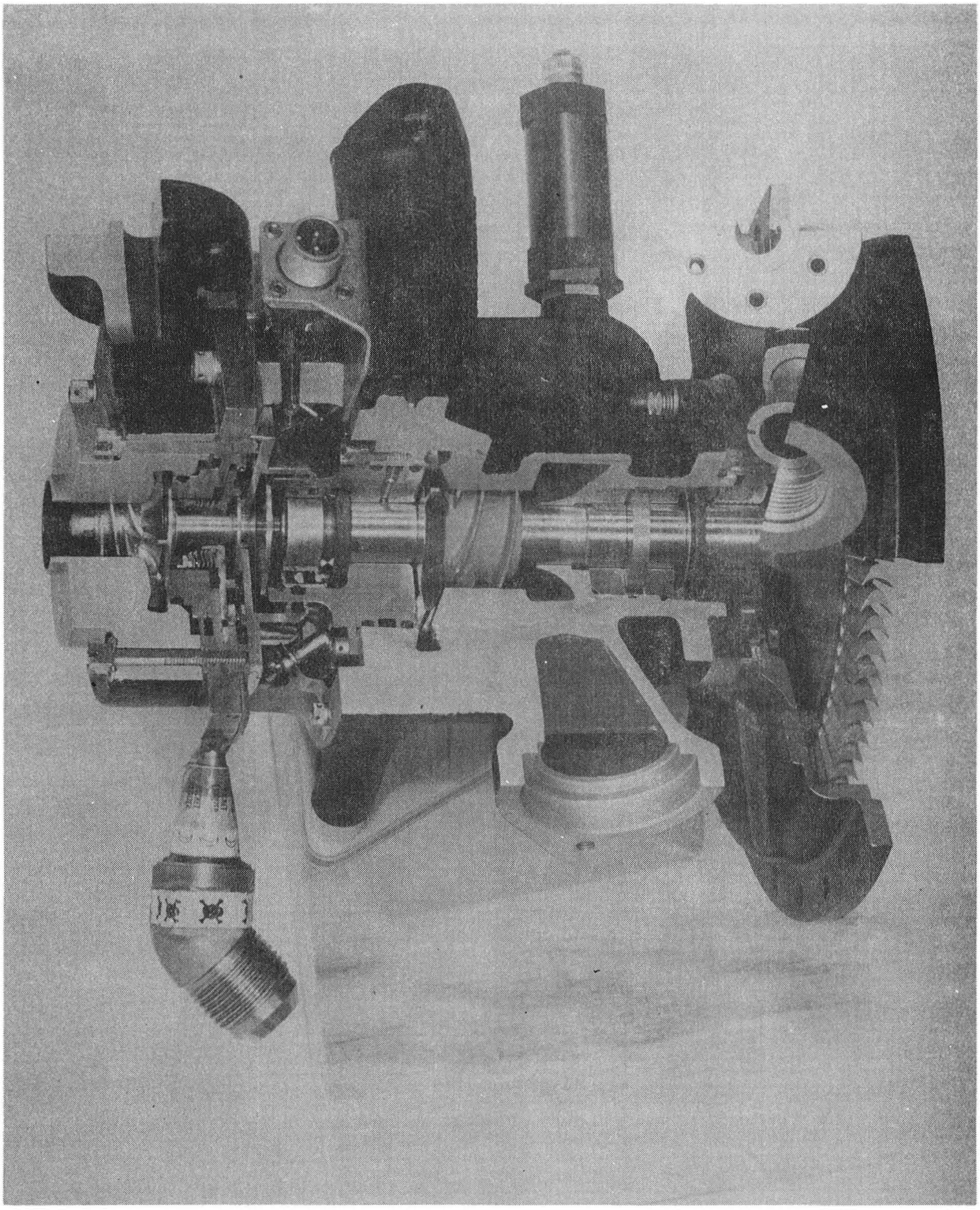

Figure 3. Auxiliary Pump Drive Assembly, Titan I

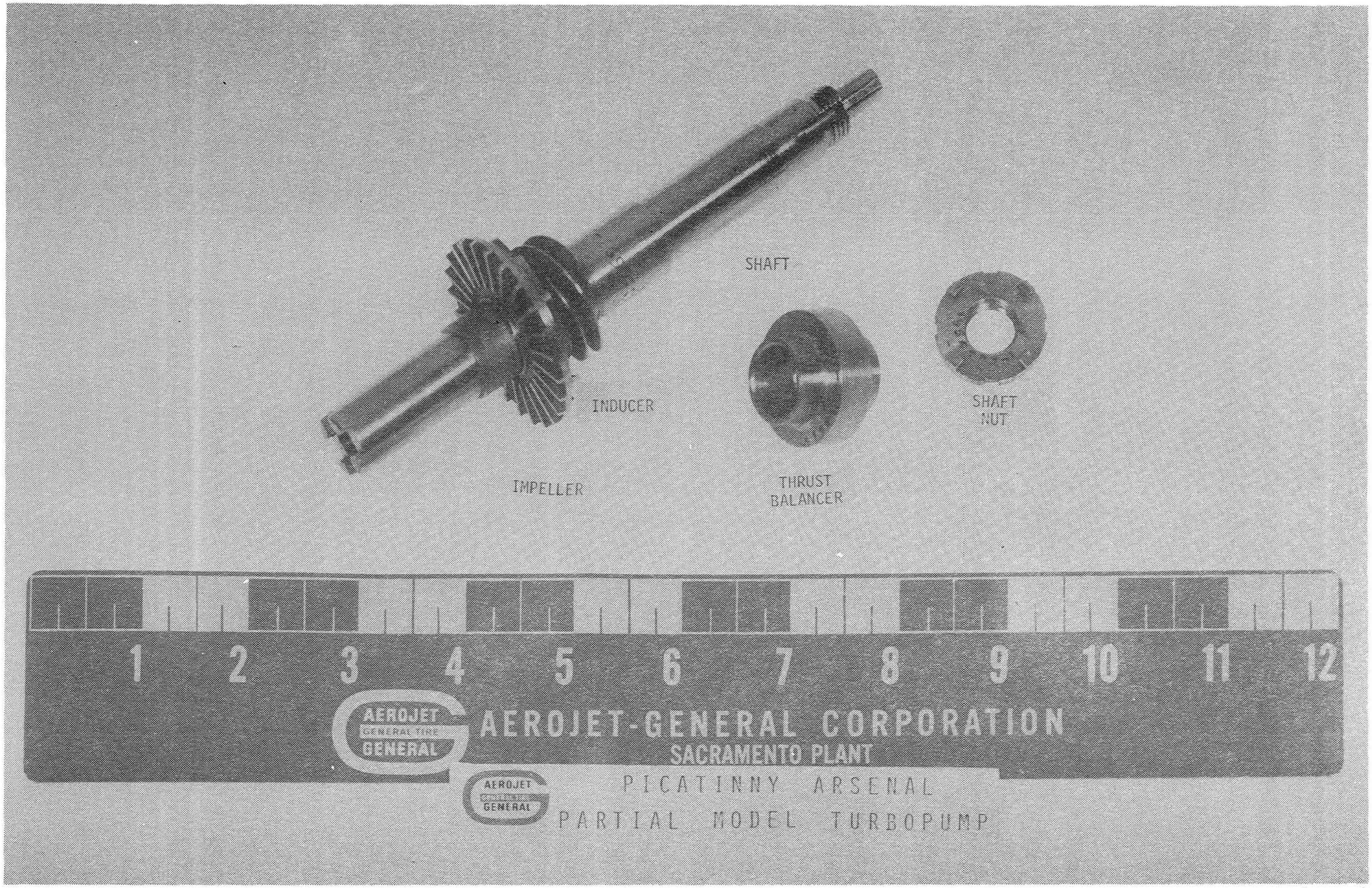

Figure 4. Picatinny Arsenal Pump Impeller

b. Literature Review

Pertinent literature is replete with design and performance information on centrifugal pumps in the 0.15-m (6-in.) and larger impeller diameter range. A significant amount of literature about smaller pumps is not available.

Historically, only two centrifugal pumps in the pressure/flow regime of interest are known to have been designed and developed. These are:

- Goddard Lox Pump 6.4 cm (2.5 in.) tip diameter

  Design Point: 1262 cm^3/s (20 GPM)
  4137 kPa (600 psi)
  29,000 RPM

- Titan I Auxiliary LOX Pump 5 cm (2.0 in.) tip diameter

  Design Point: 757 cm^3/s (12 GPM)
  6205 kPa (900 psi)
  36,000 RPM

Design and test criteria developed over the years have identified that the major potential risk in the design of small pumps is the difficulty in obtaining the efficiency levels achieved by larger pumps. Low specific speed pumps of small size are known to operate in an efficiency range of only 25 to 50%.

c. Performance Analysis

The following analysis was conducted with the objective to obtain insight into the size and performance of centrifugal pumps designed for pressure/flow combinations within the specified closed envelopes exhibited in Figure 1. For this study, the parameters of interest are limited to the following:

(A) Pump Speed = N (RPM)
(B) Blade Height = b (inches)
(C) Tip Diameter = d (inches)

(D) Specific Speed $= N_s \quad \frac{(RPM)(GPM)^{1/2}}{ft^{3/4}}$

(E) Efficiency $= \eta$

The parameters which may be assumed as given are:

Pump Pressure Rise	- ΔP (psi)	from map (Figure 1)
Pump Flow	- Q (GPM)	from map (Figure 1)
Pump NPSH	- h_{sv} (ft) = constant over map (Figure 1)	
Pump Suction Specific Speed	- S = Constant over map (Figure 1) Value specified in Table IV	
Density of Fluid	- S = Constant over map (Figure 1)	
Number of Stages	- $1 < I < 6$	

The analysis is carried out using the English Unit System exclusively. Introducing the definitions of specific speed

$$N_s = \frac{NQ^{1/2}}{\Delta H^{3/4}}$$

where ΔH is the pump head and suction specific speed is

$$S = \frac{NQ^{1/2}}{h_{sv}^{3/4}}$$

and making the assumptions

Head coefficient: $\psi = 0.560 - 7.90 \times 10^{-5}\ N_s$ — see Figure 5
Flow coefficient: $\phi = 0.08 + 1.16 \times 10^{-5}\ N_s$ — see Figure 5
Efficiency: $\eta = \eta(N_s,\ d)$ — see Figure 6

it is possible to derive the equations of the loci of the parameters of interest, (A) through (E), in the pressure/flow map.

The assumed equation used to relate head coefficient to flow coefficient is a linear function at approximately a 20° impeller discharge

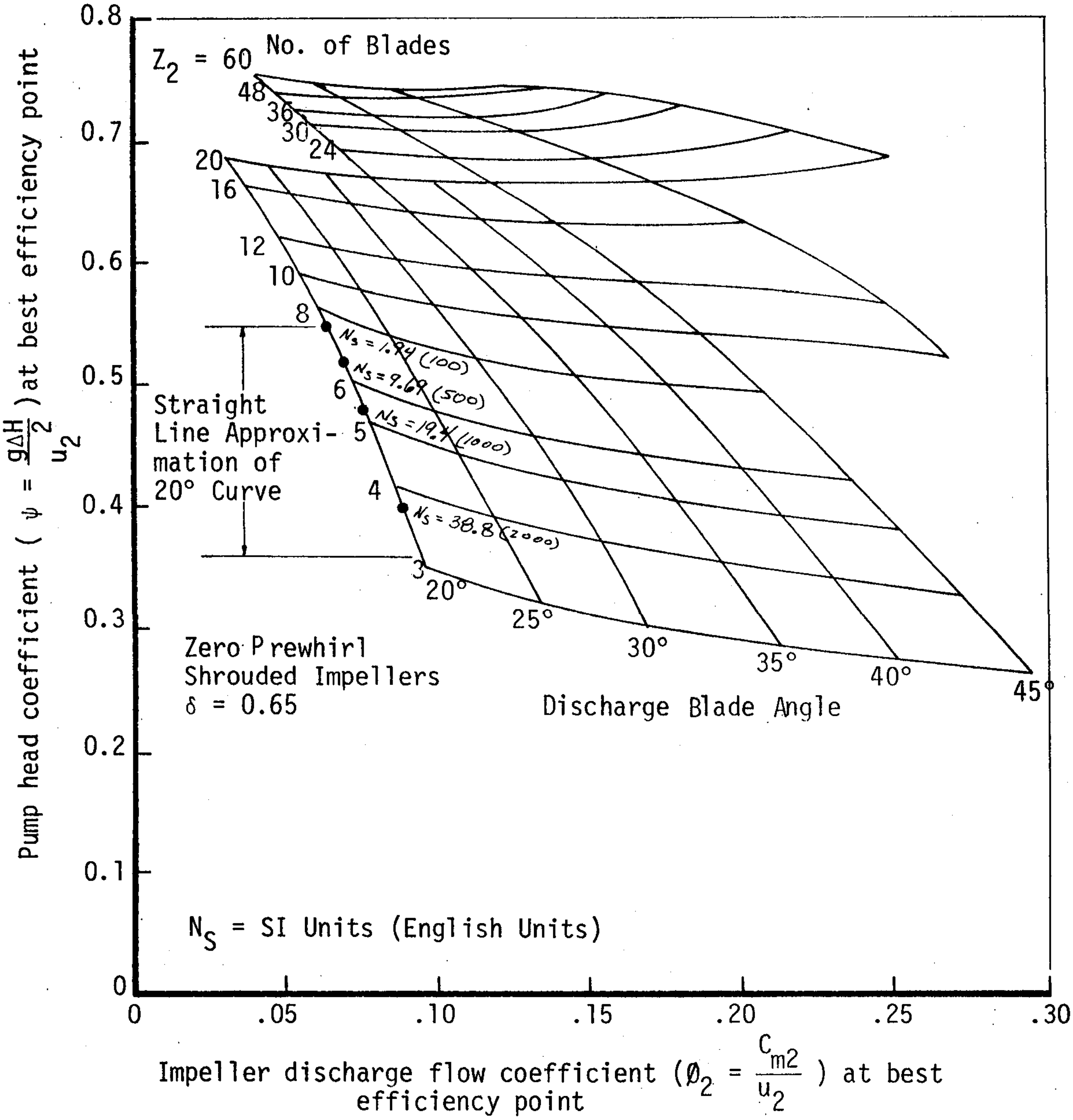

Ref: NASA SP-8109, Dec. 73

Figure 5. Head Versus Capacity Coefficient for Centrifugal Pump Designs

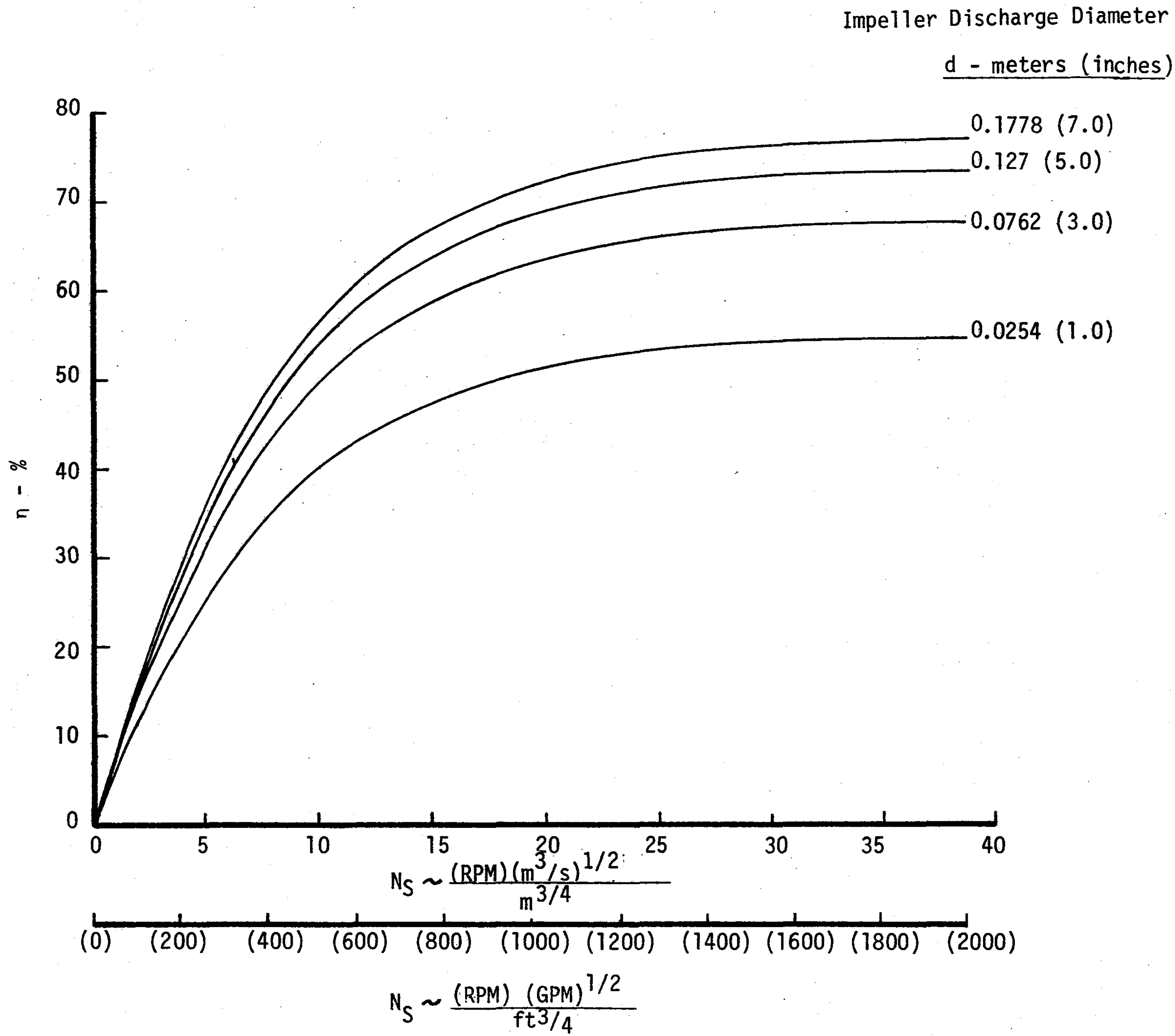

Figure 6. Efficiency as a Function of Specific Speed and Impeller Size

angle. It is within 1% of the original data and covers the range of specific speeds of

$$1.94 \frac{\text{RPM } (m^3/s)^{1/2}}{m^{3/4}} \quad \text{to} \quad 38.8 \frac{\text{RPM } (m^3/s)^{1/2}}{m^{3/4}}$$

$$\left(100 \frac{(\text{RPM})(\text{GPM})^{1/2}}{ft^{3/4}} \quad \text{to} \quad 2000 \frac{(\text{RPM})(\text{GPM})^{1/2}}{ft^{3/4}} \right)$$

This range encompasses impellers with 3 to 8 vanes. The use of more than 8 vanes for the lowest specific speed encountered in the study is judged to be a fabrication limit for vane thickness and spacing at the vane leading edges. A 20° impeller vane angle was selected for this initial study to keep impeller port widths from becoming too small.

The pump efficiency (Figure 6) is defined as a function of two independent variables: specific speed and impeller tip diameter. The data are based on information found in NASA SP-9109, AFRPL TR-72-45, and on engineering judgment.

The derived equations which specify the loci of the parameters of interest in the pressure/flow map are:

<u>(A) SPEED LOCUS - N = constant</u>

$$F\left(N, \frac{\Delta P}{I}, Q\right) = \left[\frac{S\, h_{sv}^{3/4}}{N}\right]^2 - Q = 0$$

NOTE: F is not a function of ΔP, i.e., the speed loci are vertical straight lines in the pressure/flow map.

<u>(B) BLADE HEIGHT LOCUS - b = constant</u>

$$F\left(b, \frac{\Delta P}{I}, Q\right) = \frac{23.3\, \rho\, Q^{1/2}\, S\, h_{sv}^{3/4}}{2.43 \times 10^8} \; \frac{\left[0.560 - 7.90 \times 10^{-5}\, S \left(\frac{h_{sv}\, \rho}{144 \Delta P} I\right)^{3/4}\right]}{\left[0.068 + 1.16 \times 10^{-5}\, S \left(\frac{h_{sv}\, \rho}{144 \Delta P} I\right)^{3/4}\right]} - \frac{\Delta P}{I} = 0$$

(C) TIP DIAMETER LOCUS - d = constant

$$F(d, \frac{\Delta P}{I}, Q) = \frac{\rho\,(d\,S\,h_{sv}{}^{3/4})^2}{2.43 \times 10^8\,Q}\left[0.560 - 7.90 \times 10^{-5}\,S\,\left(\frac{h_{sv}\,\rho}{144\Delta P}\,I\right)^{3/4}\right] - \frac{\Delta P}{I} = 0$$

(D) SPECIFIC SPEED LOCUS - N_s = constant

$$F(N_s, \frac{\Delta P}{I}, Q) = \frac{\rho\,h_{sv}}{144} \times \left(\frac{S}{N_s}\right)^{4/3} - \frac{\Delta P}{I} = 0$$

NOTE: F is not a function of Q, i.e., the specific speed loci are horizontal straight lines in the pressure/flow map.

(E) EFFICIENCY LOCUS - η = constant

$$F(\eta, \frac{\Delta P}{I}, Q) = \eta\left(\frac{S\,h_{sv}{}^{3/4}}{[144\frac{\Delta P}{\rho I}]^{3/4}};\ Q\right) - \eta = 0$$

The solutions for SPEED, TIP DIAMETER, and SPECIFIC SPEED LOCI are straightforward whereas BLADE HEIGHT and EFFICIENCY LOCI must be determined iteratively. The results of the functions (A) through (E) for the three candidate propellants (liquid hydrogen, liquid methane, and liquid oxygen) are as described below.

d. Analytical Results

(A) The SPEED LOCI in the pressure/flow map are given in Figures 7a, b, and c for LH_2, LCH_4, and LO_2, respectively. It is noted that the speed is only a function of the pump flow for constant suction specific speed and constant net positive suction head. Over the region of interest, the variations in speed for the three propellants are as follows: from 170,000 to 37,500 RPM for LH_2; from 125,000 to 27,500 RPM for LCH_4; and from 45,000 to 10,000 RPM for LO_2. The high speed values correspond to the low flow regime, and the low speed values correspond to the high flow regime.

(B) The BLADE HEIGHT LOCI in the pressure/flow map are given in Figures 8, 9, and 10, respectively for LH_2, LCH_4, and LO_2 for pumps with one to six stages.

Hydrogen

Methane

Oxygen

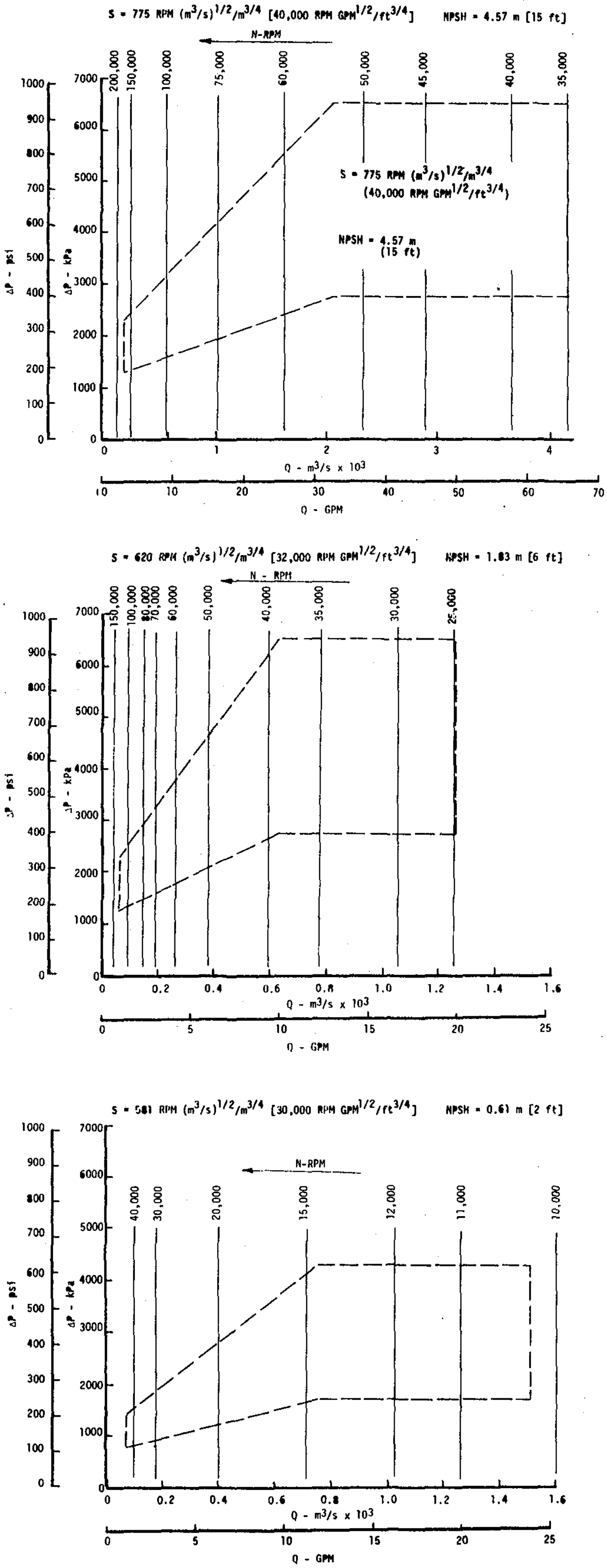

Figure 7. Speed Loci in Pressure/Flow Maps for LH_2, LCH_4, and LO_2

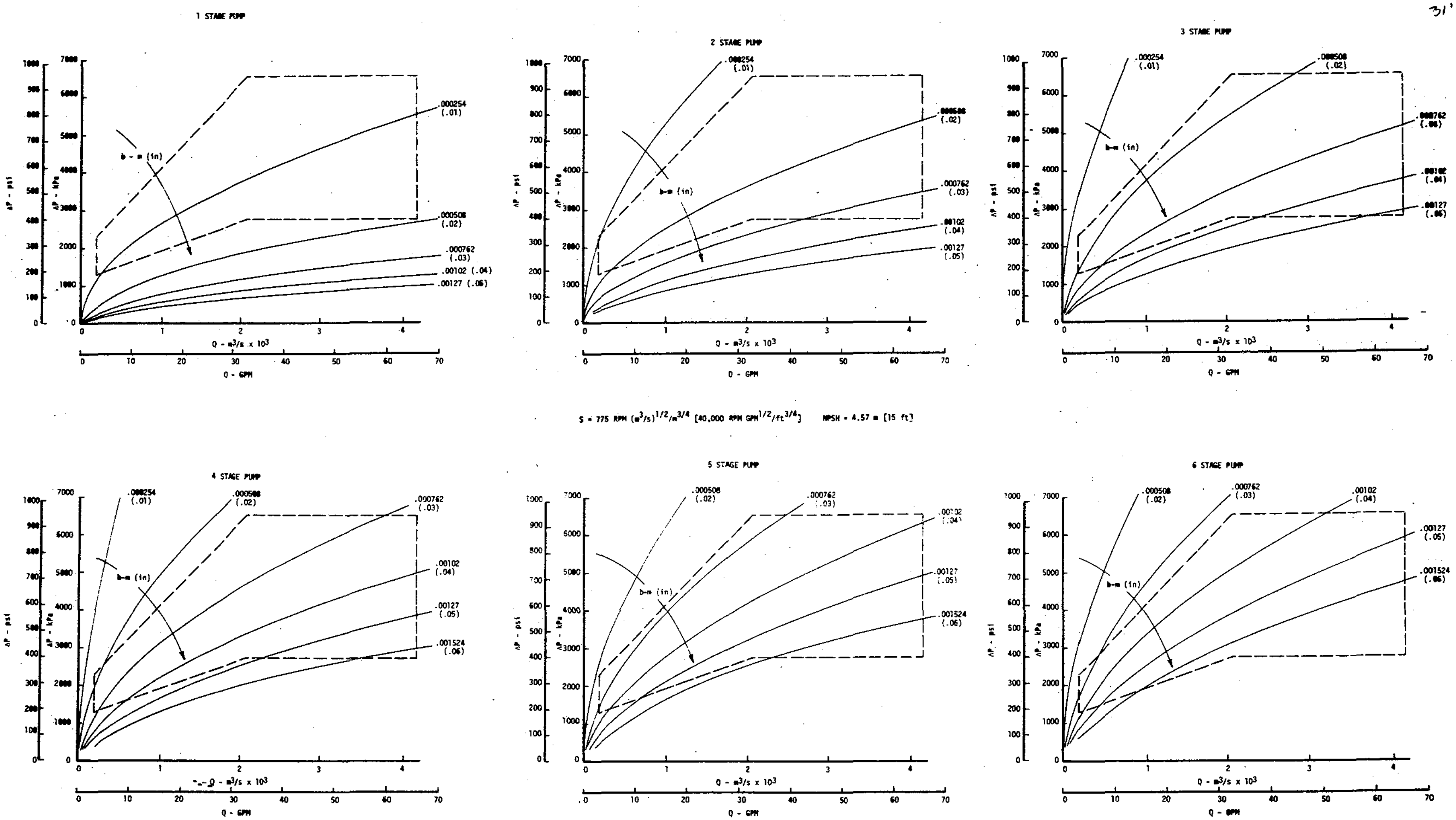

Figure 8. Blade Height Loci in Pressure/Flow Map for LH_2

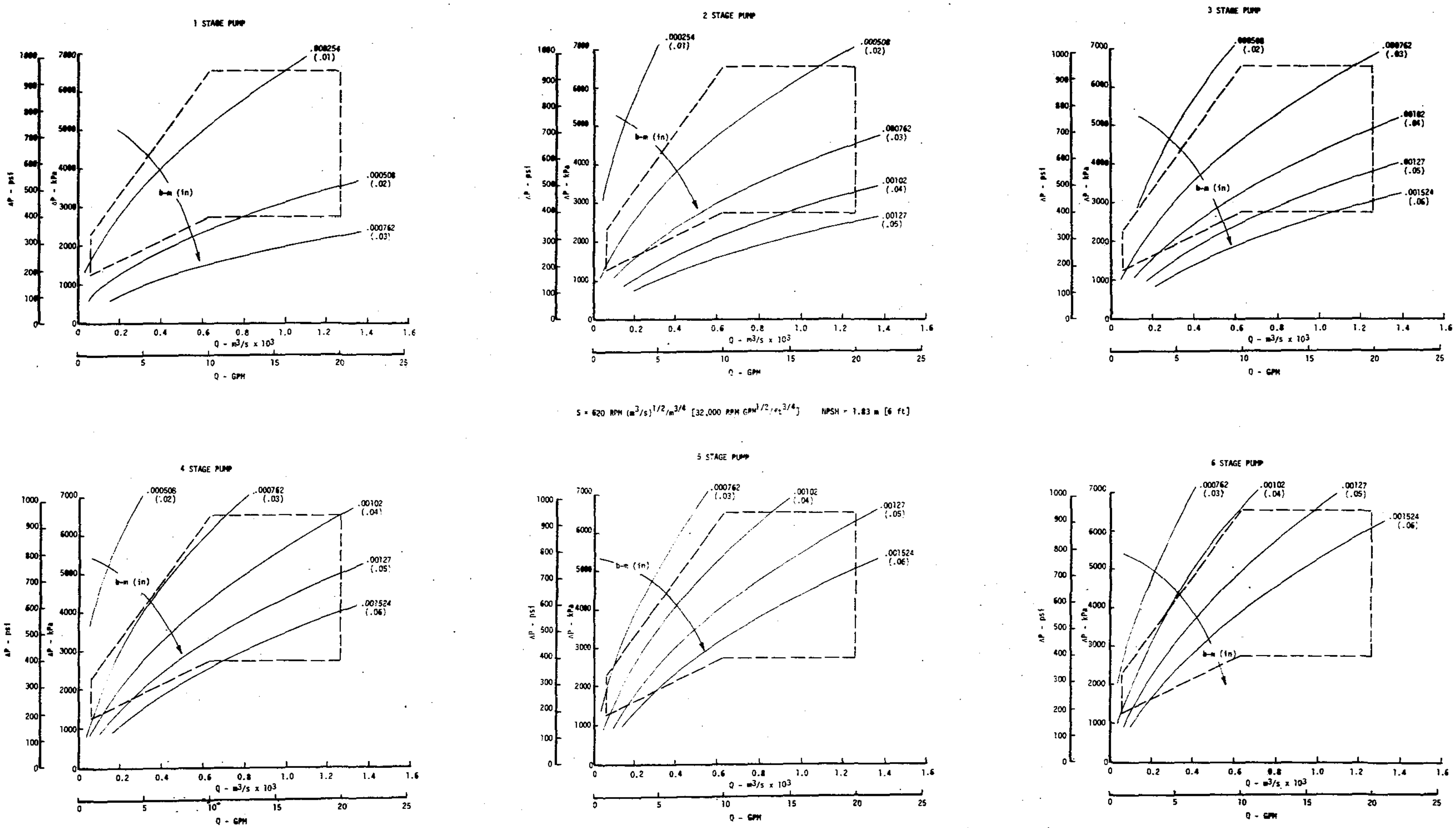

Figure 9. Blade Height Loci in Pressure/Flow Map for LCH_4

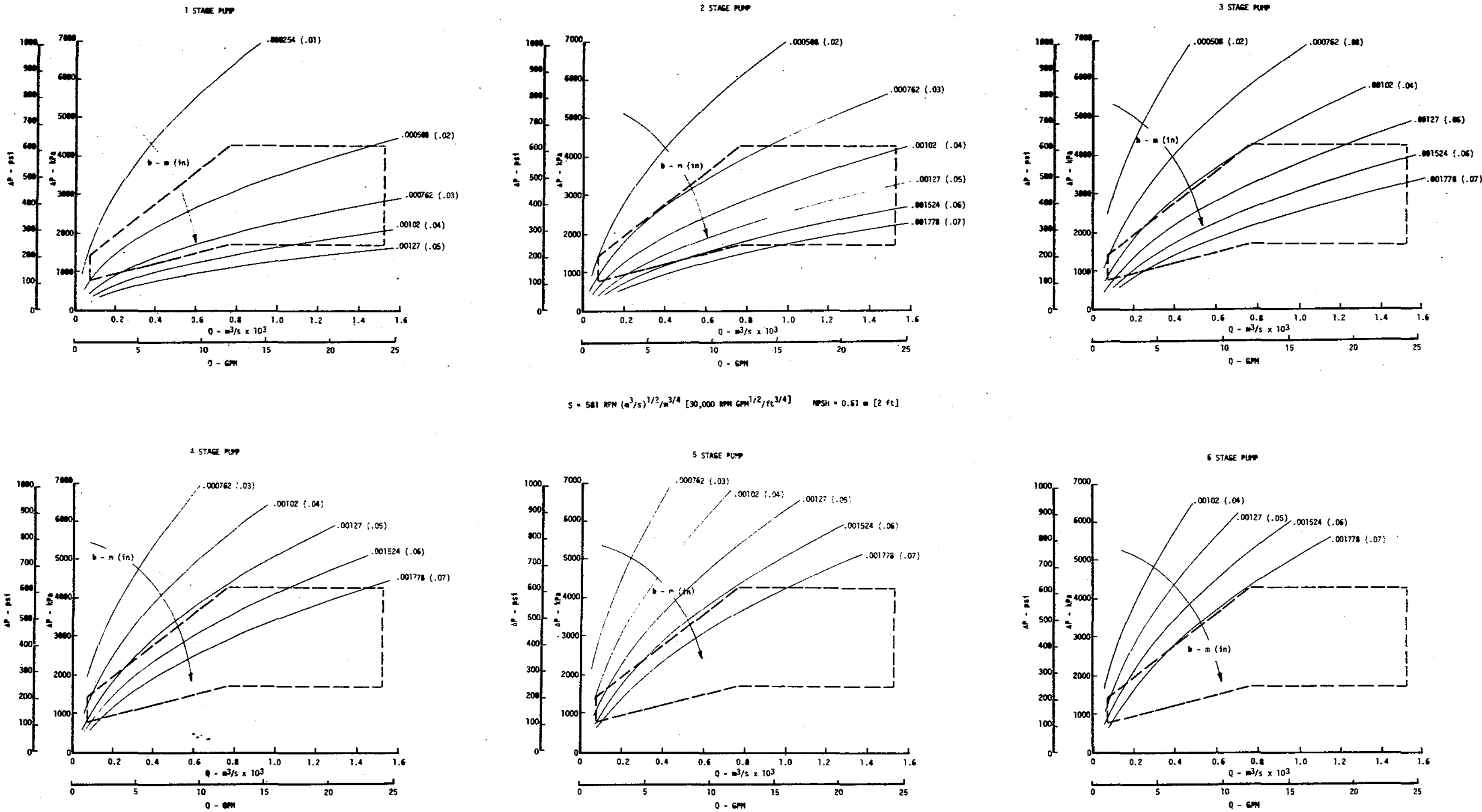

Figure 10. Blade Height Loci in Pressure/Flow Map for LO_2

Ignoring fabricational size limitations for this assessment, the respective minimum and maximum blade heights required to cover the pump design range of interest are as listed below:

MINIMUM/ MAXIMUM BLADE HEIGHT - METERS [INCHES]						PROPELLANT
NUMBER OF STAGES						
1	2	3	4	5	6	
0.000127/ 0.000508 [0.0050/ 0.0200]	0.000254/ 0.001016 [0.0100/ 0.0400]	0.000381/ 0.001397 [0.150/ 0.0550]	0.000445/ 0.001651 [0.0175/ 0.065]	0.000572/ 0.001778 [0.0225/ 0.0700]	0.000635/ 0.002032 [0.250/ 0.0800]	LH_2
0.000127/ 0.000635 [0.0050/ 0.250]	0.000381/ 0.001143 [0.0150 0.0450]	0.000508/ 0.001651 [0.0200/ 0.0650]	0.000635/ 0.002032 [0.0250/ 0.0800]	NOT REQUIRED		LCH_4
0.000381/ 0.00127 [0.0150/ 0.0500]	0.000635/ 0.002032 [0.0250/ 0.0800]	0.001016/ 0.002286 [0.0400/ 0.0900]	See Section VI.A.1.e			LO_2

(C) THE TIP DIAMETER LOCI in the pressure/flow map are given in Figures 11, 12, and 13, respectively, for LH_2, LCH_4, and LO_2 for pumps with one to six stages.

Again ignoring fabricational size limitations, the minimum and maximum tip diameters required to cover the pump design range of interest are as listed below:

MINIMUM/ MAXIMUM TIP DIAMETER - METERS [INCHES]						PROPELLANT
NUMBER OF STAGES						
1	2	3	4	5	6	
0.01778/ 0.20828 [0.7/8.2]	0.01778/ 0.1524 [0.7/6.0]	0.0127 0.127 [0.5/5.0]	0.01016/ 0.1143 [0.4/4.5]	0.00762/ 0.889 [0.3/3.5]	0.00508 0.762 [0.2/3.0]	LH_2
0.01778 0.1143 [0.7/4.5]	0.01016 0.07112 [0.4/2.8]	0.007621 0.06858 [0.3/2.7]	0.00508 0.05842 [0.2/2.3]	NOT REQUIRED		LCH_4
0.01778/ 0.127 [0.7/5.0]	0.0127 0.09398 [0.5/3.7]	0.01016 0.0889 [0.4/3.5]	See Section VI.A.1.e			LO_2

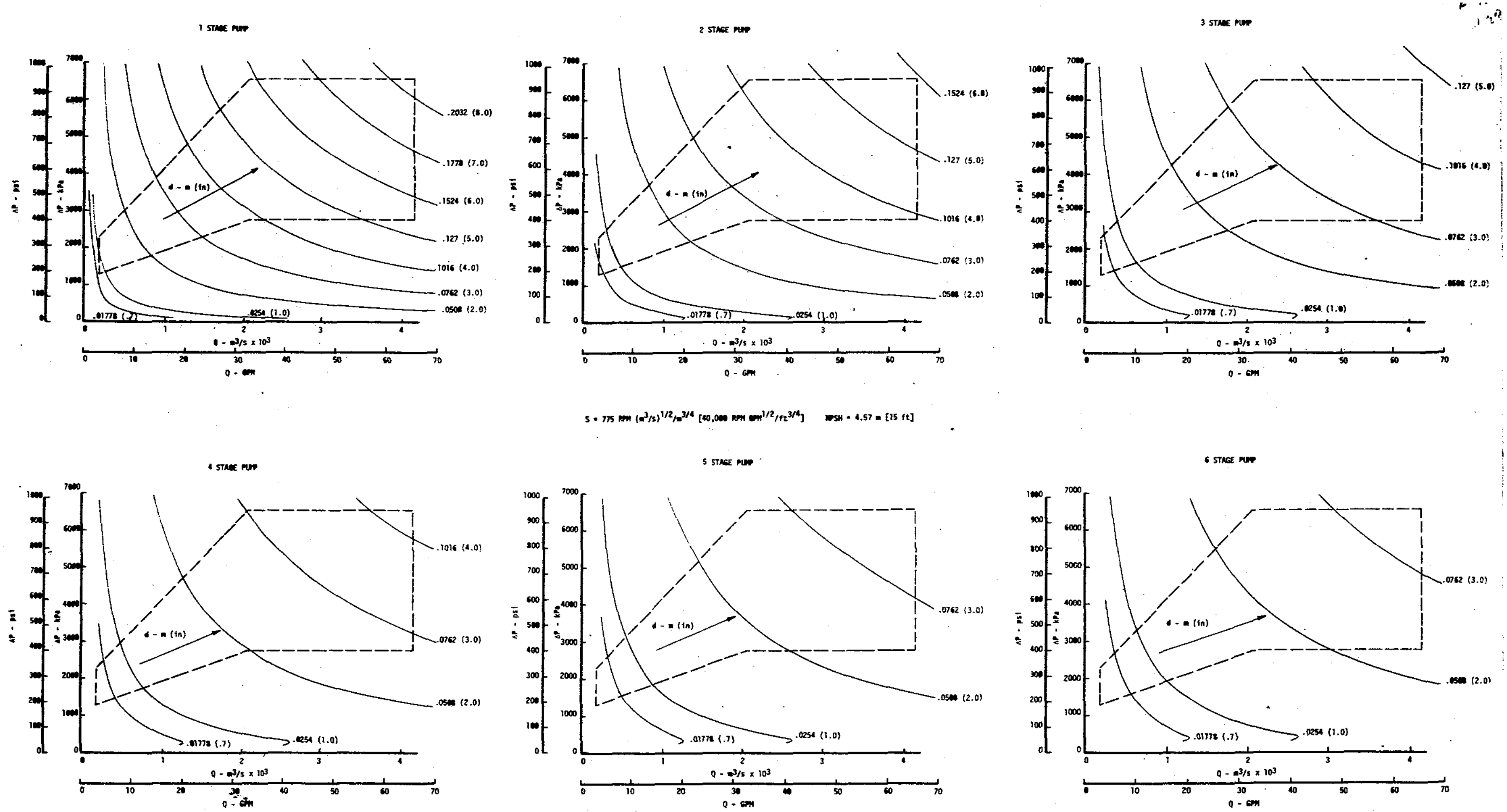

Figure 11. Tip Diameter Loci in Pressure/Flow Map for LH_2

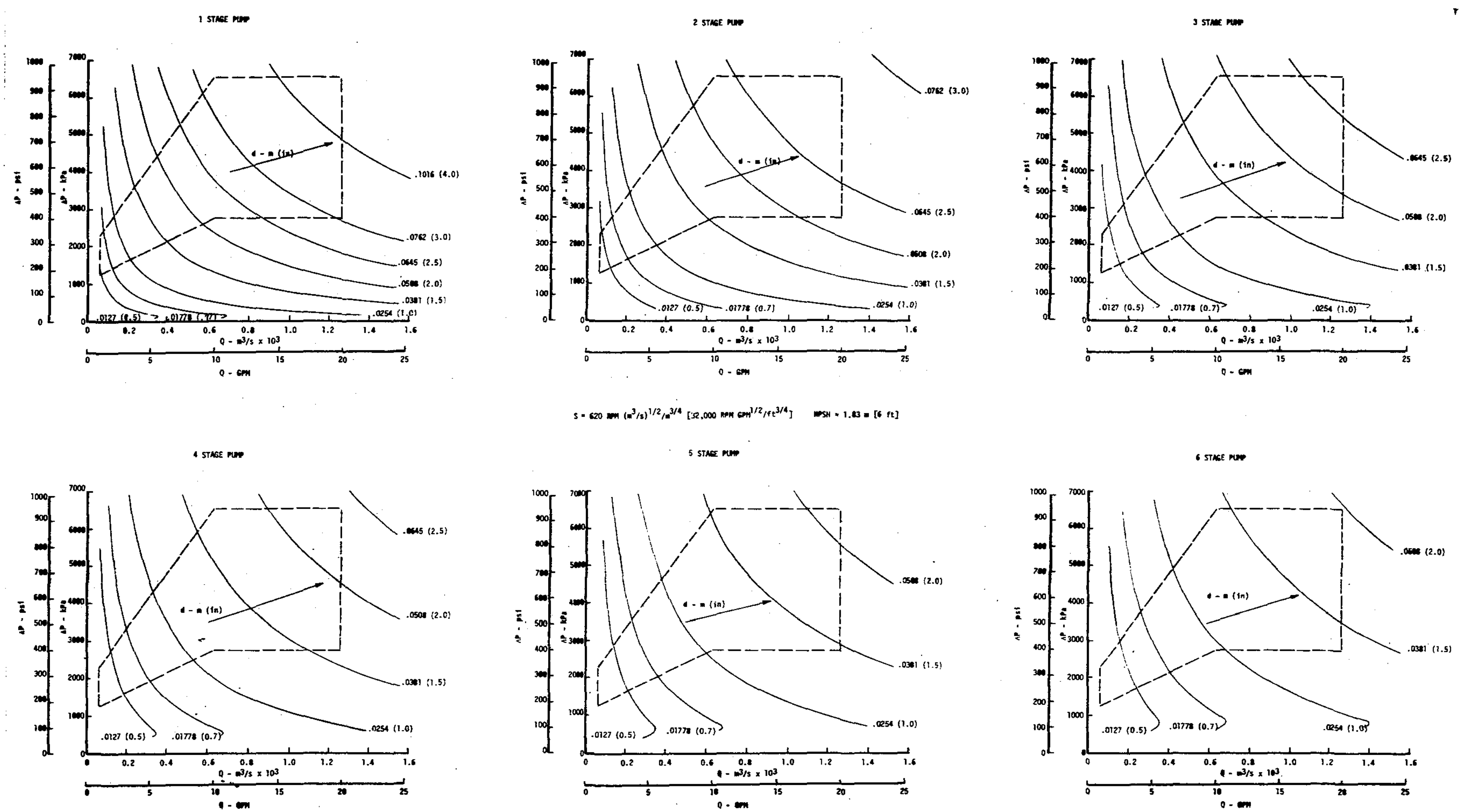

Figure 12. Tip Diameter Loci in Pressure/Flow Map for LCH_4

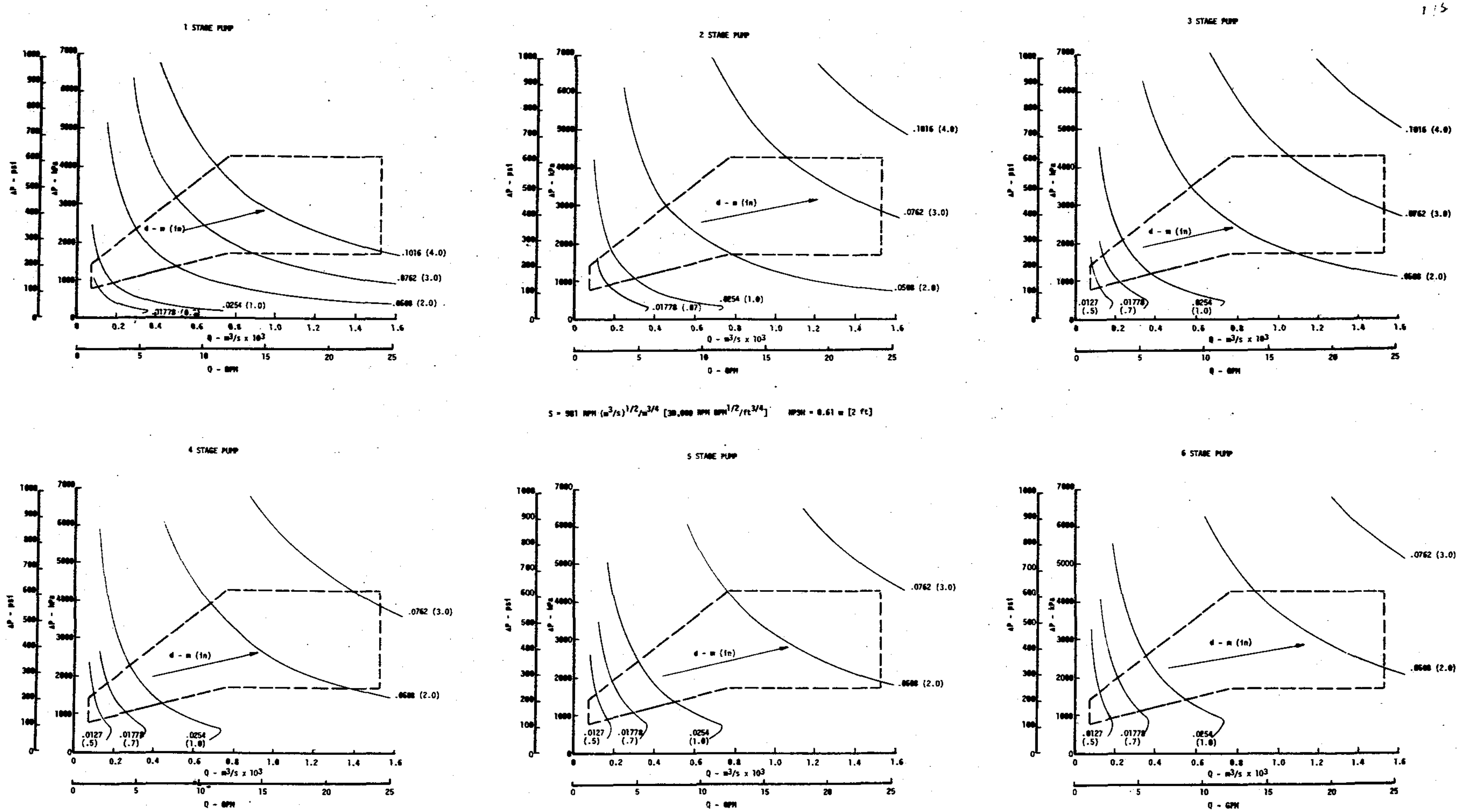

Figure 13. Tip Diameter Loci in Pressure/Flow Map for LO_2

(D) The SPECIFIC SPEED LOCI in the pressure/flow map are shown in Figures 14, 15, and 16, respectively, for LH_2, LCH_4, and LO_2 for pumps with one to six stages.

The following specific speed ranges are required to cover the pressure/flow range of interest:

STAGE SPECIFIC SPEED RANGE $\frac{(RPM)(m^3/s)^{1/2}}{m^{3/4}}$ $\left[\frac{(RPM)(GPM)^{1/2}}{ft^{3/4}}\right]$ NUMBER OF STAGES 1	2	3	4	5	6	PROPELLANT
2.519-8.721 [130-450]	4.264-14.535 [220-750]	5.620-19.768 [290-1020]	6.977-24.419 [360-1260]	8.333-29.051 [430-1499]	9.496-33.140 [490-1710]	LH_2
3.876-13.566 (200-700]	6.589-22.868 [340-1180]	8.915-30.814 [460-1590]	11.047-38.372 [570-1980]	12.985-45.155 [670-2330]	15.116-51.745 [780-2670]	LCH_4
4.457-17.054 [230-880]	7.558-28.489 [390-1470]	10.271-38.76 [530-2000]	12.597-48.062 [650-2480]	14.923-56.783 [770-2930]	17.248-64.923 [890-3350]	LO_2

(E) The EFFICIENCY LOCI in the pressure/flow map are also shown in Figures 14, 15, and 16, respectively, for LH_2, LCH_4, and LO_2 for pumps with one to six stages.

As was to be expected, the pump efficiencies approach the lines of constant specific speeds asymmetrically in large-flow regimes which is an indication of their size independence in this region. In the low-flow regime, or equivalent small-size region, the constant efficiency lines deviate from the specific speed lines significantly, indicating increased pressure drops due to relatively high internal losses. Theoretically, it can be shown that the lines of constant efficiency drop down sharply and continue in the very low (below 138 kPa [20 psi]) pressure regime at specific speeds way above

$$58.14\ \frac{(RPM)(m^3/s)^{1/2}}{m^{3/4}}\quad \left[3000\ \frac{(RPM)(GPM)^{1/2}}{ft^{3/4}}\right].$$

However, it is known that this regime is outside the operating range of centrifugal pumps, and thus these solutions are of no practical value.

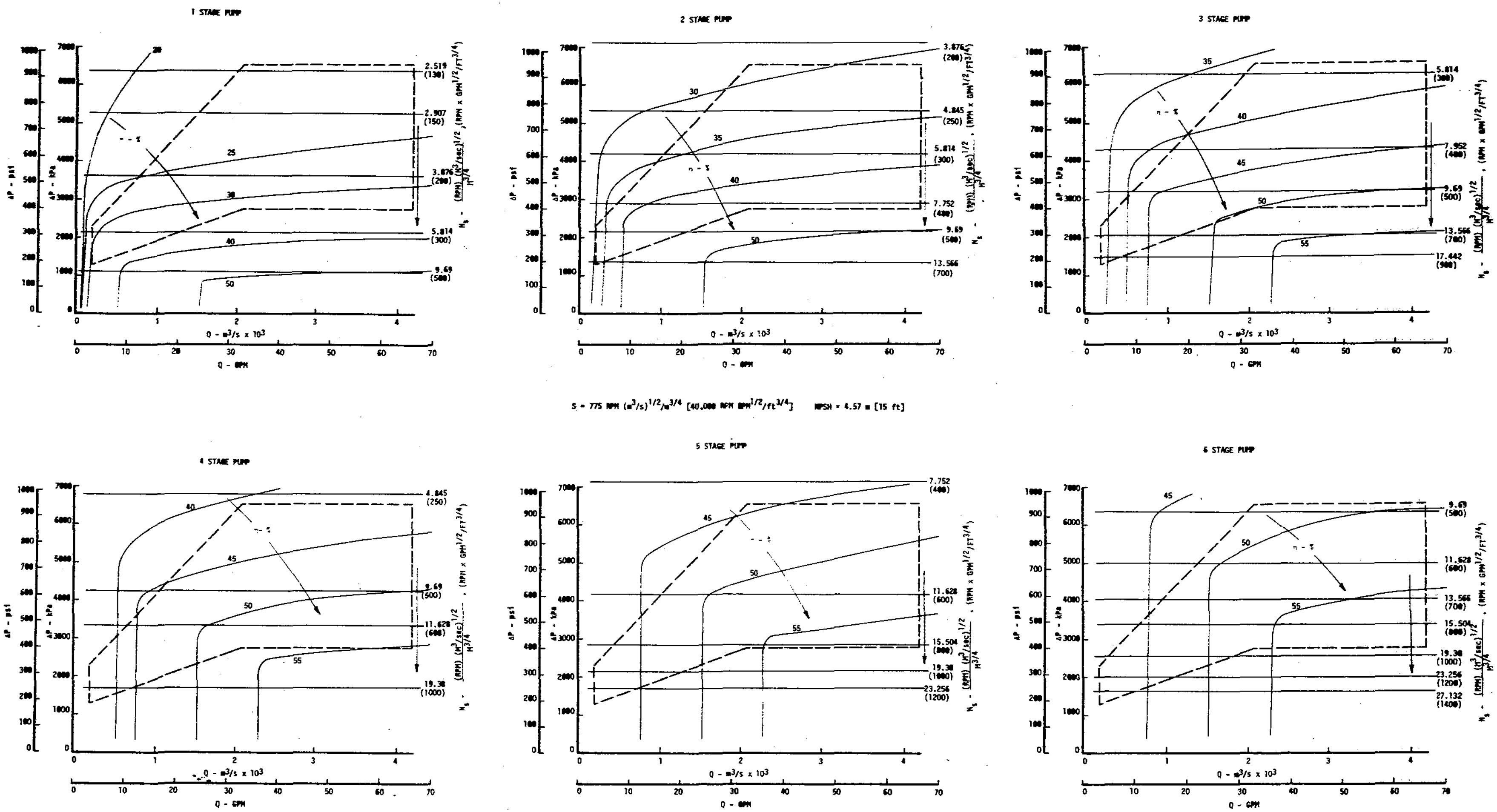

Figure 14. Specific Speed and Efficiency Loci in Pressure/Flow Map for LH_2

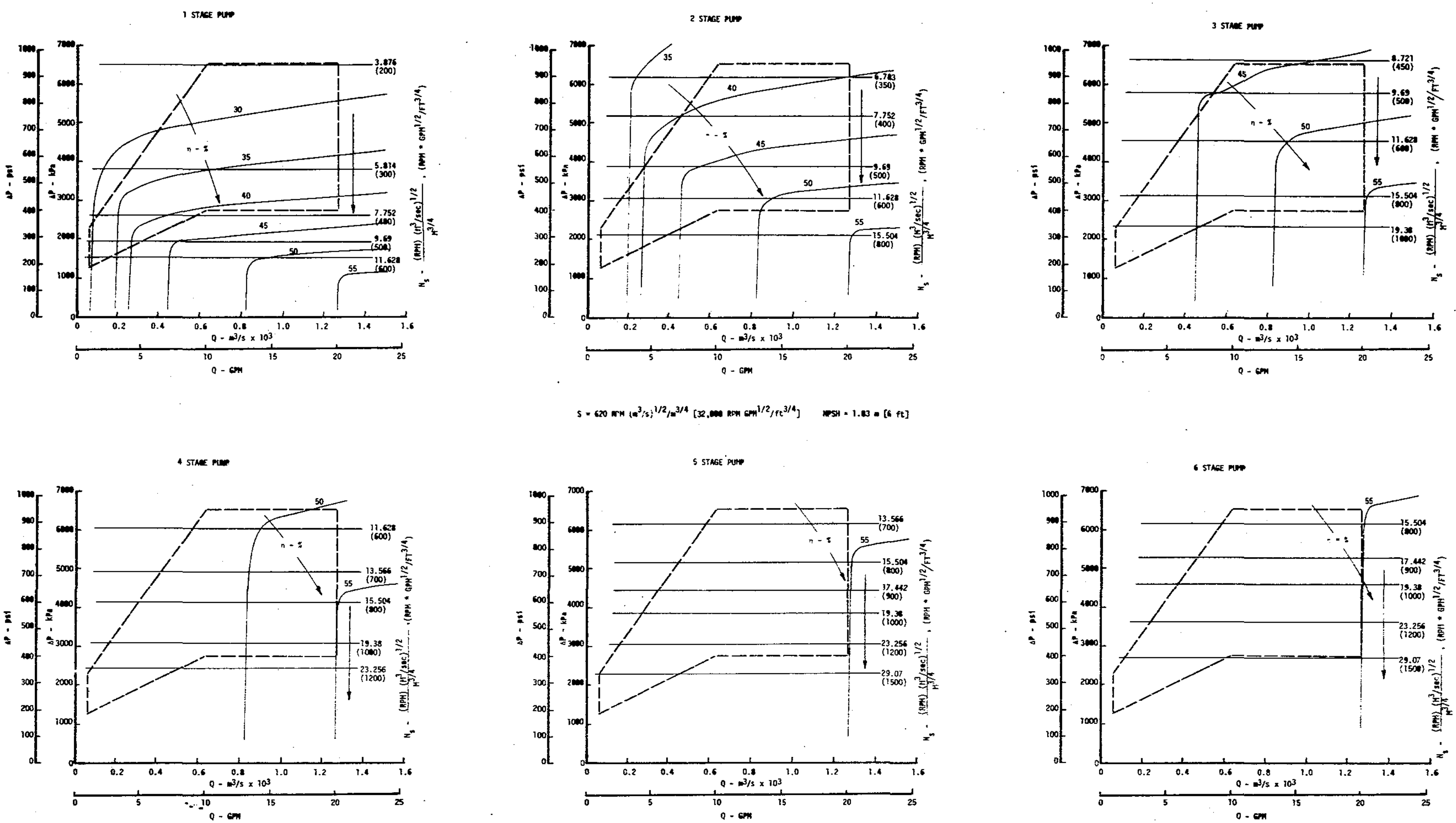

Figure 15. Specific Speed and Efficiency Loci in Pressure/Flow Map for LCH_4

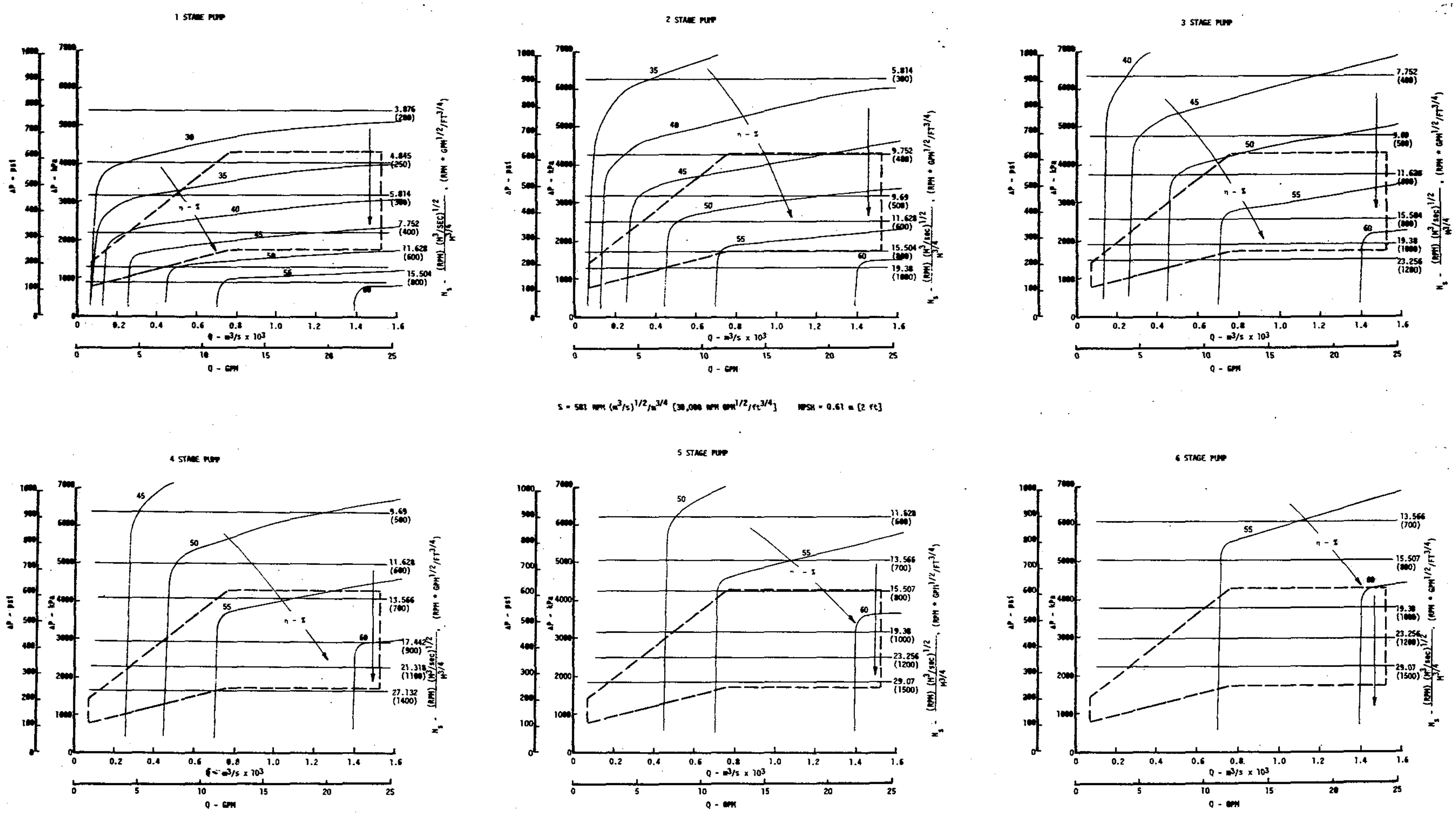

Figure 16. Specific Speed and Efficiency Loci in Pressure/Flow Map for LO_2

e. Realistic Results

The results for centrifugal pumps presented in the previous section were achieved without consideration of fabricational constraints. The results presented in this section were obtained by considering the following two limits:

(1) Blade height - 0.762 mm (0.030 in.)
(2) Tip diameter - 17.8 mm (0.700 in.)

The areas where blade heights and impeller diameters exceed these arbitrary limits are shown in Figures 17a through 17c. The results clearly indicate that conventional centrifugal pumps designed with state-of-the-art efficiencies and state-of-the-art fabrication techniques are feasible over the higher flow but not over the lower third of the range as indicated in Figure 1. Constraints due to blade height fabrication limitations make the low-flow, high-pressure regime of the map an area where centrifugal pump performance improved and/or better manufacturing techniques must be developed. Due to the use of multiple staging, pressure limitations are not encountered. The degree of required staging is as follows: 2 to 6 stages for LH_2; 2 to 4 stages for LCH_4; and 1 to 3 stages for LO_2. This relatively high degree of staging will result in complex designs and resultant problems with bearings, critical speeds, alignment, etc., which will have to be addressed in greater depth.

f. Conclusions and Recommendations

The analysis of centrifugal pumps indicates that conventional pumps will function throughout the operating maps specified in Figure 1. The limiting factors are identified as efficiency degradation due to the pumps' small size effect and the fabrication limits imposed by impeller blade height. Improvements may be achieved through applied research addressing the following areas:

(1) Reduction of impeller leakage flow.

(2) Reduction of bearing and seal losses.

(3) Reduction of blade height fabrication limits.

(4) Investigation of new configurations such as impellers designed for smaller blade height but actually built for large achievable blade heights, and/or impellers designed for partial emission through increased vane thickness at discharge and corresponding increase of required blade heights.

17a.

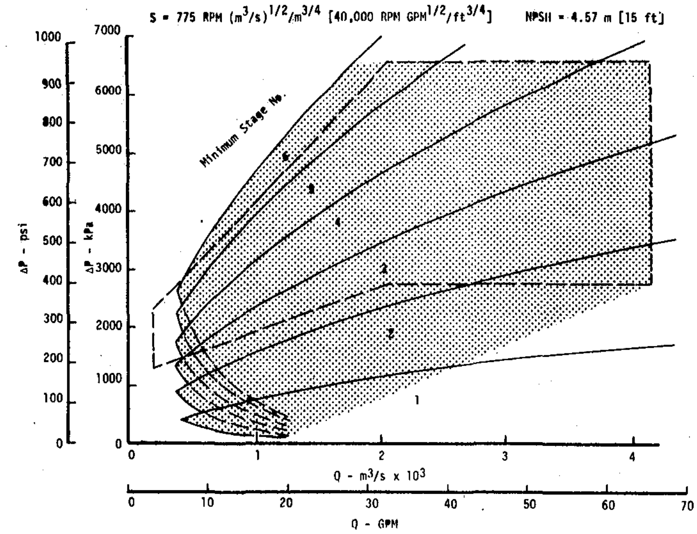

17b.

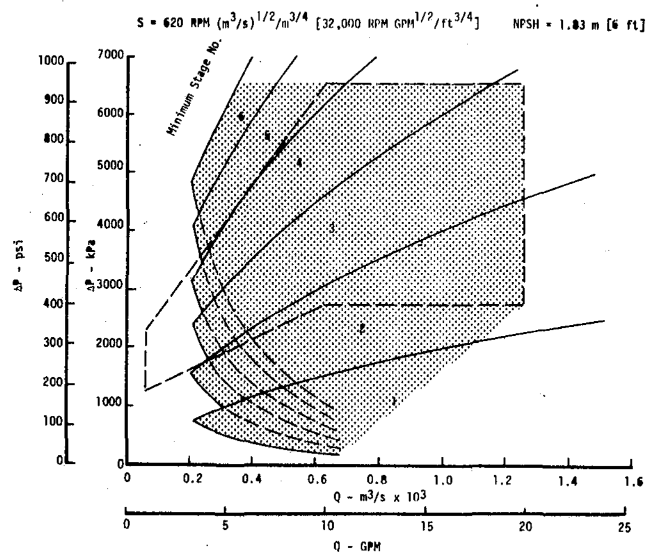

17c.

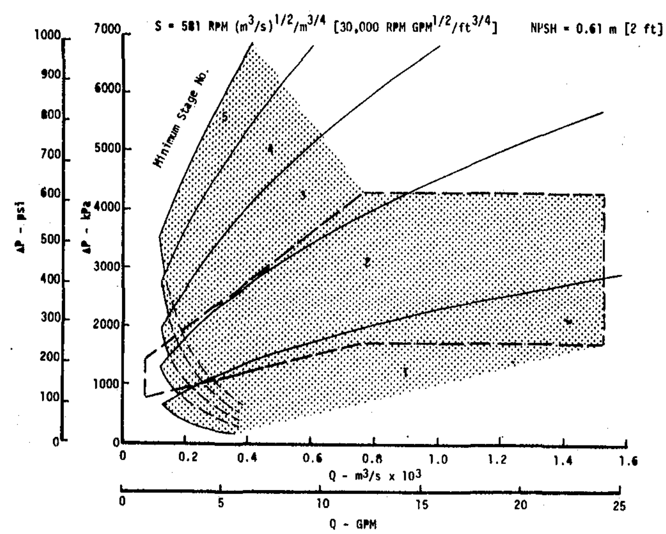

Figure 17. Operating Regime of Centrifugal Pumps

g. Summary of Centrifugal Pumps Evaluation

(1) Pressure/Flow Map

Centrifugal pumps can be designed using state-of-the-art techniques throughout the pressure/flow regime of interest except in the high-pressure, low-flow section of the map. In this area, blade height limitations present a problem. However, this area of concern is outside the operating envelope specified for this study.

(2) Efficiency

With the use of multiple staging, efficiencies of around 40 to 50% can be achieved for conventionally designed centrifugal pumps.

(3) Cavitation

Centrifugal pumps utilizing integral inducers can meet the minimum NPSH values specified for this study. Since the study did not take into account the effects of thermodynamic suppression head, the derived results may be considered conservative. This is especially true for liquid hydrogen where thermodynamic suppression heads of up to eight times the given 4.57 m (15 ft) NPSH are available.

(4) Life

The life-limiting elements in centrifugal pumps are bearings and seals. In view of the high speeds required for the pumps under consideration, bearing DN values and bearing stiffness become a major concern. Data concerning DN values applicable to 20-mm or smaller bearings are not available. Scaling from data obtained with larger bearing sizes is not directly applicable since the number of balls decreases with smaller shafts and since geometrical similarity is not maintained.

As with larger size centrifugal pumps, the interpropellant seal remains a problem. Rubbing contact seals are not desirable because of the high seal velocities. Purge systems are not applicable because they are too heavy and too complex for the long-life requirement and desired restart capability.

The solution to bearing and seal difficulties (and thus the life problem) is to utilize hydrostatic bearings with integrated seals.

(5) Weight

Due to the small size of the centrifugal pumps, a relatively low weight can be achieved.

(6) Size

Due to the high speed at which centrifugal pumps can operate, relatively small sizes can be achieved. However, the very smallness of the pumps creates a concern in terms of efficiency and fabrication techniques.

(7) Reliability

Though centrifugal pumps are made up of geometrically complex components with a high degree of accuracy, as a pumping system they represent a concept of low complexity and high reliability.

(8) Head Versus Capacity Characteristics

Centrifugal pumps have the desired negative slope head versus capacity relationship. The pumps under consideration all have small specific speed values. This results in a tendency toward flat heat versus capacity characteristics.

(9) Cost

Relative costs for high-speed centrifugal pumps are high due to very tight fabrication tolerances, surface finishes, and sophisticated design and development efforts.

(10) Drive System Requirement

Due to their high speed, centrifugal pumps lend themselves to direct drive turbine drives. For low-power pumps (less than 1 HP), cryogenically cooled electric motors are also feasible.

(11) Start Transient Characteristics

Centrifugal pumps lend themselves to through-flow type chill-downs. Due to their small size, their rotor inertia is low, and thus very high acceleration rates can be achieved.

(12) Confidence in Meeting Life Requirements

Centrifugal pumps have a high confidence level rating for meeting life requirements as they have only a small number of wear- and fatigue-sensitive life-limiting parts.

(13) Confidence in Meeting Predicted Performance

A large portion of the work done with high-pressure cryogenic propellants has been with centrifugal pumps. This extensive data base gives then a high confidence level rating for meeting predicted performance.

(14) Maintainability

Maintainability for centrifugal pumps is about average and comparable to that for other pump types.

2. Drag Pump

a. Description

The drag pump concept, shown on Figure 18, is often referred to as a turbine pump, regenerative pump, viscous pump, or friction pump. It is a single rotating disk, with radial vanes machined into each side from approximately 60 to 100% of the outside disk diameter. As the fluid passes through the open channel from suction to discharge, it repeatedly circulates through these vanes. This produces the fluid path (shown schematically in Figure 19). The process creates a circumferential pressure gradient from the suction to the discharge ports. The trapped fluid in the vanes is returned to the pump suction, representing about 40 to 60% of the delivered flow. Because a trapped cryogenic fluid tends to boil when the pressure is released, drag pumps may not be suited for this application.

b. Literature Review

Most texts on dynamic pumps contain general information on drag pumps. However, there is little specific data on cavitation limits, pressure loading on the impeller, or separation of mechanical and hydraulic efficiencies. Reference 99 presents an analytical treatment of a drag pump, and Reference 100 lists correlated test data on different configurations with a hydrodynamic model. However, neither of these references addresses the cavitation capabilities or limits.

Drag pumps have a flow range to 6.3×10^{-3} m^3/s (100 GPM), a pressure range to 6895 kPa (1000 psi), a specific speed range

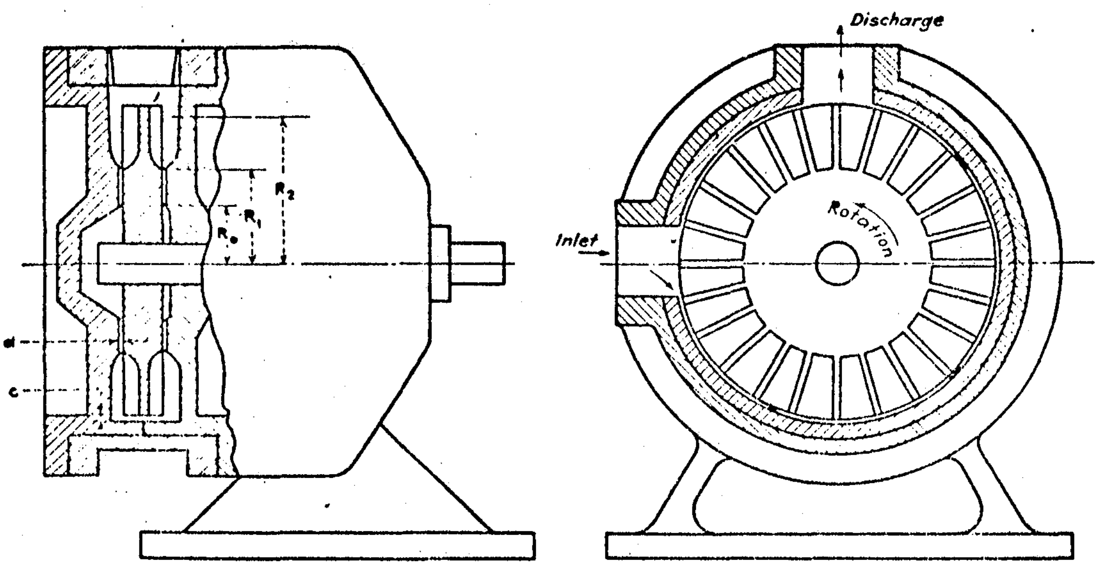

Figure 18. Drag Pump - Typical Cross Section

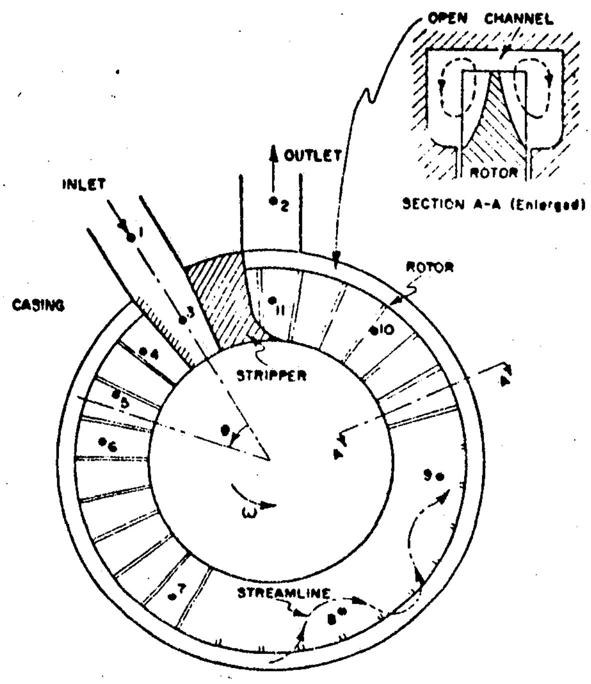

SCHEMATIC DRAWING OF REGENERATIVE PUMP
(Numbers indicate pressure taps.)

Figure 19. Drag Pump - Schematic

from

$$0.78 \text{ to } 11.6 \frac{(\text{RPM})(\text{m}^3/\text{s})^{1/2}}{\text{m}^{3/4}} \quad \left(40 \text{ to } 600 \frac{(\text{RPM})(\text{GPM})^{1/2}}{\text{ft}^{3/4}}\right),$$

and a very steep, negative head versus capacity slope. Applications for this pump include small boiler feed, chemical processes, spraying systems, car washes, etc.

The efficiency of a well-designed drag pump appears not to exceed 50%, with most falling in the 35 to 45% range.

No data or designs of drag pumps for use with cryogenic propellants were found in the literature surveyed.

c. Conclusions

The literature search did not yield any cavitation data on drag pumps. However, because the carry-over volume (from discharge pressure to suction pressure) is very high (approximately 40 to 60% of the delivered flow), the cavitation characteristics are predicted to be very poor with use of cryogenic fluids. In cryogenics, boiling liquid will be returned to suction by carry-over. This boiling at the inlet is unpredictable and can only be determined through testing.

Because cavitation affects the thermodynamic considerations presented in the gear and vane pump sections, it would appear that the drag pump concept is not suitable with LH_2 or LCH_4 and could only be used for lowest specified permissible pressure in LO_2.

3. <u>Pitot Pump</u>

a. Description

The Pitot pump obtains its name from a Pitot tube, or total pressure probe, located in the flow stream to measure both static and dynamic velocity head. In a Pitot pump, there is flow in the probe which reduces the head resulting from pipe friction loss, entrance loss, and diffusion. Most existing pump applications have a rotating drum containing the pumped fluid and a stationary probe. In theory, the probe could be rotated through the fluid. The former has one major advantage, however, and that is a low-pressure dynamic seal.

Figure 20 shows a design where the incoming fluid flows radially in passages in the drum sides. This assures that the fluid is rotating at the same velocity as the drum when it enters the cavity containing the probe. The flow rotating with the cavity then enters the probe, giving up its velocity head in diffusion to low velocity. From the probe head, the flow travels down the strut and out the drum at the center. This allows the dynamic seal to be placed at a small diameter in a low-pressure zone.

b. Literature Review

References 7 and 39 present the major design parameters for the Pitot pump. There is some discrepancy between these two references on the concept's head coefficient. Reference 7 shows a head coefficient between 0.4 and 0.5, while Reference 39 gives values as high as 0.8. The difference is apparently due to the design of the fluid entrance into the rotating drum. The application history includes high-pressure/high-temperature cleaning systems, boiler feed water and desuperheating, hydro-blast cleaning, water injection, and electrical-chemical machining. Usage life should be high because no close clearances or small tolerances need to be maintained.

Per Reference 39, one advantage of a Pitot pump is that it is seizure-proof. This type of pump can be run dry and/or operated against a closed discharge valve. In addition, the reliability will be high due to the simplicity of the design which requires no close fitting parts other than the shaft, seal, and bearing assembly. There has been no reported use in cryogenic fluids. This would not appear to present any problems, except possibly for cavitation due to heating the rotating fluid which is caused by viscous friction of the stationary probe and strut.

c. Conclusions

The cavitation limit for the Pitot pump was set at

$$145 \frac{(\text{RPM})(\text{m}^3/\text{s})^{1/2}}{\text{m}^{3/4}} \quad \left(7500 \frac{(\text{RPM})(\text{GPM})^{1/2}}{\text{ft}^{3/4}}\right)$$

and was taken from Reference 39. With use of cyrogenic fluids, this value may not be realized if the viscous heating within the drum causes the fluid to seek a temperature significantly higher than the fluid inlet temperature from the tank. With a limiting suction specific speed of

$$145 \frac{(\text{RPM})(\text{m}^3/\text{s})^{1/2}}{\text{m}^{3/4}} \quad \left(7500 \frac{(\text{RPM})(\text{GPM})^{1/2}}{\text{ft}^{3/4}}\right)$$

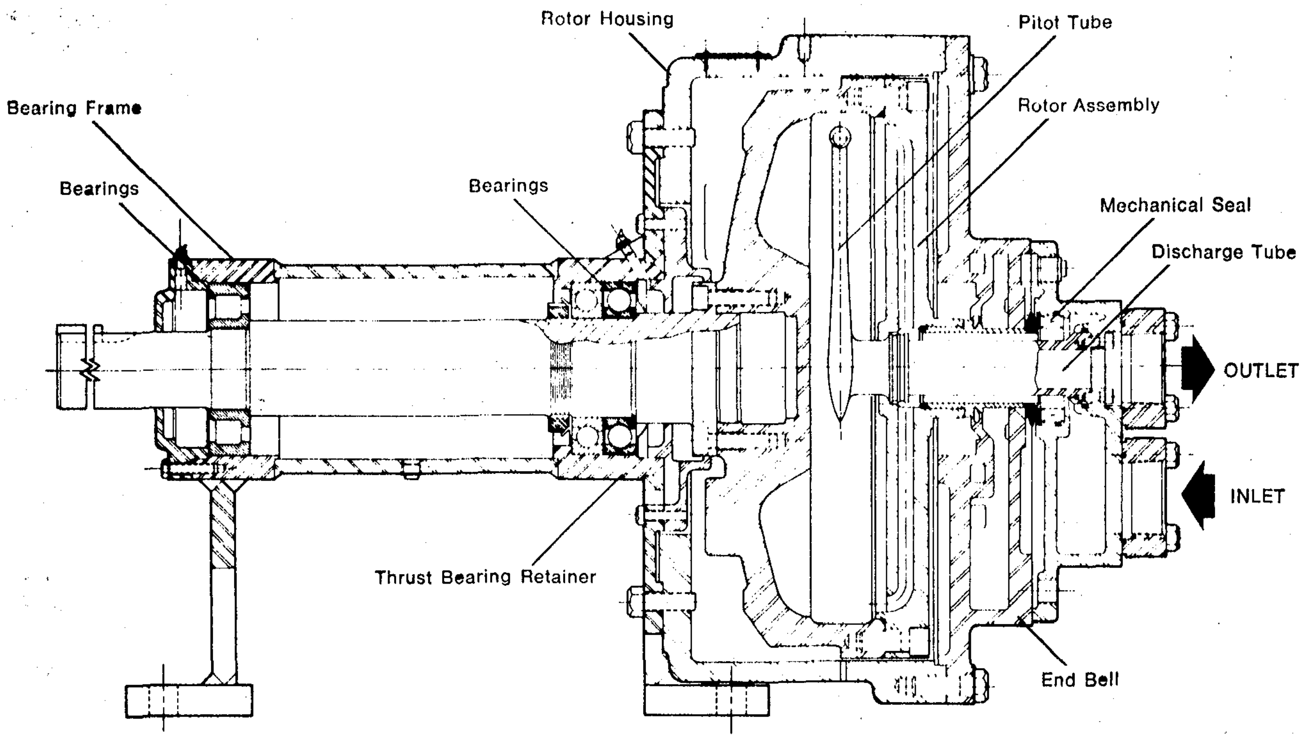

Figure 20. Pitot Pump - Rotating Housing

it appears that Pitot pumps with efficiencies less than 30% would be able to operate in LH_2. For LCH_4, Pitot pumps with only 30% efficiencies could meet the specified low pressure points of the map. Likewise, for LO_2, pumps with only 30% efficiency would meet the specified low pressure values, and a 40% efficient pump could be designed to meet the lowest specified flow and pressure rise points. The Pitot pump speeds were calculated to range from approximately 2,000 to 24,000 RPM. The specific speed range for efficiencies between 20 and 55% is

$$1.36 \text{ to } 5.8 \frac{(\mathrm{RPM})(\mathrm{m}^3/\mathrm{s})^{1/2}}{\mathrm{m}^{3/4}} \quad \left(70 \text{ to } 300 \frac{(\mathrm{RPM})(\mathrm{GPM})^{1/2}}{\mathrm{ft}^{3/4}}\right),$$

but the high efficiencies cannot be achieved for the cryogenic fluids and desired operating points specified for this study.

Prediction of performance has many variables. For example, References 7 and 39 show a wide variation in both obtainable head coefficient and efficiency. Without further testing, the performance of this pump cannot be predicted with confidence.

4. Tesla Pump

a. Description

The Tesla pump is similar in speed and construction to conventional centrifugal pumps. The main difference between the two is the impeller design. The impeller of the Tesla pump consists of a series of closely spaced disks rotating at a common speed. These disks generate flowrate and pressure by a shearing action of the disks on the fluid. Ideally, the gaps between the disks would be clear, but in practice the disks are part of a rotor that must transmit torque, maintain alignment, etc. Therefore, axial clamping pins or a device to structurally attach the disks is required. A schematic of the Tesla type pump with the pump impeller, support bearings, wear ring seals, seal package, and housing is shown in Figure 21. The flow to the impeller enters through the inside diameter of the parallel flow disk spaces and discharges at high pressure at the outside diameter. Wear ring seals of some form to limit return leakage to the low-pressure zones are required at each end of the impeller. The wear ring radii may be selected to balance axial thrust in a manner similar to centrifugal shrouded impellers. As shown in the schematic, the disk-type impeller may be supported overhung or straddle-mounted by the bearings.

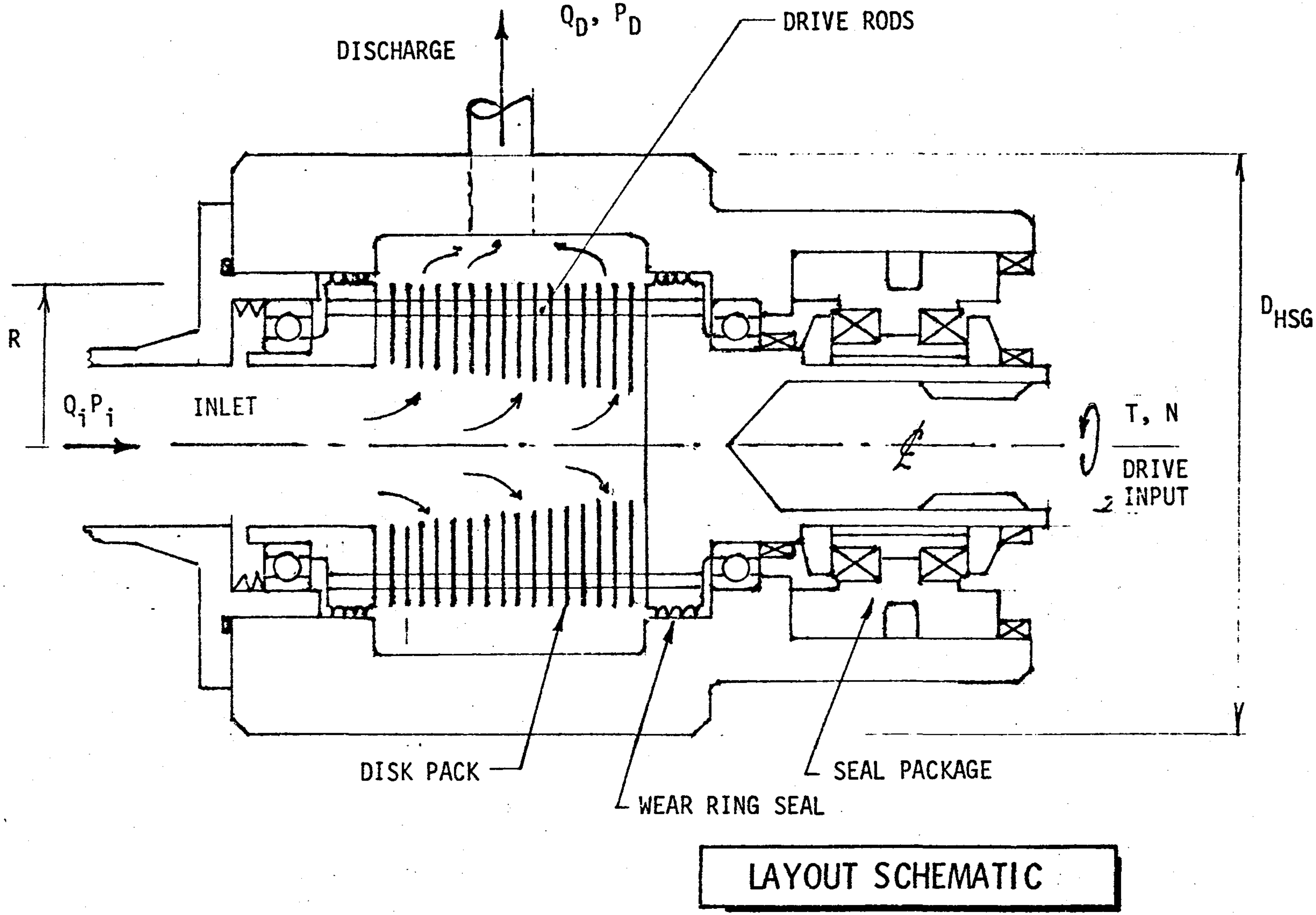

Figure 21. Tesla Pump - Schematic

b. Literature Review

Information on the Tesla (disk-type) pump can be found in References 7, 8, 26, 27, 35, 41, 61, and 62. A review of the literature has shown that while this type of pump was invented early in this century, there has been little demonstrated development or interest in it until lately. Suction performance seems to be its main feature. It would most likely make a good inducer pump. References 7 and 8 deal with a liquid fluorine pump for rocket application, but with analytically demonstrated low efficiency, not including mechanical losses. Reference 26 presents an analytical approach and design data for disk pumps having very low Reynolds numbers. Reference 27 discusses disk pump applications. Reference 35 presents a laboratory approach along with analysis and test data for a single unobstructed disk set but with turbulent flow and some stall observed at very low flows. Reference 41 describes and presents the results of analytical and experimental work for a rocket propulsion disk pump involving an investigation of disk roughness head versus capacity efficiency. References 61 and 62 both describe analytical treatment of disk pumps.

c. Conclusions

This pump offers no significant advantages (other than better suction performance) over centrifugal pumps and has much lower efficiencies (Ref. 41). The questionable structural integrity and reliability of the disk pack would also present an area of concern. Therefore, this pump concept was eliminated as a candidate for this study application.

5. Axial Flow Pump

a. Description

Axial flow pumps utilize radial vanes on a hub to impart rotation to a fluid so that it is flowing over the hub in parallel to the axis of rotation. Tangential motion is arrested by a set of stator vanes to develop a static pressure rise for a moderate specific speed range from

$$77.5 \text{ to } 155 \ \frac{(\mathrm{RPM})(\mathrm{m}^3/\mathrm{s})^{1/2}}{\mathrm{m}^{3/4}} \quad \left(4000 \text{ to } 8000 \ \frac{(\mathrm{RPM})(\mathrm{GPM})^{1/2}}{\mathrm{ft}^{3/4}}\right).$$

For specific speeds above the high end of the range, the static pressure rise is probably not a design requirement and thus no stator would have to be used. In practice, even the name axial pump is changed to propeller pump at specific speeds in excess of

$$194 \frac{(RPM)(m^3/s)^{1/2}}{m^{3/4}} \quad \left(10{,}000 \frac{(RPM)(GPM)^{1/2}}{ft^{3/4}}\right).$$

Figure 22 shows a typical axial pump.

b. Literature Review

Typical rocket engine axial flow pump data are shown in Reference 72. Typical commercial axial flow pumps are noted by Stepanoff (Ref. 22). The stage specific speeds for the rocket applications range from

$$64.5 \text{ to } 83 \frac{(RPM)(m^3/s)^{1/2}}{m^{3/4}} \quad \left(3329 \text{ to } 4284 \frac{(RPM)(GPM)^{1/2}}{ft^{3/4}}\right)$$

when used as multistaged machines and yield efficiencies in the 70% range.

c. Conclusions

The axial flow pump is best-suited for use in high specific speed applications and is not practical as a candidate for this study application. If they were used for the

$$2.5 \text{ to } 15.5 \frac{(RPM)(m^3/s)^{1/2}}{m^{3/4}} \quad \left(130 \text{ to } 800 \frac{(RPM)(GPM)^{1/2}}{ft^{3/4}}\right)$$

range of overall specific speeds of the study, it would take from 6 to 62 stages to satisfy the head-generating requirements. Axial flow pumps will only be practical for the very low-flow/low-pressure range of the study where 6 to 12 stages might meet the head requirements.

6. <u>Jet Pump</u>

a. Description

Jet pumps use flow energy with or without an expenditure of internal energy of one fluid stream to increase the pressure level of a second fluid stream. The fluid streams may be a gas driving a gas, a liquid driving a liquid, a gas driving a liquid, or a liquid driving a gas. The pump, shown in Figure 23, basically consists of a nozzle for the driving

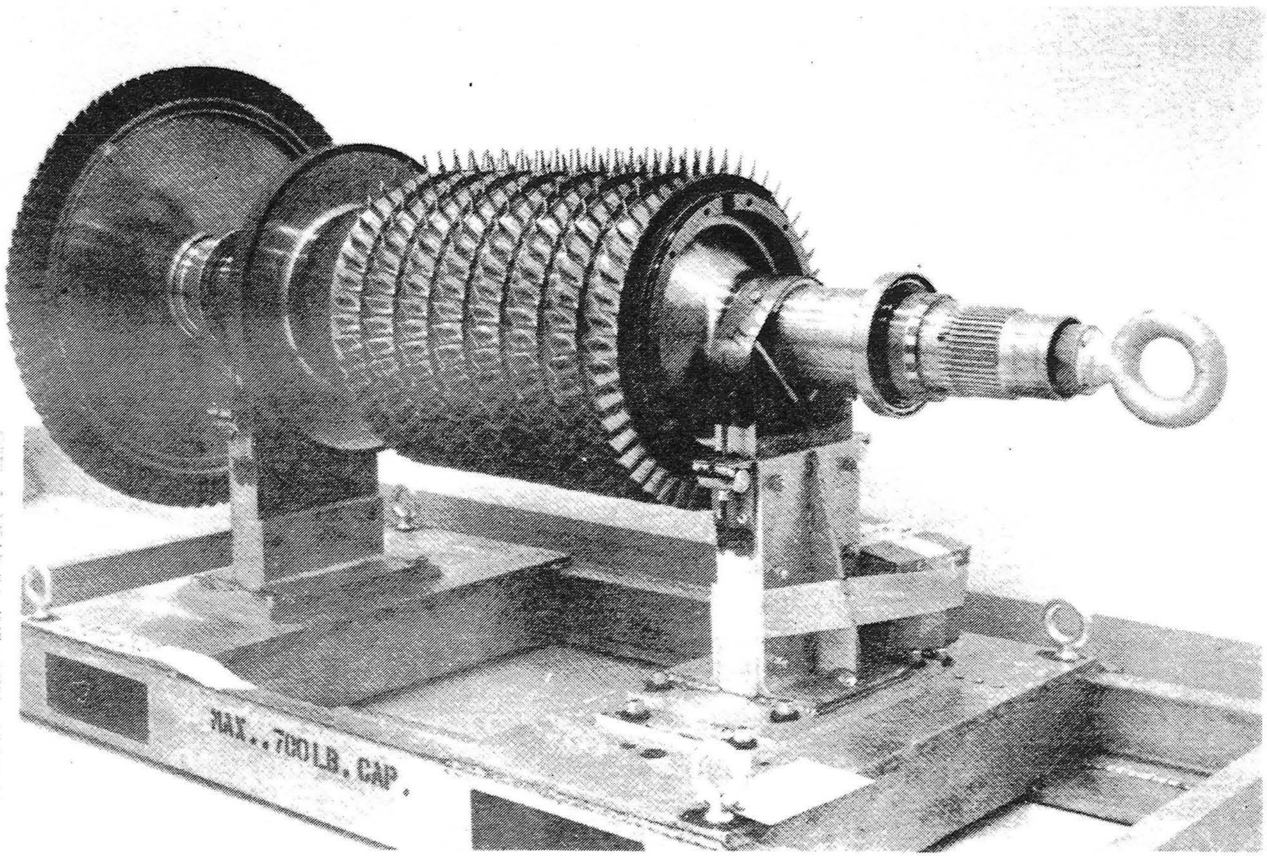

Figure 22. M-1 Axial-Flow LH_2 Pump

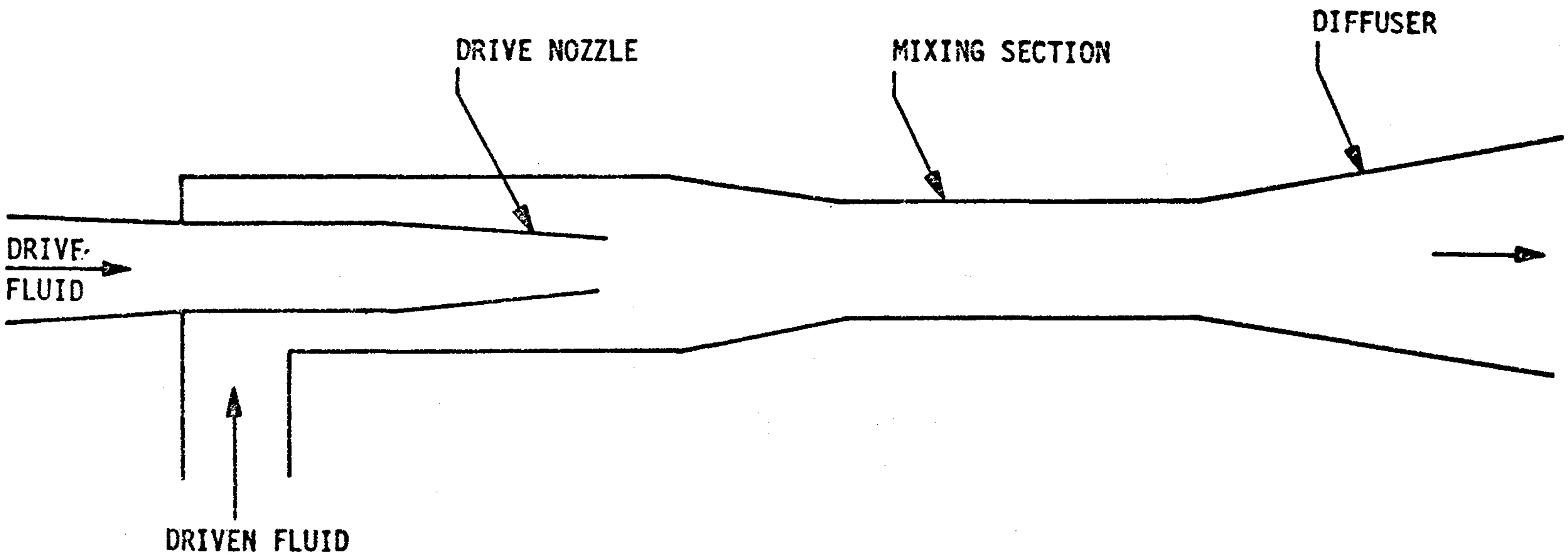

Figure 23. Jet Pump - Schematic

fluid centered in an antechamber containing the fluid to be pumped. The driving fluid, which is ejected from the nozzle at a relatively high velocity compared to the driven fluid, transmits some of its momentum to the driven fluid through viscous shear. The two streams mix in a typically constant area section, bringing the two streams to a common velocity greater than the entering driven stream. The mixing section is followed by a diffusing section which recovers some of the kinetic energy to static pressure. The pump has no moving parts but does require some means of pressurizing or energizing the driving fluid.

b. Literature Review

Although jet pumps are common and have been in use for a century, they have not been used in a flight rocket engine. The most common jet pump has been the water jet, used to boost well water from 9.1-m (30-ft) depths or more to the suction of a centrifugal pump. Discharge pressure from the centrifugal pump provides the pressure source for the driving jet stream placed at the bottom of the well.

Gosline and O'Brien analytically and experimentally investigated water driving water jet pumps at the University of California (Ref. 86). They developed the theory of momentum exchange between fluids through the use of a driven to driving flow ratio and a discharge head to driving head ratio.

Flugel (Ref. 87) made an investigation of a gas driving a liquid jet pump system. In theoretically defining the thermodynamic relationships for fluid conditions that traverse the liquid-gas phase, Flugel, by way of photography, also demonstrated the mixing vortices between the driven and driving fluid interface.

Cunningham (Ref. 85) addressed liquid-liquid jet pumps from the standpoint of understanding the effect of fluid viscosities on performance. The experimental work corroborated the best efficiency range estimates of previous investigators.

Staging of jet pumps has been suggested as one way of reducing the inherent turbulence losses in jet pumps and the cavitation effects of high jet velocities. Sidhom and Hansen investigated the possibility theoretically and compared the results with M. Hoshi's experimental data for two-staged pumps (Ref. 88). Resulting efficiencies for these were lower than for single-stage pumps.

Sangers (Ref. 89, 90, and 91) investigated jet pump performance from a cavitation standpoint. It was proposed that the jet pump head breakdown occurs when the driving fluid velocity head equals the fluid NPSH less the driven fluid friction losses. Sanger's tests with water jet pumps showed a sharp loss of head-generating capability at the onset of cavitation. This occurred when the driven fluid NPSH is no lower than 90% of the driving fluid velocity head. This severely limits the pressure-generating capability of a jet pump if the drive fluid has a low NPSH (such as those used in this study).

A previous study conducted at the University of Colorado (Ref. 92) relates gas-gas and liquid-liquid jet pump efficiencies. A correlation between driven-stream and driving-stream Mach number with efficiency was noted, in addition to the flow ratio-head ratio relations of the two streams. The authors noted that actual jet pump efficiencies were one half to three fourths of the theoretical values. No significant influence on efficiency was noted as the result of size, mixing section cross-sectional shape or convergence, use of supersonic flow conditions, or series pumps. A definite increase in efficiency was noted when the mixing section was increased up to a 7.5 diameter ratio, after which the efficiency remained constant.

An Aerojet-General Corporation Study (Ref. 93) investigated a gas driving a liquid jet pump. This study included design, fabrication, and testing. In addition to water, the fluids utilized were UDMH (unsymmetrical dimethylhydrazine) and N_2O_4 (nitrogen tetroxide). The system modeled was a rocket engine that utilized the heat energy from the pumped propellant coolant of the thrust chamber to raise the propellant enthalpy level. The testing with UDMH, N_2O_4, and water seemed to indicate that up to 3447 kPa (500 psi) chamber pressure could be achieved with UDMH, N_2H_4, kerosene, nitric acid, and ClF_3. The investigators also deduced that propellants such as OF_2, ClO_3F, and NH_3 could be included in the group if they were subcooled to their freezing points. These opinions were based on the assumption of having sufficient heat addition to the propellant to do the work, but made no claims for a chamber design that would yield the wall temperatures necessary to raise the enthalpy level through heat transfer. The same logic led the investigators to state that liquid oxygen and liquid fluorine could be pumped to 1379 kPa (200 psi) chamber pressure if the driven liquids were subcooled to within 258°K (5°F) of their respective freezing points. Propellants judged to be unsuitable for pumping were liquid hydrogen, liquid methane, nitrogen tetroxide, and NF_3.

c. Conclusions

Jet pumps, whether gas or liquid drive, have serious limitations for pumping cyrogenic rocket engine propellants. They require relatively large NPSH values, have a low pressure rise capability, and are inherently limited to low (less than 40%) efficiencies. In addition, like any other liquid drive pump, require a pressurizing source, or they must employ the unproven bootstrap start for the gas drive that uses thrust chamber coolant as an energy source.

The jet pump concept is incapable of meeting the study pressure rise requirements with the specified NPSH values for any of the propellants under consideration.

B. POSITIVE-DISPLACEMENT PUMPS

A pump in which the internal volume is decreasing with either reciprocating motion or rotating motion is classified as a positive-displacement pump. Two of the more frequently and widely used positive-displacement pumps are the vane and the gear pump. Their acceptance is due to their small size and their smooth, relatively high-speed operation while delivering high pressure at low flows and high efficiencies.

Fluid Carry-Over

All positive-displacement pumps have residual fluid, also called fluid carry-over, which is returned from the discharge pressure to the inlet pressure. Fluid carry-over represents a serious problem for cryogenic pumps insofar as it causes two-phase flow at the pump inlet which results in pump efficiency degradation. In order to avoid or minimize this negative effect, a design criterion has been defined which states that the vapor resulting from flashing of the fluid carry-over must be recondensed by the fluid entering the pump through the supply line.

A simple mass and heat balance was performed for each propellant to determine what inlet pressure would be required as a function of volumetric efficiency and discharge pressure to avoid vapor at the inlet. Figure 24 is a schematic of the pumping process which includes the internal leakage being returned to the pump inlet. This process is displayed on the enthalpy-entropy diagram showing the pump inlet flow ($\dot{W}_{in}$ at P_1) mixing at constant pressure with the pump leakage flow ($\dot{W}_L$), with the mixture enthalpy (h_m) being a saturated liquid. The mixture is pumped to discharge pressure (P_2), adiabatically, resulting in discharge enthalpy, (h_2). The return leakage ($\dot{W}_L$) is composed of the internal leakage and the entrained carry-over flow. The summation of these flows and the delivered flow determines the volumetric efficiency. To have zero head loss due to vapor in the pump inlet fluid, the mixture must be a liquid. Therefore, the required inlet pressure for each of the design points for all three fluids was selected on the basis of the calculated volumetric efficiency of the vane pumps and zero vapor volume present in the suction chamber. This analysis may be used for any positive-displacement pump with an equivalent volumetric efficiency.

The results of the analysis are shown in Figures 25, 26, and 27 for LH_2, LCH_4 and LO_2, respectively. For LH_2, this means that, at the given inlet conditions of 21°K (37.8°R) and 4.6m (15 ft) NPSH, there are no vane or gear pumps which can meet the pressure/flow points specified in Figure 1. For LH_2 for instance, it would take 206 kPa (30 psi) inlet pressure (approximately 304.6m (1000 ft) of NPSH) to prevent vapor at the inlet for point No. 5.

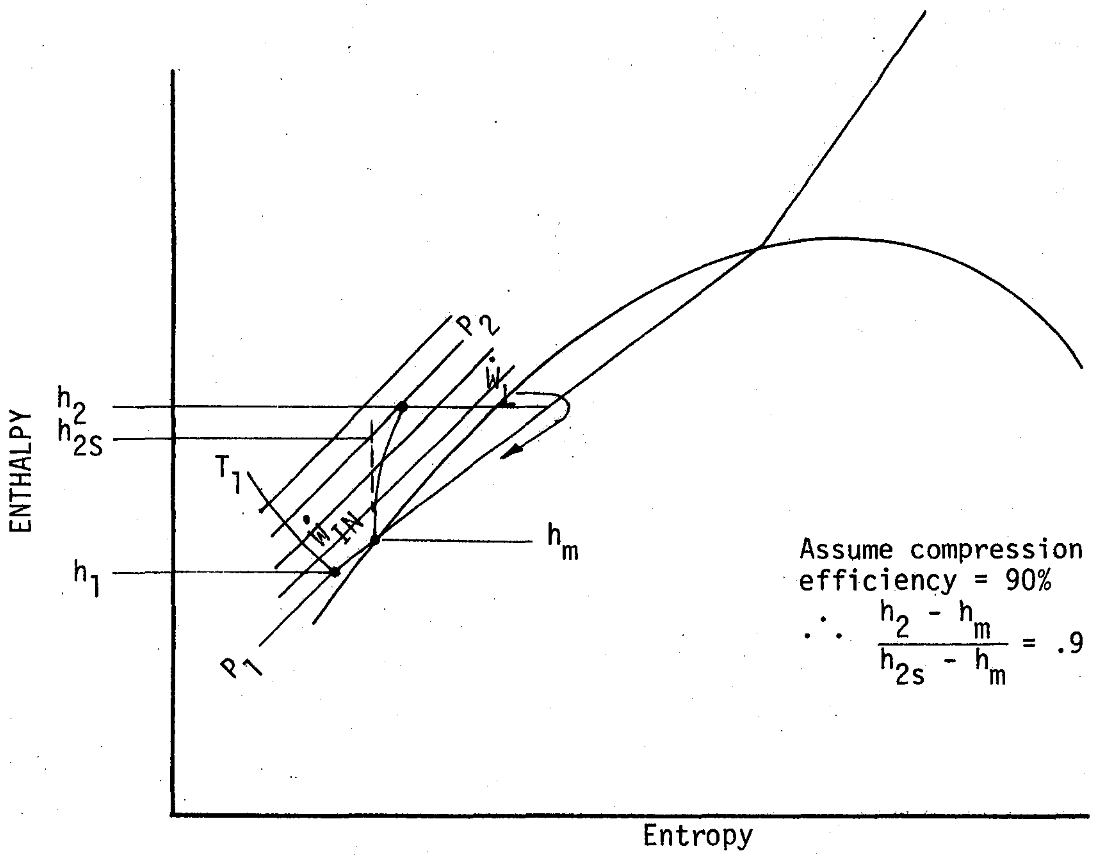

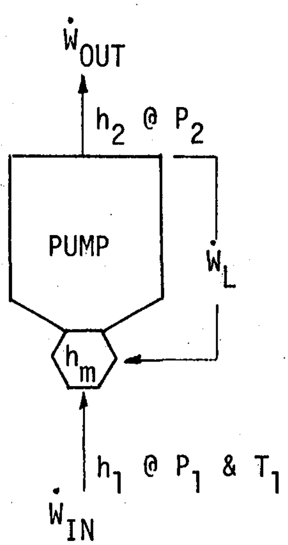

THERMODYNAMIC MODEL

$\dot{W}_{IN} = \dot{W}_{OUT}$

$\dot{W}_L$ = INTERNAL CARRY-OVER & LEAKAGE (P_2 to P_1)

① $$\eta_V \approx 1 - \frac{\dot{W}_L}{\dot{W}_{IN} + \dot{W}_L} \quad \text{(VOLUMETRIC EFFICIENCY)}$$

THEN: TO AVOID VAPOR AT THE PUMP SUCTION

② $$h_m > \frac{\dot{W}_{IN} h_1 + \dot{W}_L h_2}{\dot{W}_{IN} + \dot{W}_L}$$

WHERE: h_m = THE ENTHALPY OF THE SATURATED LIQUID AT P_1

COMBINING ① & ② $$h_m > h_1 \eta_V + h_2 - h_2 \eta_V$$

$$\eta_V > \frac{h_m - h_2}{h_1 - h_2}$$

Figure 24. Positive-Displacement Pump - Internal Leakage Flow Schematic and Enthalpy/Entropy Diagram

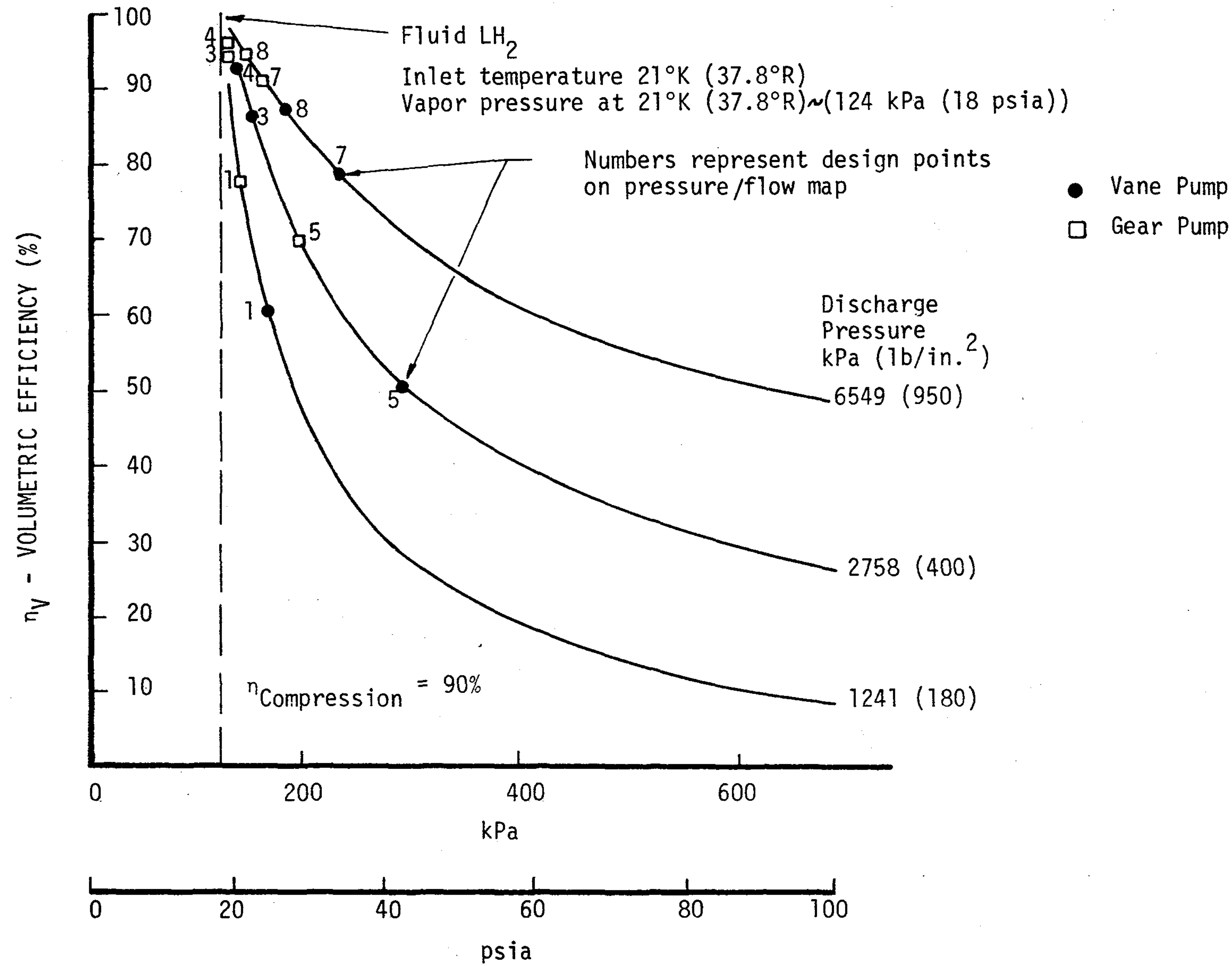

Stage Inlet Pressure Required to Avoid Vapor at Suction

Figure 25. Inlet Pressure to Avoid Vapor - LH_2

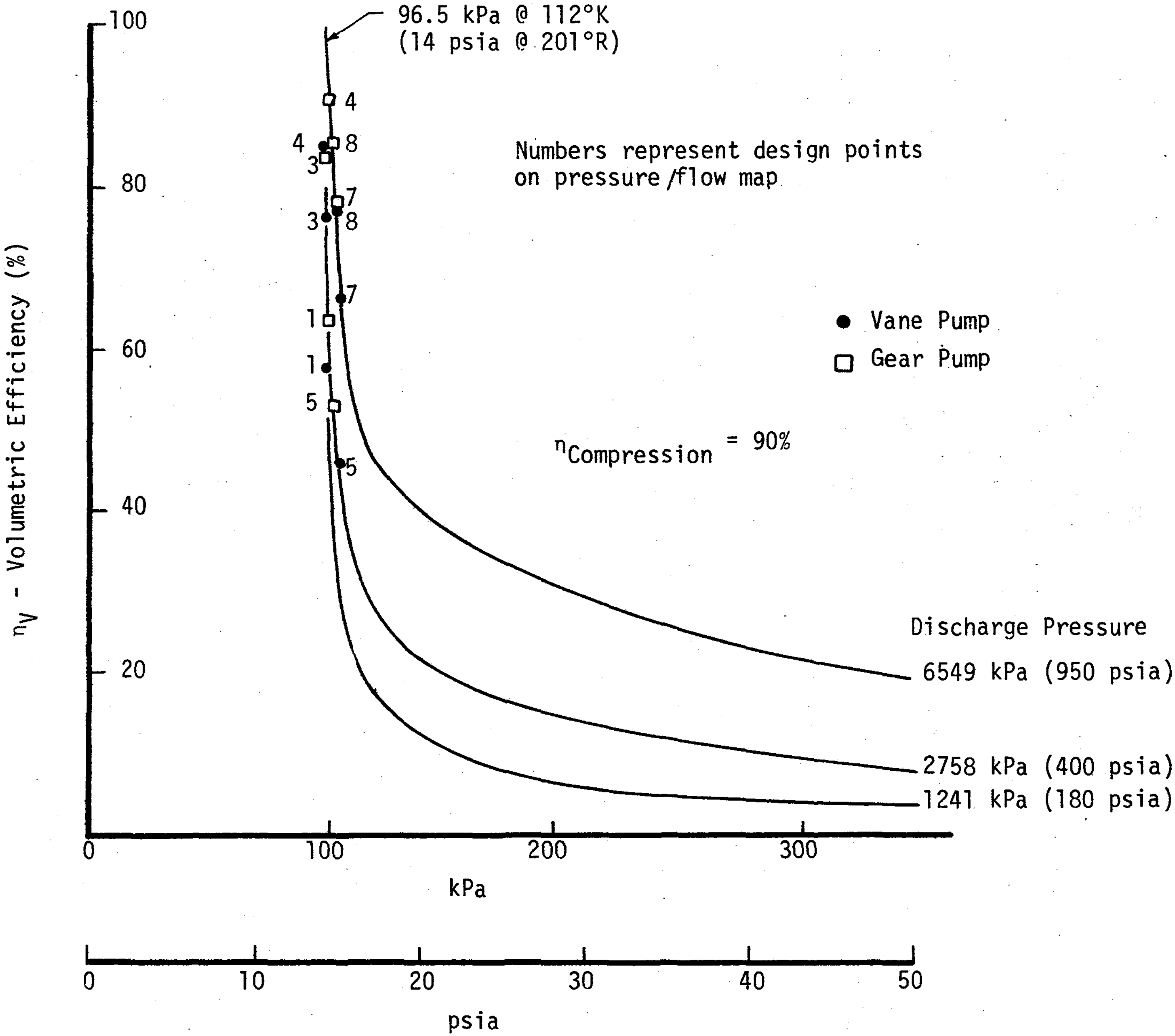

Stage Inlet Pressure Required to Avoid Vapor at Suction

Figure 26. Inlet Pressure to Avoid Vapor - LCH_4

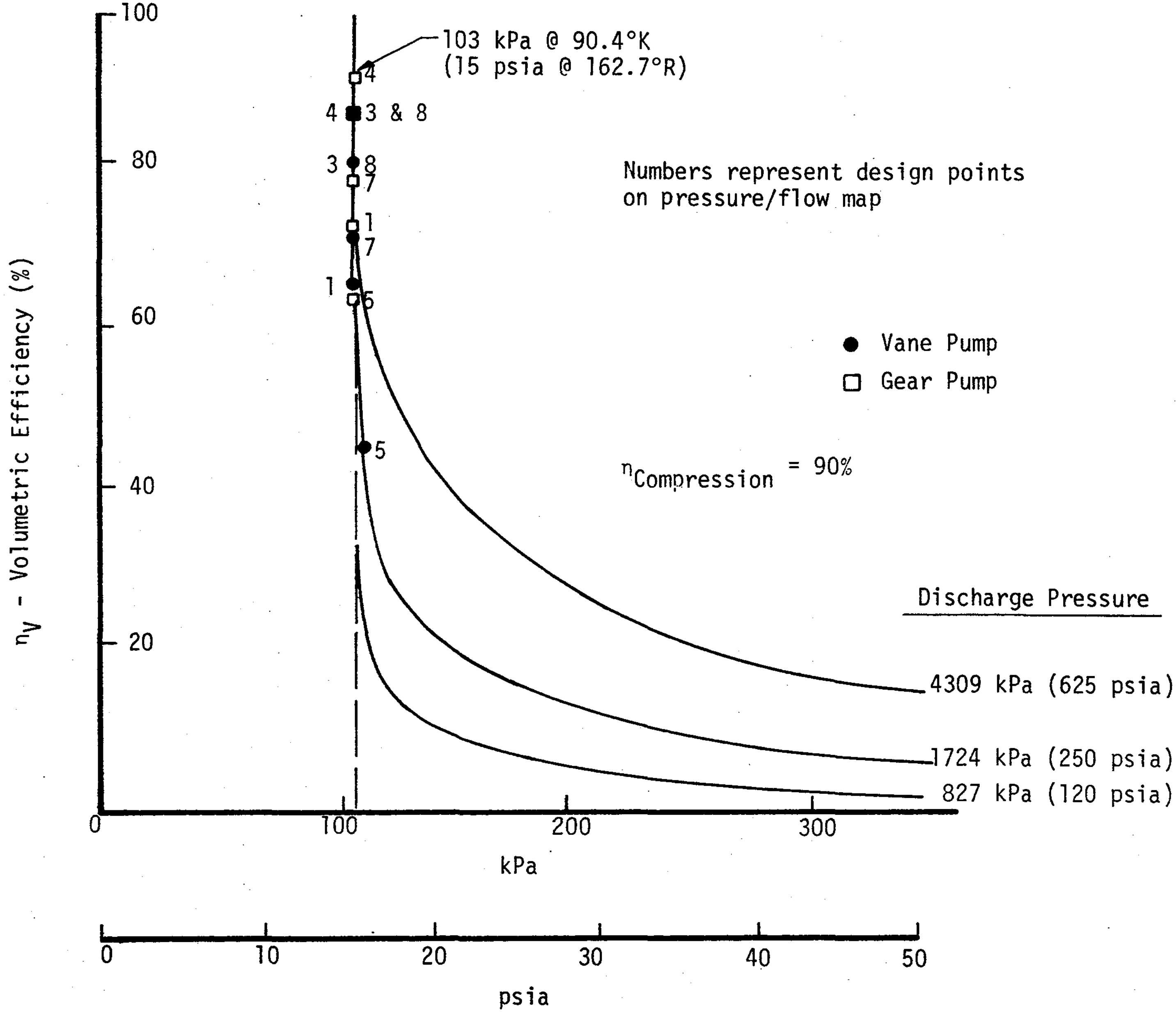

Stage Inlet Pressure Required to Avoid Vapor at Suction

Figure 27. Inlet Pressure to Avoid Vapor - LO_2

For LCH_4, it appears that, if a gear pump is used, only pressure/flow point No. 4 will have sufficient NPSH to prevent vapor in the inlet; all others will require additional inlet pressures. In LO_2, all pumps, with the possible exception of the vane pump at point No. 5, will meet all the pressure/flow points at the specified NPSH. The required suction pressure (head), which is in excess of that value given in Figure 1, would be supplied by a boost pump or an increase in tank pressure.

Vane and Gear Pumps

Each pump was evaluated on the basis of the following criteria: literature search and review, results of analysis performed, the pump's drive adaptability, and overall engineering judgment.

The majority of the vane pump data found in the literature review was taken from References 7, 8, 11, 37, 40, 46, 47, 48, 49, 51, 53, 57, 58, 59, and 109. For the gear pump, the information was taken from References 7, 8, 42, 66, 70, 72, 94, 95, and 96. Only References 7 and 8 considered pumps which were specifically designed for cryogenic use.

The parameters to be evaluated, and the results for both vane and gear pumps, are shown in Table VIII. The data from this table indicate that neither the vane nor the gear pump are particularly suited for this application. The major concern is their performance with cryogenics where wear and cavitation experience is very limited.

1. Vane Pump

a. Description

The positive-displacement vane pump employs reciprocating vanes sliding in slots over a rotating cylinder. The pumping action is created either by the rotor being eccentric or the bore of the housing being elliptical. The cavity between the vanes enlarges and closes during each cycle to allow ingestion of fluid at low pressure and to exhaust at the high-pressure side. Many variations of the basic vane concept are used in practice.

A very simple eccentric vane pump is shown in Figure 28. The sides, ends, and tips of the vanes provide the sealing of the high-pressure fluid. The vane sealing surfaces must also absorb the pressure and centrifugal loads. The vane tips can be an articulated design to conform to the housing and generate a fluid film to reduce friction and wear. This technique appears successful in fluids with reasonable viscosity, but may not be successful in such fluids as low-viscosity cryogenics. Eccentric designs have an unbalanced radial hydraulic load that must be supported by the bearings, while the elliptical

TABLE VIII. EVALUATION OF POSITIVE-DISPLACEMENT PUMPS

	Parameter	Vane	Gear
1.	Can pumps be designed to meet pressure/flow points on Figure 1.	Hydraulically yes, but with additional suction pressure (see cavitation).	Hydraulically yes, except at Pts 1 & 5 for LCH_4 where small size would not allow 10-mm bearings. Additional suction pressure required for most points.
2.	What is expected efficiency?	50 - 70%.	40 to 90%.
3.	What is expected cavitation performance?	Much lower than that of centrifugal pumps. See Figures 25, 26 and 27 for required suction pressure.	Same.
4.	Can pump operate for required life of 50 hours?	Cannot be met with current design practice.	Appears life may be met but will require special coatings on gear teeth.
5.	Weight of pump? (Excluding drive)	Lightest (after centrifugal pumps).	Heavier than vane pump because of two rotors.
6.	Size of pump?	If suction pressure can be supplied, then size is similar to that of centrifugal pump.	Somewhat larger than vane pump because of two rotors.
7.	Reliability?	Least reliable of pumps studied.	Industrial experience indicates high reliability if tooth wear can be controlled. No technical reason to expect low reliability.
8.	Head versus capacity?	Very steep head vs flow at constant speed. Pulsating pressure may not be acceptable to rocket engine system.	Same.

TABLE VIII (cont.)

	Parameter	Vane	Gear
9.	Cost?	Least expensive.	Low if standard or slightly modified gear cutting equipment is used. Cost incurred over conventional gear pumps due to special materials, tighter tolerances, and dry lubrication coatings.
10.	Will pump match with drives?	Best match is achieved with electric motors. Speed too low for direct drive turbines.	Same.
11.	What are start transient characteristics?	High starting torque. Must be bled-in and cooled to operating temperatures.	Transient speed limited by acceleration of fluid into the inlet. Must be bled-in.
12.	Confidence that pump can meet the operating life?	Low.	Low until cryogenic wear life data can be established for 100 to 500 hours of operation.
13.	Confidence that pump can meet the predicted performance?	Above average if the required suction pressure is supplied to preclude cavitation.	Same.
14.	Maintainability of pump?	Average.	Above average.

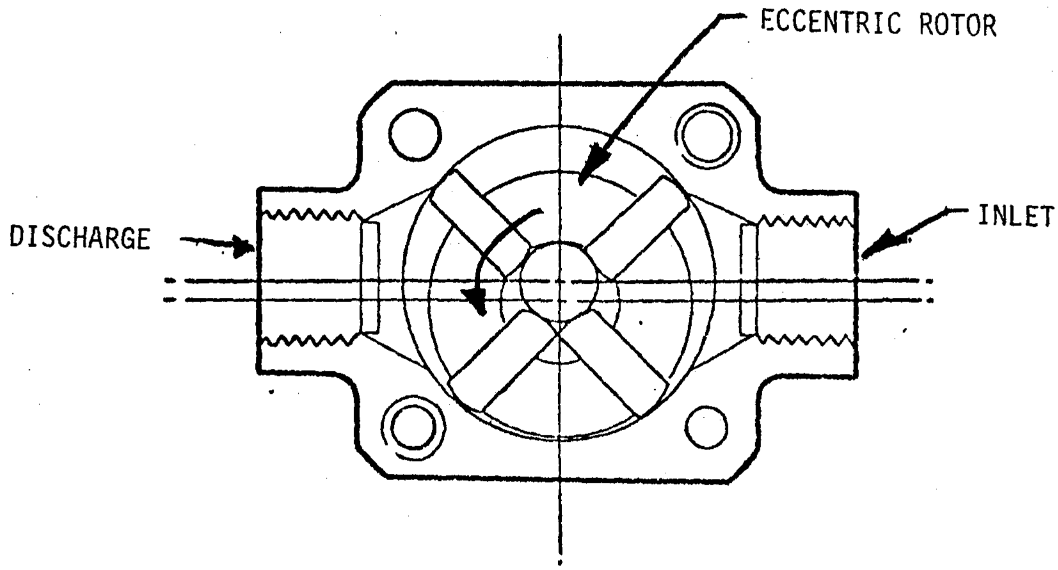

Figure 28. Positive-Displacement Vane Pump

design balances the hydraulic forces by having two intake and discharge cycles per revolution. Intake and exhaust ports may be either on the side plates or on the housing bore. The bore ports appear to have a better suction condition, especially with wide rotors, while the side ports are better from a vane rubbing aspect since the higher loaded bore surface is not interrupted. Suction performance is limited by the suction pressure and the peripheral velocity of the vane.

In order to minimize the carry-over volume of the vane pump, its vane slot depth and feed ports must be carefully determined. This portion of the vane pump design will affect the volumetric efficiency negatively as the carry-over volume increases. Feed port and undervane volume must be minimized in order to achieve high efficiency. But with small ports, the pressure developed in the undervane cavity will be high as the vane is compressed, which, in turn, loads the sliding vane tip. Excessive vane loading without lubrication will promote high friction drag, heat, and excessive wear. Wear also affects the undervane volume as the vane is shortened. This vane shortening results in a reduction of volumetric efficiency, in addition to excess vapor at the pump inlet.

A sliding vane type pump with an elliptical housing cross-section using two inlets and two outlets to balance forces is described in Reference 11. With split vanes, a volumetric efficiency of 98% was obtained. Two important design features of the vane pump are (1) the internal clearances which control the volumetric efficiency and (2) the rubbing force on the vane tip at the contact with the bore of the housing which influences pump life and frictional horsepower loss. It is not known, however, how this pump would perform for cryogenic propellants without lubrication of the tips. Careful design based on experimental data is necessary to obtain a mechanically reliable pump with reasonable life.

Reference 109 presents a detailed design for a liquid oxygen/liquid hydrogen boost and vane pump system for low-pressure/low-flow requirements. Apparently this design has not been tested as yet, but it should provide valuable data for cryogenic vane pump performance, especially with regard to efficiency, wear life, and reliability, at a future date.

b. Analysis

The analysis technique used for the vane pump characteristics was similar to that of Reference 7 with regard to modifications, additions, and corrections. Results of the analysis include discharge pressure and flowrates, internal leakages and volumetric efficiencies, shaft speed rotor size, housing size and weight, friction losses, overall efficiencies, rubbing speed, and loads of bearings, seals, and vanes. The parametric analysis was performed for vane pump designs at each of the eight pressure/flow points for each of the three fluids. (see Figure 1). Typical plots are shown in Figures 29, 30, and 31. Calculated efficiencies for LH_2 at the eight pressure/flow points are graphed as a function of gap (see Figure 29). The results of these curves show that the highest and lowest efficiencies, respectively, occur at design points No. 4 and 5. The gap effect on the other design parameters for pressure/flow point No. 5 in LH_2 is shown in Figure 30. Figure 31 shows the effect of L/D on the other design parameters, for design point No. 4 in LH_2. By using the data from plots of this type, a compromise design for each pressure/flow point was selected, the results of which are tabulated in Table IX.

c. Operating Life of Vane Pump

A cursory assessment of vane and liner wear rate was attempted to determine the order of magnitude of pump life. First, a "zero wear" stress criterion for sliding members was used on the LH_2 vane pump design. The results of this, given in Table X, show that the value of S_s does not approach the required maximum allowable value of 9245 kPa (1341 psi). Even if the coefficient of friction were to approach zero, the value of S_s would only be reduced by a factor of 2. Since the material does not meet the "zero wear" criterion, the amount of wear must be determined for the particular design point and pressure times velocity (PV) value.

An assessment of pump life can be based on two criteria: 1) when the wear equals the value as the clearance, or 2) when the wear equals a value which will cause the volumetric efficiency to decrease by 10%. The results of applying the first criterion are shown on Table XI. The life is extremely short, in the order of one second for a soft bore and a hard vane. The results of applying the second criterion are shown in Table XII. Again a very short operating life is predicted for typical material combinations.

Calculation of pump life by using an assumed material combination that would result in a 0.10 coefficient of friction appears adequate. However, obtaining a material combination that would result in a 0.10 coefficient of friction in the cryogenic fluids under consideration does not seem likely.

Another alternative is use of a pressure-balanced and lubricated vane (pivoted vane tip, etc.). A lubricated vane usually relies on a hydrodynamic fluid film, but in view of its low viscosity and low sliding velocity, hydrodynamic lubrication is not practical in this application. The possibility of using a hydrostatically lubricated vane tip still exists, but it has not yet been designed or tested.

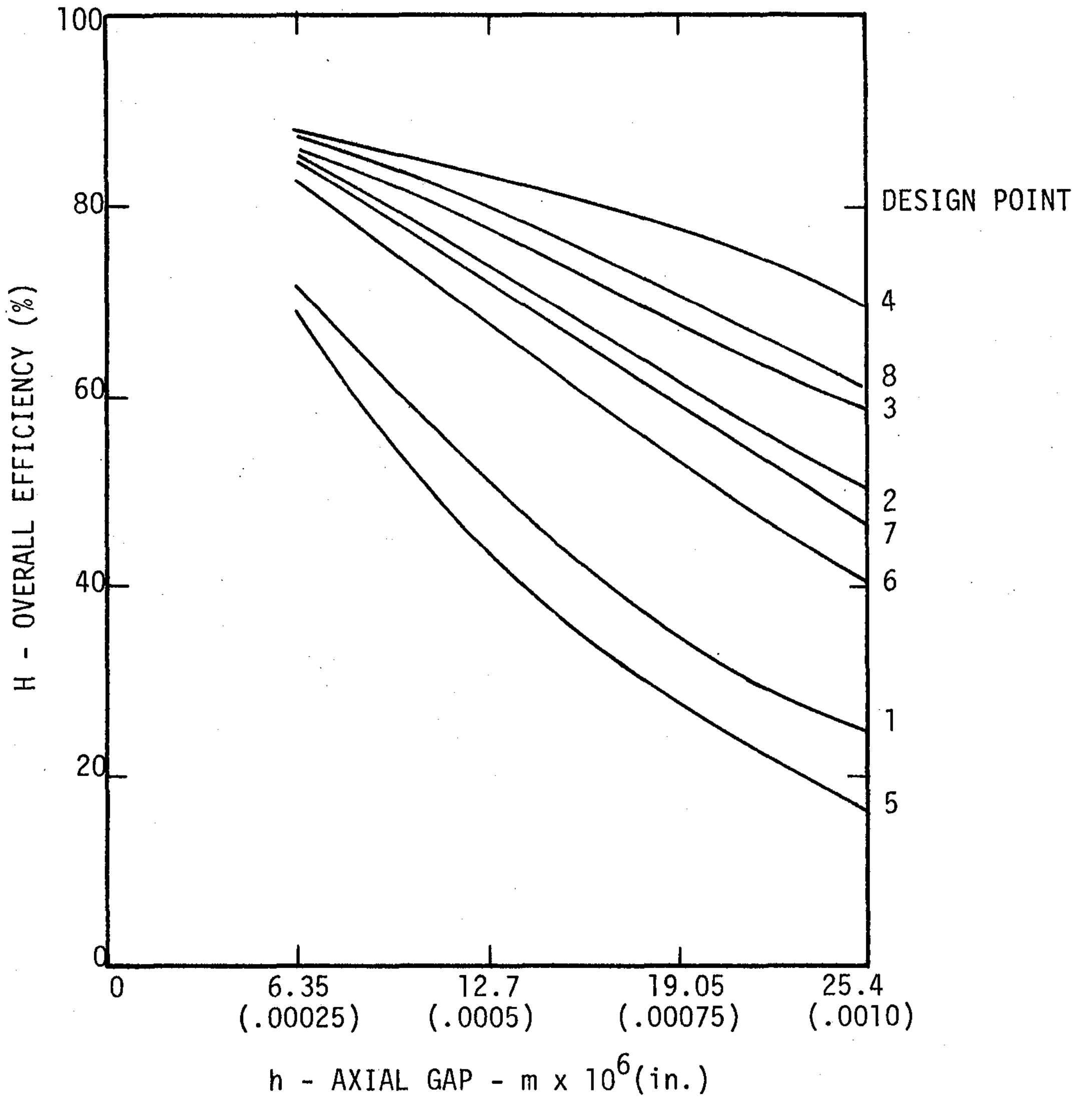

Figure 29. LH_2 Vane Pump - Efficiency versus Gap

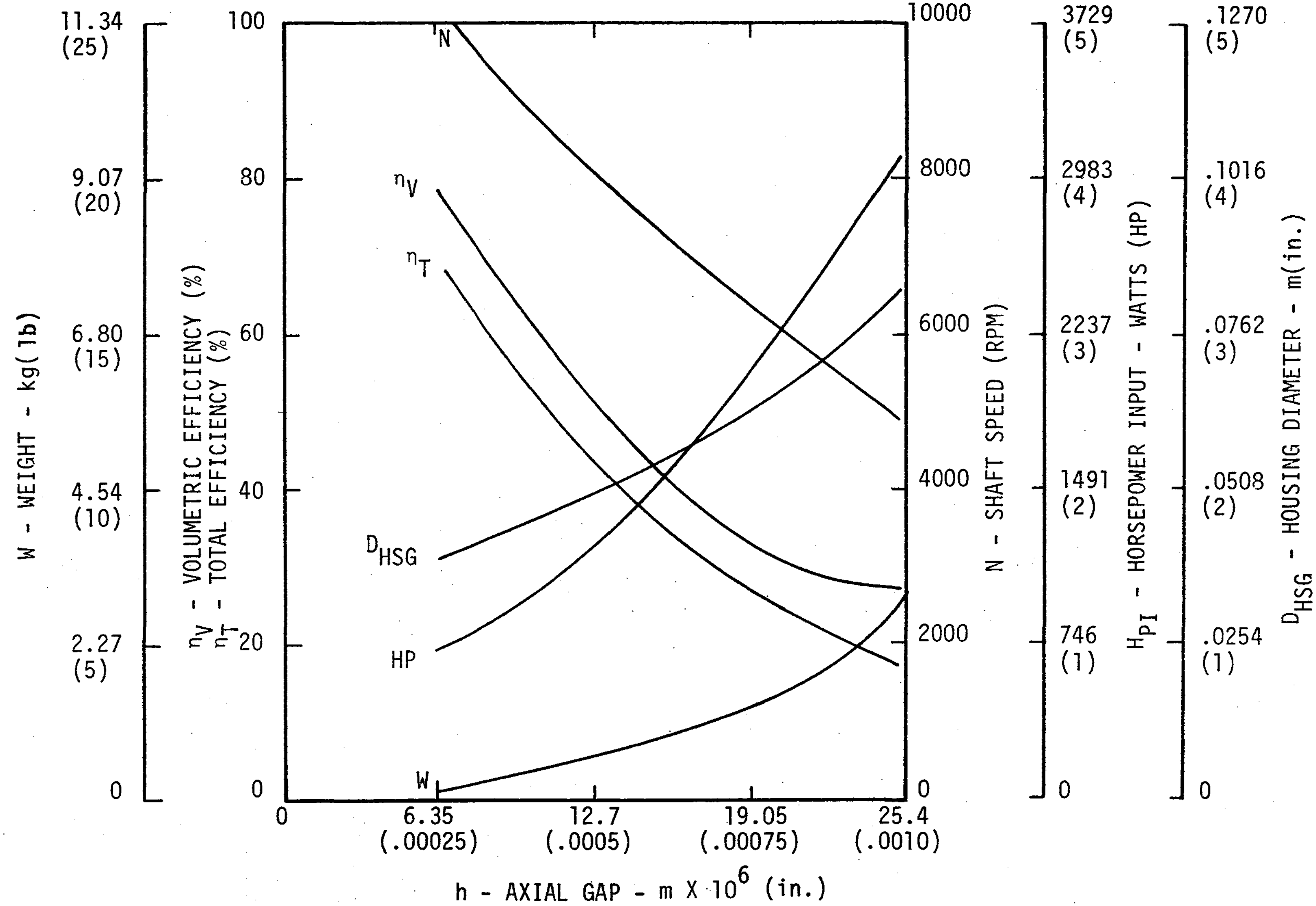

Figure 30. LH_2 Vane Pump - Influence of Axial Gap

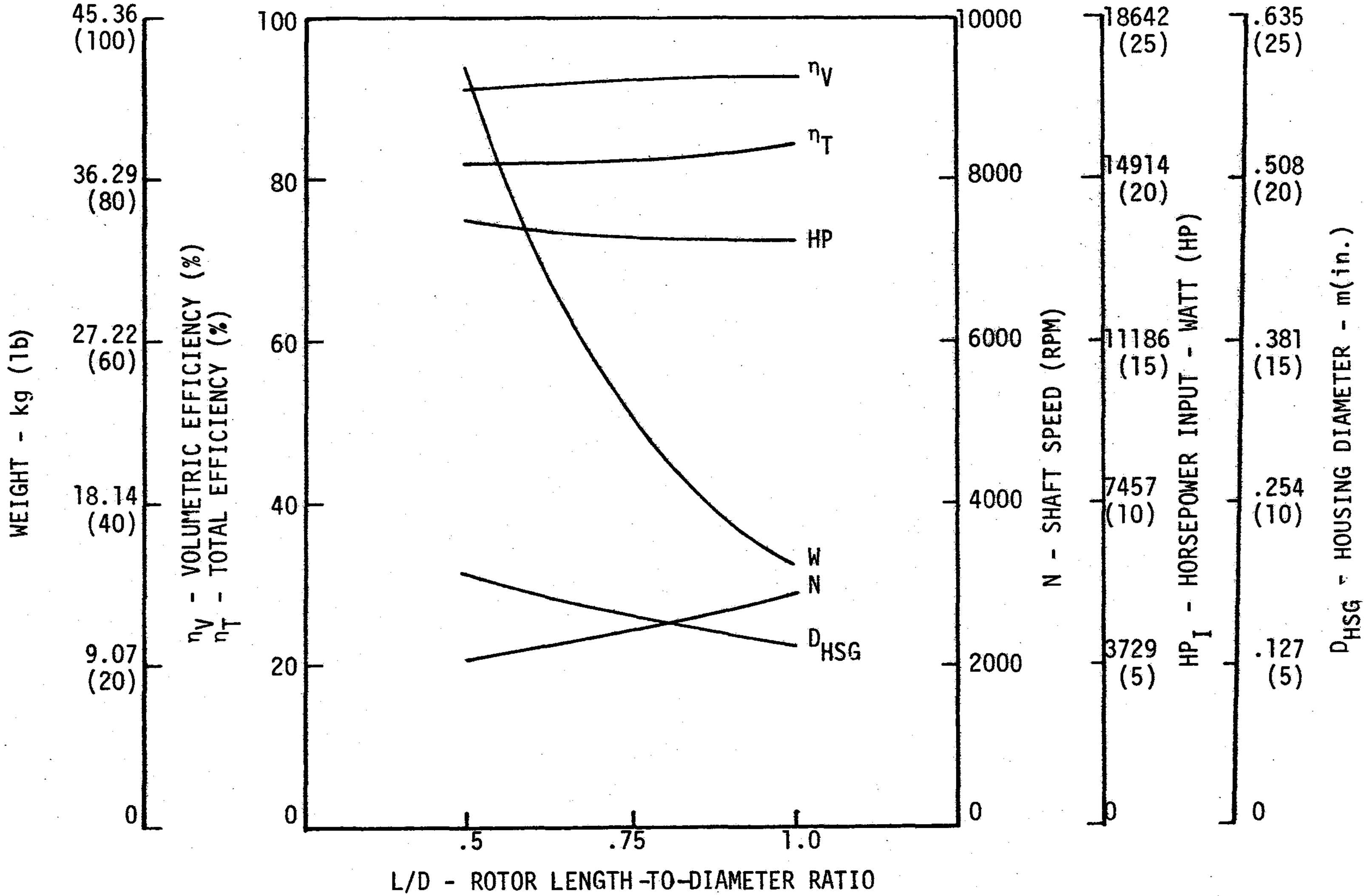

Figure 31. LH_2 Vane Pump - Influence of Rotor Size

TABLE IX. VANE PUMP DESIGN PARAMETERS

Metric Units

Design Point	n_V %	n_T %	N (RPM)	D_{HSG} (m)	W (kg)	POWER (WATT)	PV_V (kPa x m/s)	PV_S (kPa x m/s)	DN	F_{BRG} (N)	L/D	R (m)	h (m)
LH_2													
1	.611	.517	8975.	.045	.476	500	10267	376.1	50569.	.1868	0.75	.0112	.0000127
2	.829	.741	4473.	.090	3.855	3087	14282			.7518		.0211	
3	.866	.787	3397.	.119	8.800	7293	18298			1.2989		.0297	
4	.920	.825	2457.	.1645	23.260	13870	18298			2.4866		.0411	
5	.515	.432	8027.	.050	.667	1193	16840			.2313		.0126	
6	.749	.682	4249.	.095	4.491	7606	27609			.8319		.0238	
7	.797	.723	3235.	.124	10.206	18867	38380			1.4320		.0312	
8	.893	.797	2402.	.168	24.902	34154	38380			2.6023		.0419	
LCH_4													
1	.322	.259	5798.	.044	.445	293	4976	248.0	31982	.1112	0.75	.0114	.000019
2	.729	.651	3667.	.069	1.769	1201	7861			.2802		.0174	
3	.777	.695	2918.	.088	3.515	2498	10170			.4448		.0219	
4	.860	.771	2169.	.118	8.527	4504	10170			.8052		.0295	
5	.467	.417	5076	.050	3.868	835	10170			1.4680		.0126	
6	.627	.553	3347.	.076	2.327	3184	16520			.3381		.0191	
7	.673	.612	2719.	.094	4.341	6756	22870			.5116		.0235	
8	.783	.724	2090	.122	9.525	11409	22870					.0305	
LO_2													
1	.53	.423	2997.	.049	.621	136	1645	142.7	18500	.0801	0.75	.0164	.000254
2	.784	.704	1507.	.098	4.899	858	2679					.0245	
3	.822	.732	1199.	.123	9.752	1782	3511					.0307	
4	.889	.808	889.	.166	23.904	3229	3511					.0414	
5	.578	.506	2076.	.071	1.878	601	3511					.0178	
6	.685	.627	1407.	.105	6.033	2237	6012					.0262	
7	.724	.667	1137.	.130	11.421	4884	8510					.0323	
8	.822	.761	853.	.172	26.581	8576	8510					.0411	

TABLE IX (cont.)

English Units

Design Point	η_V %	η_T %	N (RPM)	D_{HSG} (in.)	W (lb)	HP_1	PV_V (psi x ft/sec)	PV_S (psi x ft/sec)	DN	F_{BRG} (lb)	L/D	R (in.)	h (in.)
LH_2													
1	.611	.517	8975.	1.775	1.05	.67	4886.	179.	50569.	.042	.75	.44	.0005
2	.829	.741	4473.	3.56	8.5	4.14	6797.	179.	50569.	.169	.75	.83	
3	.866	.787	3397.	4.688	19.4	9.78	8708.	179.	50569.	.292	.75	1.17	
4	.920	.825	2457.	6.48	51.28	18.6	8708.	179.	50569.	.559	.75	1.62	
5	.515	.432	8027.	1.98	1.47	1.6	8014.	179.	50569.	.052	.75	.496	
6	.749	.682	4249.	3.74	9.9	10.2	13139.	179.	50569.	.187	.75	.937	
7	.797	.723	3235.	4.9	22.5	25.3	18265	179.	50569.	.322	.75	1.23	
8.	.873	.797	2402.	6.6	54.9	45.8	18265	179.	50569.	.585	.75	1.65	.0005
LCH_4													
1	.322	.259	5798.	1.73	.98	.393	2368	118.	31982	.025	.75	.450	.00075
2	.729	.651	3667.	2.75	3.9	1.61	3741.			.063		.687	
3	.777	.695	2918.	3.45	7.75	3.35	4840.			.10		.863	
4	.860	.771	2169.	4.64	18.8	6.04	4840.			.181		1.16	
5	.467	.417	5076.	1.98	1.47	1.12	4840.			.033		.496	
6	.627	.553	3347.	3.00	5.13	4.27	7862.			.076		.752	
7	.673	.612	2719.	3.70	9.57	9.06	10884.			.115		.926	
8	.783	.724	2090.	4.8	21.0	15.3	10884.	118.	31982		.75	1.20	.00075
LO_2													
1	.53	.423	2997.	1.94	1.37	.182	783.	67.9	18500	.018	.75	.645	.001
2	.784	.704	1507.	3.85	10.8	1.15	1275.					.964	
3	.822	.732	1199.	4.85	21.5	2.39	1671.					1.21	
4	.889	.808	889.	6.54	52.7	4.33	1671.					1.63	
5	.578	.506	2076.	2.8	4.14	.806	1671.					.700	
6	.685	.627	1407.	4.14	13.3	3.0	2861.					1.03	
7	.724	.667	1137.	5.1	25.18	6.55	4050.					1.27	
8	.822	.761	853.	6.77	58.6	11.5	4050.	67.9	18500	.018	.75	1.62	.001

TABLE X. HYDROGEN VANE PUMP WEAR PARAMETERS

SI UNITS

Design Point	Vane Tip Radius R (m)	Pressure X Sliding Velocity PV (kPa x m/s)	Vane Area A_v (m^2)	Vane Force F (N)	Vane Tip Pressure P (kPa)	Vane Tip Stress S_s (MPa)
1	0.0112	10267	0.000037	36.2	965	120.14
2	0.0226	14282	0.000154	205.9	1337	141.70
3	0.0297	18298	0.000265	455.9	1717	160.39
4	0.0411	18298	0.000508	871.8	1710	160.37
5	0.0126	16840	0.000048	75.4	1579	153.27
6	0.0238	27609	0.000170	441.2	2599	196.60
7	0.0312	38380	0.000292	1056.8	3612	232.29
8	0.0419	38380	0.000526	1899.3	3612	232.29

ENGLISH UNITS

Design Point	Vane Tip Radius R (in.)	Pressure X Sliding Velocity PV (psi x ft/sec)	Vane Area A_v (in.^{2})	Vane Force F (lb)	Vane Tip Pressure P (psi)	Vane Tip Stress S_s (psi)
1	0.44	4886.	0.058	8.13	140.	17425.
2	0.89	6797.	0.238	46.3	194.	20552.
3	1.17	8708.	0.410	102.5	249.	23262.
4	1.62	8708.	0.787	196.	248.	23260.
5	.496	8014.	0.074	16.95	229.	22230.
6	.937	13139.	0.263	99.2	377.	28514.
7	1.23	18265	0.453	237.6	524.	33690.
8	1.65	18265	0.816	427.	524.	33690.

TABLE XI. HYDROGEN PUMP LIFE DUE TO VANE AND LINER WEAR

SI UNITS

Design Point	Vane Tip Radius R (m)	Pressure X Sliding Velocity PV (kPa x m/s)	Vane Wear h (m)	Life t (sec)
1	0.0112	10267	0.0000127	1.01
2	0.0226	14282		1.30
3	0.0297	18298		1.00
4	0.0411	18298		1.00
5	0.0126	1879		1.10
6	0.0238	27688		0.67
7	0.0312	38380		0.484
8	0.0419	38380	0.0000127	0.484

ENGLISH UNITS

Design Point	Vane Tip Radius R (in.)	Pressure X Sliding Velocity PV (psi x ft/sec)	Vane Wear h (in.)	Life t (sec)
1	0.44	4886.	0.0005	1.01
2	0.89	6797		1.30
3	1.17	8708		1.0
4	1.62	8708		1.0
5	0.496	894.		1.1
6	0.937	13139.		0.67
7	1.23	18625		0.484
8	1.65	18625	0.0005	0.484

TABLE XII. HYDROGEN VANE PUMP LIFE FOR 10% VOLUMETRIC EFFICIENCY DECREASE

SI UNITS

Vane Radius R (m)	Vane Wear h_V (m)	Life @ PV = 38,380 (kPa x m/s) t* (sec)	Life @ PV = 10,267 (kPa x m/s) t** (sec)
0.0127	0.000559	8.0	30.5
0.0191	0.000856	12.26	46.7
0.0254	0.001143	16.37	62.4
0.0381	0.001702	24.38	92.9
0.0508	0.002286	32.70	124.0

ENGLISH UNITS

Vane Radius R (in.)	Vane Wear h_V (in.)	Life @ PV = 18,625 (psi x ft/sec) t* (sec)	Life @ PV = 4886 (psi x ft/sec) t** (sec)
0.5	0.022	8.0	30.5
0.75	0.0337	12.26	46.7
1.0	0.045	16.37	62.4
1.5	0.067	24.38	92.9
2.0	0.090	32.7	124.

*Maximum PV Value at Design Point 8

**Maximum PV Value at Design Point 1

2. Gear Pump

a. Description

Displacement in a gear pump is accomplished by the meshing of gear teeth. This means that, at constant speed, the flowrate is nearly independent of pressure. There are several concepts of gear pumps, but all require at least two gears. Some examples are shown in Figure 32. Input power from the driver is connected to the extended shaft of one of the gears. In turn, this gear drives the mating gear(s). The volume displaced per revolution for a two-gear pump is approximately equal to 75% of the difference between the square of the tooth OD and ID times the tooth width. Most gear pumps have been designed to be used either as a lube oil pump or a pump used to pump hydraulic oil. Oil has two characteristics which give the gear pump attractive performance. First, the oil has high enough viscosity so that the leakage flowrate is low in comparison to flow delivered. Secondly, the oil has either enough viscosity to provide a hydrodynamic film at the tooth mesh or enough lubricity to prevent excessive tooth wear.

Data from existing designs indicate that the efficiency of a gear pump can be better than 95%. Again, this is for a lube oil pump. As indicated by the performance of automobile gear pumps and lube pumps for stationary power plants, these pumps have extremely long life.

Most gear pumps have been made with involute-type teeth; however, one objectionable characteristic of the gear pump is its pulsating discharge pressure. Unless special gearing is manufactured or an accumulator is used on the discharge, these pressure pulses would have an adverse effect on the combustion chamber. If an accumulator is required, its weight and size must be considered before an overall evaluation of the gear pump is made. Attempts have been made to use cycloidal tooth forms since there is less fluid trapping between the teeth during mesh (see Ref. 42 and Figure 33). This tooth shape is basically a cycloidal form and, per Reference 95, has many theoretically kinematic advantages. However, the practical difficulties of producing it accurately are largely responsible for its non-use in commercial gears.

Two characteristics of the pump limit the suction performance. One is the peripheral speed of the gear at the opening of the inlet cavity. The relative velocity between the gear and the incoming fluid in this cavity must be maintained low enough to avoid cavitation. This limitation is defined in Reference 72. The other characteristic is that the recirculating leakage from the high-pressure discharge zone to the low-pressure inlet zone may cause vapor at the inlet of the pump. When mixed with the low-energy inlet fluid, the high-energy, high-temperature recirculating fluid must result in a liquid mixture as opposed to a liquid-vapor mixture. If this vapor/liquid ratio does not approach zero, the gear pump will choke or cavitate.

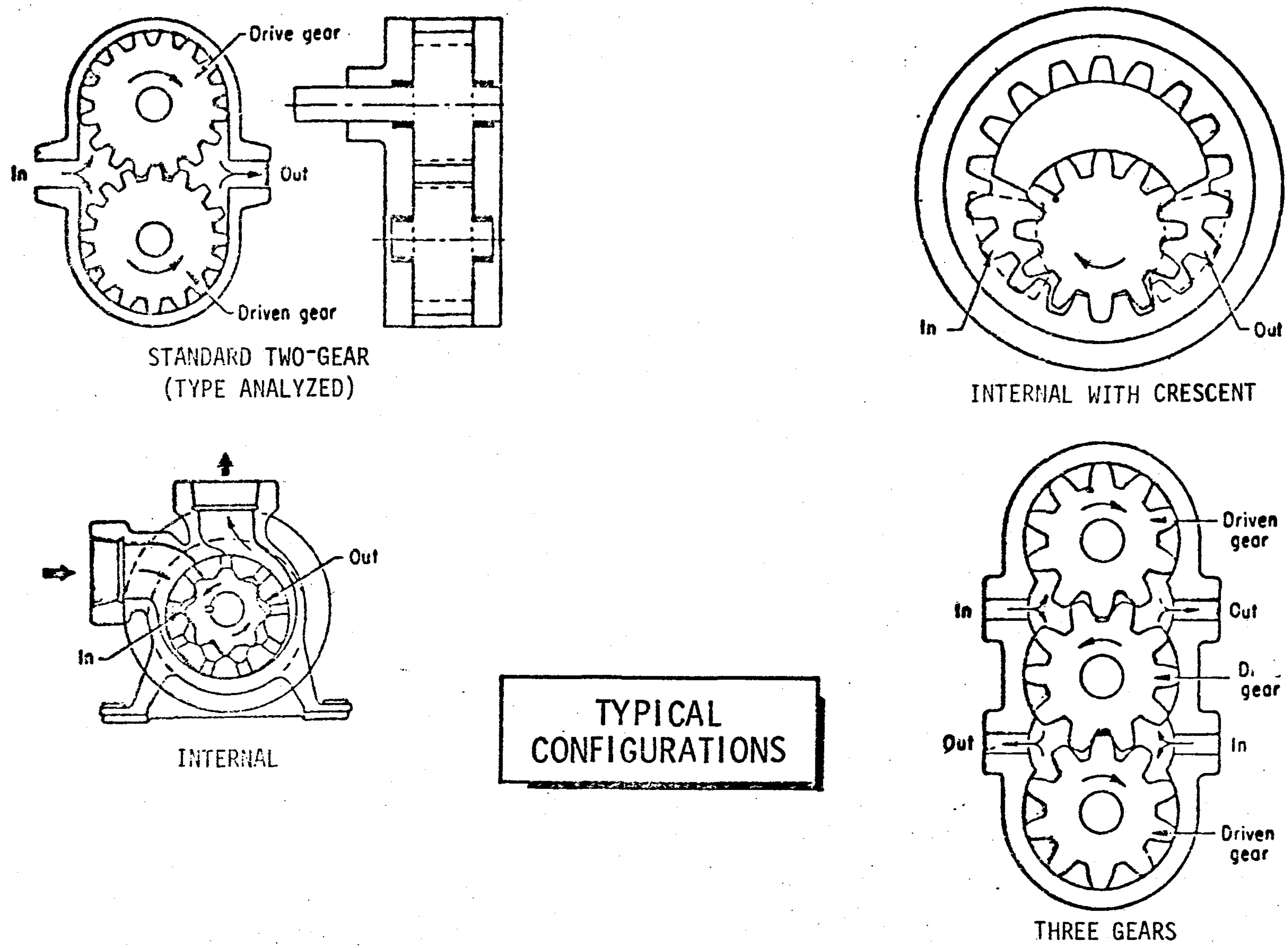

Figure 32. Types of Gear Pumps

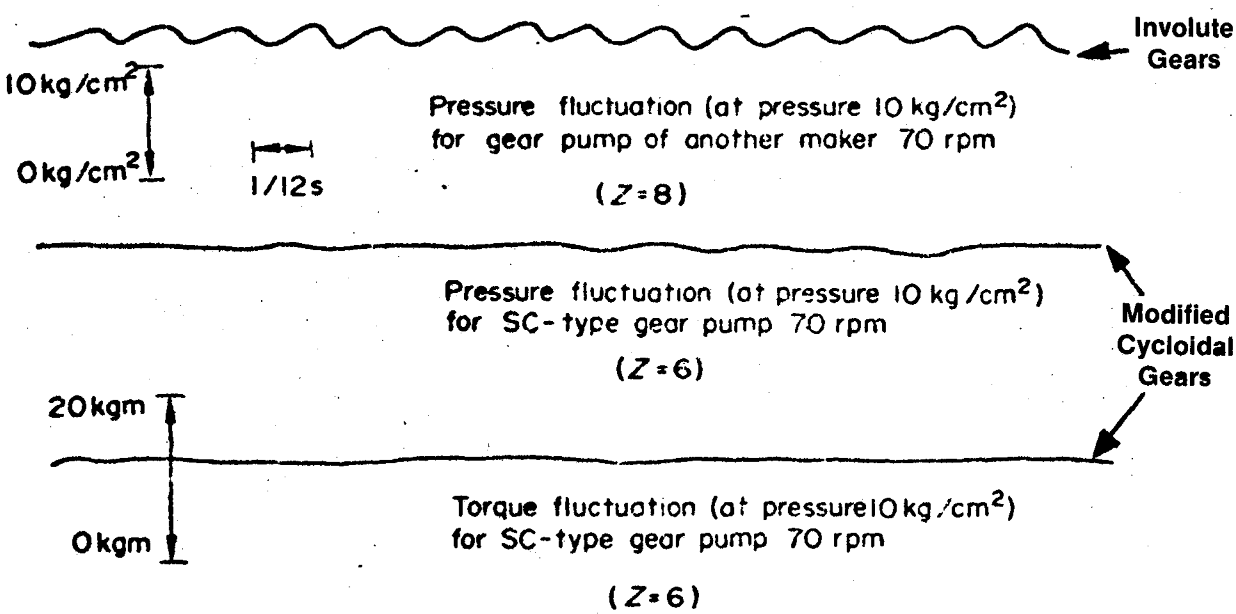

Figure 33. Recording Example of Pressure and Torque Fluctuation

b. Analysis

The three design parameters which will affect gear pump size, efficiency, weight, and speed are 1) number of teeth, 2) gear width to gear diameter ratio, and 3) gear to housing clearances. In order to evaluate these design parameters, a computer model was developed on the basis of the logic described in Reference 80. The following description of the design parameters gives some insight into their influence on gear pump performance characteristics and on some of the physical limitations.

Number of Teeth

The number of teeth were varied from 6 to 15. Increasing the number of teeth causes the gear-tip-diameter to gear-root-diameter ratio to increase (high number of finer teeth). This, in turn, increases the overall gear diameter so that a given flowrate can be passed through. When the overall gear diameter is increased, the leakage path width increases, causing higher leakage flow. This can be seen by the following equation:

$$\frac{D_{RD}}{D_{TD}} = \frac{1-\frac{2C_2}{N}}{1+\frac{2C_1}{N}}$$

where

D_{RD} = gear tooth root diameter

D_{TD} = gear tooth tip diameter

N = number of teeth

C_1&C_2 = constants for a particular pressure angle and tooth form.

The number of teeth selected was 12. Again this represents a compromise between high efficiency and large pulses for a lower number of teeth versus low efficiency and small pulses for a larger number of teeth. With a low number of teeth on a gear (7 to 15, depending on the pressure angle), special designs must be implemented to avoid undercutting during manufacturing (see Ref. 96 for this criterion). Since gear strength is not critical, higher numbers of teeth will also have better wear characteristics and run more quietly.

Gear Width/Gear Diameter

As the ratio of gear width to gear diameter is increased, the efficiency increases. The theoretical flow is given by:

$$Q_{TH} = \frac{D_{TD}^{2}\left[1 - \frac{D_{RD}}{D_{TD}}^{2}\right]}{} \times W \times RPM$$

where Q_{TH} = delivered flow with zero clearance

W = gear width

RPM = pump speed.

For a constant delivered flow, the width has to increase when the diameter decreases. This causes the width of the leakage path (not to be confused with the height or clearance) to decrease. In turn, this reduces the leakage flow and, consequently, increases the efficiency. The effect is less at either high flow or low pressure. A ratio of 0.3 was selected because it was approximately at the "knee" of the weight curve; also, it represents a compromise between high efficiency and wide gears which will be less tolerant to misalignment. An exception to the 0.3 ratio was made on pressure/flow points No. 1 to 5. It was necessary to reduce the ratio to 0.1 in order to obtain a gear diameter large enough to place the smallest bearing (10 mm) within the envelope.

Clearance

The clearance was varied over a range of 0.005 to 0.0356 mm (0.0002 to 0.0014 in.). This is not only the clearance between the side of the gear and the housing, but also between the tips of the gear teeth and the housing. A separated clearance study was not conducted. However, from the calculated values, the tip leakage flow is 1% to 3% of the side leakage flow; consequently, tip clearance will have a secondary effect. Again the low flows and high pressure points were more sensitive to clearance. One clearance which affects not only the volumetric efficiency but also the thermodynamics at the inlet was not included in the analysis. This is the clearance between the tip of one gear and the root of the mating gear. This clearance produces carry-over volume and was estimated to be 3% by Reference 7 (depending on tooth form). The more detrimental effect is the expansion of this trapped fluid back into the inlet.

The efficiency can be improved by reducing the clearance to some practical limit. The gear pump of Reference 8 was designed for a clearance of 0.025 mm (0.0001 in.) per side and, because of rubbing, was later increased to 0.028 mm (0.0011 in.). This is an indication that, in practice, the clearance may be greater than anticipated in the design. For the LH_2 pumps, a clearance value of 0.177 mm (0.0005 in.) was selected. For the LCH_4 pumps, a clearance of 0.19 mm (0.0075 in.) for the small pumps and 0.025 mm (0.0010 in.) for the large pumps was selected. This increase in clearance over that used for LH_2 was justified since the efficiencies did not drop off because of the higher viscosity of LCH_4. For LO_2 pumps, where rubs could cause catastrophic damage, the clearance was increased to 0.025 mm (0.0010 in.) for the small pumps and 0.0381 mm (0.0015 in.) for the larger pumps.

Results of Sensitivity Study

Using the computer model, a sensitivity study of each design parameter was made and graphs for six pressure/flow points and for all three propellants were plotted. From these plots, acceptable values for each design parameter were determined. Typical plots have been selected to display the influence of the design parameter on gear pump characteristics and to demonstrate how the data contained in Table XIII were generated.

Figure 34 shows how efficiency varies as a function of number of gear teeth for each of the pressure/flow points. The highest efficiency is obtained at the highest flow low-pressure point while the lowest efficiency occurs at the lowest flow high-pressure point. The other pump parameters are shown in Figure 35 at the lowest flow high-pressure point. This shows how the weight increases and the speed decreases as the number of teeth are increased. The gear width-to-gear diameter ratio design parameter is shown in Figure 36. For all pressure/flow points, the efficiency does not fall off significantly until the ratio drops below 0.3. Below a ratio of 0.3, the weight increases very rapidly, as shown in Figure 37. The design parameter for clearance is shown in Figures 38 and 39. Since this parameter has a strong effect on efficiency, the design value selected should be as low as practical.

Again, Figures 34 through 39 were selected to show how the pump characteristics vary with the three design parameters. In all cases (both pressure/flow and propellants), the trends were similar; however, the magnitude differed. It is interesting to note the change in efficiency that results from designing for different fluids. At the same flowrate and pressure (126 cm^3/s, 1241 kPa) (2 GPM, 180 psi) and at the same number of teeth (12), width-to-diameter ratio, and clearance (7.6, and 0.025 mm) (0.3 and 0.001 in.), the efficiency of a gear pump would be 56%, 80%, and 87% in LH_2, LCH_4, and LO_2, respectively. This indicates the effect of fluid properties, namely viscosity and density.

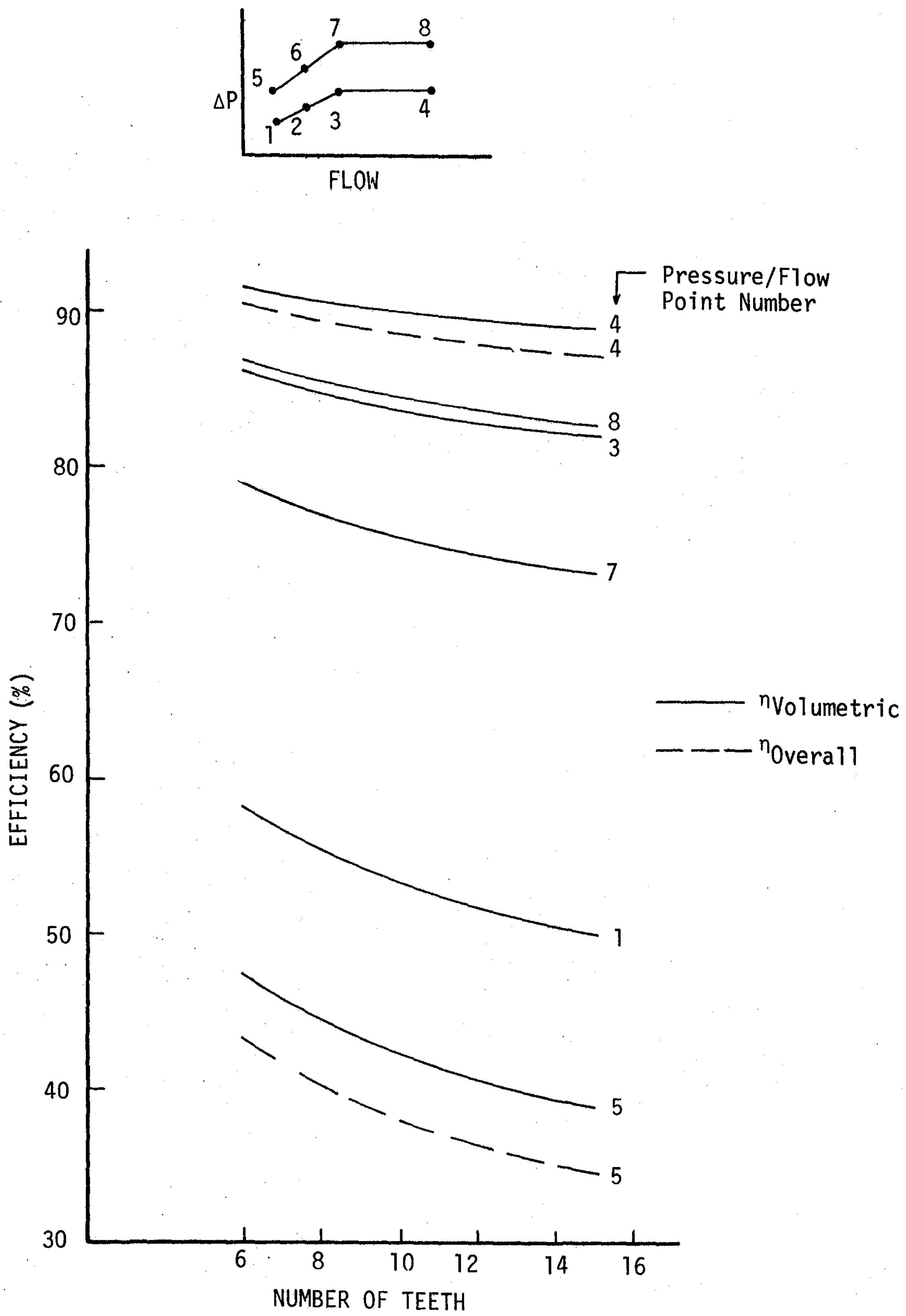

Figure 34. LH_2 Gear Pump - Efficiency Versus Number of Teeth

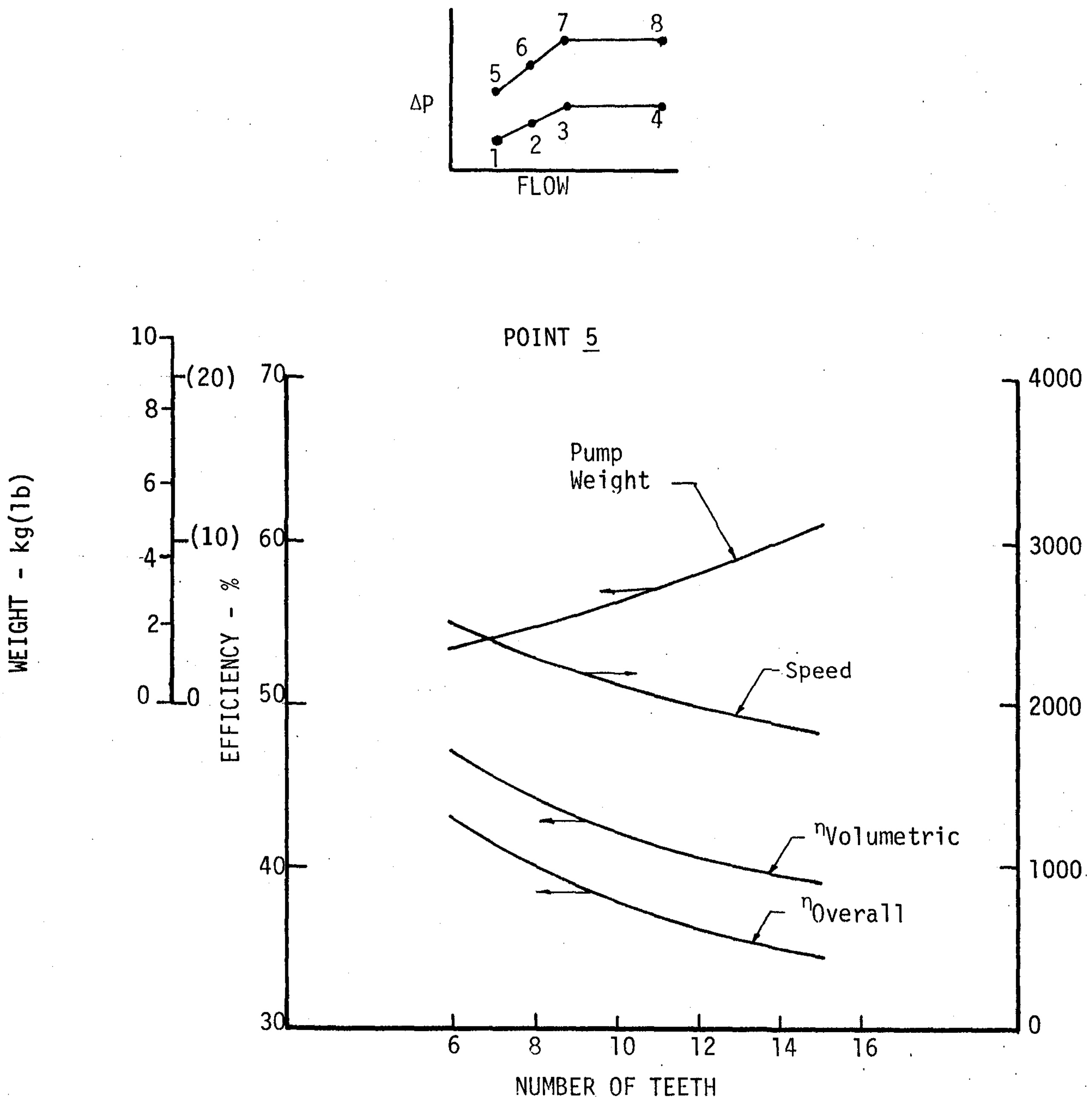

Figure 35. LH_2 Gear Pump - Efficiency and Weight Versus Number of Teeth, Point 5

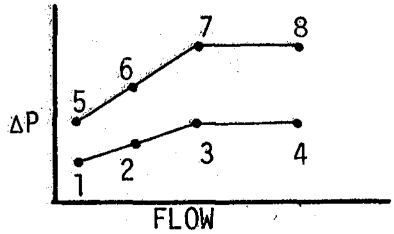

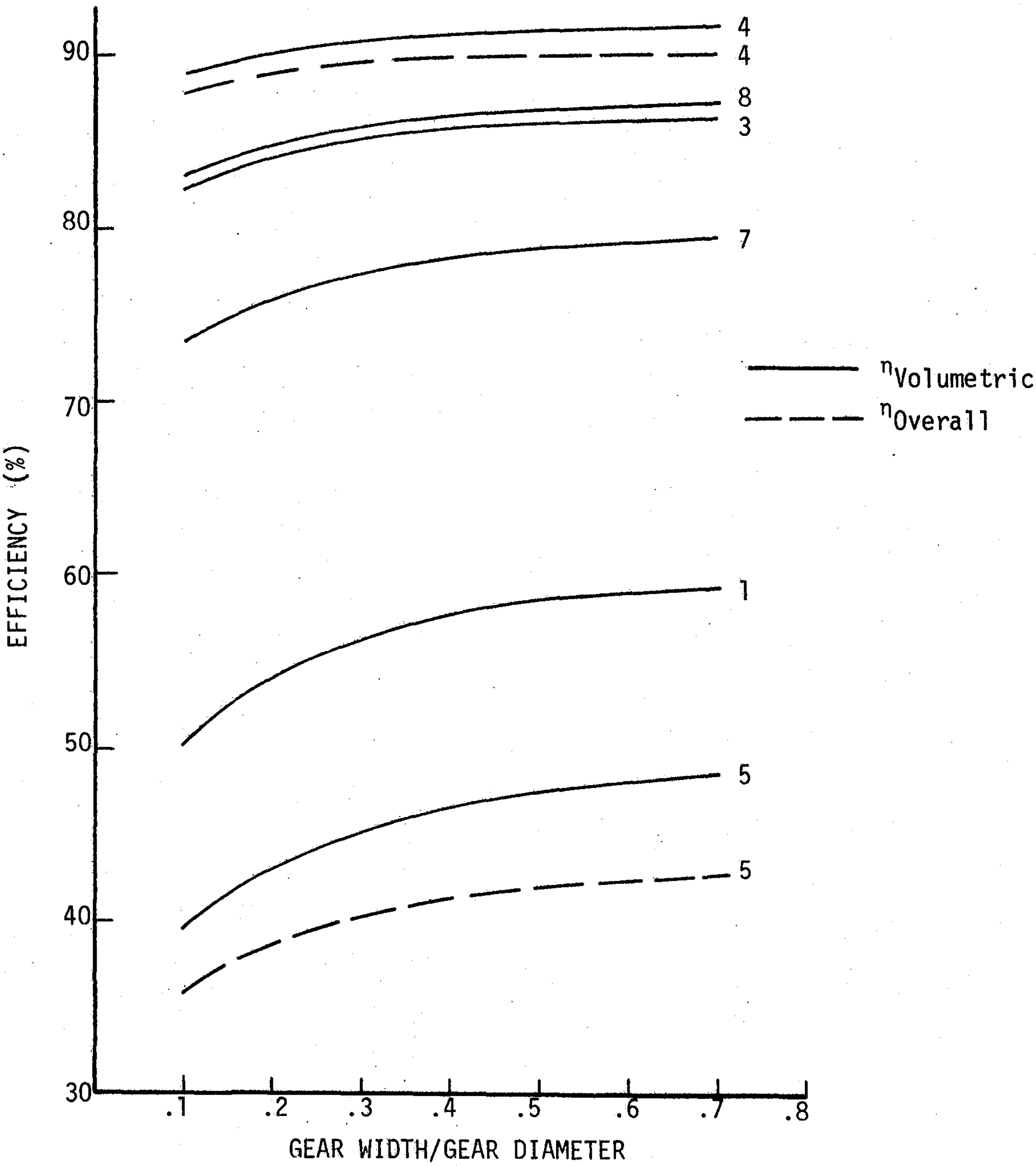

Figure 36. LH_2 Gear Pump - Efficiency Versus Gear Size

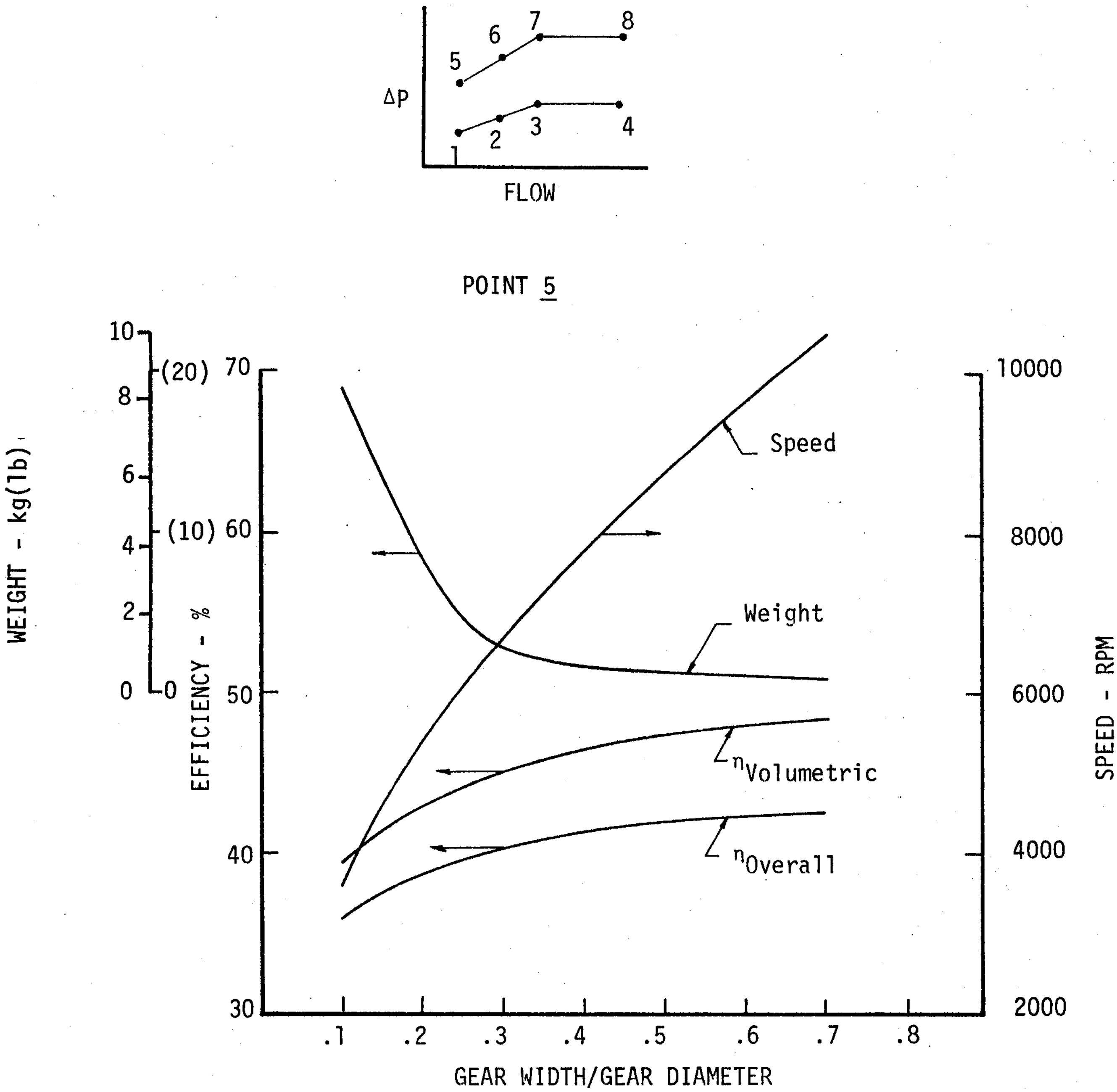

Figure 37. LH_2 Gear Pump - Efficiency and Weight Versus Gear Size, Point 5

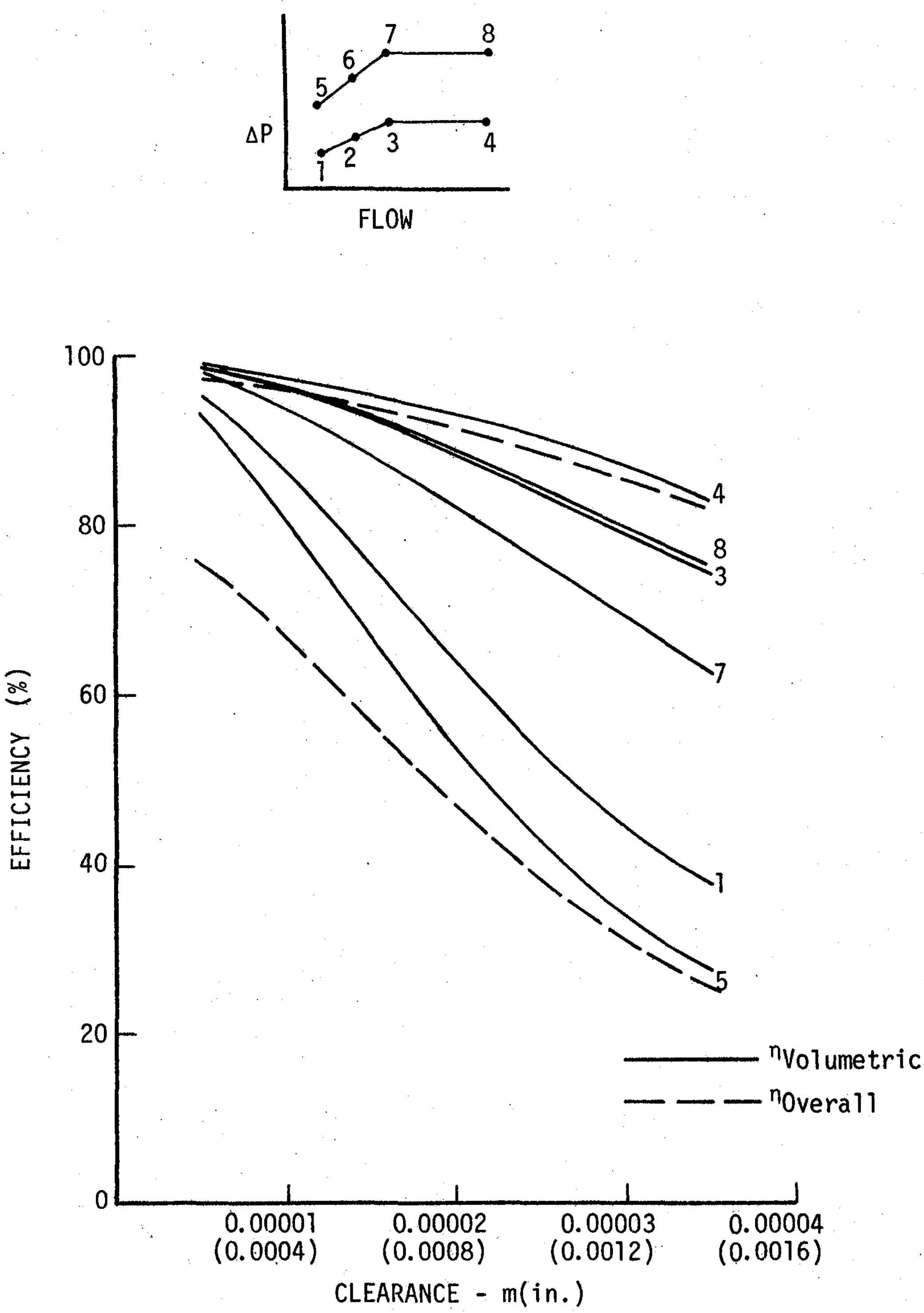

Figure 38. LH_2 Gear Pump - Efficiency Versus Clearance

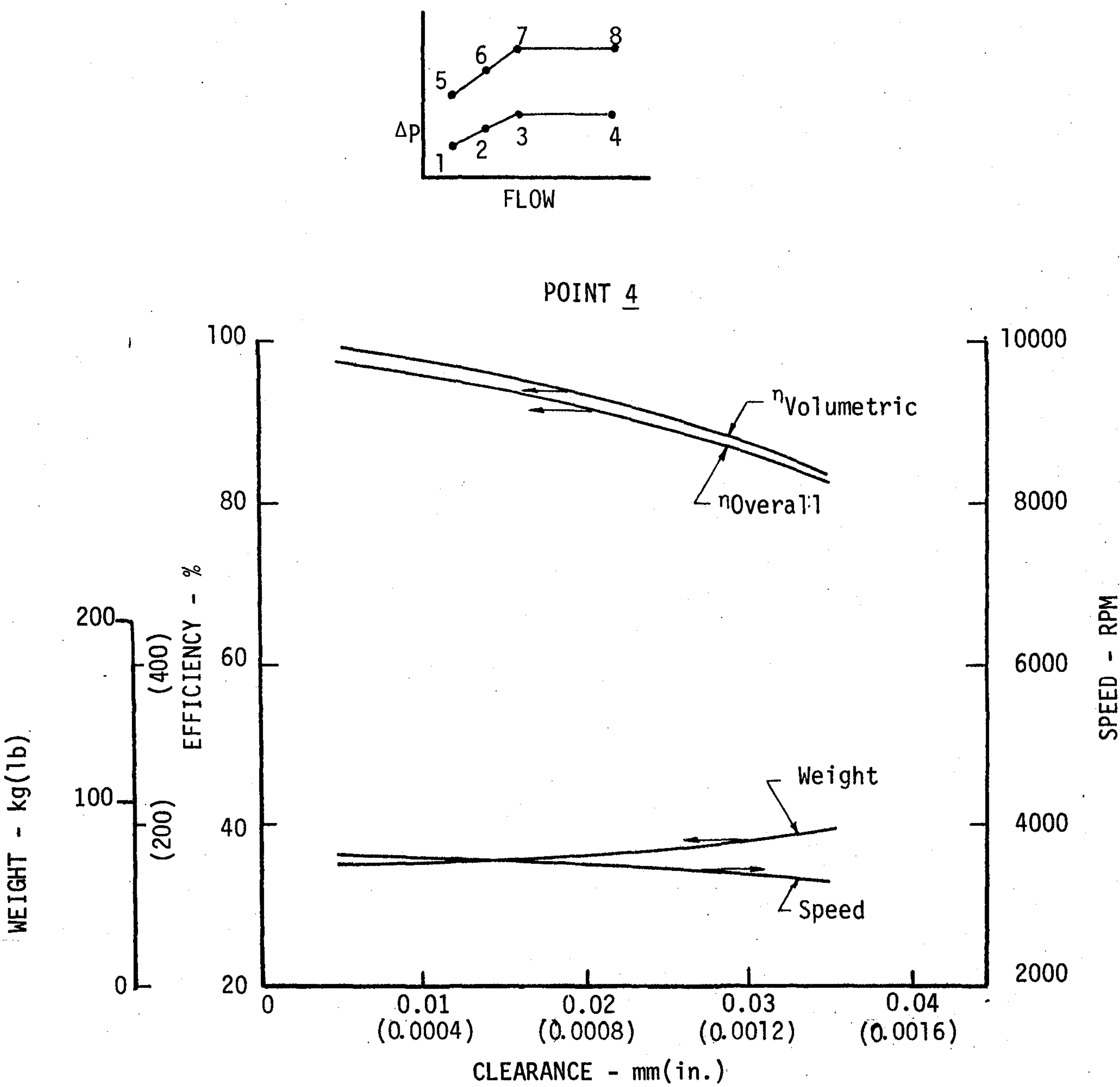

Figure 39. LH_2 Gear Pump - Efficiency and Weight Versus Clearance, Point 4

Gear Pump Life

Calculation of gear pump life will be based on three factors: 1) bearing DN and fatigue life; 2) seal life: and 3) gear life. The DN values are relatively low, less than 70,000, 43,000, and 27,000 mm for the LH_2, LCH_4 and LO_2 pumps, respectively. The bearings fatigue life is a minimum of 60 times the required life. However, operating in cryogenics will mean that these values will be difficult to obtain since the fluid will only provide coolant and not a hydrodynamic film.

The seal life should not be a limiting factor. Many seals (face seals or shaft-riding carbon-type) have operated in cryogenics. The seal can be pressure-balanced so that the product of the face pressure times the velocity can be controlled to a value within acceptable limits.

The gear life is determined by the tooth load and the properties of the pumped fluid. Reference 94 indicates that satisfactory operation can be obtained if the tooth load in cryogenics is below 70 N/mm (400 lb/in.) of face width. In addition, it is recommended that a dry-film lubricant, such as a mixture of molybdenum disulfide and graphite, be applied to the gear teeth to a thickness of 0.0127 to 0.0508 mm (0.5 to 2.0 mils), using varnish as the carrier. Table XIII shows that the tooth load in all cases is below 52.5 N/mm (300 lb/in.).

3. Piston Pump

a. Description

This pump consists of a piston which operates with a reciprocating motion within a cylinder and a valving or porting arrangement which provides inlet and discharge flow from the cylinder at the appropriate times of the piston cycle. The basic piston pump schematic is shown in Figure 40. The reciprocating motion can be generated by a conventional crank or camshaft or by a variety of angled swashplates, eccentric external cams, "Z" cranks or bent axis rotating cylinders. In most crankshaft and camshaft designs, the force exerted on the piston results in a side load between the piston and cylinder. For pumping oils and hydrocarbon fuels, there is enough viscosity to provide an adequate lubricating film at the sliding interface. With low-viscosity cryogenic fluids, this hydrodynamic lubrication is insufficient to prevent scuffing at the expected piston speeds. Therefore, special care must be taken with cryogenics to minimize these loads and speeds, and an acceptable rubbing combination or special hydrostatic lubrication must be provided. Usually, piston rings are used to seal the high-pressure fluid, and this also creates a rubbing surface that requires special attention. A successful design for cryogenic fluids would be a compromise of those components that minimize rubbing loads, piston speeds, leakage areas, thermal leakage and, for rocket engine application, the pressure pulsations.

TABLE XIII. GEAR PUMP DESIGN PARAMETERS

SI UNITS

DESIGN POINT	n_V (%)	n_T (%)	N (RPM)	N_S $\frac{(RPM)\ (m^3/s)}{m^{3/4}}$	S	P.D. (m)	DIA. (m)	WT. (kg)	DN	BEARING LOAD (N)	BEARING LIVES (**)	TOOTH LOAD (N/m)
LH_2												
1*	78	54	4590	23.26	2112	.0376	.1143	4.08	55000	111	>2000	4203
3	95	92	2770	23.26	4089	.0625	.1897	18.14	70000	2046	1200	15235
4	97	95	1980	23.26	4089	.0874	.2652	49.90	70000	4004	3200	21364
5*	70	58	4350	11.63	2016	.0399	.1207	4.54	65000	267	>2000	8756
7	91	89	2720	11.63	3973	.0635	.1930	19.50	67000	5027	60	37125
8	95	94	1960	11.63	4050	.0884	.2677	52.16	68000	9742	160	51660
LCH_4												
1*	64	36	3810	40.70	1938	.0287	.0864	1.81	- -	67	- -	3152
3	85	80	2400	46.51	3837	.0457	.1387	7.26	40000	1112	2000	11032
4	91	88	1750	46.51	3954	.0625	.1897	18.14	43000	2046	2000	15235
5*	51	40	3480	23.26	1764	.0315	.0955	2.27	- -	156	- -	6830
7	77	75	2280	23.26	3643	.0480	.1455	8.16	39000	2891	94	27669
8	86	84	1700	23.26	3837	.0645	.1953	20.41	42000	5649	120	37125
LO_2												
1*	73	43	1620	60.08	2035	.0391	.1184	4.54	19000	76	>2000	2627
3	86	83	970	60.08	3876	.0653	.1979	20.87	24000	1379	>2000	9807
4	92	89	710	62.02	3992	.0897	.2718	54.43	25000	2669	>2000	13659
5*	65	48	1530	36.82	1938	.0414	.1245	5.44	23000	151	>2000	4903
7	79	77	920	29.07	3702	.0683	.1994	22.68	53000	3870	460	25917
8	86	86	690	29.07	3876	.0922	.2794	58.97	27000	6984	>2000	35024

*Design points 1 and 5 have gears with width/diameter ratios = 0.1; all others = 0.3

**Required life exceeded by number of lives

Clearance: LH_2 - All design points: 0.0000127 m
LCH_4 - 1 and 5: 0.0000190 m; 3, 4, 7, and 8: 0.0000254 m
LO_2 - 1 and 5: 0.0000254 m; 3, 4, 7, and 8: 0.0000381 m

TABLE XIII. GEAR PUMP DESIGN PARAMETERS (cont.) ENGLISH UNITS

	DESIGN POINT	η_V (%)	η_T (%)	N (RPM)	N_S $\frac{(RPM)(GPM)^{1/2}}{ft^{3/4}}$	S	P.D. (in.)	DIA. (in.)	WT (lb)	DN	BEARING LOAD (lb)	BEARING LIVES (**)	TOOTH LOAD (lb/in.)
	1*	78	54	4590	12	1090	1.48	4.50	9	55×10^3	25	> 2000	24
	3	95	92	2770	12	2090	2.46	7.47	40	70	460	1200	87
LH_2	4	97	95	1980	12	2110	3.44	10.44	110	70	900	3200	122
	5*	70	58	4350	6	1040	1.57	4.75	10	65	60	> 2000	50
	7	91	89	2720	6	2050	2.50	7.60	43	67	1130	60	212
	8	95	94	1960	6	2090	3.48	10.54	115	68	2190	160	295
	1*	64	36	3810	21	1000	1.13	3.40	4	--	15	---	18
	3	85	80	2400	24	1980	1.80	5.46	16	40×10^3	250	2000	63
LCH_4	4	91	88	1750	24	2040	2.46	7.47	40	43	460	> 2000	87
	5*	54	40	3480	12	910	1.24	3.76	5	--	35	---	39
	7	77	75	2280	12	1880	1.89	5.73	18	39	650	94	158
	8	86	84	1700	12	1980	2.54	7.69	45	42	1270	120	212
	1*	73	43	1620	31	1050	1.54	4.66	10	19×10^3	17	> 2000	15
	3	86	83	970	31	2000	2.57	7.79	46	24	310	> 2000	56
LO_2	4	92	89	710	32	2060	3.53	10.70	120	25	600	> 2000	78
	5*	65	48	1530	19	1000	1.63	4.90	12	23	34	> 2000	28
	7	79	77	920	15	1910	2.69	7.85	50	53	870	460	148
	8	86	86	690	15	2000	3.63	11.00	130	27	1570	> 2000	200

*Points 1 and 5 have gears with width/diameter ratios = 0.1; all others = 0.3

**Required life exceeded by number of lives

Clearance: LH_2 - All design points: 0.0005 in.
LCH_4 - 1 and 5: 0.00075 in.; 3, 4, 7, and 8: 0.0010 in.
LO_2 - 1 and 5: 0.0010 in.; 3, 4, 7, and 8: 0.0015 in.

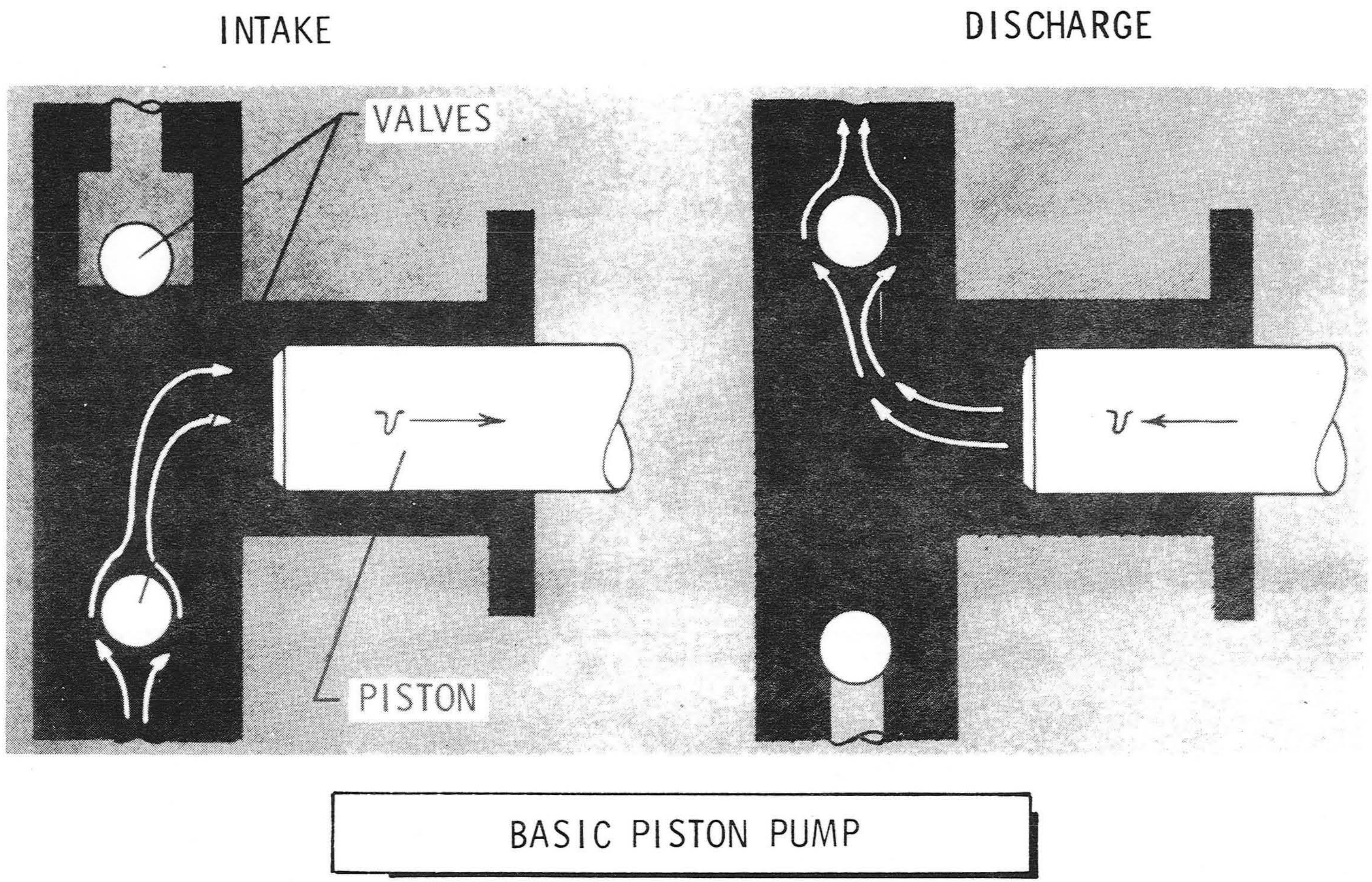

Figure 40. Basic Positive-Displacement Piston Pump

b. Literature Review

Piston pump literature reviewed included References 7, 8, 10, 19, 20, 44, 50, 65, 82, 101, 102, and 103. Reference 1 shows several types of manufactured piston pumps. They consist of radial and axial pistons, with various mechanical devices for achieving the reciprocating piston motion and various valves and ports for providing the inlet and discharge flow. Figure 41 shows a radial piston arrangement with the eccentric internal in one case and the eccentric external in another case. Figure 42 shows two schematics of an axial piston pump: one with the cam plate rotating and a check valve arrangement; the other with a stationary swashplate with rotating cylinder and pistons and a valve port plate.

The literature review uncovered a wide variety of piston pump designs, all with useful features, but none exactly suited to meet the pressure/flow requirements of this study. Those which are either directly or potentially applicable for use with cryogenic fluids are briefly discussed herein.

Biermann (Refs. 19 and 20) presented design and operation information on a piston pump run in JP-5, LN_2, and LH_2. The design, shown in Figure 43, is a low-speed, low-pressure, and low-flowrate pump. Operation in LH_2 was successful, although the pump size and weight were large for the flowrate. Volumetric and overall efficiencies were high in all three fluids tested, and reasonable life and reliability were also demonstrated.

Reference 3 shows pump designs for use with hydraulic fluids, but some of these have desirable features for cryogenic operation. Figure 44 shows a design in which the rotating assembly is supported on rolling contact bearings that can operate in cryogenic fluids. This design avoids oscillating wrist pins, which are difficult to lubricate, and also eliminates the crank which is associated with large side loads on pistons. The reciprocating motion is provided by an eccentric bearing in contact with the radial pistons. Figure 45 shows a design with all-fluid film bearings. This feature is desirable for long life but degrades the efficiency because of additional leakage.

c. Conclusions

The conclusions were derived from the literature review, and further analysis was not considered necessary.

(1) The piston pump concept appears to be applicable to the entire study pressure/flow map with all three fluids.

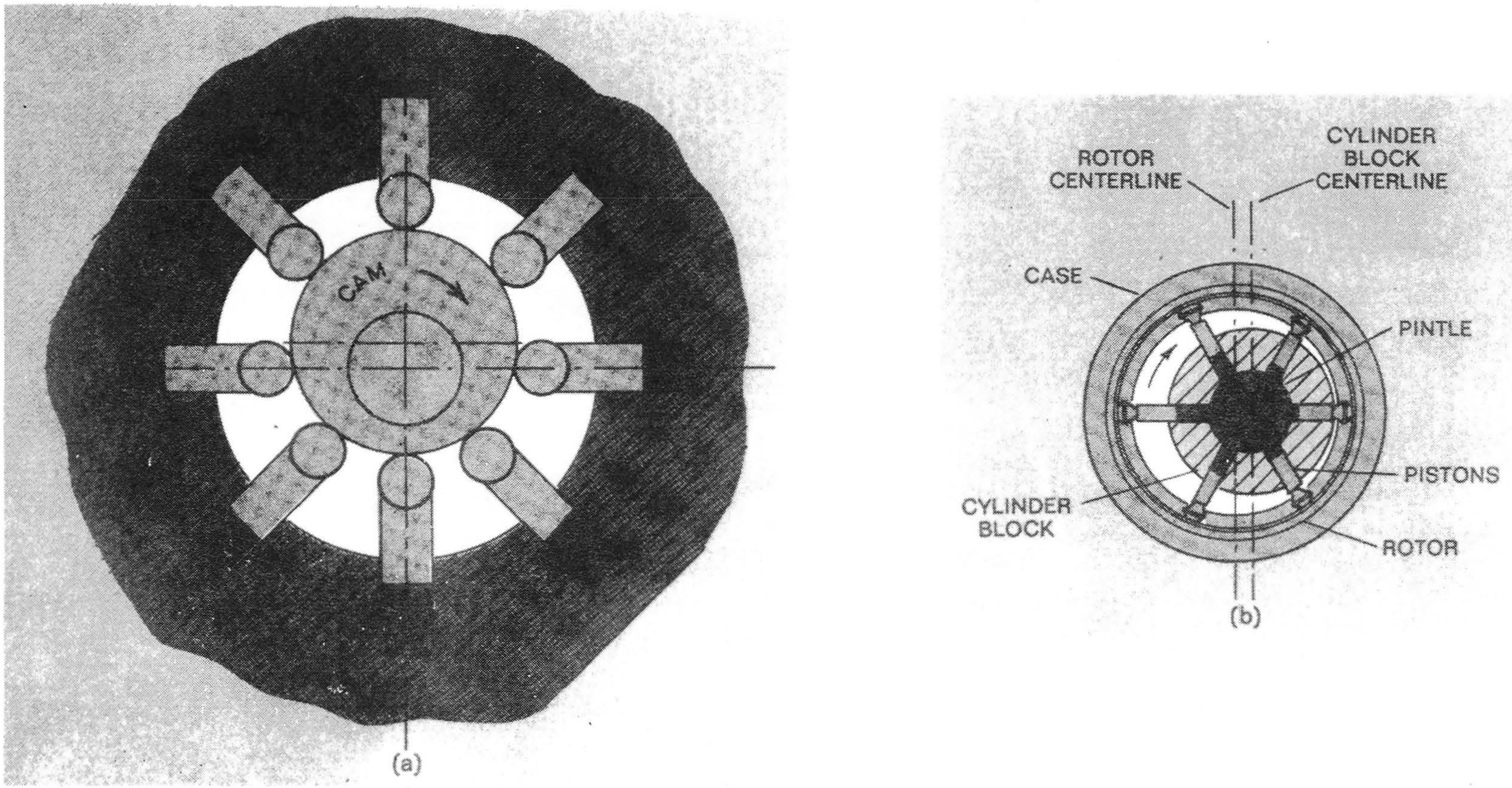

RADIAL PISTON PUMP

Figure 41. Radial Piston Configuration

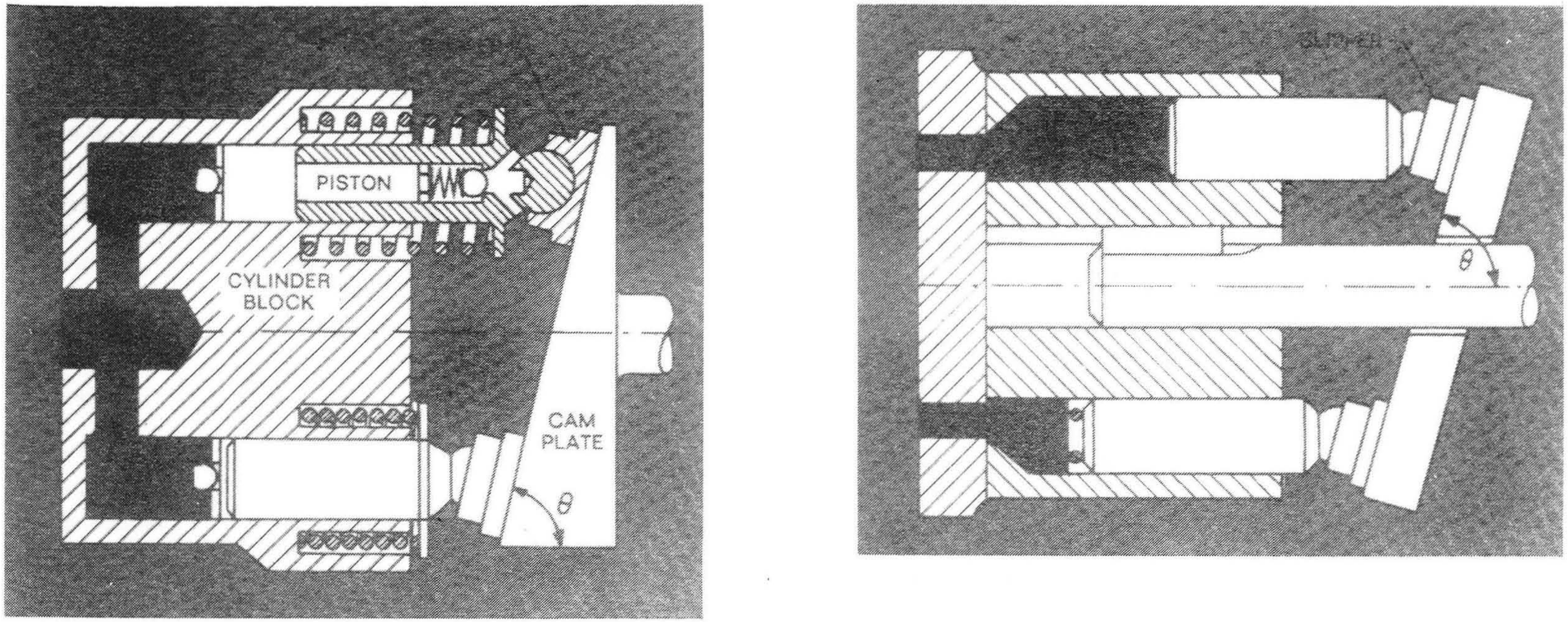

AXIAL PISTON PUMP

Figure 42. Axial Piston Configuration

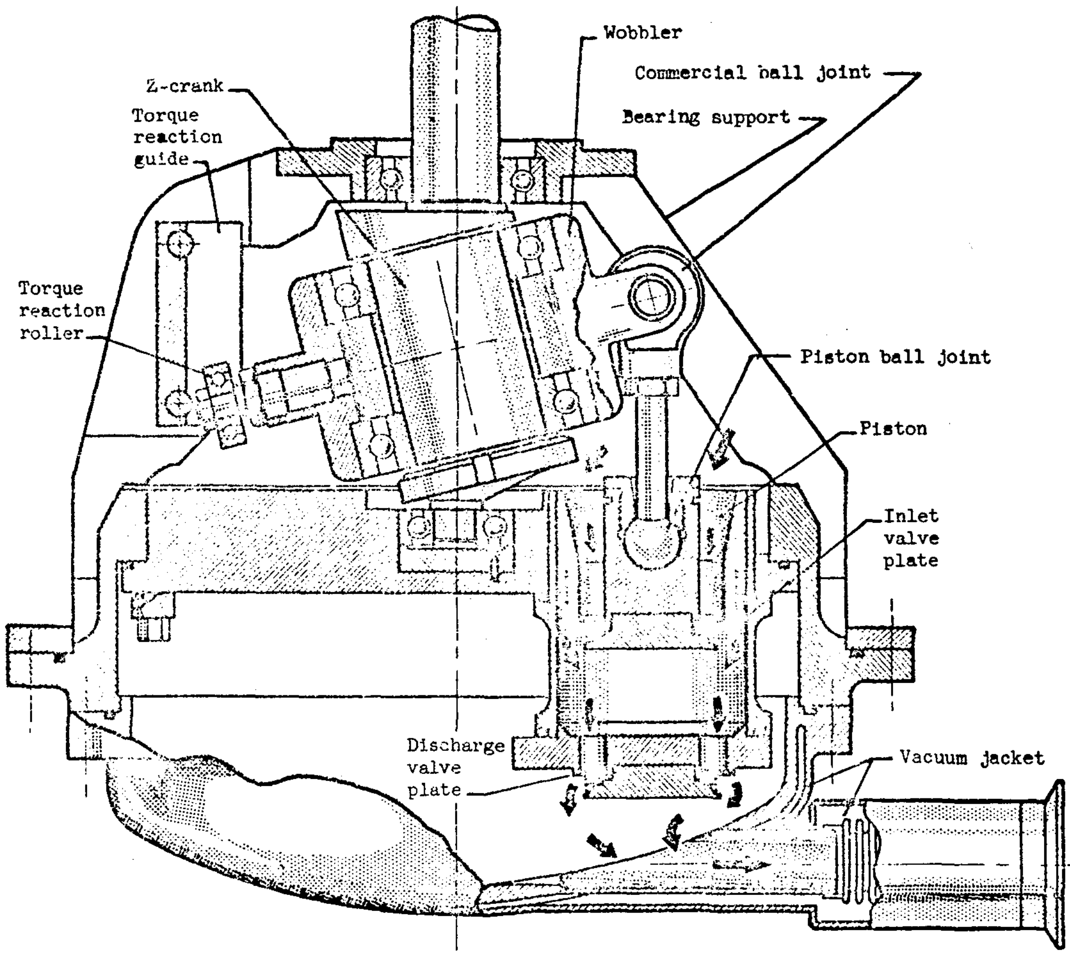

Figure 43. NASA LH_2 Piston Pump

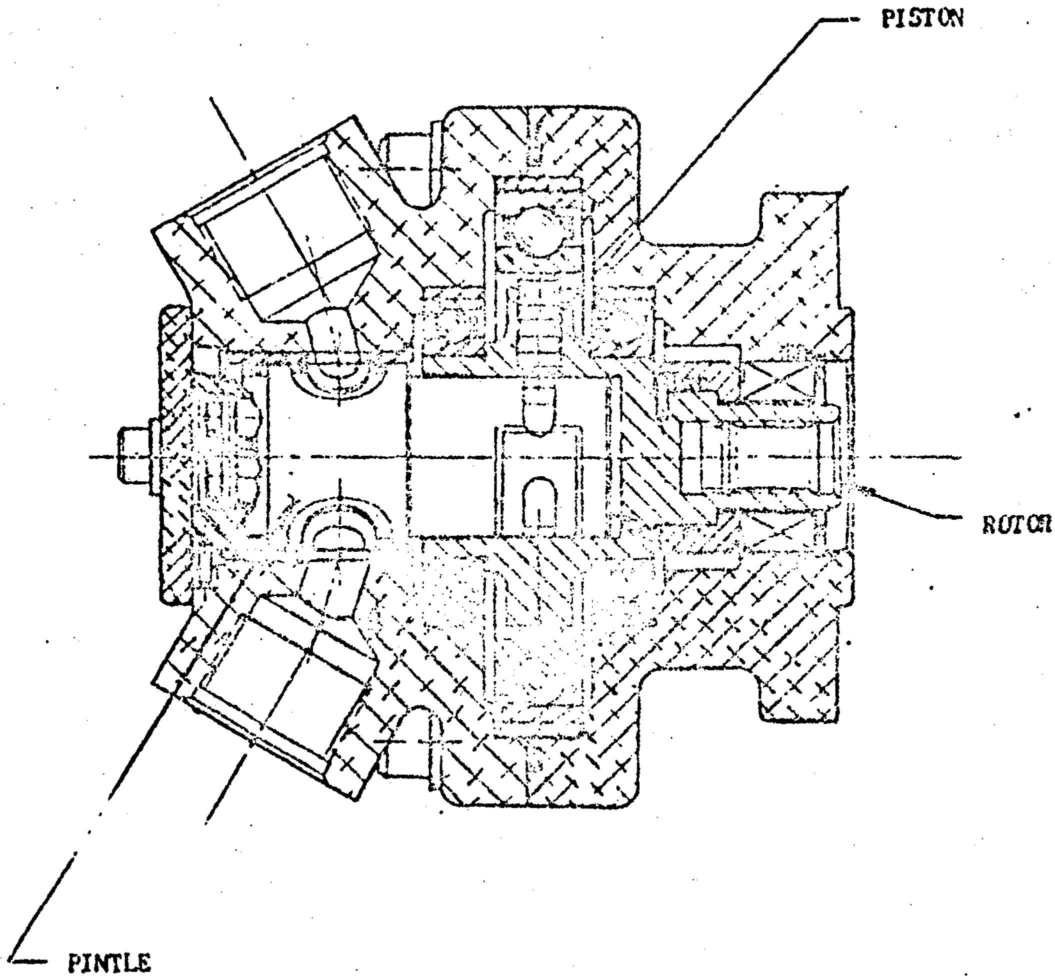

Figure 44. Radial Piston Pump - External Eccentric Rolling Contact Bearings

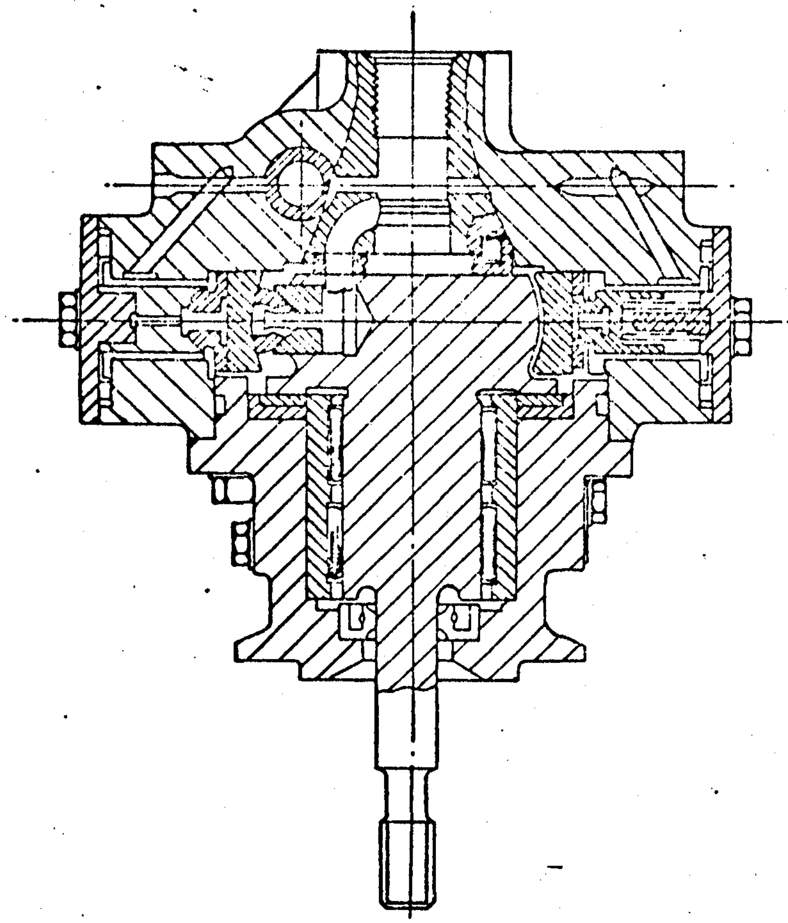

Figure 45. Radial Piston Pump - External Eccentric Fluid Film Bearings

(2) Very high volumetric and overall efficiency has been demonstrated in LH_2 (see Refs. 19 and 20).

(3) Cavitation is typical of positive-displacement pumps. A piston design with small clearance volume is desirable.

(4) Drive speeds are low (20-10,000 RPM).

Some major remaining areas of concern are as follows:

(1) Life is determined by piston rings, piston-to-cylinder, wrist pin, and crank or cam bearing wear characteristics.

(2) Piston pump designs for use with cryogenic fluids are large and heavy.

(3) Reliability is dependent on selected design details, e.g., rubbing and sizing of sliding surfaces.

(4) Pressure pulsations. The amplitude is inversely proportional to the number of pistons and speeds.

4. Lobe and Roots Pump

a. Description

The lobe pump and the Roots blower are basically gear pumps with fewer teeth, usually 2 to 4, as shown in Figure 46. Both types are considered to be positive-displacement pumps, with a discharge pulse occurring with each passing lobe. The Roots blower is usually used for moving gases in supercharging, gas line compression, or driving air into a furnace. As the lobes are not self-driving, they require a second set of drive- or timing gears to keep the lobes synchronized. The action between two full-cycloidal-form rotors uses conjugate gear-tooth action, but the pressure angle between the two varies from 0 to 90 degrees so that one rotor will not drive the other rotor through the whole cycle of operation. This means the clearance (leakage gap) must be large enough to accommodate manufacturing errors and tolerance in both the drive gears and the lobes. The magnitude of this leakage gap causes considerable loss in performance. The advantage of a lobe pump over a gear pump is found in the elimination of fluid being trapped between the lobes and in a larger displacement per revolution which results in fewer deeper pulses.

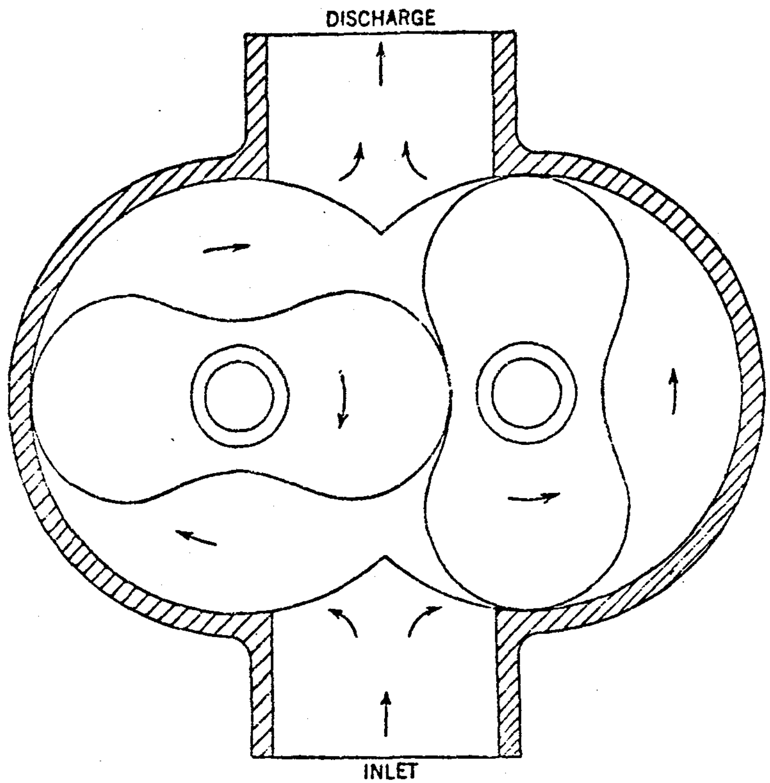

TWO-LOBE ROTARY PUMP.

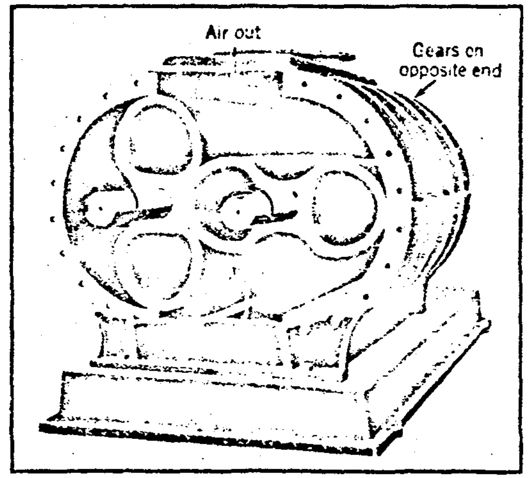

ROOTS BLOWER

Figure 46. Typical Lobe and Roots Pump

b. Literature Review

References 3, 7, 31, and 95 provide the basis for evaluation of the lobe pump. Many pumps of this type have been manufactured and are presently in service. The public utilities use the lobe compressor as displacement meters, low-pressure pipe-line boosters, vacuum gas-well gathering systems, and as a supercharger for gas and diesel engines.

Efficiencies for low-pressure application are as high as 90% but generally fall between 60 and 80% for well-designed (minimum clearance) pumps. Since there is no contact between lobes, the life is very high and determined by the drive gears which operate in oil. The literature search of lobe pumps revealed no experience with cryogenic fluids.

c. Conclusions

The lobe pump appears to be best-suited for operation with gases. Because of high leakage flow, efficiencies in low-viscosity cryogenic fluids can be expected to be very low. For this reason, this concept was dropped from further consideration.

5. <u>Diaphragm Pump</u>

a. Description

The diaphragm pump is considered to be a positive-displacement pump which moves fluid by displacement of a flexible diaphragm. When the diaphragm flexes in one direction, a check or poppet valve opens which allows the pressurized fluid to flow out the discharge side. Flexing in the opposite direction causes another check valve to open. This permits the suction flow to fill the cavity. The diaphragm is driven either by a solid connecting rod, as shown in Figure 47, or by a secondary fluid, as shown in Figure 48. The use of a secondary fluid, usually oil, has the advantage of essentially pressure-balancing the diaphragm, giving it long life.

b. Literature Review

References 7, 97, and 98 were used to evaluate the diaphragm pump. References 7 and 97 describe pumps using a metal diaphragm, and Reference 98 describes a diaphragm pump employing a secondary fluid. The latter type cannot be used with cryogenic fluids since the secondary fluid would freeze, thus only a pump concept where the diaphragm is mechanically attached to the drive rod is practical for use with cryogenics.

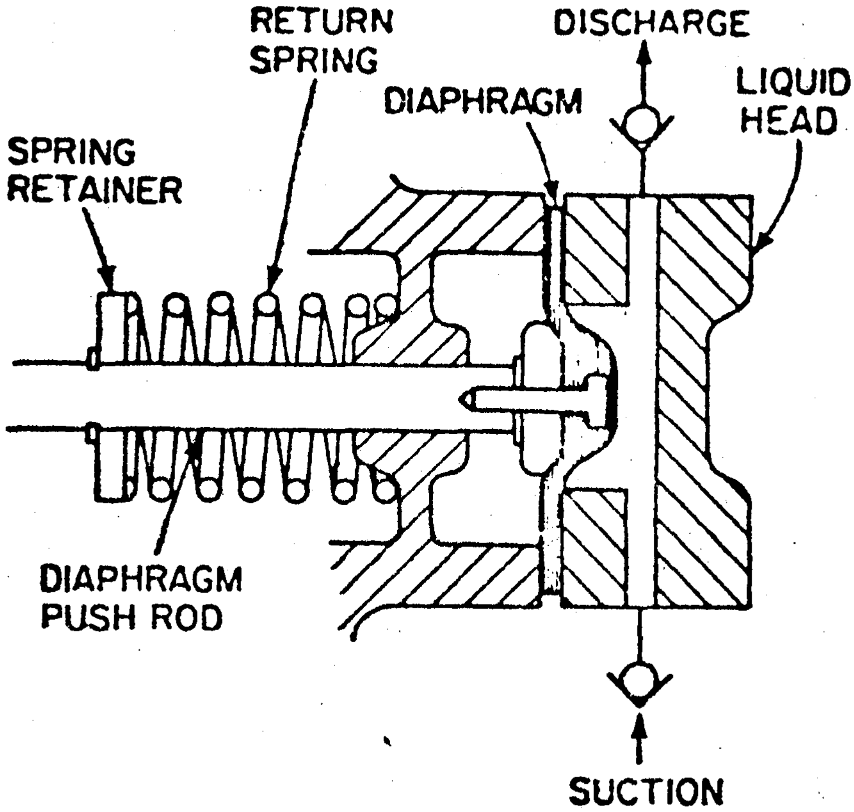

Figure 47. Mechanically Actuated Diaphragm

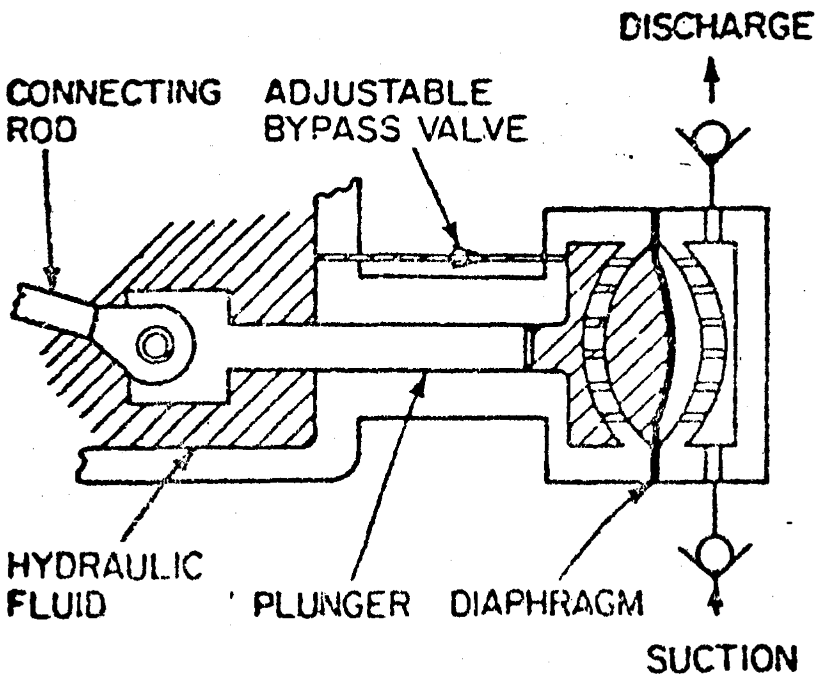

Figure 48. Hydraulically Actuated Diaphragm Pump

As outlined in Reference 98, pressure/flow limits are 1034 kPa (150 psi) and 15.8 cm^3/s (0.25 GPM) with an attached diaphragm and 6895 kPa (1000 psi) and 1260 cm^3/s (20 GPM) with a hydraulically driven diaphragm. The first could possibly be improved by contouring the diaphragm-to-push-rod attachment. As shown in Reference 7, an extension of the state of the art was attained by designing a diaphragm pump with 5 radial double-acting pistons (effectively 10 cylinders) which would deliver 757 cm^3/s (12 GPM) at 10.34M Pa (1500 psi). This design, while not yet built or tested, does have some unique features for extending diaphragm fatigue life at that pressure. The delivery flow is limited to the number of radial pistons that can be arranged, the diameter of the pistons, and the flexing (stroke) of the diaphragm.

The cavitation performance of a diaphragm pump is similar to that of a piston pump. Reference 72 shows where the piston (diaphragm) velocity cannot exceed 2.1 times the square root of the inlet NPSH. The maximum velocity of the diaphragm will equal

$$2 \pi \times \frac{N}{60} \times \frac{S}{2},$$

where N is the speed in RPM and S is the total stroke.

Operation of diaphragm pumps in cryogenics has not been demonstrated.

c. Conclusions

The high flow points specified for this study are not obtainable due to the size and complexity of multi-radial cylinders stacked axially on the shaft. The high pressure points have limiting diaphragm stresses and fatigue life.

One feature which causes the diaphragm pump to have a questionable use in cryogenics is the clearance volume. This is the volume contained between the discharge side of the diaphragm, the discharge check valve, and the suction check valve. This volume will expand irreversibly due to heat transfer and will limit the volume drawn into the suction. If this expansion causes the final state point to fall below the saturation liquid/vapor dome, the liquid will boil and a significant increase in volume will take place, choking the inlet.

As per Reference 7, the efficiency of diaphragm pumps ranges from 30 to 40%. This does not account for the possible re-expansion and boiling at the inlet. If this occurred, the pump would have to be much larger to deliver the same mass flowrate and would consequently be less efficient.

Since the diaphragm pump appears to be limited to the low flow and low pressure rise regimes, has questionable performance in cryogenics, and is life-limited, it was dropped from further consideration.

C. DRIVERS CONSIDERED

1. Gas Turbine Drives

a. Description

The gas turbines required to drive the pumps designed within the pressure flow requirements of Figure 1 have to meet a wide range of power and speed:

PARAMETER	PROPELLANT PUMPED LH_2	LCH_4	LO_2
Speed Range - RPM	37, 500 to 170,000	27,500 to 125,000	10,000 to 45,000
Power Range kw (HP)	1.19 to 57.4 (1.5 to 77.0)	0.373 to 17.9 (0.5 to 24.0)	0.2987 to 17.9 (0.4 to 24.0)

The following types of turbines were considered:

- Axial Flow
- Impulse
- Single Stage
- Full and Partial Admission

An example of a partial-admission turbine (4% admission) is the auxiliary pump drive assembly turbine of the Titan I rocket engine shown in Figure 3.

Gas turbines convert the energy of pressurized gas to shaft power by accelerating the gas through a nozzle at the expense of pressure. The high velocity gases are directed through the moving rotor blades, developing a driving force as the gases are turned by the blading. The resulting force provides the relatively constant torque that is required to drive the pump. Pressure drop across the rotor blading is kept to a minimum by proper selection of blade angles and flow area. Axial thrust on the bearing system is thereby kept to a minimum.

b. Literature Review

Little literature is available on specific design experience with small hot-gas turbines. Specific design descriptions include those for a few very small cryogenic expanders flowing helium (Ref. 38) and very old (Goddard, Ref. 110) or very recent (Ref. 113 and 114) rocket engine turbines. General criteria are summarized in the NASA design criteria handbook on Liquid Rocket Engine Turbines (Ref. 112). General size and efficiency calculations are based in part upon Balje's similarity relationships (Ref. 115).

c. Analysis

Studies conducted for the Low-Thrust Chemical Rocket Engine Study (Contract NAS 3-21940, Ref. 80) indicate that the expander cycle (heated hydrogen) can supply the energy to drive the engine propellant pumps of an oxygen/hydrogen-fueled engine. Cycles include direct drives (shown in Figure 49) and turboalternator-motor drives (shown in Figure 50) as possible gas turbine drive systems. Heated methane has limitations in view of the relatively low energy level of the gas and the temperature being limited by coking at elevated temperatures. The gas generator cycle (shown in Figure 51) has a much higher energy level per unit flowrate but does incur an engine specific impulse loss as it exhausts into vacuum at a lower energy level. Its high spouting velocity may also result in lower turbine efficiency. In view of the unknown engine and propulsion system penalties that might influence the type of drive cycle selected for this study, it was decided to amend the expander cycle for direct drive turbines for the parametric analysis. The investigation limited itself to an evaluation of the following four configurations:

No.	Pump Propellant	Turbine Drive Gas
1	LH_2	GH_2
2	LCH_2	GCH_4
3	LO_2	GH_2
4	LO_2	GCH_4

The turbine evaluations conducted are based on the following assumptions:

- Separate fuel and oxidizer turbopump assemblies.
- Turbines in series.

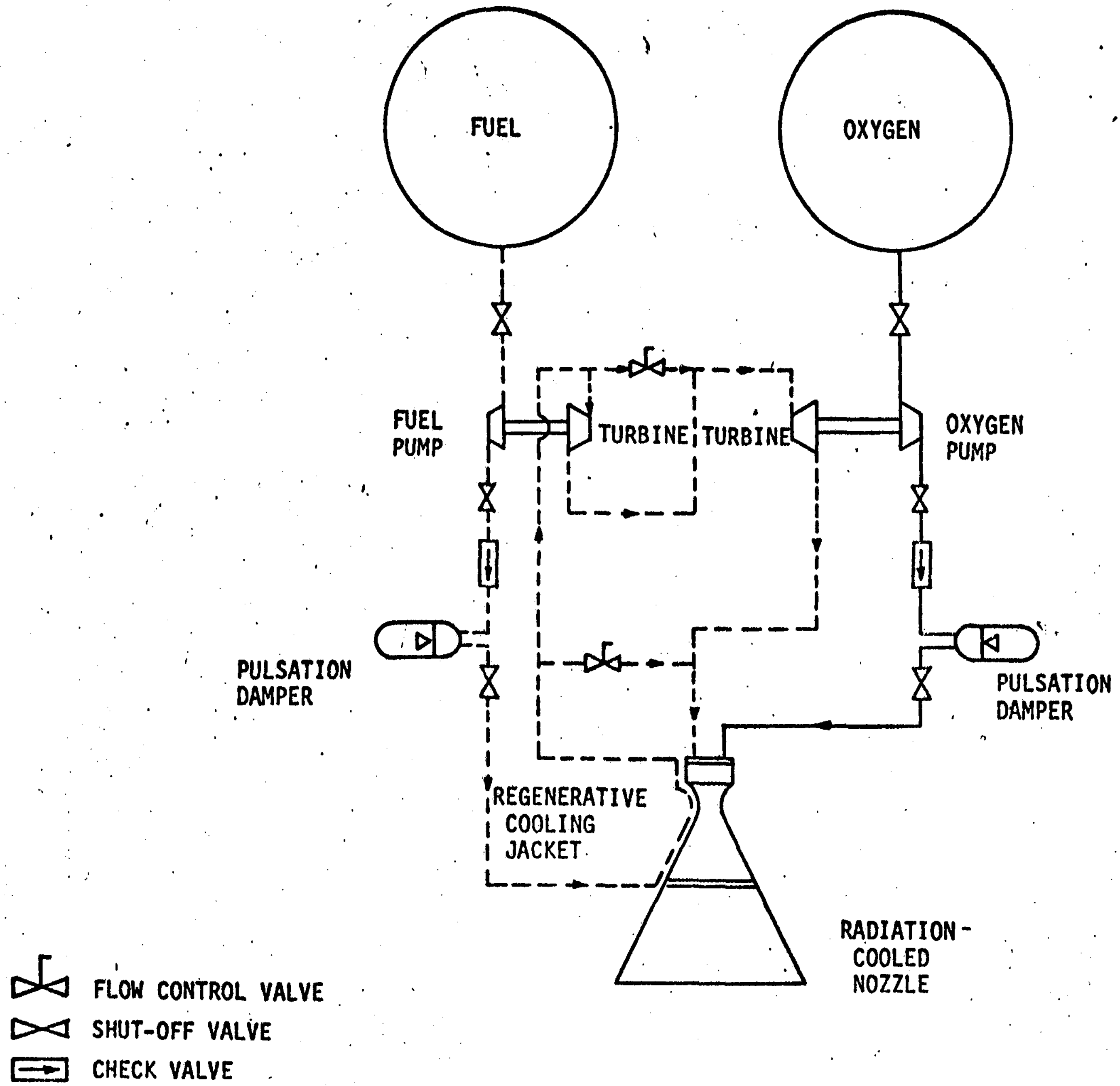

Figure 49. Expander Cycle Flow Diagram

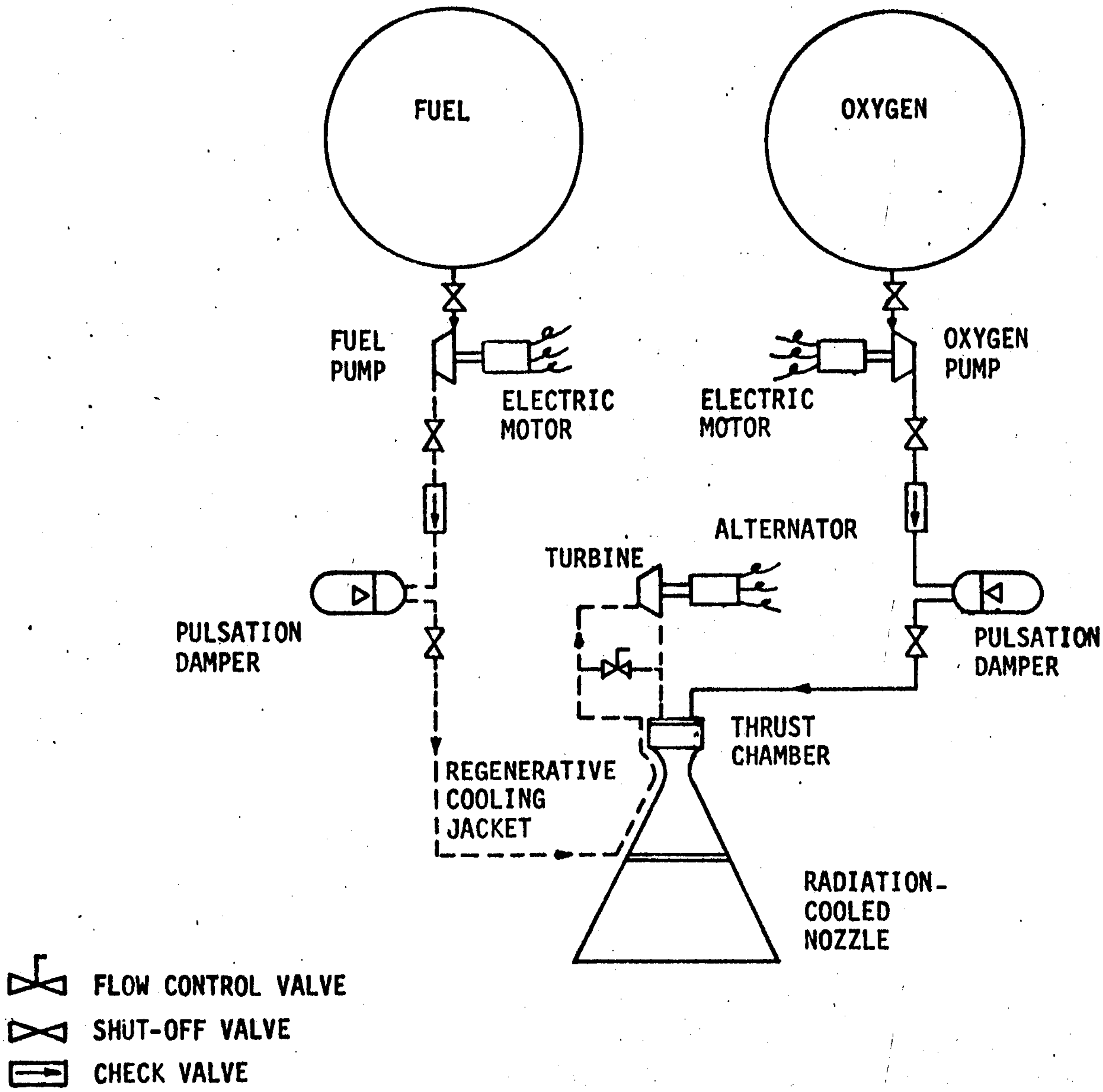

Figure 50. Turboalternator Cycle Flow Diagram

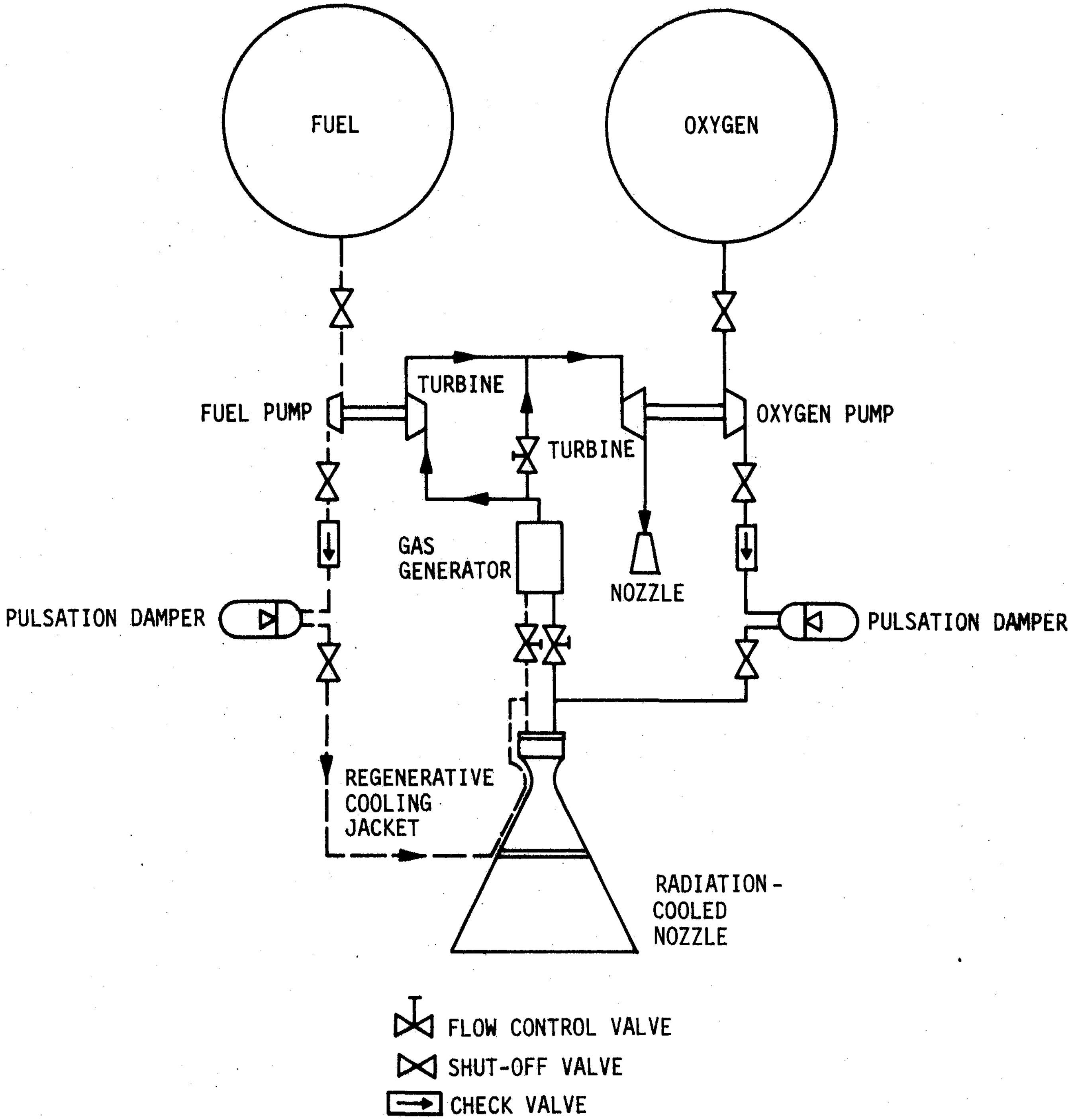

Figure 51. Gas Generator Cycle Flow Diagram

- 100% fuel flow first through fuel pump turbine, then through oxidizer pump turbine.
- Engine mixture ratio is equal to 6.
- Fuel pump turbine inlet pressure is equal to 58% of fuel pump discharge pressure.
- Oxidizer pump turbine inlet pressure is equal to exit pressure of fuel pump turbine.
- Fuel pump turbine inlet temperature is 366°K (660°R) for GH_2 and 555°K (1000°R) for GCH_4.
- All turbines are single-stage, full- or partial-admission types.
- Turbines match pumps which operate at stage levels giving the highest achievable efficiencies for the particular design pressure/flow point.

In this study, the turbine parameters of interest were limited as follows:

(A) Speed
(B) Exhaust Pressure
(C) Efficiency
(D) Admission
(E) Tip Diameter
(F) Blade Height

The analysis was performed with the aid of a computer program called "TURBO." "TURBO" is a design tool to establish preliminary performance and size characteristics of turbopumps. For given interface parameters specifying the pump and turbine fluid and theromodynamic inlet and outlet conditions, the program will determine major turbopump operating conditions. Design constraints in terms of size and operating limits can be imposed, and the program will search for solutions within these limits.

d. Results

(1) It is assumed that the turbine and the pump operate with a single shaft. Therefore, the turbine speeds in the pressure flow maps of Figure 1 are identical with the pump speeds given in Figure 7 for the three propellants.

(2) The loci of the exhaust pressure for the four TPA configurations under consideration are given in Figure 52. The significance of this parameter is that the exhaust pressure of the fuel pump turbine equals the inlet pressure of the oxygen pump turbine, and the exhaust pressure of the oxygen pump turbine equals the inlet pressure to the injector. As can be observed on all four pump-turbine combinations, the turbine exit pressures are generally determined by the pump pressure independently of the pump flow. A secondary influence from the pump flow occurs only in the low-flow regime. There, due to decreasing pump efficiencies, the turbine power needs to be increased which can be accomplished by increasing the pressure drop across the turbine.

The results given in Figure 52 are also useful in determining the rough pressure flow/schedule for either a LH_2/LO_2 - GH_2 or a LCH_4/LO_2 - GCH_4 engine system. The figure gives an example for an oxygen-hydrogen system, as follows:

(1) Select a pressure/flow value for the hydrogen pumps 5515 kPa (800 psi) and 2080 cm^3/s (33 GPM). The flow through the two turbines in series is 2080 cm^3/s (33 GPM).

(2) The 755 cm^3/s (12 GPM) flow for the oxygen pump is determined by the engine system mixture ratio.

(3) The hydrogen pump turbine inlet pressure (3199 kPa (464 psi)) is 58% of the discharge pressure. The hydrogen pump turbine exit pressure (2758 kPa (400 psi)) is obtained from Figure 52.

(4) The oxidizer pump turbine inlet pressure is assumed to be equal to the hydrogen pump turbine exit pressure (2758 kPa (400 psi)). The exit pressure of the oxidizer pump turbine is within 5% of the inlet pressure (2620 kPa (380 psi)). This 5% value is valid throughout the power range of all oxidizer turbines considered.

(5) The available oxidizer pump discharge pressure is obtained from Figure 52 (4309 kPa (625 psi)). The available pressure drop in the oxidizer system is then obtained to be 56%.

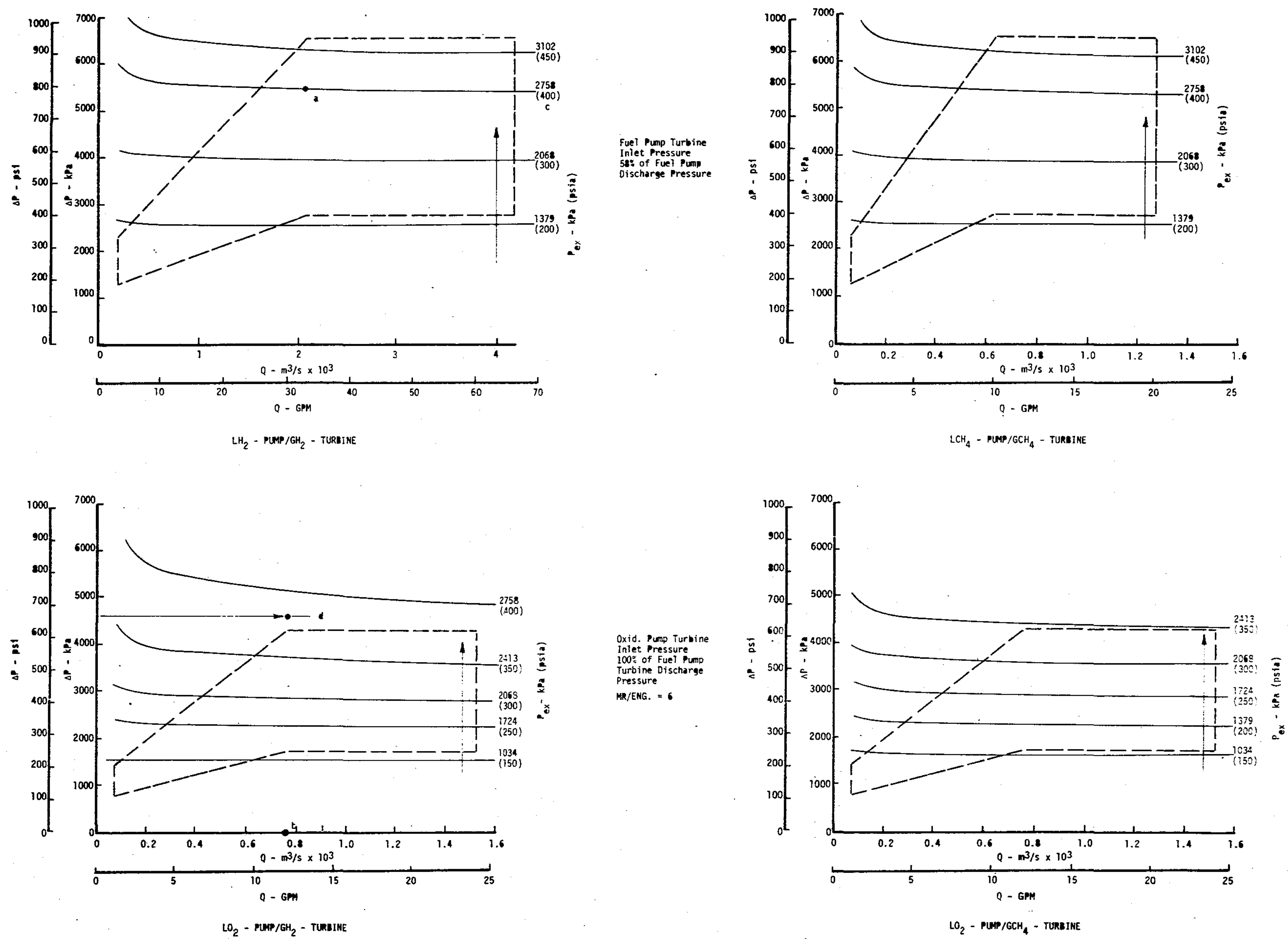

Figure 52. Loci of Constant Exhaust Pressure in the Pressure/ Flow Map

The following exit pressure values can be obtained over the range of interest:

TPA Configuration	Exit Pressure, kPa	Exit Pressure, psi
LH_2/GH_2	689 - 3240	100 - 470
LO_2/GH_2	689 - 2620	100 - 380
LCH_4/GCH_4	689 - 3240	100 - 470
LO_2/GCH_4	689 - 350	100 - 350

The higher exit pressures are obtained at the higher pump discharge pressures.

The loci of constant turbine efficiency for the four TPA configurations are given in Figure 53. As can be seen, the turbine efficiency lines are generally parallel to the pump discharge pressure lines, indicating their insensitivity to pump and turbine flow. In the low-flow regime, the flow has an influence insofar as higher pump discharge or equivalently higher turbine inlet pressures are required to maintain constant efficiencies. The following efficiency values can be obtained over the range of interest.

TPA Configuration	Efficiency, %
LH_2/GH_2	74 - 82
LO_2/GH_2	68 - 82
LCH_4/GCH_4	76 - 82
LO_2/GCH_4	68 - 82

The high efficiencies are obtained at the low pump discharge pressures.

The loci of constant turbine admission for the four pump-turbine combinations are given in Figure 54. Again it is primarily the pressure which determines the amount of admission. The flow becomes only of significance in the low-flow regime. The following admission values are required:

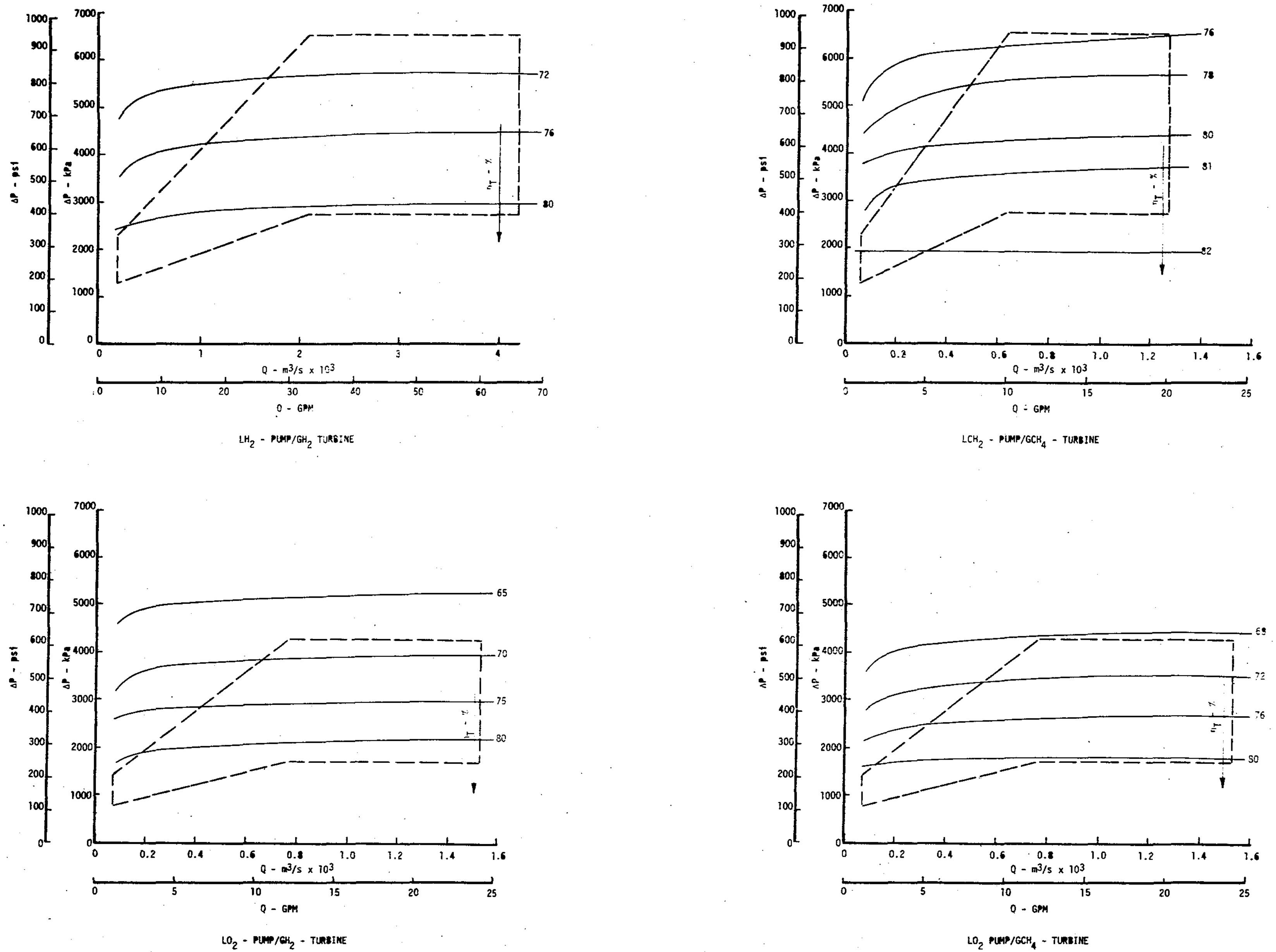

Figure 53. Loci of Constant Turbine Efficiency in the Pressure/Flow Map

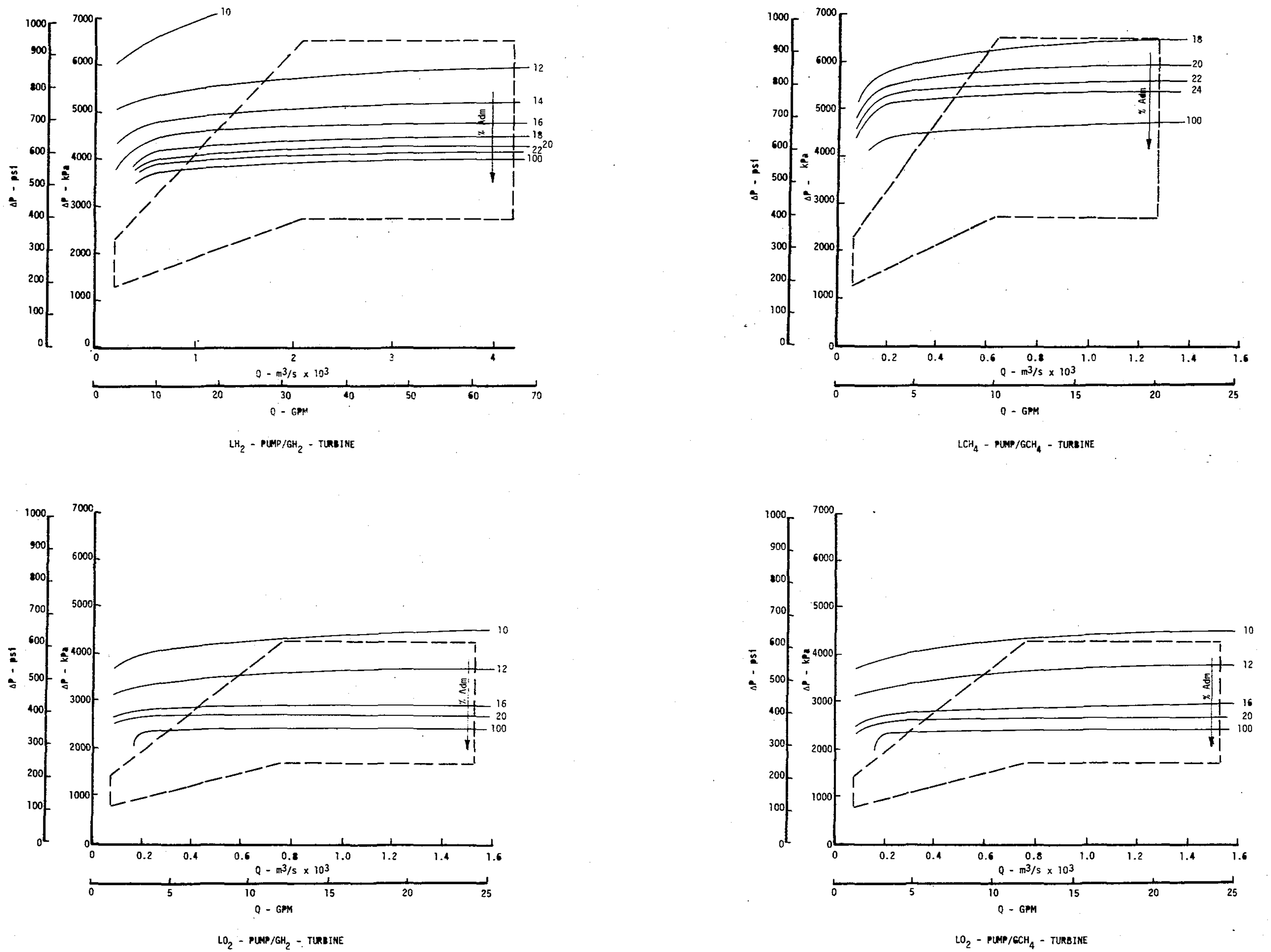

Figure 54. Loci of Constant Admission in the Pressure/Flow Map

TPA Configuration	% Admission Partial 5% - 22% kPa (psi)	Full 100% kPa (psi)
LH_2/GH_2	above 3792 (550)	below 3792 (550)
LO_2/GH_2	above 2913 (350)	below 2413 (350)
LCH_2/GCH_4	above 5171 (750)	below 5171 (750)
LO_2/GCH_4	above 2413 (350)	below 2413 (350)

The loci of constant turbine tip diameter are given in Figure 55. The tip diameters are basically a function of the pump flow, in the sense that larger flows require larger tip diameters. In the high-pressure regime, i.e., in the regime utilizing partial-admission turbines, both fuel and oxidizer turbines require larger tip diameters than the turbines in the mid-range pressure regime. The same is true for the fuel turbines in the low-pressure regime where full-admission, high-efficiency turbines are utilized. The oxidizer turbines, on the other hand, do not exhibit this behavior. Although the curves show the same trend in the low-pressure regime, the extent of curving back on the graph is not pronounced enough to result in the minimum values in the mid-pressure range that were observed for the fuel turbines.

The following turbine tip diameters are required to cover the pressure flow range of interest:

TPA Configuration	Tip Diameter, cm (in.)
LH_2/GH_2	2.54 to 15.3 (1.0 to 6.0)
LO_2/GH_2	3.8 to .24 (1.5 to 9.3)
LCH_4/GCH_4	2.03 to 8.4 (.8 to 3.3)
LO_2/GCH_4	2.54 to 16.6 (1.0 to 6.5)

The lower and higher limits apply to the low-flow and high-flow applications, respectively.

The loci of constant blade height are given in Figure 56. The locus which divides the turbines in partial- and full-admission engines is also shown in the plot of Figure 56 because, at this line, the blade heights change

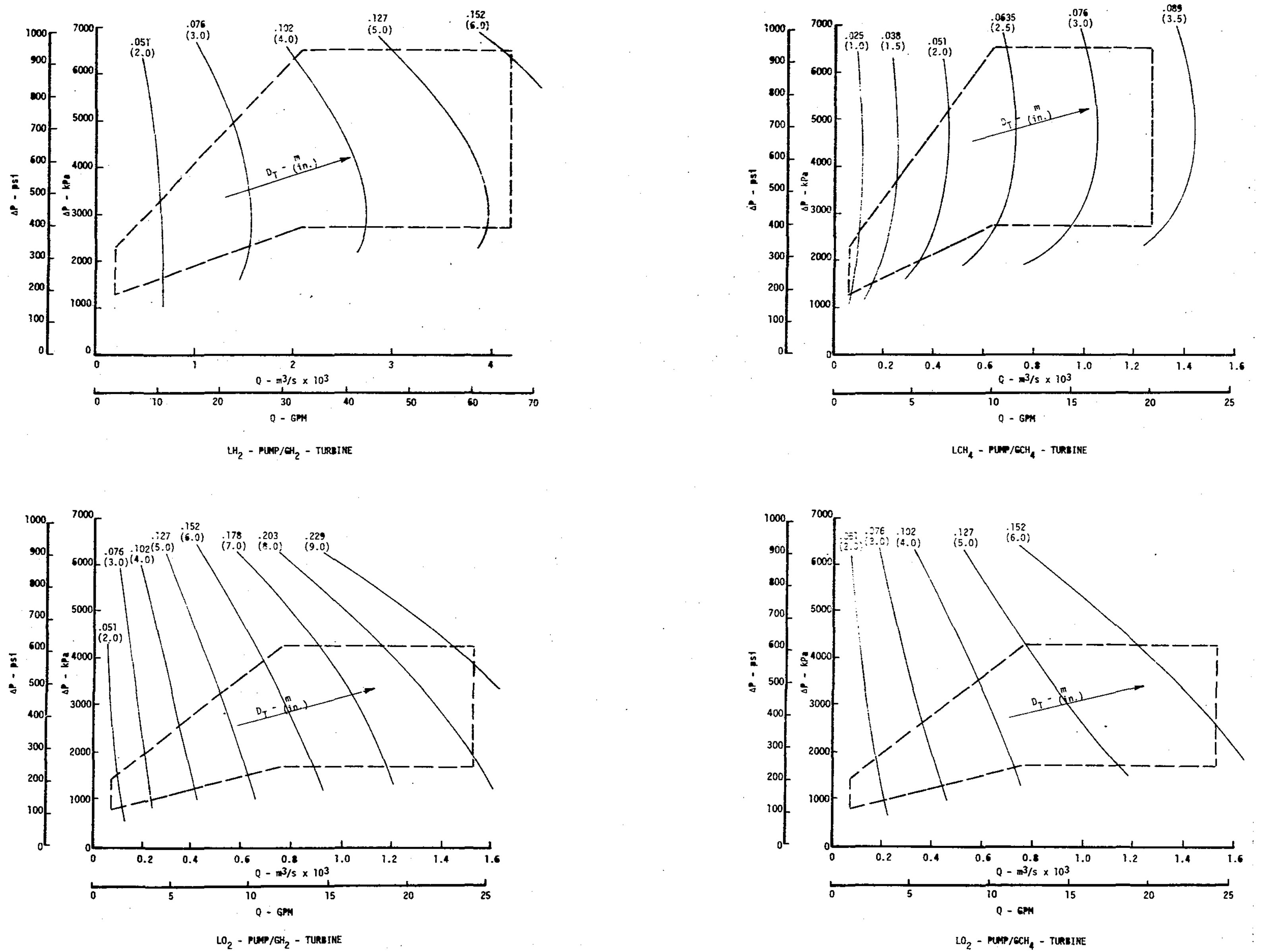

Figure 55. Loci of Constant Turbine Tip Diameter in the Pressure/ Flow Map

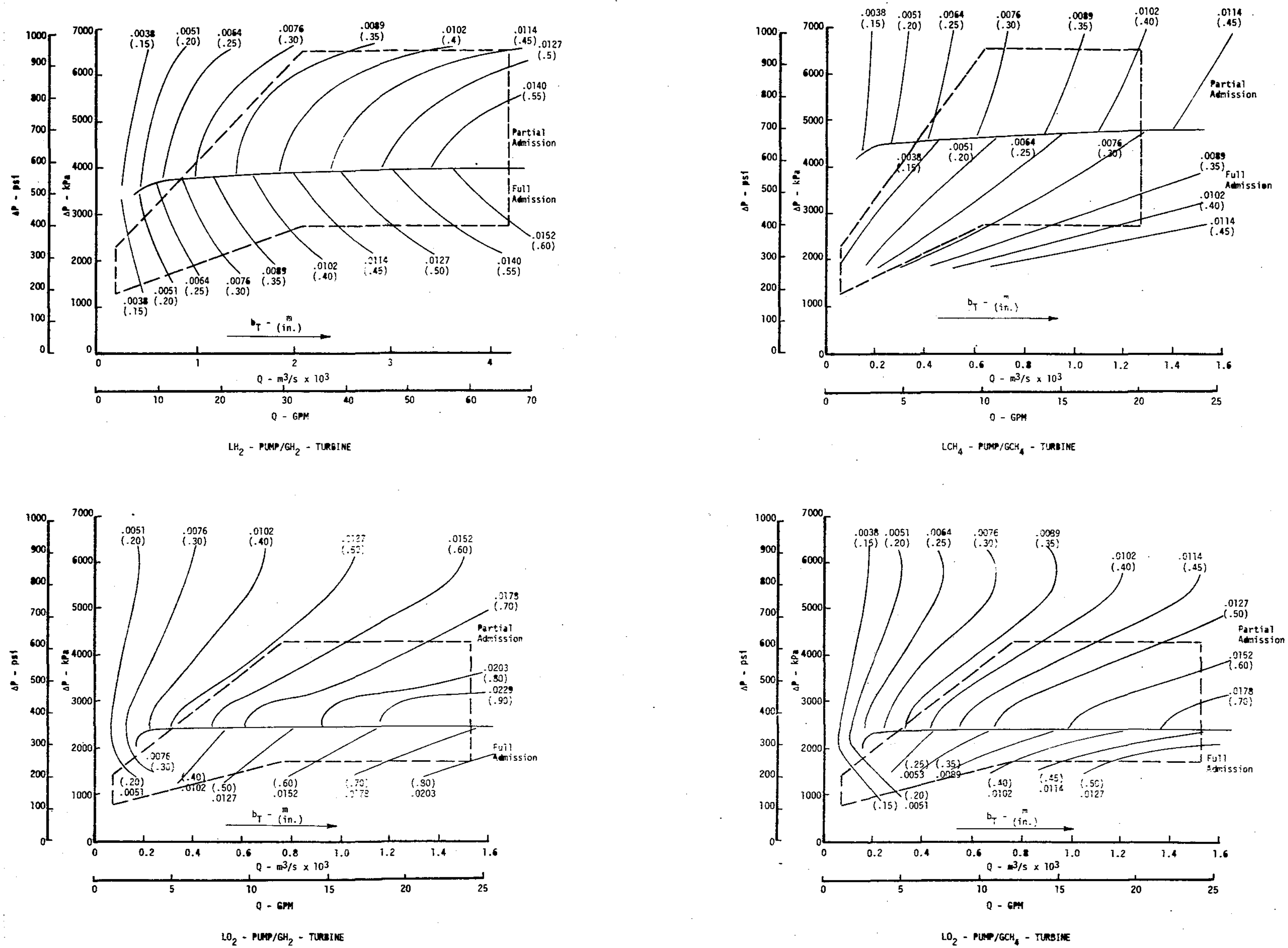

Figure 56. Loci of Constant Blade Height in the Pressure/Flow Map

abruptly. This blade height discontinuity does not come as a surprise as it is already incorporated in Balje's turbine map which was used as the basis for this analysis (see Ref. 3 and 115).

The blade heights required to cover the pump pressure/flow regimes of interest are as follows:

TPA Configuration	Blade Height, mm (in.)
LH_2/GH_2	3.8 to 16.6 (0.15 to 0.65)
LO_2/GH_2	3.8 to 25.4 (0.15 to 1.00)
LCH_4/GCH_4	3.8 to 11.5 (0.15 to 1.45)
LO_2/GCH_4	3.8 to 17.8 (0.15 to 0.70)

It is important to recognize that for blade heights under 7.6 mm (0.30 in.), special efforts are required to control the blade tip clearance if the efficiencies predicted in Figure 53 are to be maintained.

e. Conclusions and Recommendations

Single-stage turbines are feasible over the entire pressure/flow maps given in Figure 1. These turbines do vary over a wide range of size and specific speed, but they do not require new design methods except that, for blade heights below 7.6 mm (0.30 in.), special consideration must be given to the blade tip clearance. The predominant design deficiency is the lower efficiency which occurs in the high-pressure region of all pump-turbine combinations.

f. Summary of Gas Turbine Evaluation

(1) Pressure/Flow Map

Gas turbines can be designed to meet the speed and power conditions of all three propellant pressure/flow maps.

(2) Efficiency

Efficiencies of gas turbines designed to meet centrifugal pump power-speed requirements range from 68 to 82%. The lower efficiencies occur in the high-pressure portion of the map.

(3) Life

Life can easily be met for the relatively low-temperature gas turbine drives assumed for the expander cycles.

(4) Weight

Gas turbines are relatively light drivers with a range of 0.122 to 1.22 kg/kw (0.2 to 2.0 lb/HP).

(5) Size

Gas turbines are relatively small drivers with a range of 4.3 to 21.5 cm^3/kw (0.2 to 10 $in.^3$/HP).

(6) Reliability

A high reliability may be expected for the relatively cool gas turbines that are required to match engine system requirements.

(7) Cost

Conventional design methods and materials make gas turbines a relatively inexpensive driver.

(8) Drive System Requirements

Gas turbines match the power/speed requirements of centrifugal pumps over their full range.

(9) Start Transient Characteristics

Acceleration rates of all gas turbines are more than adequate for this application, in spite of the relatively slower rate of the partial-admission turbines compared to those with full admission.

(10) Confidence in Meeting Life Requirements

There is no question that gas turbines meet the life requirements.

(11) Confidence in Meeting Predicted Performance

There is a high confidence level in gas turbines meeting the predicted performance requirements.

(12) Maintainability

Gas turbines for the applications considered require little maintenance.

2. Electrical Drive Systems

a. Description

The electrical drive system assumed for this study is comprised of electric motors mounted integral with the pumps and operated from turboalternators, generators, or fuel cells. Ancillary equipment includes solid-state inverters for operating AC machines from DC power supplies and cycloconverters for operating permanent magnetic motors from permanent magnetic alternators.

(1) Motors - Candidate motors include polyphase induction (squirrel cage), permanent magnet (PM), and convential DC brush motors.

The conventional squirrel cage induction motor consists of a wound stator, laminated rotor stack with bare, solid aluminum, or copper bars cast or pressed into peripheral slots, bearings, and end bells.

Except for the rotor assembly, the design and construction of the PM motor are similar to that of the induction motor. Figure 57 consists of a rotor assembly drawing for a 200-kva (268-HP) machine. Figure 58 depicts one of the seven rotor disk assemblies (Ref. 106). The rotor (field) magnets are contained by a shrink ring which consists of bimetallic sections that have been welded together. The disk assemblies are assembled to the shaft by cooling the shaft in liquid nitrogen and pressing it into the seven disk assemblies all at once while they are held in an aligning fixture. When compared on the same speed/horsepower basis, the PM motor stator is identical to that of the polyphase induction motor except for certain detail dimensioning differences.

The conventional brush-type DC motor consists of solid magnetic iron field pole pieces, wound armature, commutator, and brushes.

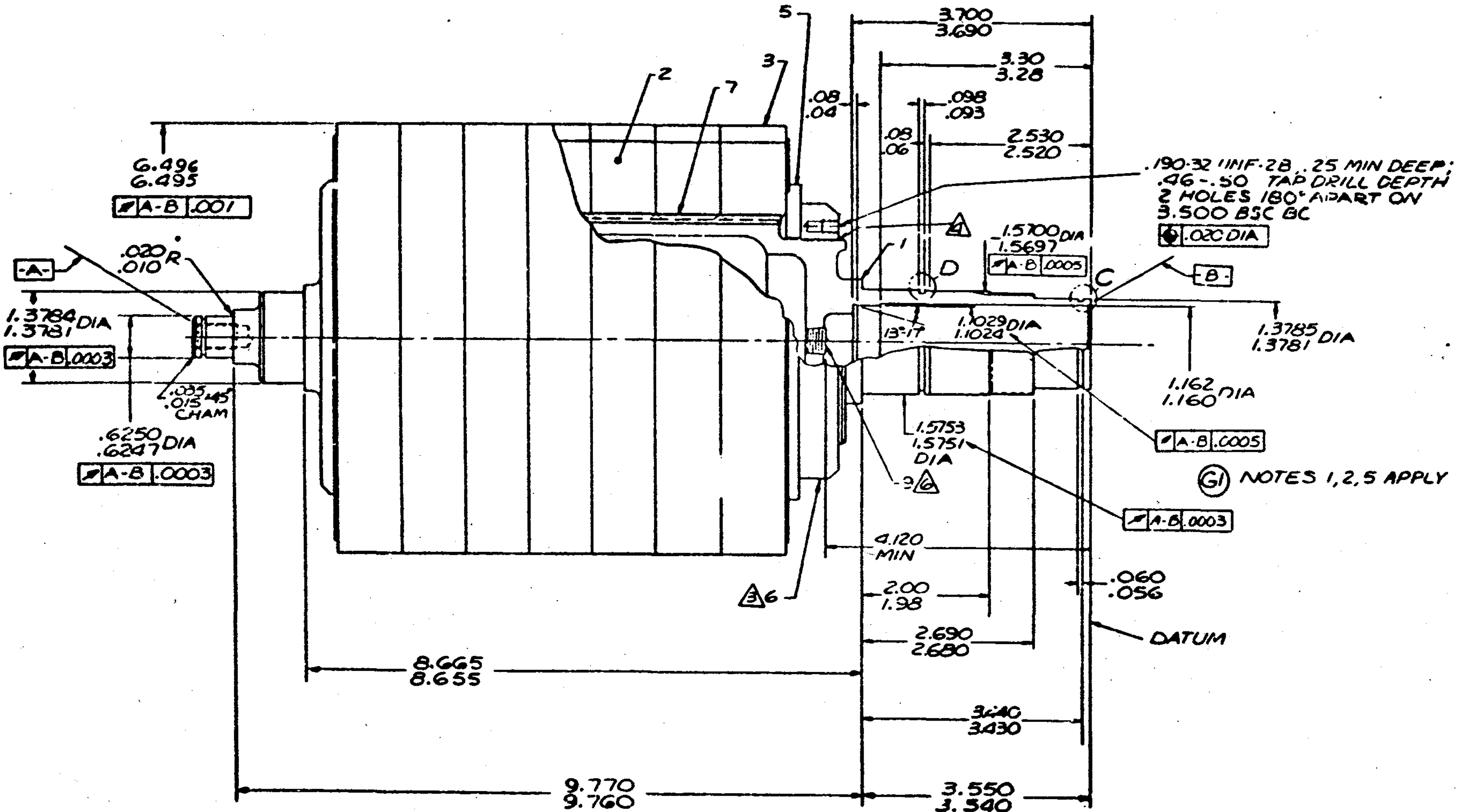

Figure 57. Rotor Assembly - Induction Electric Motor

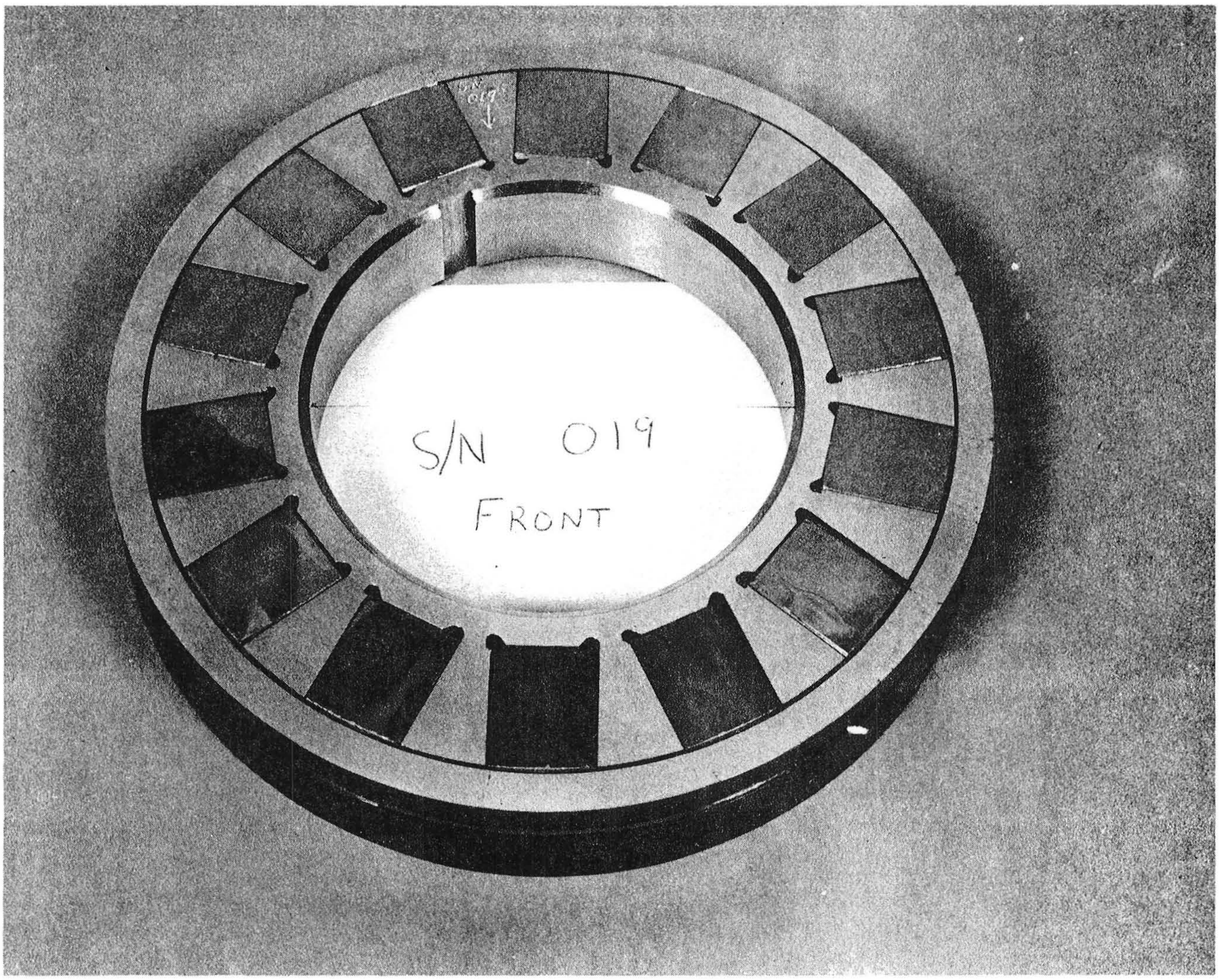

Figure 58. Disk Assembly - Induction Motor Rotor

The shaft, bearings, retainers, end bell, and housing materials for all three machines were selected for their compatible thermal expansion coefficients over the operating cryogenic temperature range and to preclude interference at 70°F. The induction motor rotor bars (and end rings) are fabricated from special copper alloy materials (bronze) to provide the high resistance necessary for producing the required stall torque (usually about 1.5 x run torque) at cryogenic temperatures. The performance of motors designed for cryogenic service is degraded at ambient temperatures because of the increased winding resistance; however, no-load operation is possible at that temperature.

All three motor designs have been successfully operated while submerged directly in liquid helium. Cryogenic induction motors have seen service as pump drives submerged in liquid hydrogen, such as on the Saturn program.

(2) Alternators - Candidate alternators include the following designs:

AC Brushless (Wound Rotor)
AC Permanent Magnet
AC Induction or Lundel (Homopolar)
DC Generator

The AC brushless alternator is widely used in aerospace and, along with the DC generator, constitutes the "conventional" design. Field excitation is provided by a permanent magnet alternator mounted in tandem with the rotor assembly. The (3-phase) PM alternator output is rectified by means of a full wave bridge mounted in the rotor assembly to provide DC to the rotor field windings. The construction of the rotor assembly limits the rotational velocity to about 12,000 RPM for machine ratings up to about 30 kva. Current development is aimed at increasing ratings to 90 kva at this speed.

The AC permanent magnet alternator design/construction is essentially identical to that of the PM motor described above.

The induction (homopolar) or Lundel (bonded rotor) alternator consists of a conventional stator and winding, a solid (or solid bonded) rotor fabricated from high strength magnetic materials, and separate DC excitation via coil windings located behind or between the stator windings. Magnet polarity of the field flux is determined by the rotor configuration and the relative location of the exciter windings. Unidirectional flux paths are established through the rotor and the stator back iron. This significantly increases the size/weight of the machine compared to that of other designs.

However, the solid rotor configurations permit rotational speeds of 1.5 to 2 times that of the other designs.

The DC generator design/construction is essentially the same as that of the DC motor.

(3) Batteries/Fuel Cells - The hydrogen/oxygen fuel cell power plant developed by Pratt & Whitney (Ref. 111) for the Space Shuttle was reviewed as a potential candidate for the pump drive electrical system. The power density curves of Figure 59 reflect this basic design, scaled up to provide 115-120 volts output by connecting 4 of the basic 30-volt power plants in series.

The basic power plant is a low-temperature alkaline unit which employs an electrolite solution of potassium hydroxide contained in an asbestos capillary matrix. The only identified maintenance item is the CO_2 scrubber which has a design life of 2000 hours.

Major elements are the reactor stack, thermal and reactant controls, water removal system, and startup controls. Waste heat is removed via liquid coolant pumped through the plant to a suitable heat rejection system. Product water is removed from the reactor stack by circulating hydrogen steam, then condensed and delivered to a suitable water storage system. Electrical power is generated in the reactor stack which consists of 99 liquid-cooled cells assembled between two steel honeycomb end plates. Hydrogen and oxygen supplied from the vehicle are preheated and scrubbed of CO_2 before flowing through the reactant regulator to the stack. Water storage and heat rejection system weights are not included in the curves shown in Figure 59.

In a similar manner, silver-zinc aerospace battery assemblies manufactured by Yardney Electric Corporation were reviewed as possible candidates for the pump drive electrical system energy source. Weight versus energy curves for this type of cell are shown in Figure 60. As shown in Figures 59 and 60, the enormous weight penalties incurred for fuel cells and batteries in general preclude their being considered as feasible electrical pump drive energy sources.

(4) Electrical Systems - The following electrical systems (comprised of the electric motors, alternators, DC generator, and fuel cell design described above) are considered feasible candidates for further consideration as pump driver elements and will be referenced periodically in the remainder of the report.

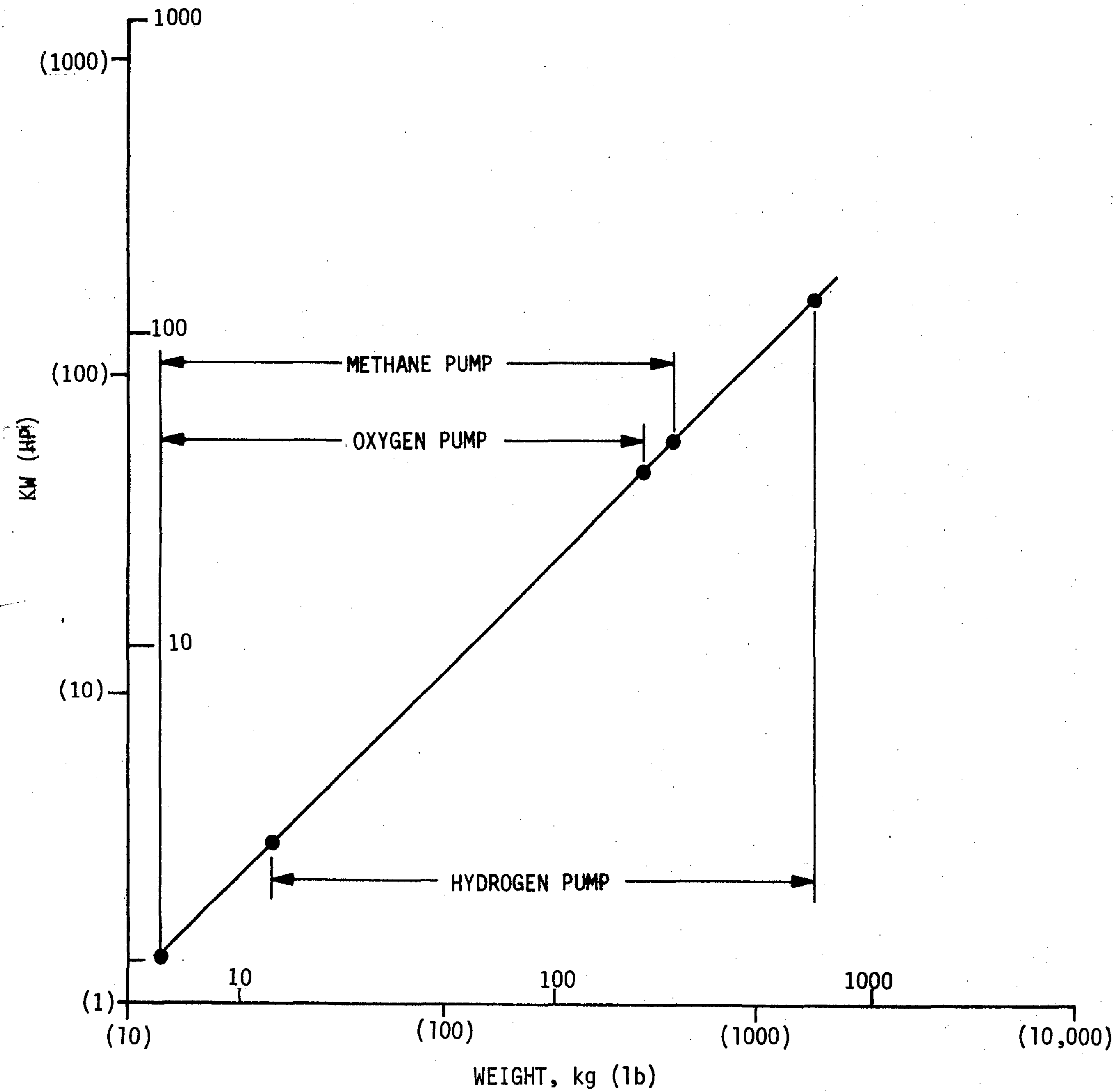

Figure 59. Hydrogen/Oxygen Fuel Cell, Power Versus Weight

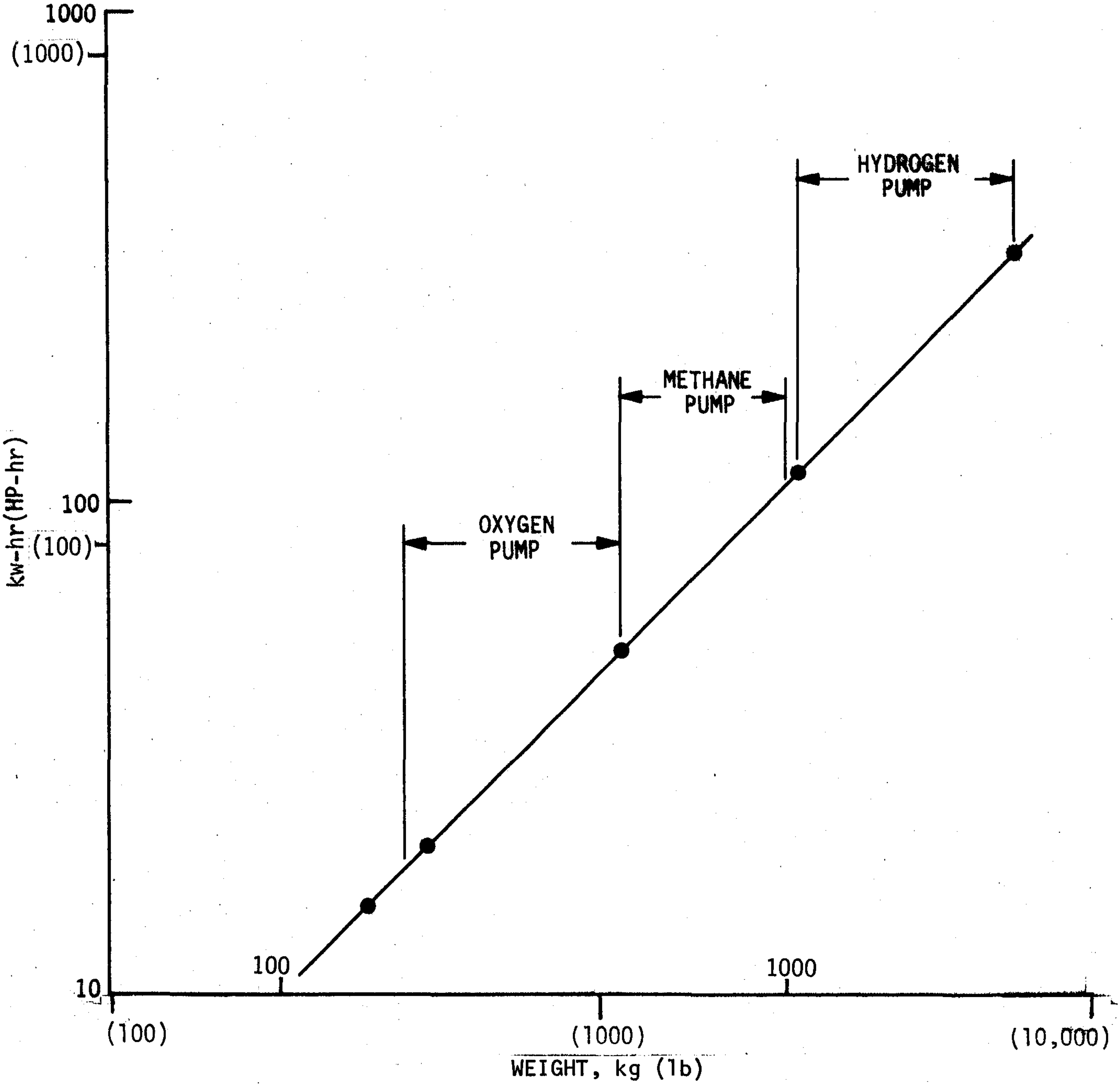

Figure 60. Silver-Zinc Battery, Power Versus Weight

System Number	System Description
(1)	Fuel Cells or DC Generator/DC Motor
(2)	Fuel Cells or DC Generator/Inverter/PM or Induction Motor
(3)	Brushless Alternator/PM or Induction Motor
(4)	PM Alternator/Induction Motor
(5)	PM Alternator/Cycloconverter/PM Motor
(6)	Induction or Lundel Alternator/PM or Induction Motor
(7)	DC Generator/DC Motor

b. Literature Review

Supplier and literature reviews provided the following weight and performance data for AC alternators, batteries, and fuel cells (Ref. 57 through 61). Electric drive motor data were updated and assessed in terms of the pump load/speed ranges for each of the three propellant pumps. Weight versus power/speed and efficiency curves were generated for electrical system components which reflect the pump loads/speeds presented in Figure 61.

c. Analysis

Motors - Figures 62 through 66 present motor weight, speed, and horsepower for AC induction (squirrel cage), permanent magnet (PM), and conventional brush-type DC machines plotted against pump horsepower/speed for the respective hydrogen, methane, and oxygen pumps. Motor selections and weights are based upon operation at cryogenic temperature (50-75°K), (90-135°R), with the weights including electromagnetic (core, rotor, and winding), shaft, bearing, and end bell weights. Figure 67 delineates these components.

Induction and DC motor size versus horsepower/speed ranges were determined from internal design files and discussions with suppliers. PM motor electromagnetic weight (EM_W) and performance data were supplied by AiResearch and General Electric for a range of PM machines being developed for aerospace, military, and industrial applications. These data are scaled for cryogenic environments based on induction motor configurations. Total PM weights are determined by the following equation (Ref. 104):

$$W_T = EM_W + C_W(EM_W)$$

where C_W = ranges from 1.2 to 1.8

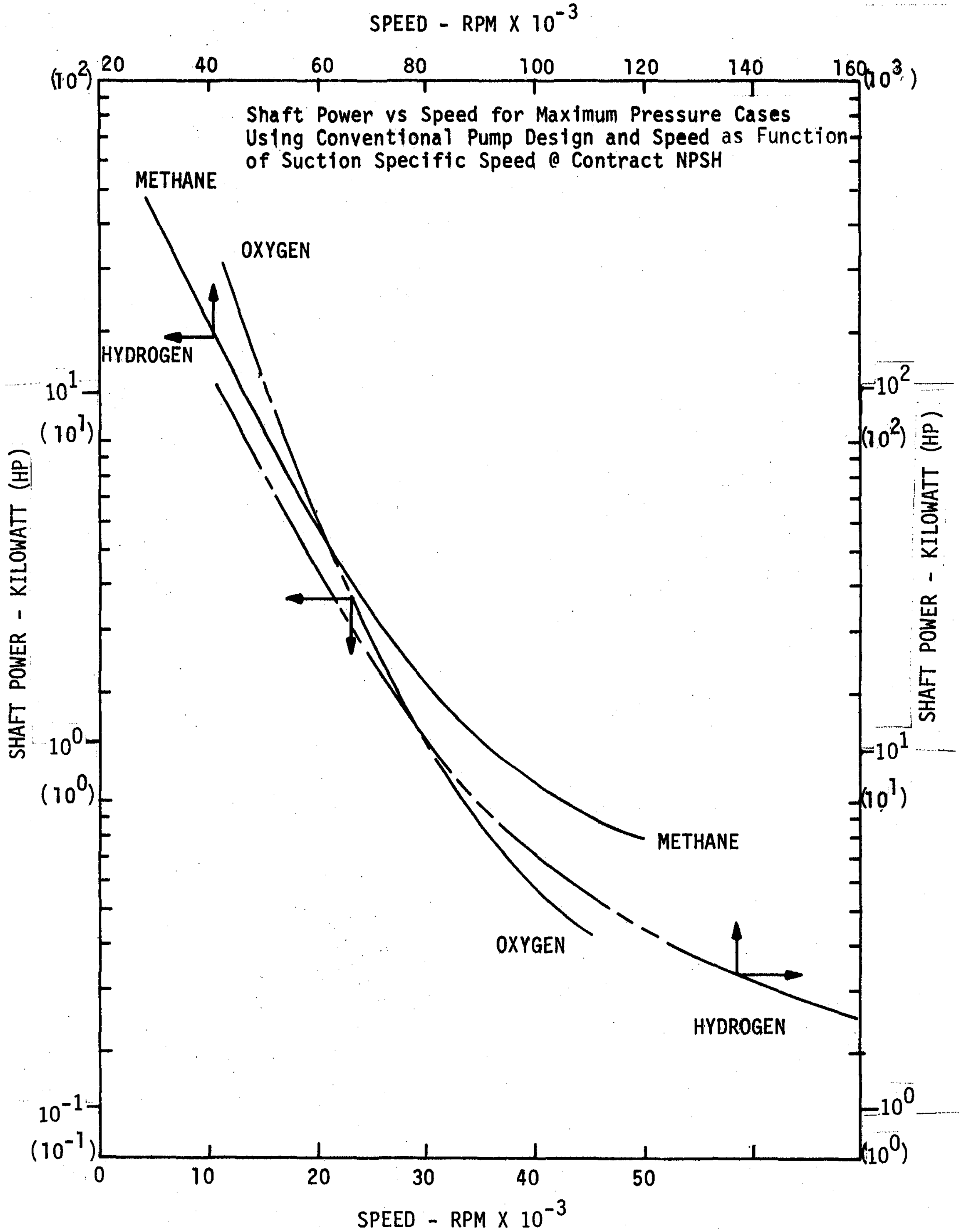

Figure 61. Preliminary Pump Shaft Power Versus Speed

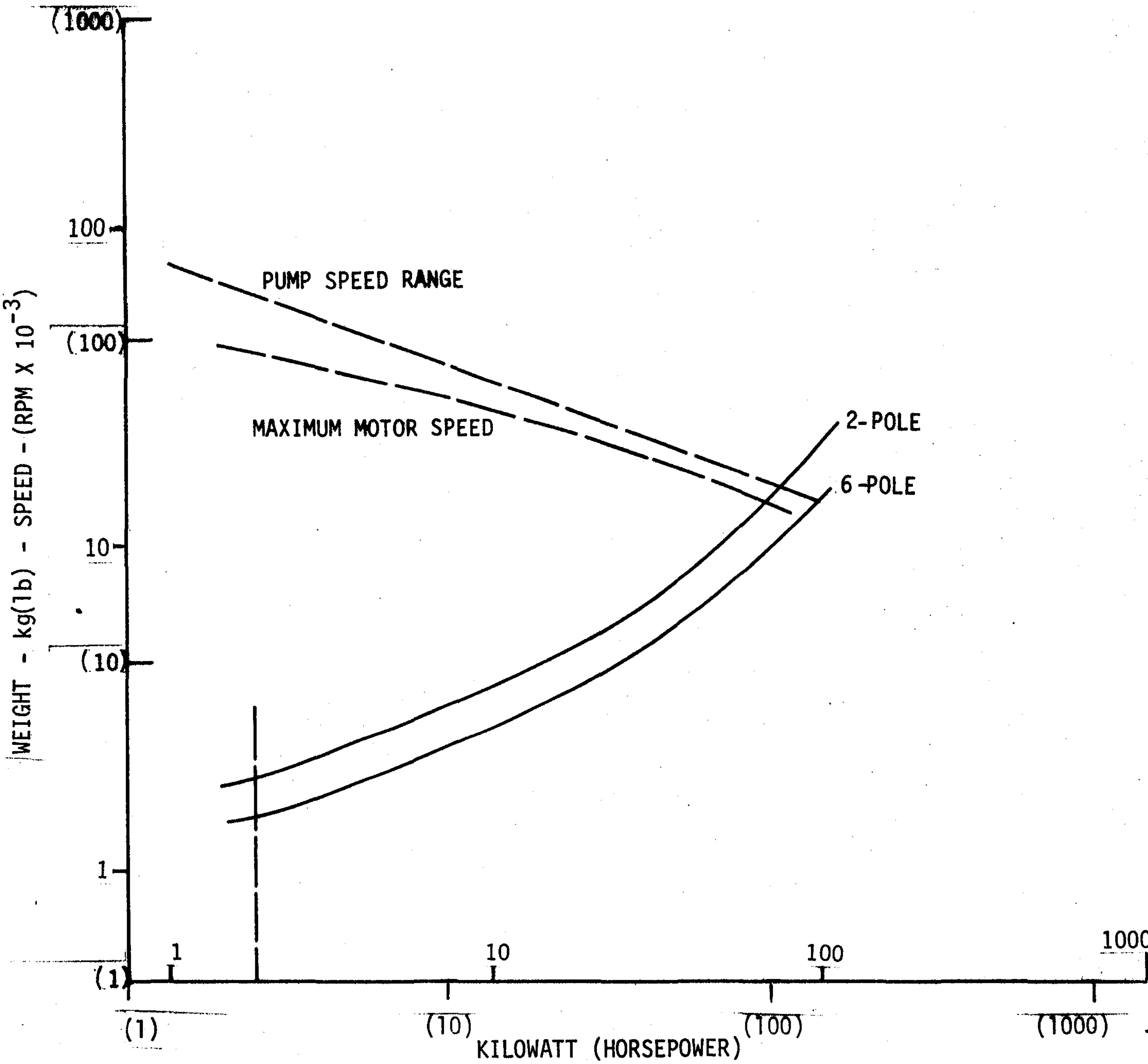

Figure 62. Hydrogen Pump Induction Motor - Weight and Speed Versus Power

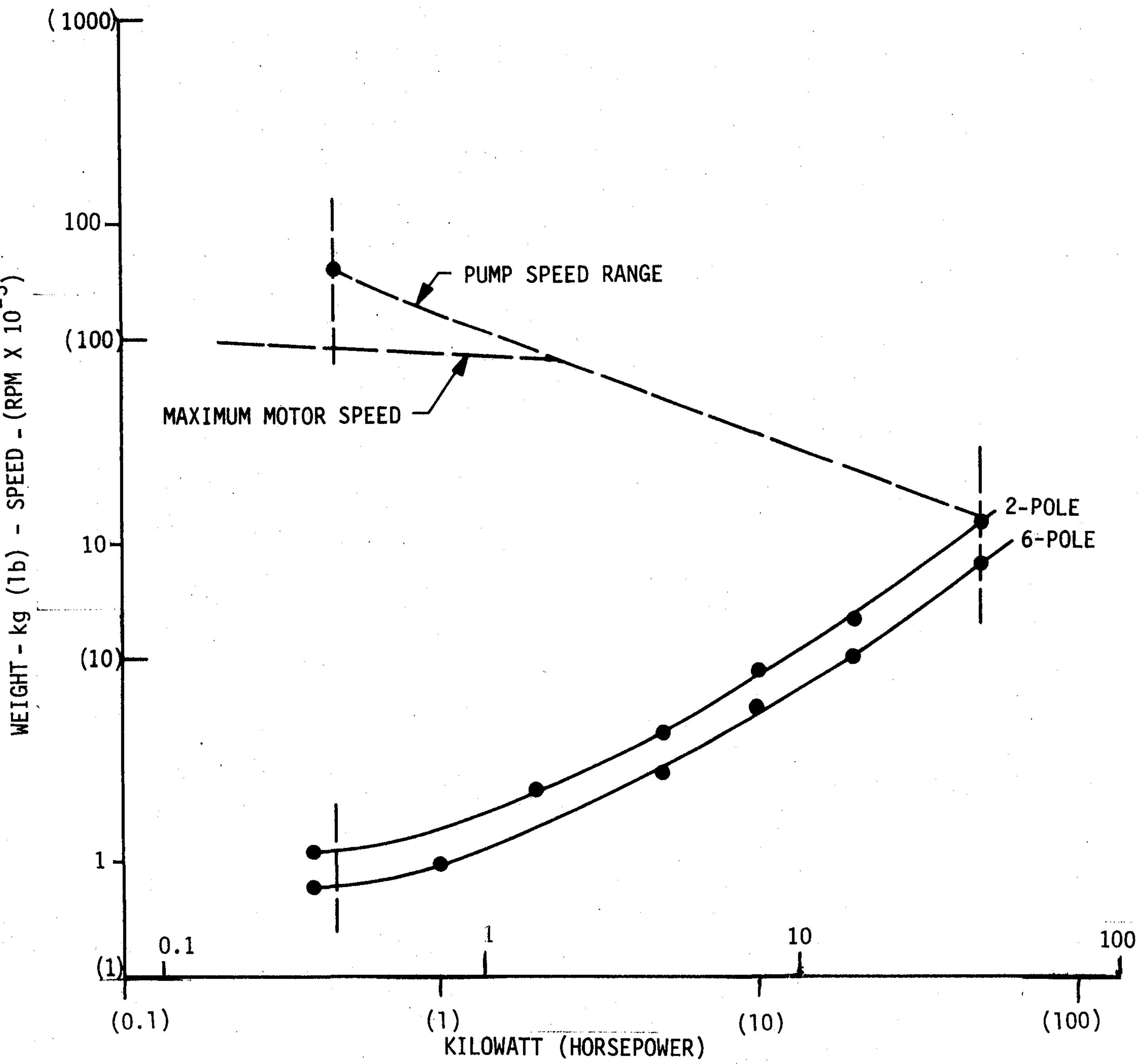

Figure 63. Methane Pump Induction Motor - Weight and Speed Versus Power

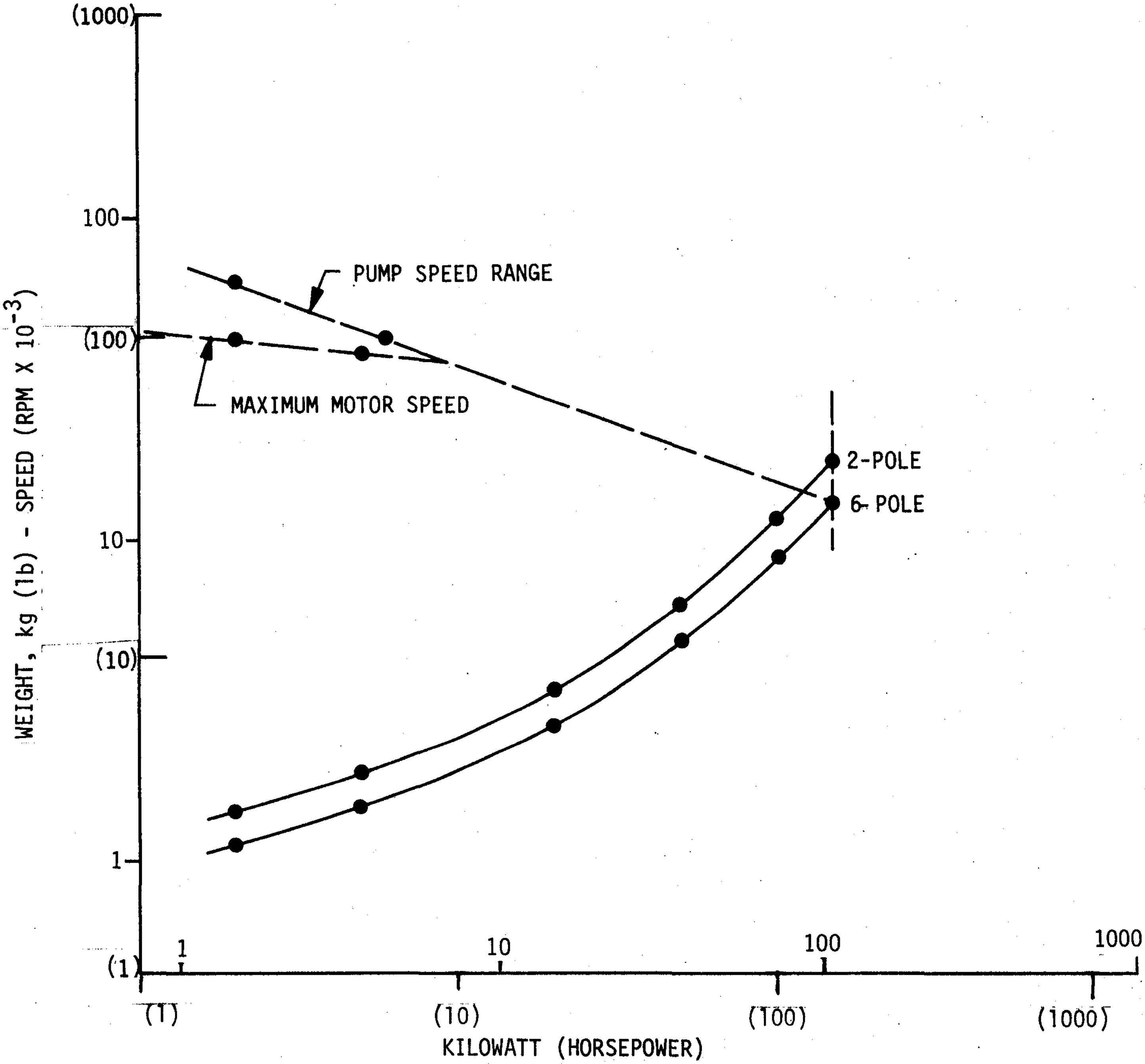

Figure 64. Hydrogen Pump Permanent Magnet Motor - Weight and Speed Versus Power

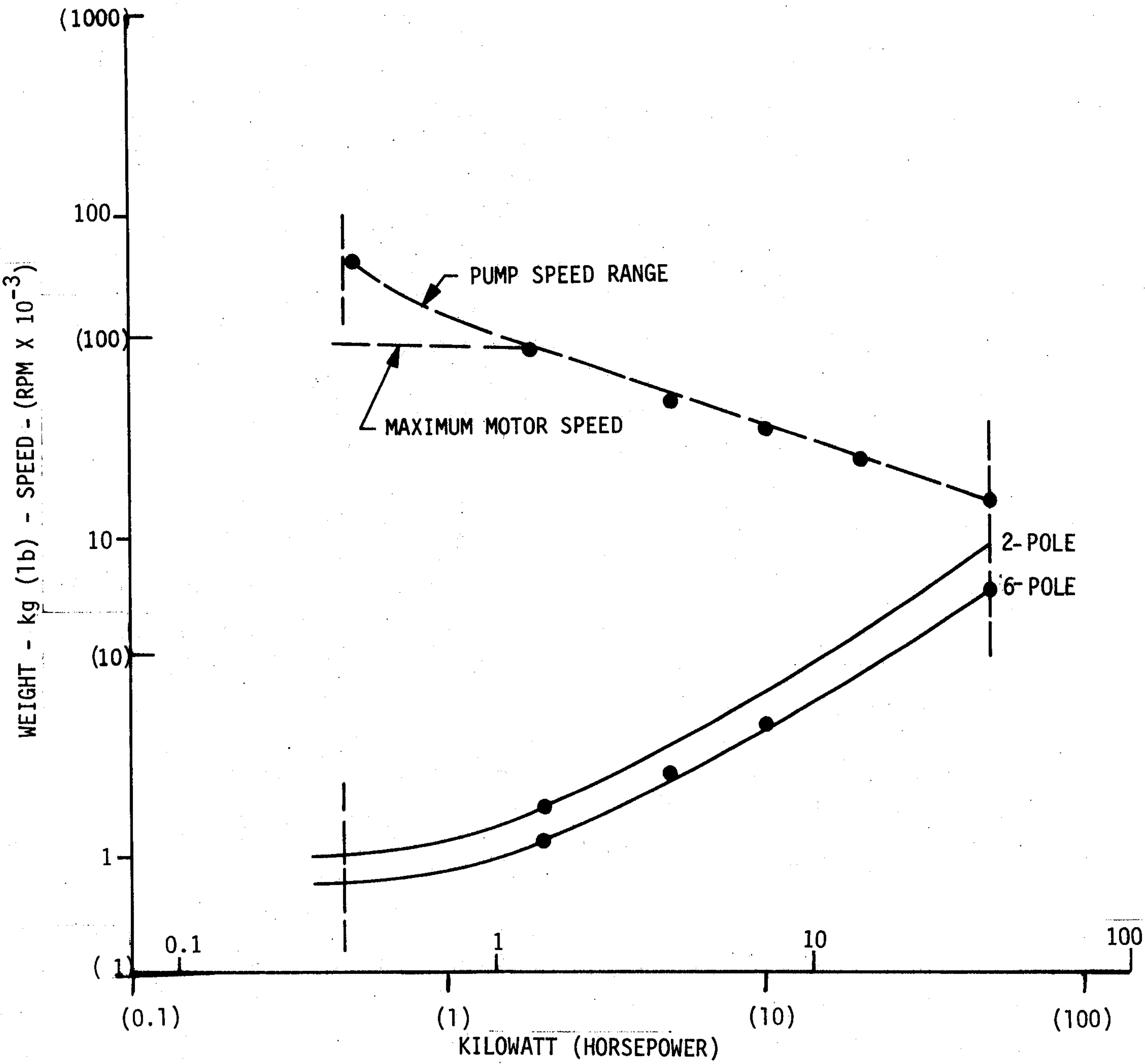

Figure 65. Methane Pump Permanent Magnet Motor - Weight and Speed Versus Power

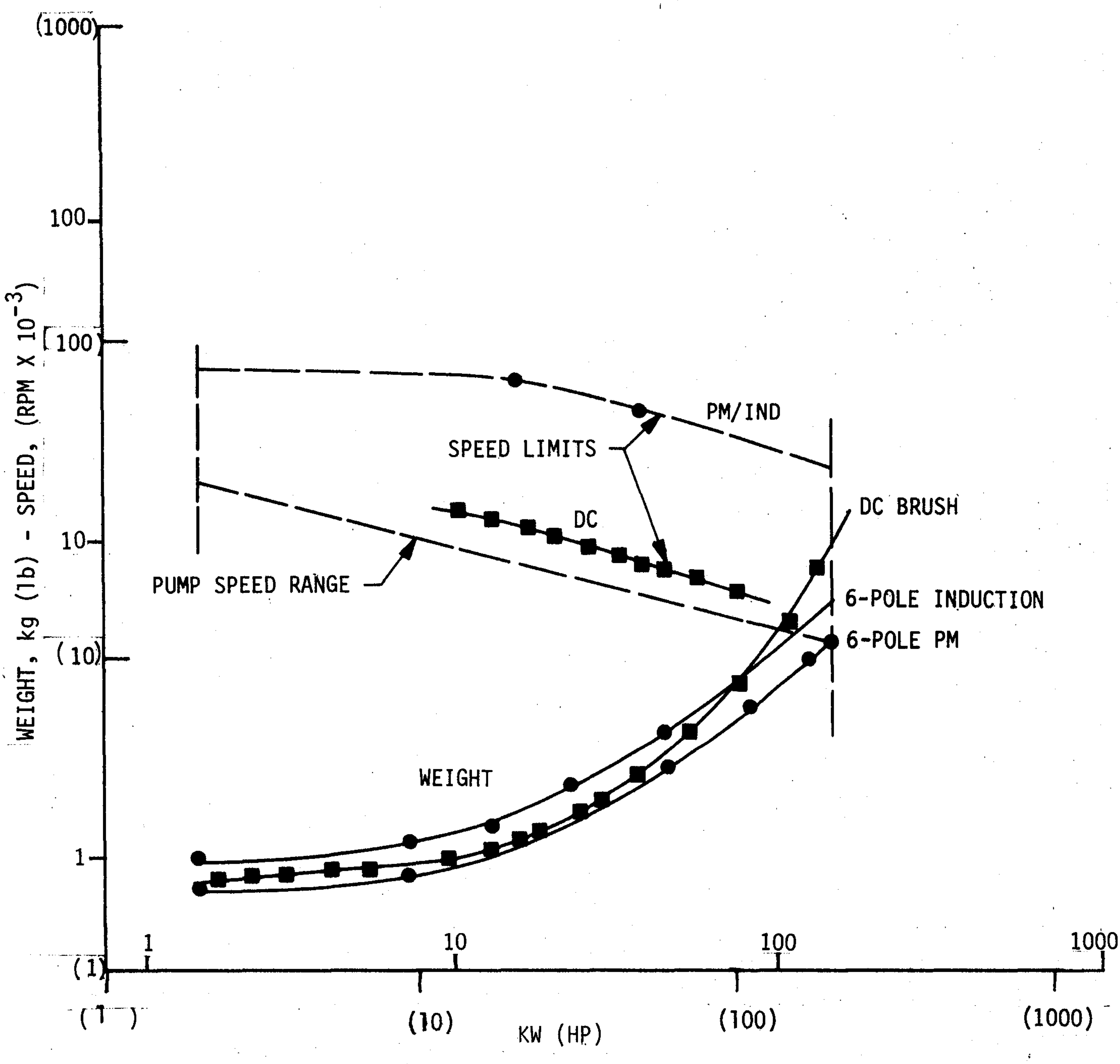

Figure 66. Oxygen Pump Permanent Magnet Motor - Weight and Speed Versus Power

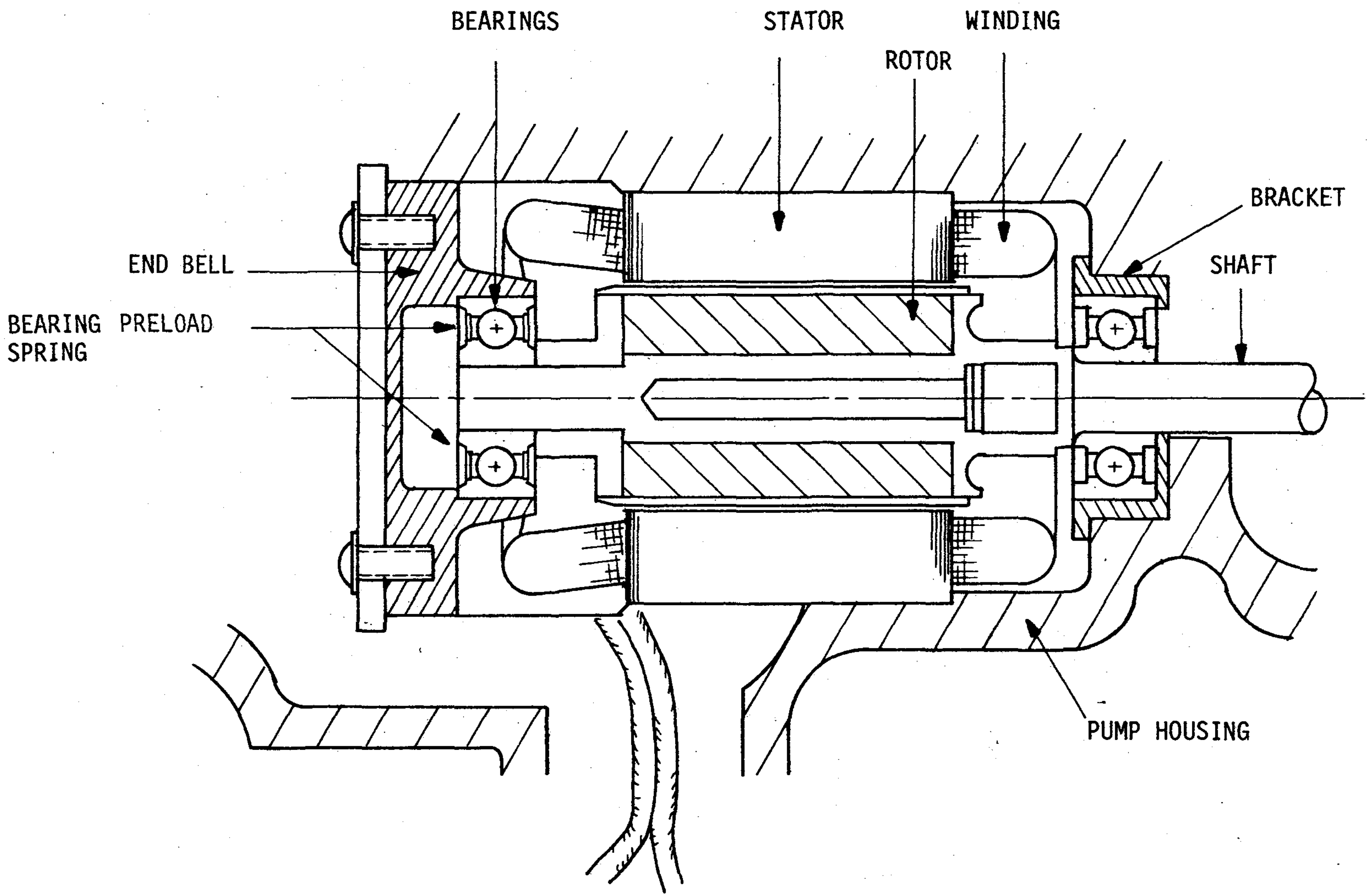

Figure 67. Typical Alternating Current Motor Components

Methane and hydrogen pump load/speed ranges are outside acceptable commutation limits for DC brush-type motors (shown in Figure 68) and are included with induction and PM motor plots for the oxygen pump only (Figure 66). The graph indicates insignificant variation in weight between all three motor types for loads up to about 10 horsepower.

Design weight variations generally exist between PM and induction motors and, for a given horsepower and speed, will usually vary with the number of poles. Both induction and PM motor parameters for 2-pole and 6-pole machines are plotted for the hydrogen and methane pump loads to assist in the final selections and tradeoff studies.

Motor Performance - On the basis of similar performance at a given load and speed, induction motors are found to operate at lower efficiencies and to require larger active volumes than comparable PM machines. This is primarily due to the increased rotor losses of the squirrel cage rotor, including I^2R, core, tooth, and windage losses. Additionally, the induction motor operates at a lagging power factor which increases power supply capacity and weight. Table XIV summarizes predicted efficiencies and power factors for the range of applicable induction and PM machine ratings. DC brush motor efficiencies approximate those listed for PM machines.

Motor Speed Limits - Tip speed limits for electric motors and alternators which employ laminated and/or wound rotors are significantly below those of the induction (homopolar) design which utilizes a solid, single-material rotor or the bonded Lundel design which utilizes a solid bimetallic rotor. The literature (Ref. 105) indicates a tip speed limit of up to 365 m/s (1200 ft/sec) for a 19.1 cm (7.5 in.) solid-rotor alternator rated at 215 kva (188 HP). In comparison, the tip speed of a comparable PM machine (Ref. 106) with a 16.5 cm (6.5 in.) diameter rotor reached the maximum rotor stress limit at 203 m/s (667 ft/sec). The supplier/literature search did not reveal any applications of solid-rotor machines for drive motors. One reason is weight, since the weight of a solid-rotor machine is 2.5 to 3 times that of a similarly rated PM or induction motor (see Figure 59).

Mechanical commutation problems limit the speed of DC brush motors as power rating increases. The driver for induction and PM machines, on the other hand, is the mechanical limitation imposed by the laminated rotor assemblies. The field magnets of the PM machines are contained by a shrink ring consisting of bimetallic sections that are welded together. The radial thickness of the shrink ring must be constrained (as a function of rotor diameter) to preclude interference with the magnetic circuit, and thus rotational velocity is limited by maximum stress in the ring. The laminated

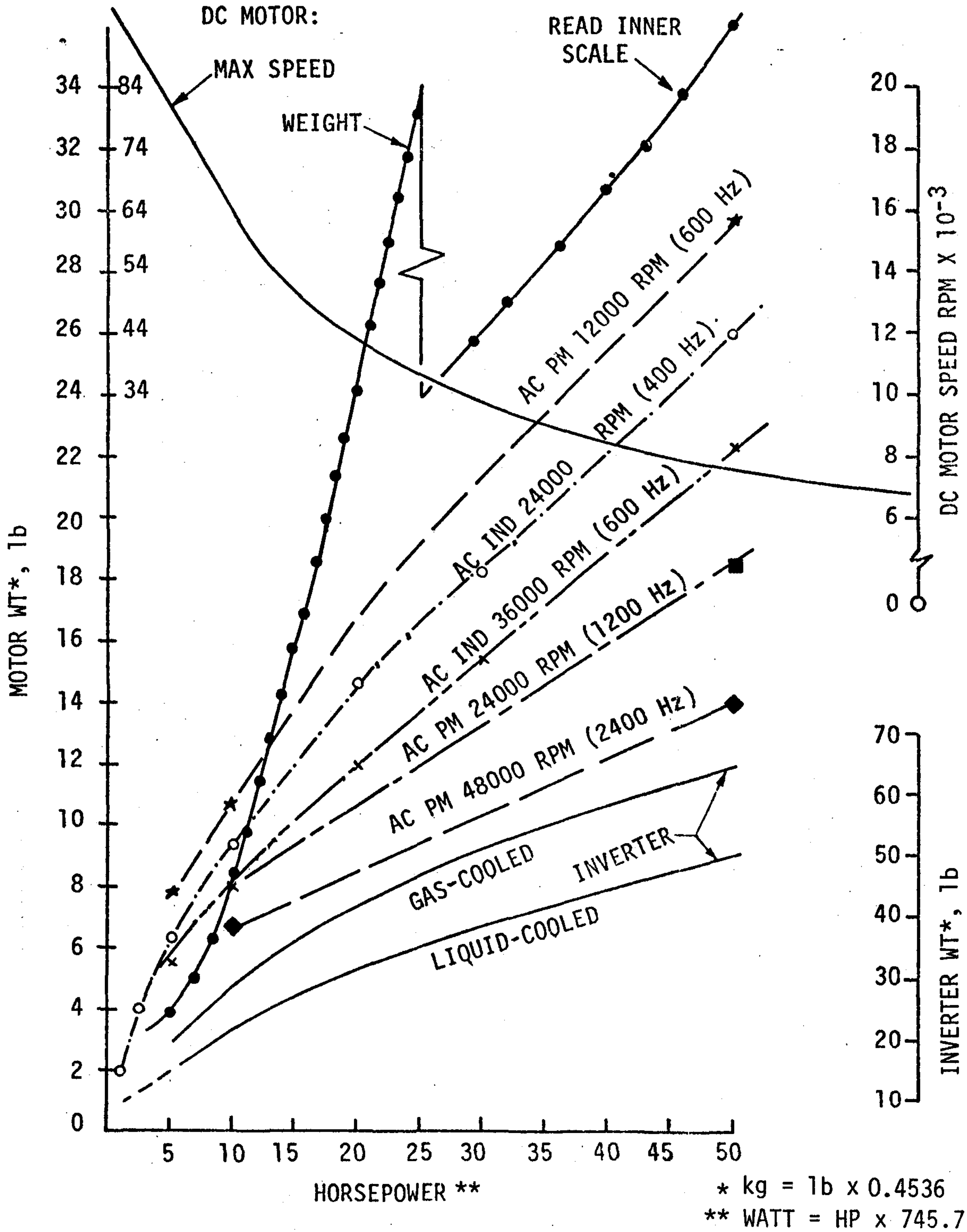

Figure 68. Cryogenic Electric Motor/Inverter - Weight and Speed Versus Power for Various Frequencies

TABLE XIV. PREDICTED EFFICIENCIES AND POWER FACTORS FOR ELECTRIC MOTORS

Motor Type	HP Range**	Efficiency	Power Factor
Permanent Magnet	0.5 - 5	0.70	NA*
Induction	0.5 - 5	0.65	0.70
Permanent Magnet	7 - 15	0.87	NA
Induction	7 - 15	0.80	0.80
Permanent Magnet	15 - 30	0.90	NA
Induction	15 - 40	0.83	0.85
Permanent Magnet	50 - 150	0.92	NA
Induction	50 - 150	0.88	0.90

*NA - Not Applicable

**SI Units Watt = HP x 745.7

rotor stack of induction machines contains copper or aluminum rotor bars near the periphery which require the addition of metal wedges or similar retention methods for peripheral velocities of 97 m/s (320 ft/sec) and upwards.

Motor speed limiting for the methane and hydrogen pump machines is assessed by assuming a maximum tip speed of 207 m/s (680 ft/sec) for PM machines and 177 m/s (580 ft/sec) for induction machines. The estimated maximum speeds for this condition are shown in Figures 62 through 66. The calculation of windage losses is based upon extrapolation of losses determined for lower-speed machines operating in liquid hydrogen for which certain assumptions about propellant state, viscosity, etc., had been made. Additional research (and perhaps actual testing) may be required to accurately set motor speed limits.

<u>Alternators</u> - The results of the study conducted to determine alternator power density/speed relationships are depicted in Figure 69. The solid rotor, PM, and rotating rectifier (brushless) types were researched, whereas the DC brush machine was assumed to reflect the curves previously developed for the brush motor. The curves reflect data extrapolated from Reference 105 for the induction/Lundel machine and from Reference 106 and 107 for the PM design. The brushless machine curve is based upon discussions with Bendix and reflects development above 30 kva (40.2 HP) and 12,000 RPM.

The extrapolation is based upon the proportionality of active volume to power density, i.e.,

$$D^2L = C\,\frac{kva}{N}$$

D = Rotor Diameter

L = Stack Length

N = RPM,

and rotor stress to rotational velocity, rotor diameter, and density, i.e.,

$$N = 1000\left(\frac{12\ Sat}{D^2 28.4\gamma}\right)^{1/2}$$

Sat = Rotor stress limit, psi

γ = 0.3.

L/D is assumed to be constant over the kva/speed range. An alternator voltage of 120/208 is assumed to minimize corona effects.

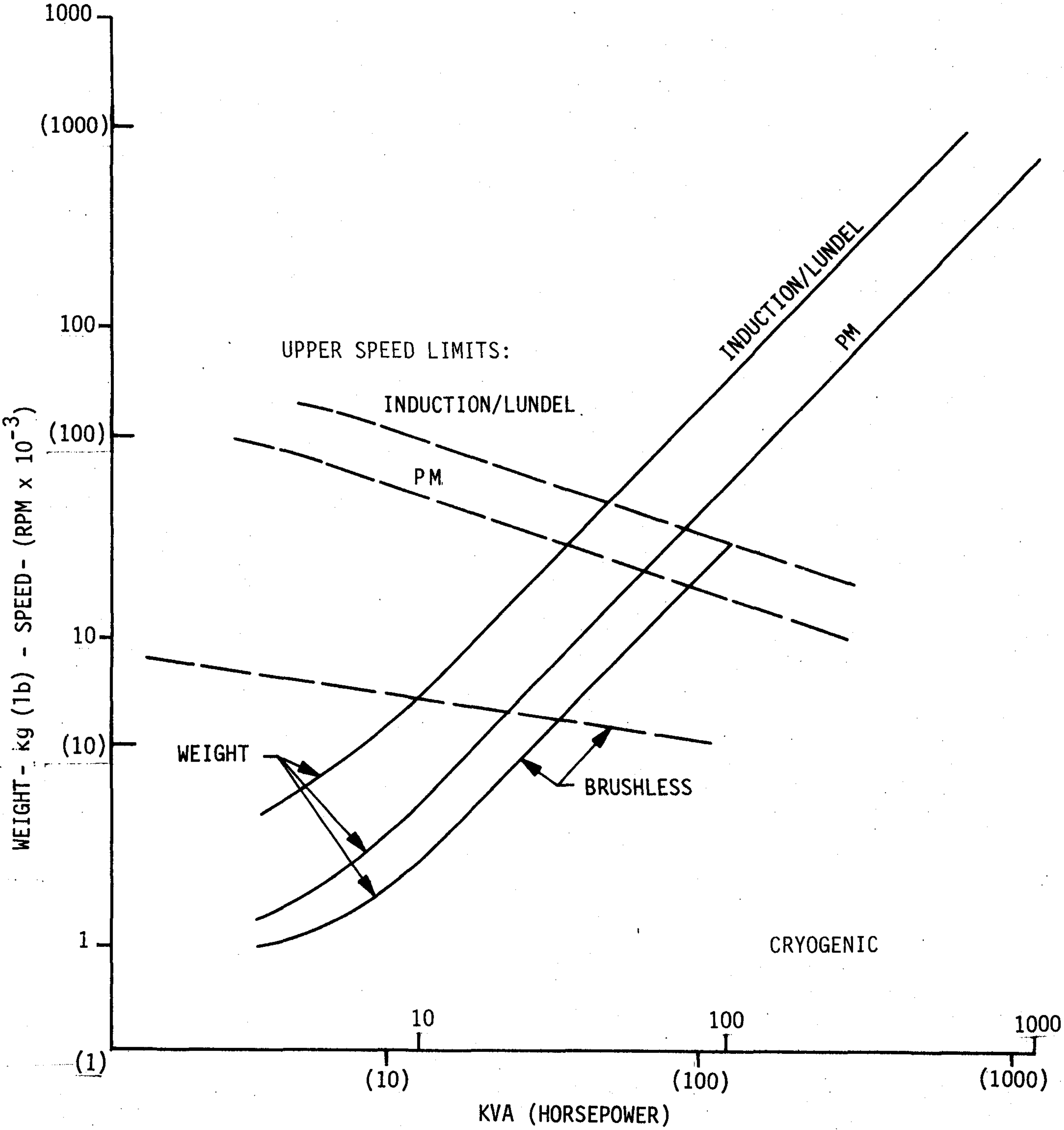

Figure 69. Alternator Weight and Speed Versus Power

The curves provide reasonable power density/speed data for PM machines of up to 14 poles, solid-rotor machines of 2 to 10 poles, and brushless machines of 4 to 20 poles, all scaled for operation at cryogenic temperatures.

The relationship of output frequency and speed for alternators and motor RPM/input frequency is

$$f = \frac{RPM*P}{120}$$

where:

$$RPM = \frac{120\ f}{P}$$

$$P = \text{Number of poles}$$

DC Power Supplies - Figures 59 and 60 present the result of discussions with Yardney and Pratt-Whitney design engineers and provide an update of the design file for aerospace battery and fuel cell weight versus kw-hr/kw. 115 volt supplies were selected to minimize corona effects; however, higher voltages should be considered for the larger motors to reduce the voltage drop across the power inverters. The end points of the three pump ranges, shown in Figure 60, are the kw-hr loads for the minimum motor load applied for 50 hours and the maximum load applied for 2.5 hours. The same applies to Figure 59, except that the loads are in kilowatts.

Inverter/Speed Control Components - Operation of induction and PM motors from a DC power supply requires the use of electronic inverters and variable voltage/frequency control. Figure 70 presents the power density and efficiency plots for current state-of-the-art inverters. Cryogenic "cold plate" cooling is assumed. The weights of cooling ducts and plates are included in the curves.

The design of PM motors based on brushless or induction alternator design criteria is accomplished by controlling the alternator field excitation as a function of speed (voltage/frequency) during start and operation under load. The weight of the excitation system is included in the power density curves of Figure 68. Operation of PM motors from PM alternators require the use of external power modulation equipment which significantly increases system weight.

Cycloconverters (Ref. 107) are currently used between the PM alternator and motor to provide the variable voltage/frequency control

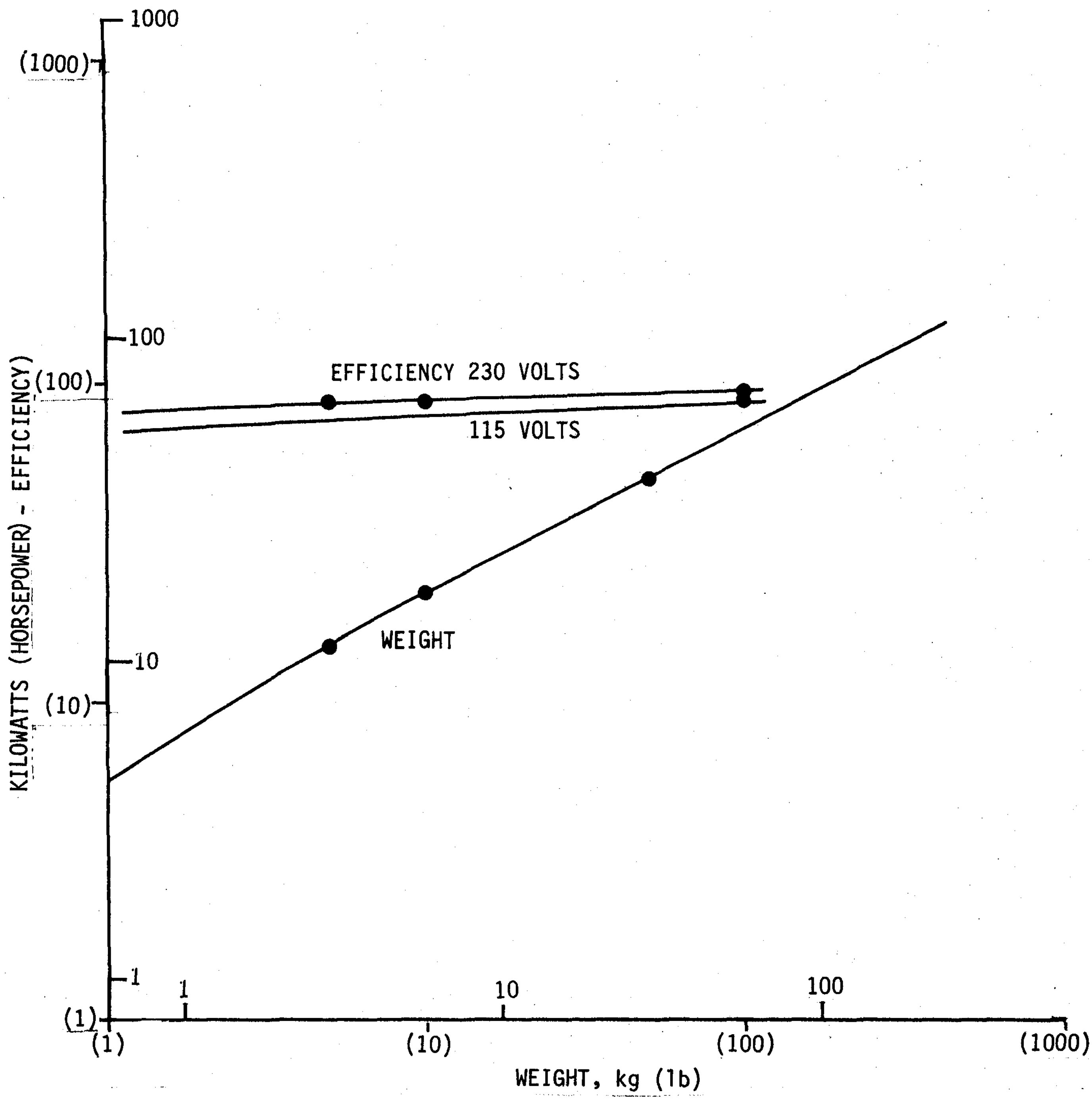

Figure 70. Inverter Power and Efficiency Versus Weight

necessary to start and run the PM motor under load. The cycloconverter is essentially a speed reducer which modulates the alternator input frequency to produce variable output frequency to the motor. The maximum output frequency is approximately 1/3 of that of the alternator to ensure adequate voltage/current waveforms. For loads above 40-45 kva (54-60 HP), the maximum alternator input frequency decreases to approximately 2400 Hz due to the longer turnoff time of the higher power solid-state switches (thyristors). Converter weight is increased when the speed difference between the two pump drive motors is greater than about 6 to 1 and the total load is above 45 kva (60 HP). Separate dedicated converters must be provided for this condition, each utilizing the higher frequency capability of power switching transistors. An increased converter weight of about 60% will result. Induction motors can be operated directly from all alternators considered, similarily to DC motors being operated from a DC power supply.

System Performance - Based upon the vendor/literature review, the electrical systems listed below were considered to be acceptable pump drive candidates. Because of the high minimum loads and long burn times, the weight and size of batteries becomes enormous (see Figure 60), making them unsuitable as an electrical system energy source. The following systems are listed in descending order on the basis of their performance in terms of system stability, efficiency, and demonstrated reliability.

System Number	
(1)	Fuel Cells/DC Brush Motors
(3)	Brushless Alternator/Induction or PM Motors
(2)	Fuel Cells/Inverter/PM Motor
(7)	DC Generator/DC Motors
(4)	PM Alternator/Induction Motors
(5)	PM Alternator/Cycloconverter/PM Motors
(6)	Induction/Lundel Alternator/PM Motors
(6)	Induction/Lundel Alternator/Induction Motors

Power/Speed Match Between Between Motors, Alternators, and Pumps

Power/speed limits for cryogenically cooled electric motors and alternators are great enough to satisfy all pump needs over the complete flow maps for hydrogen, methane, and oxygen pumps, the only exceptions being high-pressure, low-flowrate hydrogen and methane centrifugal pumps. All other types of rotary pumps operate at lower speeds than centrifugal pumps and therefore sustain no limit to electric/motor application other than the weight penalty.

Both induction and permanent magnet electric motors can power a portion of the hydrogen pump map (see Figure 71). Points No. 2, 3, and 4 may be driven by induction motors. Permanent magnet motors extend the range to include point No. 8 and all but the highest speed pumps at thrust levels less then 1334N (300 lbF). Permanent magnet alternators, operating at the hydrogen pump shaft speed, limit speed to approximately that found at the low-pressure boundary points 1 through 4 (Figures 1 and 69). The induction/Lundel type can be run faster than any of the fastest hydrogen pumps.

Permanent magnet/induction motors are the best electric motor candidates for powering methane pumps. It is only the highest-speed machines, at thrust below 2224N (500 lbF), that exceed the electric motor speed limits (see Figure 72). To illustrate the effect of increasing design NPSH, Figure 73 presents the same permanent magnet/induction electric motor speed limit for methane pump speeds which are dependent on 3.35 m (11 ft) NPSH rather than the 1.82 m (6 ft) used for the parameters of Figure 72. All of the high-pressure cases (5 through 8) allow the pumps to operate at higher speeds than the electric motors. Only the 2669N to 890N (200 to 600 lbF) thrust, low-pressure range cases can be powered by electric motors.

Oxygen pumps are not restricted at all by electric motor speed (see Figure 74). Their much smaller power level and 0.61 m (2 ft) NPSH design requirement keeps their speed at about half that of the electric motor speed limits.

d. Conclusions

The following summary evaluations are based on the same categories used for rating the pumps. Systems are numbered as described above in Section VI, C, 2, a, (4).

(1) Pressure/Flow Map

Hydrogen pumps for thrusts greater than the 1779 to 2669N (400 to 600 lbF) thrust range and less than 4481 kPa (650 psi) pressure rise can be driven by either induction or permanent magnet electric motors. Permanent magnet electric motors reach a higher pressure level than induction motors. Methane pumps for thrusts above 890N (200 lbF) may be driven by permanent magnet electric motors beyond the 6549 kPa (950 psi) pressure rise

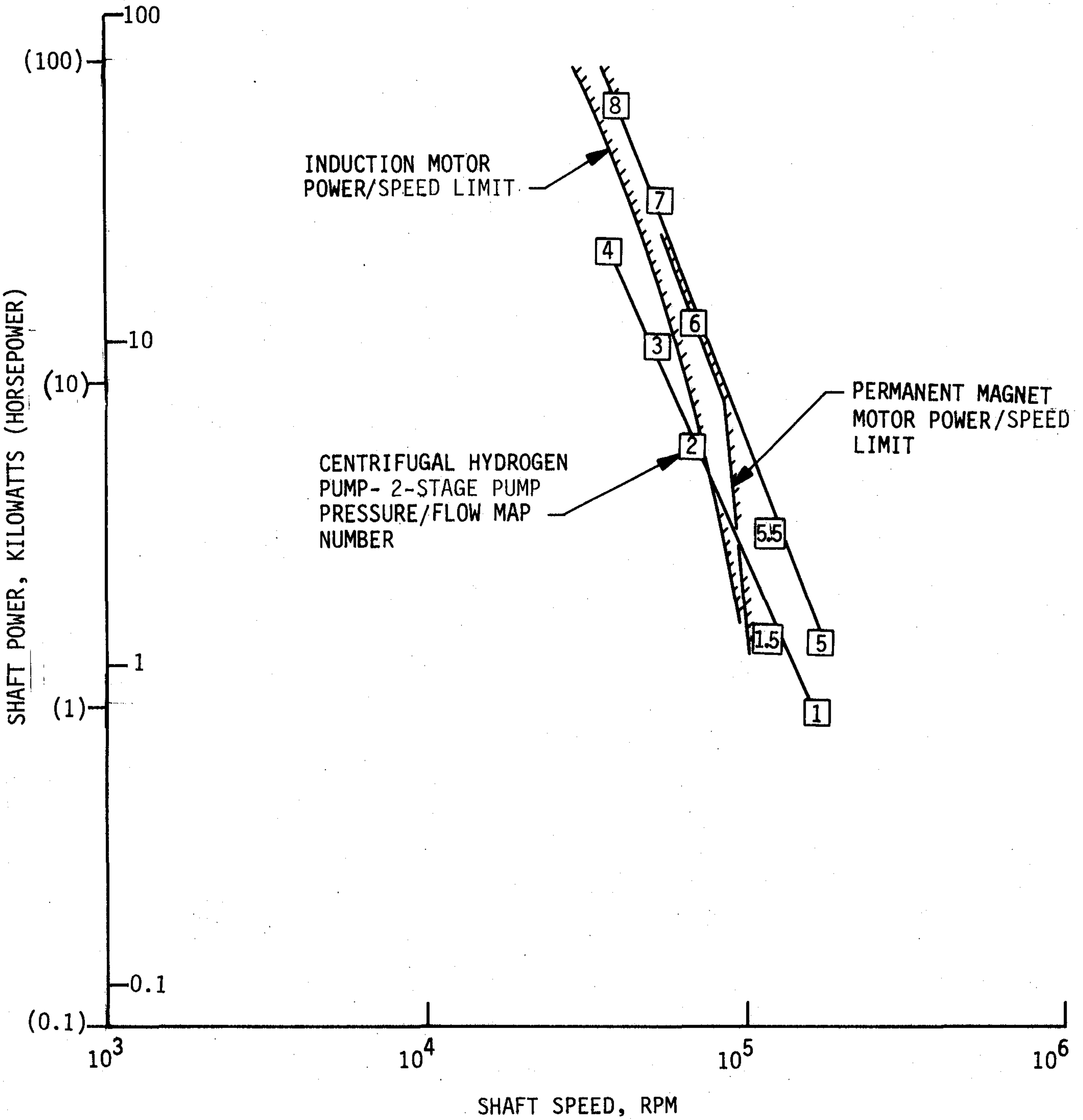

Figure 71. Electric Motor Power / Speed Limits for Centrifugal Hydrogen Pumps at 4.57 m (15 ft) NPSH

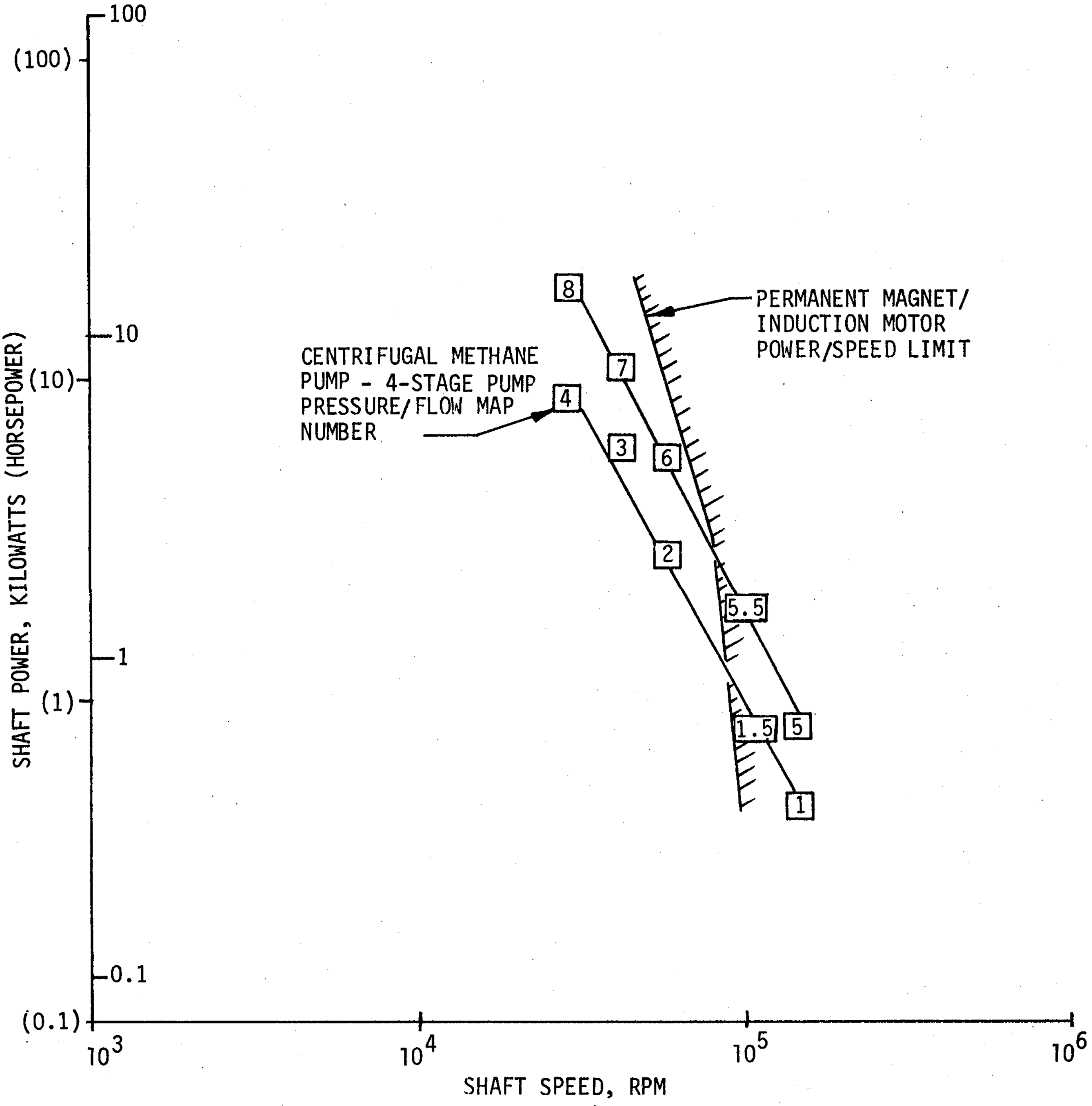

Figure 72. Electric Motor Power / Speed Limits for Centrifugal Methane Pumps at 1.83 m (6 ft) NPSH

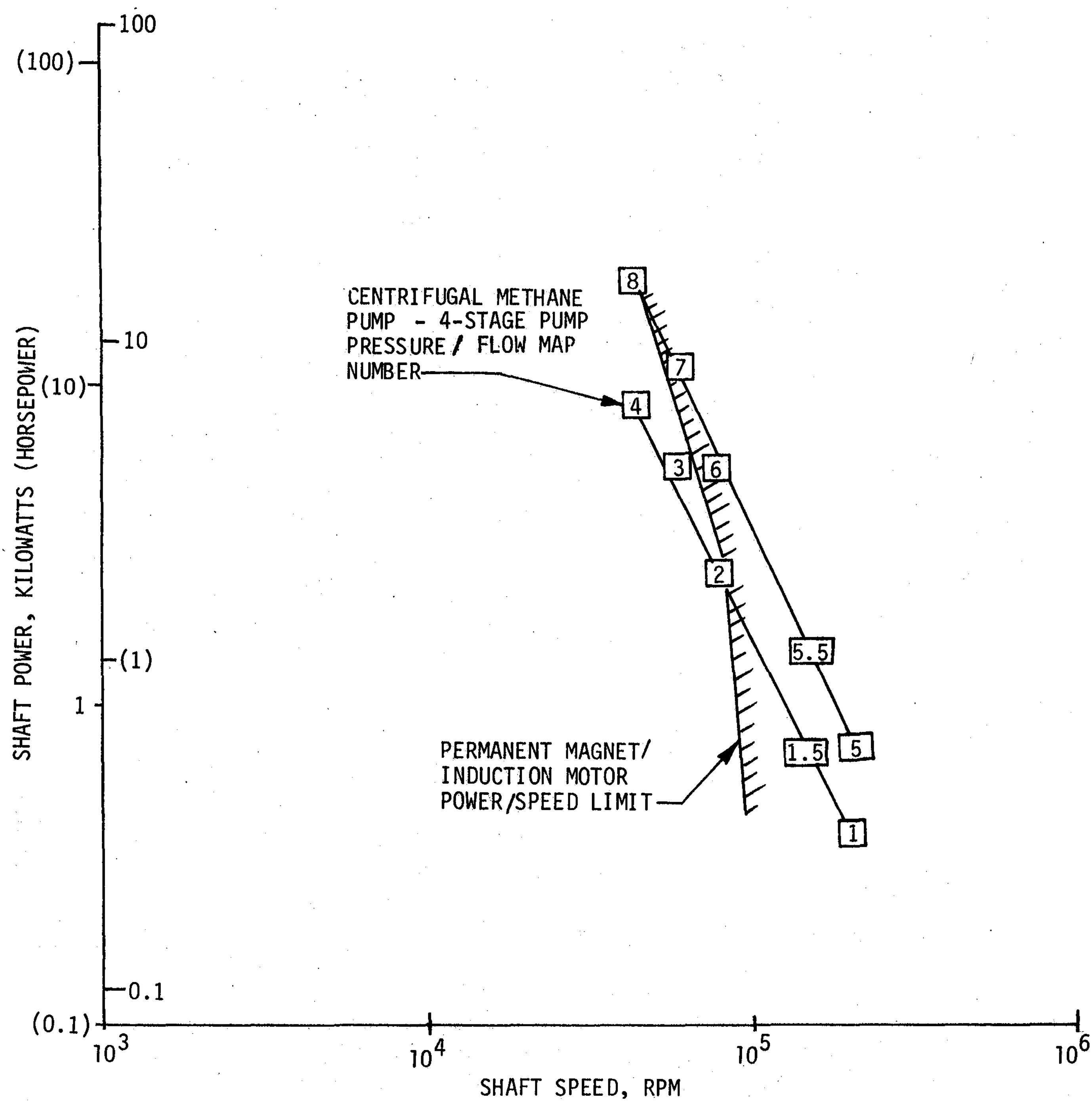

Figure 73. Electric Motor Power / Speed Limits for Centrifugal Methane Pumps at 3.35 m (11 ft) NPSH

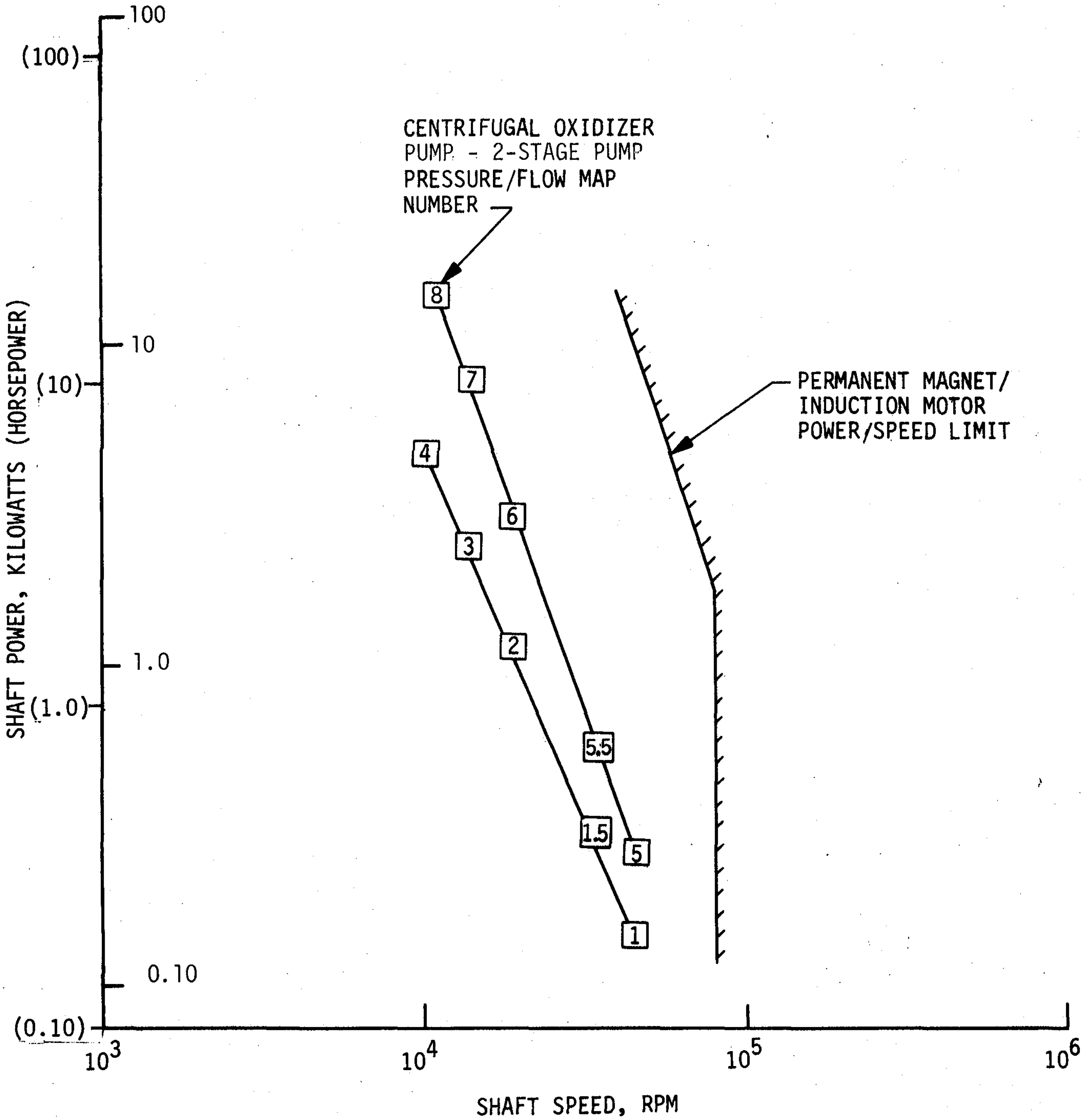

Figure 74. Electric Motor Power / Speed Limits for Centrifugal Oxygen Pumps at 0.61 m (2 ft) NPSH

level. The entire pressure rise/flowrate map can be powered by permanent magnet/induction-type electric motors.

(2) Efficiency

Overall efficiency estimates for the following systems are as follows:

System No.	Type System	Percent
(1)	Fuel Cells or DC Generator plus DC Motor	59-62
(2)	Fuel Cells or DC Generator plus Inverter plus Permanent Magnet or Induction Motor	59-62
(3)	Brushless Alternator/Permanent Magnet or Induction Motor	72-77
(4)	Permanent Magnet Alternator plus Induction Motor	69-76
(5)	Permanent Magnet Alternator/Cycloconverter plus Permanent Magnet Motor	69-76
(6)	Induction or Lundel Alternator plus Permanent Magnet or Induction Motor	80-84
(7)	DC Generator plus DC Motor	69-76

(3) System Performance

An overall rating of electrical stability efficiency and demonstrated reliability for equal weighting of each was estimated to be as follows:

System No.	Component	Life Estimate
(1)	Fuel Cell -	2000 hours
	DC Generator or DC Motor -	50 hours
(3),(4)	Permanent Magnet Alternator -	100 hours
	Permanent Magnet or Induction Motor -	200 hours
(5),(6),(7)	Lundel Alternator -	50 hours
	DC Motor -	50 hours
	Permanent Magnet or Induction Motor -	200 hours

System Number	Relative Rating
(3)	1.0
(4),(5),(7)	0.8
(1),(2),(6)	0.6

(4) Life

Estimated limiting life for previously identified systems was estimated in descending order of longevity:

System Number	Component	Life
(2)	Fuel Cell -	2000 hours
	Permanent Magnet or Induction Motors -	200 hours

(5) Weight and Size

Weight estimates for the defined systems at 7.46 kw (10 HP) are listed in descending order of unit weight. Size is assumed to vary with the cube root of weight.

System Number	System Type	Kg/Watt	lb/HP
(1)	Fuel cell plus DC Motor	7.94	13.0
(2)	Fuel cell plus Inverter plus Permanent Magnet or Induction Motor	7.8	12.8
(1),(2),(5)	DC Generator plus Inverter/ Permanent Magnet Motor; or Induction Motor or DC Motor; or Permanent Alternator/ Cycloconverter/Permanent Magnet Motor	1.22	2
(6),(7)	Induction or Lundel Alternator plus Permanent Magnet Motor, or DC Generator plus DC Motor	1.22	2
(3),(4),(5)	Brushless Alternator plus Induction Motor; or Permanent Magnet Alternator plus Permanent Magnet or Induction Motor	0.915	1.5

(6) Reliability

The seven assumed systems are listed in decreasing order of relative reliability:

System Number	Relative Reliability
(4)	1.0
(5)	0.8
(3)	0.5
(1),(2),(6),(7)	0.3

(7) Cost

Cost of electric motors and alternators using cryogenic propellant cooling is the same as that for comparable quality aircraft and rocket engines. A development program will be required, however, as there is no established market for these machines at this time.

(8) Start Transient

All electric power generating motor drive systems, except for the No. (4), permanent magnet/induction motor system, are stable enough not to present a start transient problem. Since this system has not been sufficiently developed, it cannot be predicted with confidence whether it will be able to go through a rapid start transient without a problem. All other systems are believed to be able to follow the torque/speed capability of the prime mover. "Tank head starts" may limit the maximum acceleration rate of the turboalternator.

(9) Confidence in Meeting Life Requirements

There is high confidence that the stated reliability requirements of design point No. 6 can be met.

(10) Confidence in Meeting Predicted Performance Requirements

Except for the No. (4) system (the permanent magnet alternator driving an induction motor), all of the seven other electrical power conversion systems studied have a high confidence rating for meeting predicted performance requirements.

(11) Maintainability

Maintenance requirements will be similar to those for other currently used alternator motor systems.

3. Positive-Displacement Drive Motors

a. Description

Positive-displacement drive motors are candidate prime movers for small rocket engine pumps. Of the twelve types of pumps studied, only the centrifugal, Pitot, and Tesla operate at a speed sufficiently high to match directly with a hot-gas turbine. For this reason, a low-speed prime mover, such as a positive-displacement hot-gas motor, will be required to match the speed of the other candidate pumps (i.e., the vane, gear, piston, lobe or Roots, drag, and diaphragm). These pumps generally have speeds below 10,000 RPM.

A positive-displacement motor can be either internal combustion (similar to the Otto or diesel engine shown in Figure 75), external combustion (where two fluids are combusted in a gas generator before entering the motor where expansion occurs, as shown in Figure 76), or a single fluid, heated externally (as shown in Figure 77). Thermal efficiency is highest for the internal combustion cycle, with external combustion and heated gas, respectively, being much lower. The overall rocket engine performance for the externally heated gas cycle is not degraded as significantly as the low thermal efficiency might indicate if the gas motor is exhausted to the rocket engine thrust chamber for combustion therein. The design tradeoff is between the high thermal efficiency of the internal combustion and its innate small size versus the external combustion or heated gas systems of lower thermal efficiency but larger duct and equipment size and weight.

b. Literature Review

The literature available on positive-displacement gas drives is limited; however, some work has been done which is reported in References 64, 65, and 116. Reference 116 shows two concepts of external combustion drives (shown in Figures 78 and 79). The data from the motor shown in Figure 79 are plotted in Figure 80. These data were taken from high-performance, lightweight aircraft engines and from outboard motors (both being internal combustion engines). The reason that the external combustion motors of Reference 116 have a higher performance than the internal combustion engines is that the molecular weight of the gas for the former

INTERNAL COMBUSTION

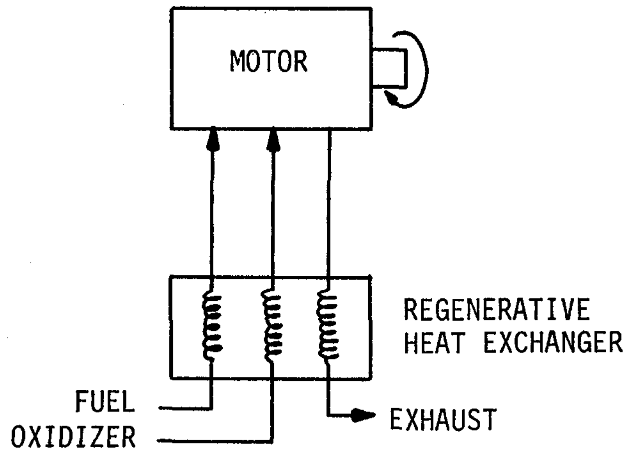

Figure 75. Internal Combustion Motor - Flow Schematic, Regenerative Cycle

EXTERNAL COMBUSTION

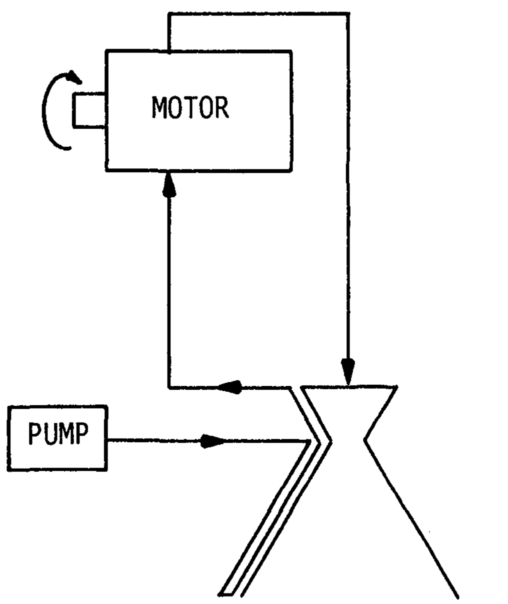

Figure 76. External Combustion Heated Propellant Motor - Flow Schematic

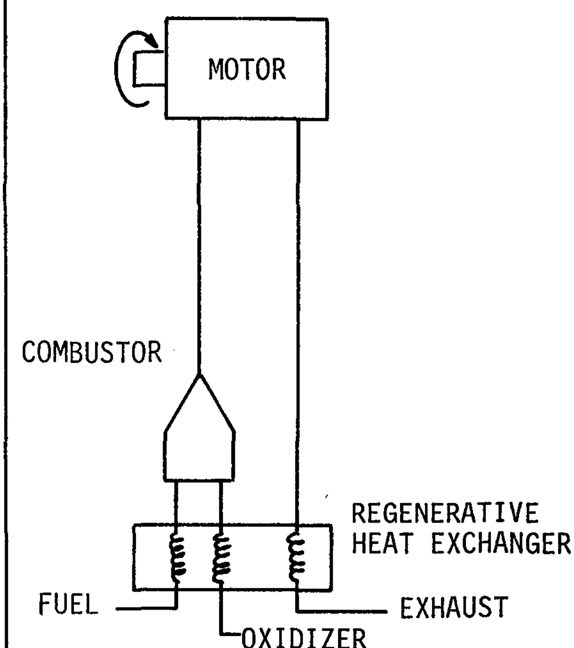

Figure 77. External Combustion Motor - Flow Schematic, Regenerative Cycle

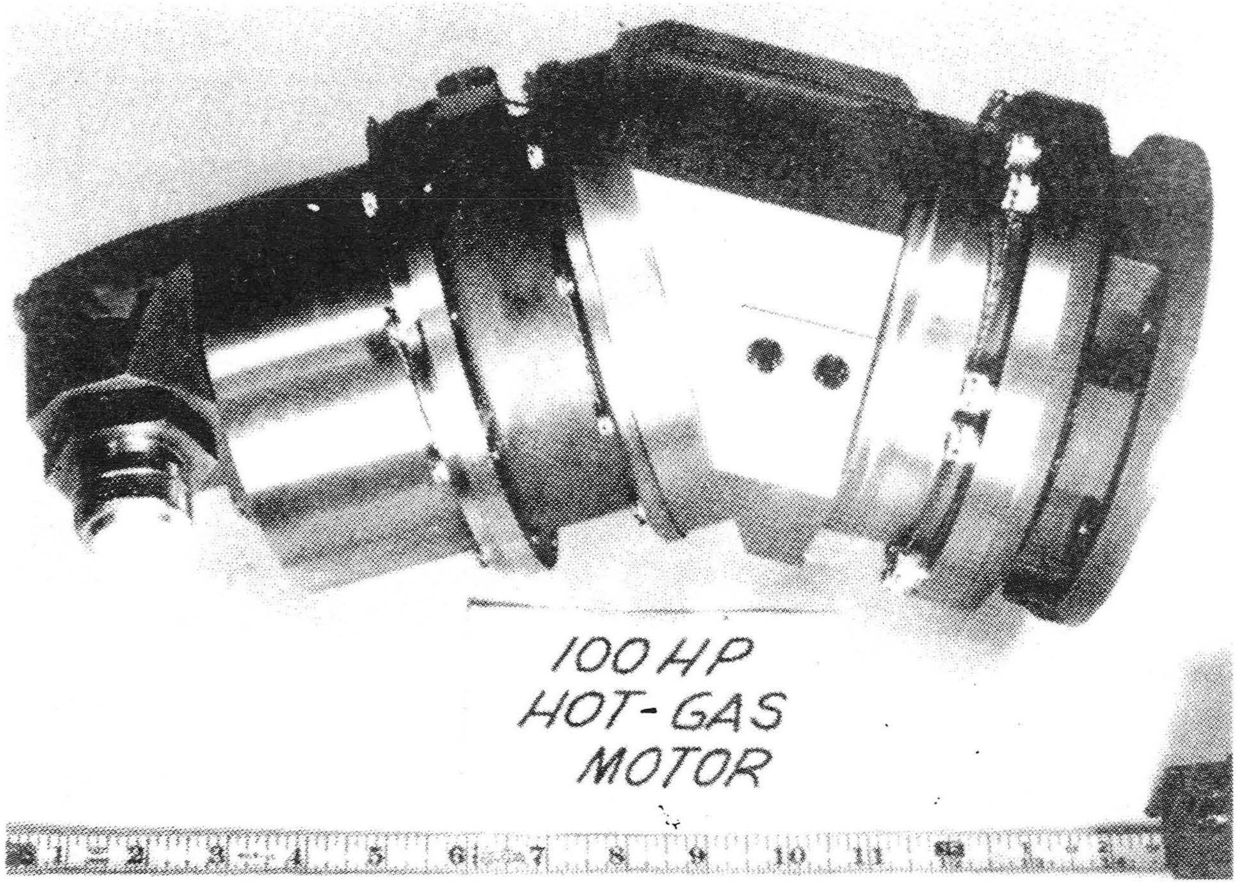

Figure 78. 74.6 kw (100 HP) Hot-Gas Motor

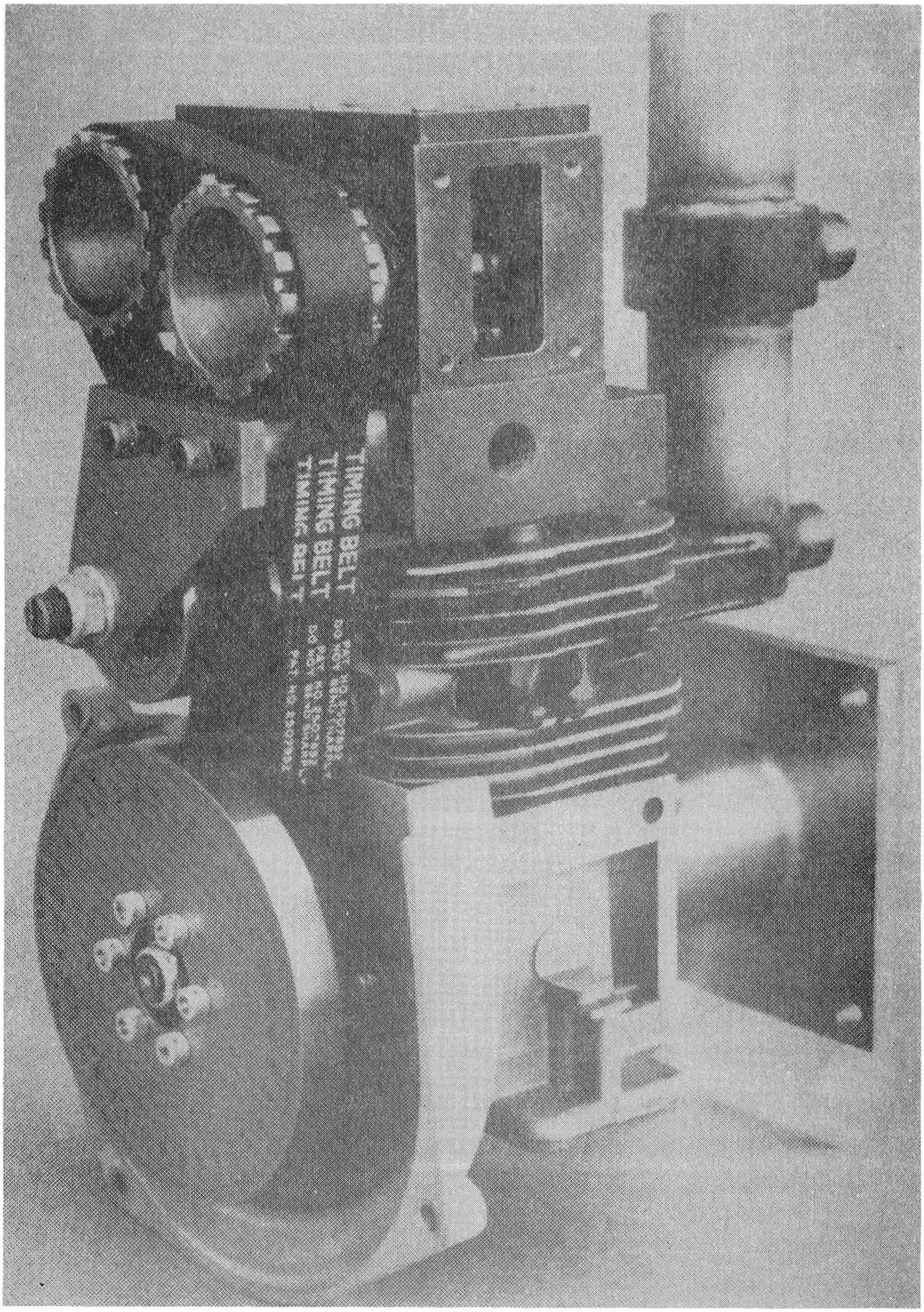

Figure 79. Experimental Single-Cylinder Expansion Engine

(GO_2 and GH_2) is much less than that of the latter (air and hydrocarbon). These data give the approximate shaft horsepower versus speed that can be expected from a positive-displacement drive motor.

c. Analysis

Figure 80 depicts the envelope for 1-, 3-, and 5-cylinder positive-displacement motors at their peak efficiencies. The area does not match the requirements of centrifugal pumps or those of gear, vane, Pitot, and nearly all drag pumps. A 2:1 to 5:1 speed increase would be required for the centrifugal pumps, and a 2:1 to 10:1 speed reduction would be required for most of the others. The peak efficiency for these internal combustion engines would fall between 25 and 35%. Since these are air-breathing engines, it should be possible to increase the efficiency to between 35 to 45% by using O_2/H_2 or O_2/CH_4.

On one hand, it would seem that the internal combustion cycle (shown in Figure 75) is more desirable than the external combustion cycle to obtain high engine efficiency even though it would result in "venting" the exhaust gas overboard, thus reducing the engine specific impulse. On the other hand, using the external combustion cycle (shown in Figure 76) would result in lower motor efficiency (this being a secondary effect on overall engine efficiency) and a significantly higher motor weight. The percentage loss in engine specific impulse for the internal combustion motor or the external combustion motor or the external combustion with overboard dump can be represented by the following equation:

$$\% \text{ Loss} = K \frac{W_{OB}}{W_{TC} + W_{OB}}$$

$K = 0.43$

W_{OB} = Overboard dump weight flow

W_{TC} = Thrust chamber weight flow

In existing rockets which use engine cycles with overboard dump, the weight flow is usually 2 to 4% of the thrust chamber flow; this results in a 1 to 2% reduction in Isp. The pumps and drives being considered in the study will have efficiencies approximately one half of those in the larger existing rocket engines. The loss in Isp will be 2 to 4%. This seems to be too high of a penalty to pay for the bleed cycle, and therefore only pumps and drives which adapt to the topping or expander cycle should be considered.

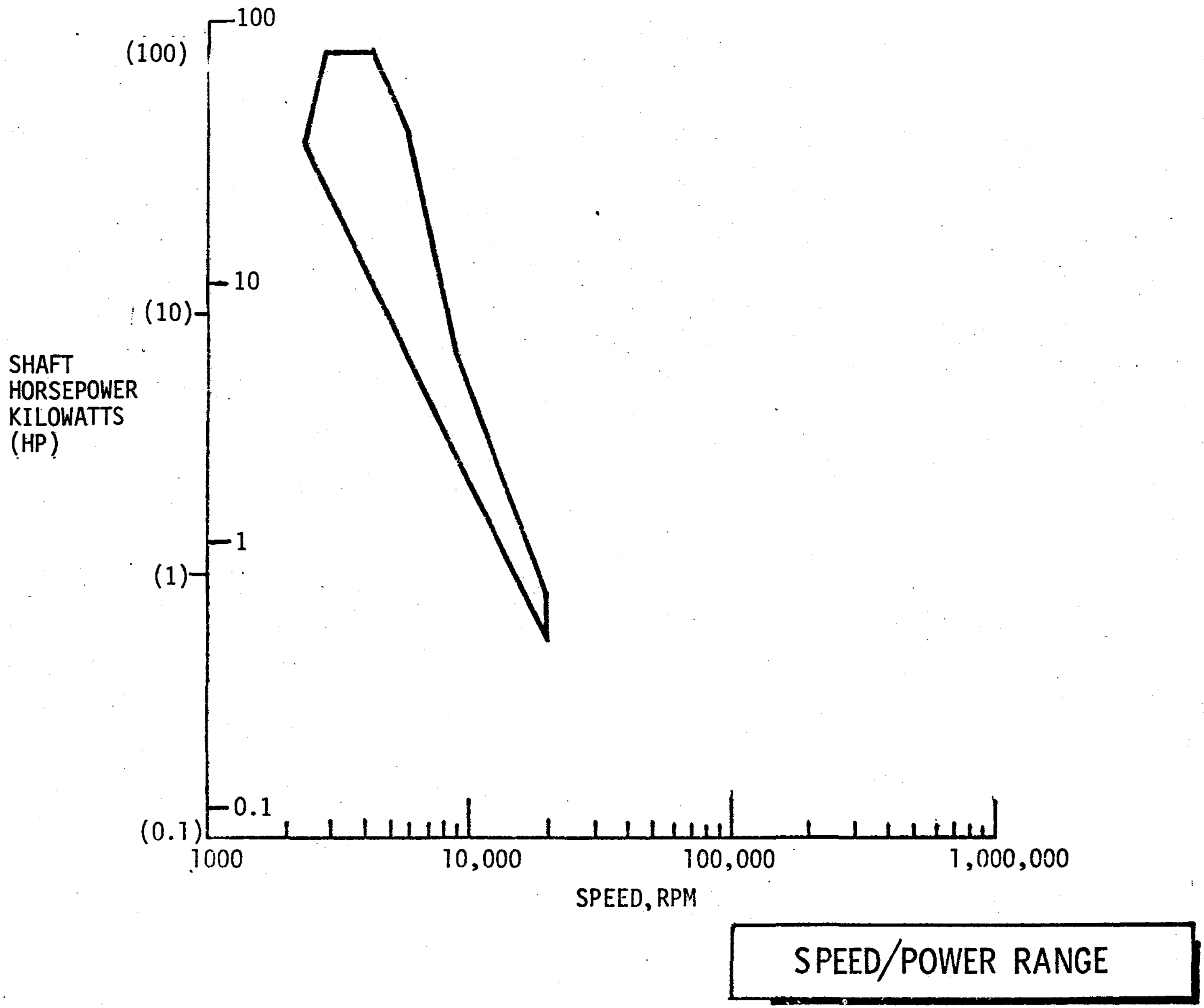

Figure 80. Power Versus Speed Range for Positive-Displacement Drivers

d. Conclusions

(1) Pressure/Flow Map

Positive-displacement motors will meet only the Pitot and drag pump requirements of 0.746 kw (1 HP) and less in the 10,000 to 20,000 RPM range without a speed change between driver and pump.

(2) Efficiency

Thermal efficiency of the positive-displacement drives ranges from 35 to 45%.

(3) Life

Life of positive-displacement motors is indeterminable at this time due to lack of developed drivers. It is estimated that it will be less than for gas turbines for the same degree of development.

(4) Weight and Size

The typical weight of 6895 kPa (1000 psi) external-combustion powered positive-displacement engines is 0.61 to 1.22 kg/kw (1 to 2 lb/HP). The physical size of multiple axial piston motors is 1.3 to 1.72 cm^3/kw (6 to 8 $in.^3$/HP) with a length-to-diameter ratio of 2.

(5) Reliability

Insufficient numbers of hot-gas positive-displacement motors have been developed to be able to assess their reliability. The potential goal should be to match the reliability standards achieved by aircraft internal combustion piston engines which are lower than those of gas turbines.

(6) Start Transient

Positive-displacement motors accelerate faster than gas turbines. Internal combustion engines will need an ancillary starter motor not required by externally pressurized motors.

(7) Confidence in Meeting Life Requirements

Confidence in meeting life is lower for the the positive-displacement motors than for the gas turbines.

(8) Confidence in Meeting Performance

Confidence in meeting performance will be less than for gas turbines due to the smaller body of experience with small, high-speed positive-displacement motors than with small gas turbines.

(9) Maintainability

Maintainability parameters for hot-gas positive-displacement motors will be more extensive than for gas turbines.

VII. SELECTION OF PUMP/DRIVE SYSTEMS FOR FURTHER STUDY

Pumps and compatible drivers which will satisfy the overall study requirements of hydrogen, methane, and oxygen propellants can be compared and ranked by reviewing the individual analyses and applying subjective judgment of the rotating machinery designers. Two selection processes have been employed: (1) a numerical assessment of features technique and (2) a sorting by function and characteristics technique.

The portion of the pressure/flow map representing the most challenging requirements is the low-thrust/high-pressure area for all three propellants. In these operating areas, the pumps will be small and the operating speeds will be high; close tolerances will be required for good efficiency. For the drives, the options are either electric motor or turbine. While electric motors provide the design option of not requiring the additional complexity, shaft length, and purge gas penalty of an inner propellant seal, there is a motor speed limit, and turbines will probably be required for the highest-speed pumps. All pumps are assumed to be directly driven.

A. PUMP/DRIVE MATCHING

Eleven types of pumps were evaluated for their applicability to the low-thrust propulsor. The preliminary results indicated that the axial-flow, rotordynamic pumps are not suitable for this application because they require too many stages. Also, since the jet pump does not require a mechanical driver, pump/drive matching analyses were performed only on the remaining nine pump types.

The power versus speed demands for centrifugal, drag, Pitot, vane, and gear pumps are shown in Figure 81. The centrifugal pump speed limits are set at 12,000 to 100,000 RPM, and the peak power is approximately 55.95 kw (75 HP). The drag and Pitot pumps have lower speed limits and their power limits are approximately 7.460 kw (10 HP) and 0.746 kw (1 HP), respectively. The vane and gear pumps, because of their good efficiency, have a maximum power requirement of 2.984 kw (40 HP). The maximum speeds are 10,000 and 5,000 RPM, respectively.

The upper speed limits for electric motors are shown in the same scale as those for pumps in Figure 82. The power/speed limits for permanent magnet motors are shown to be lower by a factor of 3 than those of the induction motors. The highest permissible speed for the induction motor is about 100,000 RPM at 1.492 kw (2 HP) whereas a permanent magnet motor is limited to about 0.149 kw (0.2 HP) at 30,000 RPM.

The power/speed envelopes for positive-displacement drivers (shown in Figure 30) are limited by two significant operational considerations. One is the minimum speed because of efficiency considerations; the other is the minimum practical physical size. The minimum speed limit is

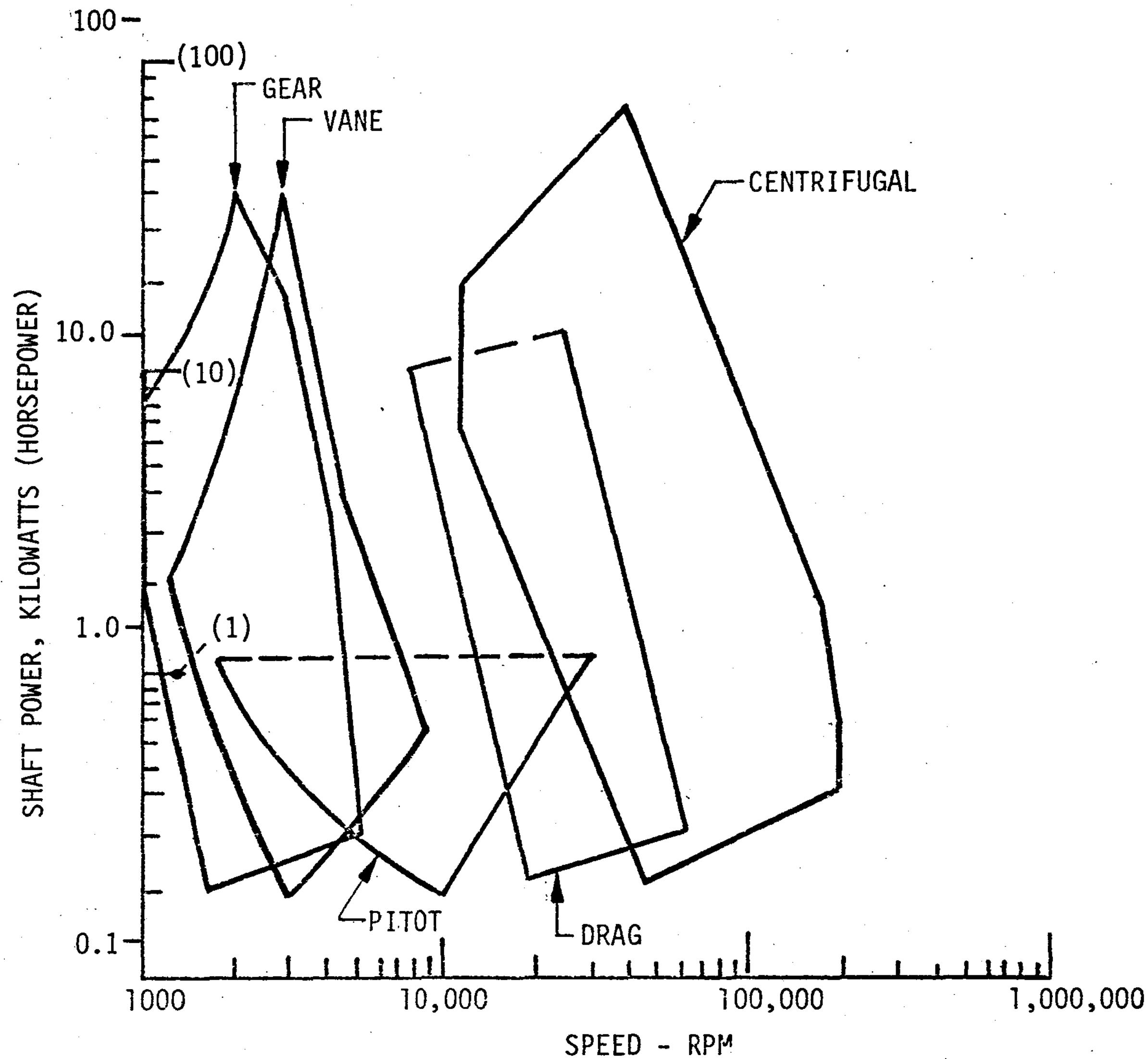

Figure 81. Power Versus Speed Demands for Centrifugal, Drag, Pitot, Vane, and Gear Pumps

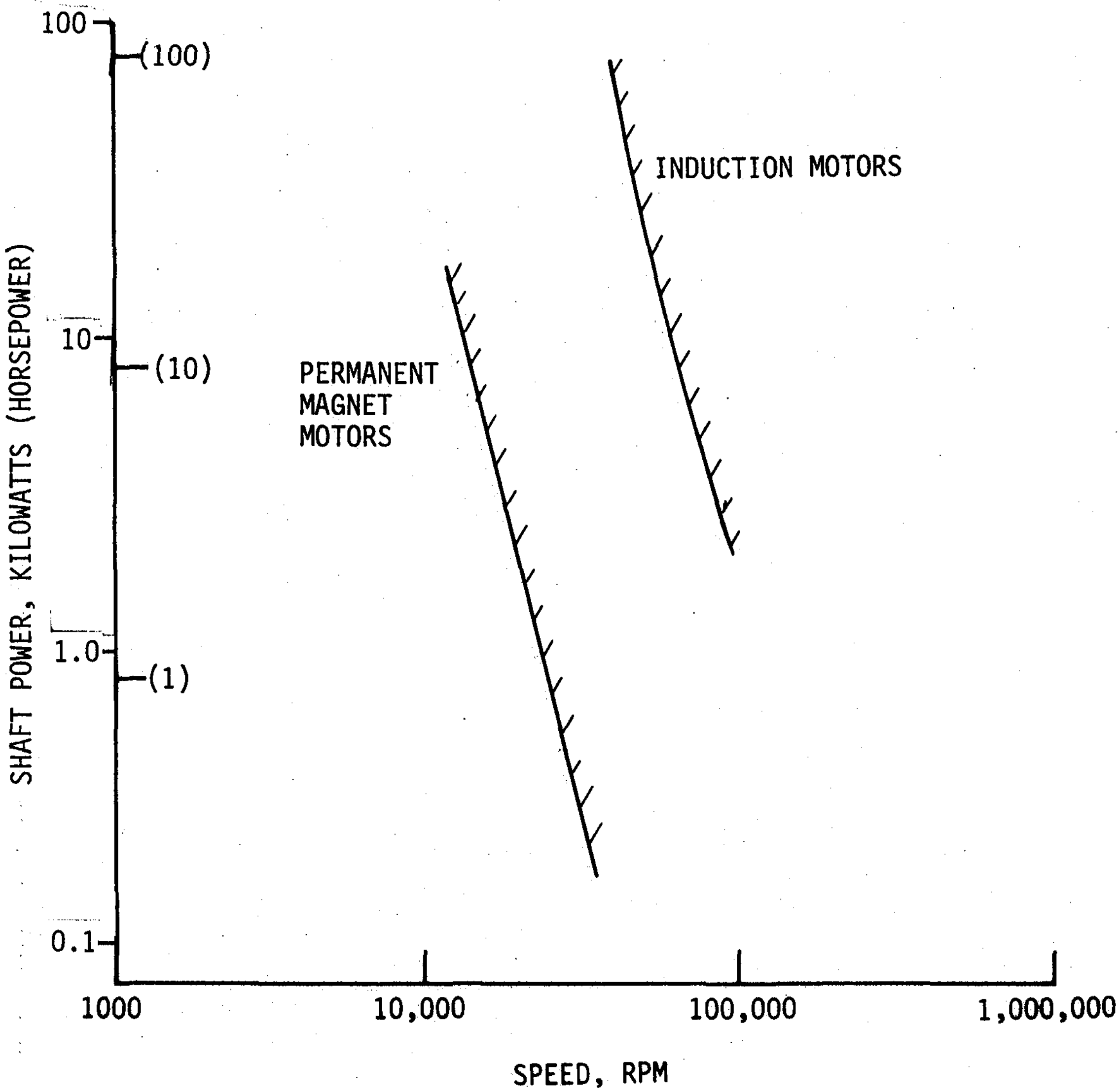

Figure 82. Electric Motor - Speed Limits

set at 10,000 RPM; the minimum practical size limit is at approximately 1 HP at 10,000 RPM.

When the drivers and pumps are matched, it is immediately evident that there is no one single type of driver which is suitable for all pump requirements. Since the gas turbine (Figure 83) is a high-speed driver, it is best-suited for the high-speed centrifugal and drag pumps; it is not suitable for the positive-displacement pumps. Electric motors can be used for all low-speed and some of the high-speed pumps; the only area where they cannot be used is in those applications which call for ultrahigh-speed centrifugal pumps. The hot-gas positive displacement motors have very limited operating envelopes. Typically, they are too fast for the positive-displacement pumps and too slow for the dynamic pumps.

B. PUMP/DRIVE SYSTEMS COMPARISON AND RANKING

1. Comparison Factors

The ultimate worth of a pump/drive system is its potential for application to the low-thrust rocket propulsion system. This potential is evaluated for the 13 following categories:

- Head versus Capacity Characteristics
- Cavitation-free Operation Potential
- Efficiency
- Size and Weight (Envelope)
- Life
- Reliability
- Maintainability
- Structural Integrity
- Matching Drive System
- Confidence in Meeting Predicted Performance
- Confidence in Meeting Life Requirements
- Cost
- Ease of Startup

The pump head versus capacity characteristics are important only in so far as the propulsor system requirements are met. For this assessment, the pump capable of meeting the widest range of operating conditions within the operating envelope of the propulsor has the highest utility.

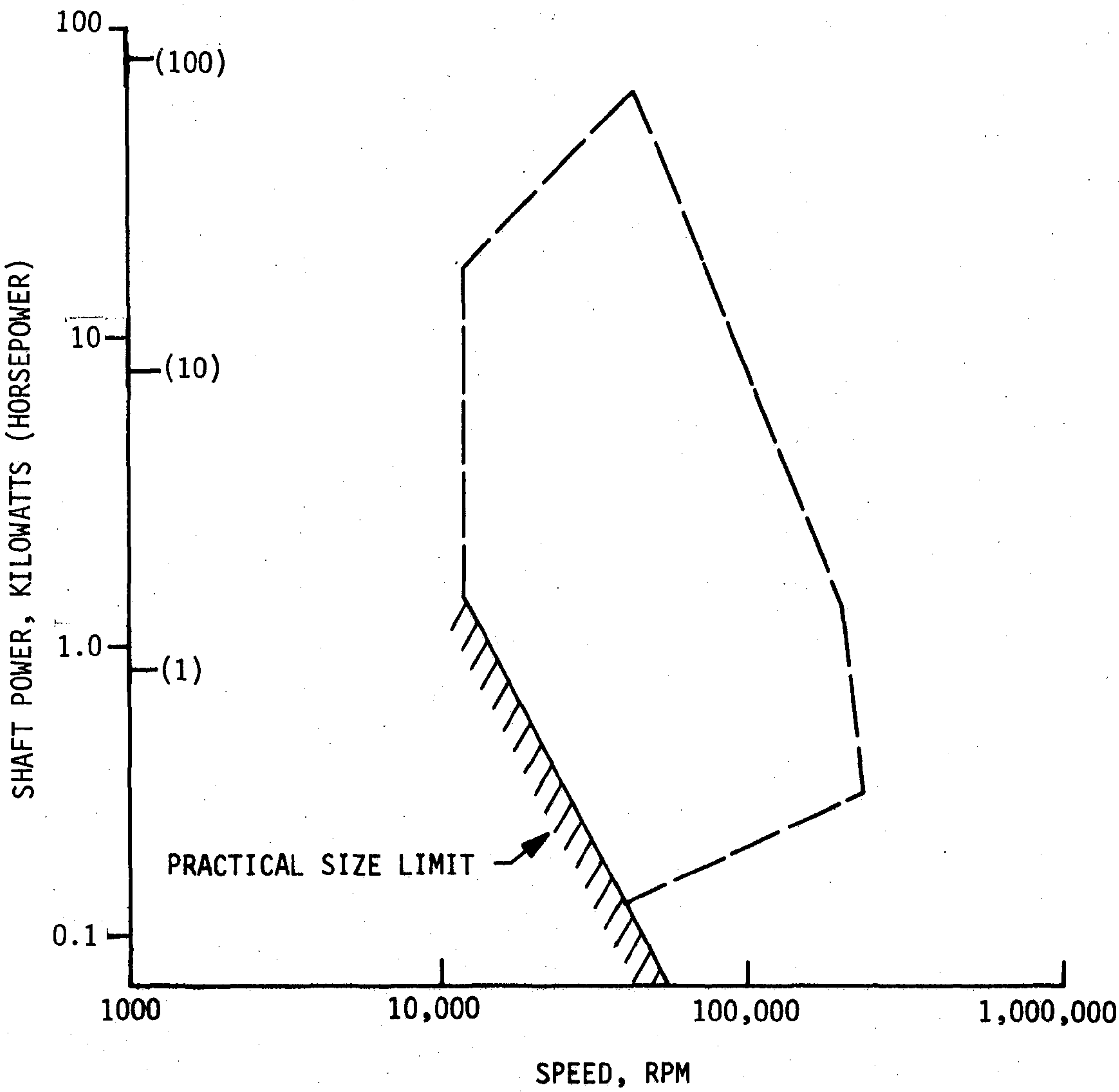

Figure 83. Gas Turbine - Operating Envelope

The ranking index for cavitation is based on the capability of the propulsor system to run without pressure surges. Pumps that run with periodic cavitation and recovery, or pumps that require extraordinary means (e.g., an elaborate boost pump system) to maintain steady operation, could have a very low utility.

Pump efficiency reflects the amount of chemical energy that is dissipated in the pump drive rather than utilized for thrust propulsion. In general, pumps with efficiencies below 40% have very little utility. However, there is only a small difference in the worth of a 70% efficient and a 80% efficient pump.

The size of the pump is restricted by the available envelope. If a given pump can be fitted into the envelope, it will get a positive rating. Beyond that, the smallest pump will be the most desirable. The weight of the pump has a direct influence on the system payload. Because of this relationship, the worth of each pump concept will be inversely proportional to the weight.

Life is one of the directly stated requirements for the propulsion system. A pump must be capable of achieving the stated life requirement before it has an utility. Beyond that, having a longer life capability adds very little to the worth of the pump.

Reliability is based only on the probability of indeterminate failures. Factors that influence life (e.g., wear and erosion) are included only insofar as they contribute to these random failures.

Maintainability has only a small utility for space equipment. Unless the maintenance procedure is simple, it cannot be implemented in space. However, if a simple maintenance procedure can enhance reliability and life significantly, it would certainly be beneficial.

The structural integrity of the pump system affects the entire propulsor system. It basically reflects the capability of a pumping system to absorb unplanned for forces and loads without ill effect.

The pumps have to be driven by a power source. The pump that has the highest utility is the one that can be matched up against a drive system which has all the desirable attributes of the pump (light weight, high efficiency, high reliability) at the pump speed.

Confidence in meeting the predicted performance is basically a matter of experience. Concepts that have been proven in service will have a high rating. Conversely, concepts that are still in preliminary stages of development will have a low rating.

Confidence in meeting life requirements can only come from direct experience; analytical life assessments have very low accuracy. As in the case of performance, concepts that have been proven in service will have a higher rating than those still under development, even if the given development system were to show longer theoretical life potential.

As the cost of the pump is only a small part of the overall cost of the propulsion system, this factor is not considered to be of primary importance.

A pump's ease of startup has high utility because it can minimize the impact of the startup procedure on the entire propulsion system. However, if ease of startup is attained at the expense of complicated support equipment, then the pump's utility is compromised.

2. Ranking of Comparison Factors

Weighting values are assigned to the comparison factors on the basis of their importance to the overall propulsion system. Of the thirteen factors considered, pump efficiency and the availability of a matching drive are deemed most important, whereas the startup capability is considered least important. The weights given to each factor are grouped as follows:

	Weighting Values
° Efficiency; Matching Drive	10
° Cavitation	8
° Size/Weight; Life; Reliability	5
° Head versus Capacity Characteristics	4
° Maintainability; Structural Integrity; Confidence in System Performance; Confidence in Meeting Life Requirements	3
° Cost	2
° Startup	1

The actual evaluation of these rating considerations is shown in Figures 84 and 85. For each rating factor, each pump type is rated on the basis of one to 10, 10 being the highest worth. The ratings are then multiplied by the relative weighting values. Finally, all of the weighted factors are summed up for each pump type. These numerical sums then become figures of merit for each type of pump.

CATEGORY / CANDIDATE	HEAD VS CAPACITY CURVE	CAVITATION	EFFICIENCY	SIZE/WEIGHT	LIFE	RELIABILITY	MAINTAINABILITY	STRUCTURAL INTEGRITY	MATCHING DRIVE SYSTEM	CONFIDENCE IN MEETING PREDICTED PERF.	CONFIDENCE IN MEETING LIFE REQUIREMENT	COST	STARTUP
WEIGHT	4	8	10	5	5	5	3	3	10	3	3	2	1
CENTRIFUGAL	7	10	3	7	10	10	6	8	10	10	7	6	10
VANE	5	2	5	6	2	3	7	8	5	5	1	8	-
GEAR	5	2	4	4	4	4	8	6	5	5	2	7	-
PISTON	4	5	7	2	5	3	4	6	2	7	4	7	-
ROOTS & LOBE	5	2	4	3	4	3	5	6	5	5	1	6	-
DRAG	7	1	2	6	8	10	7	8	6	5	5	9	10
PITOT	7	7	3	2	8	8	5	8	5	6	5	7	10
TESLA	5	7	2	5	8	6	6	2	8	3	2	6	10
DIAPHRAGM	4	2	3	2	5	3	4	3	2	6	2	5	0

BEST RELATIVE RATING

SECOND-BEST RELATIVE RATING

Figure 84. Numerical Technique for High-Flow Range Ranking

CATEGORY / CANDIDATE	HEAD VS CAPACITY CURVE	CAVITATION	EFFICIENCY	SIZE/WEIGHT	LIFE	RELIABILITY	MAINTAINABILITY	STRUCTURAL INTEGRITY	MATCHING DRIVE SYSTEM	CONFICENCE IN MEETING PREDICTED PERF.	CONFIDENCE IN MEETING LIFE REQUIREMENT	COST	STARTUP
WEIGHT	4	8	10	5	5	5	3	3	10	3	3	2	1
CENTRIFUGAL	7	10	5	10	10	10	6	8	10	10	8	6	10
VANE	5	2	6	9	2	3	7	8	5	5	1	8	0
GEAR	5	2	8	7	4	4	8	6	5	5	3	7	0
PISTON	4	5	7	5	5	3	4	6	2	7	5	7	0
ROOTS & LOBE	5	2	7	6	4	3	5	6	5	5	2	6	0
DRAG	7	-	-	8	8	10	7	8	6	5	6	9	10
PITOT	7	7	4	4	8	8	5	8	5	6	6	7	10
TESLA	5	7	4	8	8	6	6	2	8	3	3	6	10
DIAPHRAGM	4	2	4	5	5	3	4	3	2	6	3	5	0

BEST RELATIVE RATING

SECOND-BEST RELATIVE RATING

Figure 85. Numerical Technique for Low-Flow Range Ranking

The results of the ranking effort are shown in Table XV. The points shown have been normalized to 100 for the centrifugal pump. The dynamic pumps took the five highest ratings, with the positive-displacement pumps all receiving lower values, except for the jet pump which followed in tenth place.

A second ranking system, the sorting technique (shown in Figure 86), was applied to ensure that the weighting values of the numerical system were not too biased. All of the categories, except cost, were collected into four major groups. These groups are as follows:

- Function and Fluid Performance
  - Head versus Capacity Curve
  - Cavitation
  - Efficiency
  - Matching Drive System
  - Startup
- Physical Characteristics
  - Size/Weight
  - Structural Integrity
- Life, Reliability, Maintainability
- Design Confidence
  - Meeting Predicted Performance
  - Meeting Predicted Life

The five best pump types are then ranked in each of these areas. The results of the sorting method show that the dynamic pumps also rated more favorably than the positive-displacement types. Axial flow pumps generally rate high, but are deemed impractical because of the large number of stages required for high flows and the problem of manufacturing the large number of very thin section blades on the one- and two-inch-diameter rotors. The results suggest that the most practical pumps are the centrifugal, piston, and gear pumps, in that order.

The ranking procedures have shown the best pump types for the low-thrust propulsion system. These high-ranking pump types will be used as the basis of further studies and investigations. Specific recommendations for the pump/drive systems are as follows:

TABLE XV

RANKING OF PUMP/DRIVER SYSTEMS

Candidate	Figure of Merit	Rank	
Centrifugal	100	1	Rotating Dynamic Pumps
Pitot	71	3	
Tesla	69	4	
Drag	65	5	
Gear	58	6	Positive-Displacement Pumps (Excluding the Jet Pump)
Vane	57	7	
Piston	56	8	
Roots/Lobe	52	9	
Diaphragm	40		

RANK	FUNCTION AND FLUID PERFORMANCE	PHYSICAL CHARACTERISTICS	LIFE RELIABILITY MAINTAINABILITY	DESIGN CONFIDENCE
1	CENTR.	CENTR.	CENTR.	CENTR.
2	PITOT	DRAG	TESLA	PISTON
3	TESLA	GEAR	PITOT	PITOT
4	DRAG		GEAR	DRAG
5	PISTON	ROOTS/LOBE	PISTON	DIAPHRAGM

- DYNAMIC PUMPS (TOP TWO)
  - (1) CENTRIFUGAL (4 CATEGORIES)
- POS.-DISPLACEMENT PUMPS (TOP TWO)
  - (3) PISTON (3 CATEGORIES)
  - (4) GEAR (2 CATEGORIES)

Figure 86. Results of Sorting Technique

- Liquid Hydrogen Pump
  - Centrifugal/Turbine
  - Piston/Electric Motor
  - Gear/Electric Motor
- Liquid Oxygen Pump
  - Centrifugal/Turbine

VIII. TECHNOLOGY RECOMMENDATIONS

The results of this program clearly indicate that there are three pumping systems which appear attractive for the low-thrust propulsion system. These are:

- ° Centrifugal pump, driven by a gas turbine
- ° Piston pump, driven by an electric motor
- ° Gear pump, driven by an electric motor

In order to ascertain the merits of these concepts and to ensure that the technology for producing these pumps is in place, the following technology program is suggested. This basic program plan, displayed on the flow chart of Figure 87, should culminate in a technology readiness appraisal as generated through three basic paths:

(1) Hydrogen Pump/System Evaluation

(2) Oxygen Pump/Seal Evaluation

(3) Methane Pump/Positive-Displacement Pump

The interchange between the various programs provides design, technology, and system-level information.

1. Point Design Evaluation (a. hydrogen, b. methane, c. oxygen)

A program should be conducted to thoroughly evaluate the design issues and system performance of these three candidate concepts. This program would first select an appropriate design point for the three propellants of interest. Once the technology readiness date has been established, a preliminary design should be created to identify the following:

- ° Areas requiring further design emphasis
- ° Parasitic performance losses
- ° Manufacturing requirements
- ° Areas of reliability uncertainty

The next phase would then be to conduct detailed designs of the major components for each pumping system. Following these detailed designs, an assessment of the areas requiring further technology considerations (e.g., technological advancement, elimination of hydraulic uncertainties, and driver/power requirements) will be made. This information, together with the results of the pre-design effort, will be utilized to define 1) realistic performance for system trades and 2) definitized near-term technology programs.

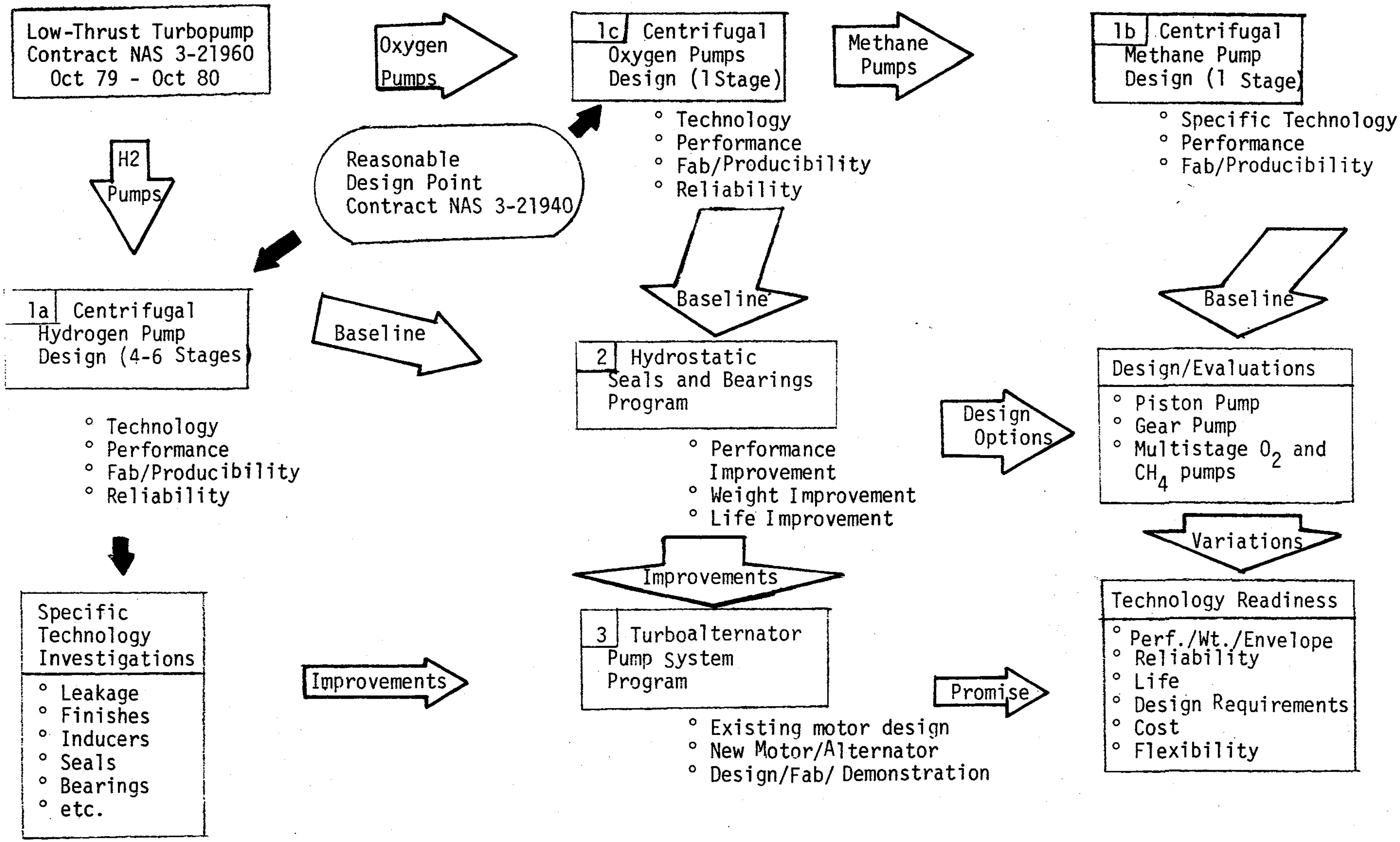

Figure 87. Low-Thrust Turbopump Technology Program

2. Hydrostatic Seals and Bearings

A primary life/performance-limiting aspect of all candidates evaluated during the study was in the area of bearings and seals. In general, pump impeller and shaft seal leakages become a large percentage of the total pump flow if conventional seal designs are incorporated. In addition, bearings and seals do not scale proportionally to impellers and turbines and thus affect the length and complexity of small machines. In summary, the efficiency of small pumps is greatly reduced due to operating clearances. Bearing life is controlled by shaft speed, size, and critical speed and is dictated by the limits of rolling contact bearings. All these shortcomings can be improved by employing hydrostatic devices. A three-part program is envisioned to accomplish this evaluation.

The program would start with the development of a state-of-the-art turbopump design employing rolling contact bearings which would contain these aforementioned limits. The bearings and seals would be changed to hydrostatic types. Subsequently, the operating design point would be changed. A pre-design would follow which would display the characteristics of the hydrostatic elements. Following this activity, a competitive assessment would be made between conventional and hydrostatic approaches. This information would then supply the technical justification necessary to support definitized technology investigations.

3. Turboalternator Cycle Turbopump

The most attractive pumps evaluated during the study were centrifugal pumps with gas turbine power drives. This configuration is limited, however, by two problems: 1) pump speed cannot be increased to a level yielding high turbine efficiencies and 2) oxygen pumps must be driven by fuel-rich gases which unfortunately produce a combustible mixture in the shaft seal area. To avoid the undesirable conditions and improve efficiencies, the following design approach is proposed.

The fuel pump will utilize an encapsulated alternator to supply the electrical power for driving the oxidizer pump drive motor. In so doing, the bipropellant seal is eliminated and the turbine efficiency is improved.

To thoroughly evaluate the merits of this concept, a design/analysis program is recommended. Starting with an assumed preliminary design point for a LOX/hydrogen low-thrust propulsion system, the basic pump/turbine characteristics for the encapsulated alternator concept would be determined. A preliminary design of both pump/driver concepts would set the stage for more detailed design evaluations. Starting with the alternator/motor driver, a review of existing hardware would be conducted. This study would identify the need for a new alternator/motor combination or the promise of an existing motor modification. If the latter looks attractive, then a design iteration would be conducted. Following this evaluation, the pump design would proceed. At the completion of this effort, the areas requiring critical technology investigation would be identified, and a plan for a "breadboard" demonstration would be defined. In addition to basic pump/alternator/driver demonstration data, this program would also provide general system data (e.g., chilldown and pressure transients) in conjunction with the engine system configuration requirements.

IX. REFERENCES

1. NASA, "Liquid Rocket Engine Centrifugal Flow Turbopumps," NASA SP8109, 1973.

2. Bashta, T.M., "Calculations and Physical Designs for Aircraft Hydraulic Devices," trans. from the Russian, FTD-TT-63-939/1+2, 1963.

3. Baljé, O.E., "Performance of Turbomachines in Terms of Similarity Parameters," Private Report, October 1962.

4. Gibson, W.H. and Fox, L., "A New Development in High-Speed Variable Delivery Vane Pumps," SAE Paper No. 700792, October 1970.

5. Campbell, W.E., Robertson, C.F., and Yoshikawa, D.K., "The Design and Evaluation of an Axial-Flow Impulse Pump," ASME Paper 63-AHG5-52.

6. Kempf, D.D., "A Program to Demonstrate the Feasibility of an Idling Shroud High-Pressure Centrifugal Pump," F.M.C. Corporation Report CE 333, October 1972.

7. Rocketdyne, "Rotating and Positive-Displacement Pumps for Low-Thrust Rocket Engines," Volume 1, Evaluation and Design, Final Report, NASA CR-72965 (R-8494-1), February 1974.

8. Rocketdyne, "Rotating and Positive-Displacement Pumps for Low-Thrust Rocket Engines," Volume 2, Fabrication and Testing, Final Report, NASA CR 72966 (R-8494-2), February 1974.

9. Pearsall, I.S., "The Supercavitating Pump," Proceedings of the Institution of Mechanical Engineers, Vol. 187, 54/73 (1973), pp. 649-665.

10. Burton, J.D., Lobo, J., and Guerrero, U., "Induced Flow Reciprocating Pump Theory Supported by New Performance Data," Transactions of the American Society of Mechanical Engineers, Journal of Basic Engineering (Dec. 1972), pp. 706-714.

11. Gill, W. and Shouman, A.R., "State-of-the-Art Review of Sliding Vane Machinery," ASME Paper, 76-DET-90.

12. Anderson, W.J., "Bearings, Gearing and Lubrication Technology," SAE Paper 780077, 1978.

13. Thomas, D.L. and Catterson, R.K., "A 30,000 RPM Vane Pump for Aircraft Hydraulic Systems," SAE Committee A-6, Meeting No. 72.

14. Brooks, R.D., Eckard, S.E., Frank, R.G., and Barber, K.F., "Design of Reciprocating Single Cylinder Expanders for Rankine Cycle Engines," SAE Paper 729051.

15. Marsters, G.F., and Ogbuefi, E., "Rotary Vane Expander Development: Some Design Considerations," SAE Paper 729048.

16. Wolgemuth, C.H. and Olson, D.R., "A Study of Breathing in Vane Type Expanders."

17. NASA Space Vehicle Design Criteria, "Turbopump Systems for Liquid Rocket Engines," NASA SP-8107, 1974.

18. Baljé, O.E., "A Study on Design Criteria and Matching of Turbomachines, Part B - Compressor and Pump Performance and Matching of Turbo Components," Transactions of the American Society of Mechanical Engineers, Journal of Engineering for Power (Jan. 1962), pp. 103-114.

19. Biermann, A.E. and Kohl, R.C., "Preliminary Study of a Piston Pump for Cryogenic Fluids," NASA Memo 3-6-59E, 1959.

20. Biermann, A.E. and Shinko, W.G., "Performance Study of a Piston-Type Pump for Liquid Hydrogen," NASA TN D276, 1960.

21. Barske, U.M., "Development of Some Unconventional Centrifugal Pumps," Proceedings of the Institution of Mechanical Engineers, Vol 174, No. 11 (1960), p. 452.

22. Stepanoff, A.J., Centrifugal and Axial Flow Pumps, John Wiley & Sons, 1962.

23. Pfleiderer, C., Die Kreiselpumpen, Springer, 1961.

24. Nichols, J.F., "Study of Liquid Oxygen/Liquid Hydrogen Auxiliary Propulsion Systems for the Space Tug," Final Report, Contract NAS 3-18913, NASA CR-134790, Space Division Rockwell International, 15 June 1975.

25. NASA "Liquid Rocket Engine Axial-Flow Turbopumps," NASA SP-8125, 1978.

26. Crawford, M.E. and Rice, W., "Calculated Design Data for the Multiple-Disk Pump Using Incompressible Fluid," Transactions of the American Society of Mechanical Engineers, Journal of Engineering for Power (July 1974), pp. 274-281. (Contains 42 references.)

27. O'Keefe, W., "New Efforts Aim at Practical Application of Multiple-Disk-Pump Concept in Industry," Power (Dec. 1974), pp. 51-53.

28. Green, W.L., "Fluid Power Circuits - Their Design and Application," Machinery and Production Engineering (11 Sept. 1974), pp. 298-301.

29. Neerken, R.F., "Selecting The Right Pump," Chemical Engineering (3 April 1978), pp. 87-98.

30. Pump Manual, American Institute of Chemical Engineers.

31. Scheel, L.F., "A Technology for Rotary Compressors," Transactions of the American Society for Mechanical Engineers, Journal of Engineering for Power (July 1970), pp. 207-216.

32. Winn, L.W., Eusepi, M.W., and Smalley, A.J. (M.T.I.), "Small, High-Speed Bearing Technology for Cryogenic Turbo-Pumps," NASA CR-134615, July 1974.

33. Kittredge, C.P., "Estimating the Efficiency of Prototype Pumps from Model Tests," Transactions of the American Society of Mechanical Engineers, Journal of Engineering for Power (April 1968), pp. 129-148.

34. Wassell, A.B., "Reynolds Number Effects in Axial Compressors," Transactions of the American Society of Mechanical Engineers, Journal of Engineering for Power (April 1968), pp. 149-156.

35. Bakke, E. and Kreith, F., "Disk Pump Performance in Turbulent Flow," ASME Paper 77-WA-FE-26, December 1977.

36. Engel, J. and Walter, H., "Design of a Small Centrifugal Pump for Subcooled and Boiling Liquids ($77<T<300°K$)," Fifth International Cryogenic Engineering Conference, 5th Proceedings, Kyoto, Japan, May 1974, Paper N 11, pp. 384-386.

37. Johnson, H.T. and Michell, R.K., "Advanced High-Speed Fuel Pumps for Small Gas-Turbine Engines," Task 1G162203D14416, Contract DAAJ02-67-C-0037, USAAVLABS Technical Report 69-12. Prepared by Battelle Memorial Institute for the U.S. Army Aviation Material Laboratory, Fort Eustis, Virginia, April 1969.

38. Ammann, H.H. and Morihara, H., "Miniature Turbo-Expander for a Closed Cycle Helium Refrigerator," Air Force Flight Dynamics Laboratory Technical Report AFFDL-TR-68-58 (Union Carbide), May 1968.

39. Erickson, J.W. and Grumet, W.H., "A New Pump for Industry - The Roto Jet," ASME Paper 74-Pet-31, 1974.

40. Johnson, H.T. and Mitchell, R.K., "A Turbine-Speed Fuel Pump for Small Gas-Turbine Engines," ASME Paper 69-GT-45, 1968.

41. Barske, U.M., "Investigations on the Pumping Effect of Rotating Discs," Proceedings of the Institution of Mechanical Engineers, Vol. 189, 36/75 (1974).

42. Togashi, S. and Iyoi, H., "The Synthesis of Tooth Profile Shapes and Helical Gears of High Hydraulic Performance for Rotary Type Pumps," Mechanism and Machine Theory, Vol. 8 (1973), pp. 105-123.

43. Hollis, C.R., "A Review of Five Types of Electrical Adjustable Speed Drives and Their Application to a Centrifugal Pump."

44. Palmer, K.P, "Double Row Radial Hydraulic Piston Pumps for Aircraft Hydraulic Systems," Paper B1, 5th International Power Symposium, 13-15 September 1978.

45. Stepanoff, A.J., "Cavitation Properties of Liquids," Transactions of the American Society of Mechanical Engineers, Journal of Engineering for Power (April 1964), pp. 195-200.

46. Johnson, H.T. and Mitchell, R.K., "Hydrodynamic Pivoting-Pad Vane Tips for High Speed Vane Pumps."

47. Johnson, H.T., "A Turbine-Speed, Main-Engine Fuel Pump," ASME Paper 71-GT-24, 1971.

48. Thomas, D.L., Swain, J.C., Wilcox, J.P., Mitchell, R.K., and Netter, D.E., "Investigation of a 30,000 RPM Turbine-Driven Hydraulic Pump," Battelle Memorial Institute Contract AF 33(615)-2723, Quarterly Progress Report, 29 July 1966.

49. Thomas, D.L., Dechow, J.P., Catterson, R.K., et al. "30,000 RPM Vane-Pump Demonstration," Battelle Columbus Laboratories, Technical Report AFAPL-TR-72-9, Contract F33615-69-C-1302, March 1972.

50. Dyett, D., "Design and Testing of a Small Feedwater Pump," Defense Science and Technology Organization, Aeronautical Research Laboratories, Melbourne, Australia, Report AR-000-858, October 1977.

51. Perian, F.W., "Investigation of a High-Speed Directly Driven Engine Hydraulic Pump," Aerospace Division Vickers, Inc., Technical Report AFAPL-TR-66-103, October 1966.

52. Humphries, W.R., "Pump/Control System Minimum Operating Cost Testing," Tennessee Technological University, Report DOE/NASA CR-150604, Contract NAS 8-31564, 7 December 1977.

53. Johnson, H.T., "Design and Evaluation of Advanced High-Speed Fuel Pumps," Final Report, Battelle Columbus Laboratories Contract DAA J02-69-C-0072. USA AMRDL Technical Report 71-37, July 1971.

54. Bunjes, J.H., "Design Principles and Test Data of Pump Impellers with Improved Cavitation Behavior," VMF/DFO Engineering Consultants.

55. Ruggeri, R.S. and Moore, R.D., "Method for Prediction of Pump Cavitation Performance for Various Liquids, Liquid Temperatures, and Rotative Speeds," NASA TN D-5292, June 1969.

56. Ramprasad, B.S. and Radha, T.S., "On Some Aspects of Rotary Vane Pumps," Vacuum, Vol. 23, No. 7, pp. 245-249.

57. Engel, V.Y. et al., "Parameters of Throttling Grooves of Sliding-Vane Pumps," Russian Engineering Journal, Volume LI, No. 12, pp. 22-24.

58. Zaichenko, I.Z., "Theory and Design of an Automatic Mechanism to Control the Supply from Sliding Vane Pumps for Hydraulic Drive Machinery," Russian Engineering Journal, Vol. LV, No. 9, pp. 7-10.

59. Thomas, D.L., "High Performance Vane Pump for Aircraft Hydraulic Systems," Battelle Columbus Laboratories, Technical Report AFAPL-TR-75-94, December 1975.

60. Lewis, G.W., Tysl, E.R., and Hartmann, M.J., "Design and Experimental Performance of a Small Centrifugal Pump for Liquid Hydrogen," NASA Technical Memorandum X-388, 1960.

61. Baljé, O.E., "A Study on the Performance Potential of Conventional and Shear Force Pumps," Aeronautical Research Laboratories, Report ARL 65-118, Contract AF 33(615)-1915, June 1965.

62. Murata, S., Miaoke, Y., and Iemoto, Y., "A Study on a Disk Friction Pump," 1st Report, Bulletin of the Japanese Society of Mechanical Engineers, Vol. 19, No. 128 (Jan. 1976), pp. 168-178.

63. Murata, S. et al., "A Study of a Disk Friction Pump," 2nd Report, Bulletin of the Japanese Society of Mechanical Engineers, Vol 19, No. 136 (Oct. 1976), pp. 1160-1171.

64. Breaus, D.K., Burriss, W.L., and Schultz, R.L., "Missile and Space Vehicle Non-Propulsive Power Concepts, "SAE Paper 234A, October 1960.

65. Klemach, F., "Positive-Displacement Motors for APU Power Requirements," SAE Paper 53R, 1959.

66. Rock, E.J., "Modern Gear Pumps are 95% Efficient or Better," SAE Paper 770782, 1977.

67. Tyler, S.R., "Application of the Vapour Core Pump to Aero Engine Fuel Systems," Journal of the Royal Aeronautical Society, Vol. 70 (Oct. 1966), pp. 923-935.

68. Aerojet Liquid Rocket Company Advanced Study Group, "The Aerojet Platelet Disk Pump."

69. Brown, A. and Wilcox, K.J., "Rotary Pumps," Engineering Materials and Design (Nov. 1974), pp. 23-25.

70. Stuart, R. and Holdeman, J., "Hydraulic System Pumps - 2-Gear Pumps," Machine Design (28 May 1970), pp. 142-147.

71. Mansoorian, H., Capps, E.F., Gielen, H.L., Eubank, P.T., and Hall, K.R., "Compact Magnetic Recirculating Pump for Wide-Range Temperature and Pressure Operation," Rev. Sci. Instrumentation, Vol. 46, No. 10 (Oct. 1975), pp. 1350-1351.

72. Wilson, W.E., "Cavitation in Positive-Displacement Pumps," Product Engineering (March 1959), pp. 47-49.

73. Lewis, G.W., Tysl, E.R., and Hartman, M.J., "Design and Experimental Performance of a Small Centrifugal Pump for Liquid Hydrogen," NASA TM X-388.

74. Maddocks, F.E., "Application of Turbomachinery to Small-Capacity Closed-Cycle Cryogenic Systems," Advances in Cryogenic Engineering, (1967), pp. 463-473.

75. Baljé, O.E., "A Study on the Performance Potential of Conventional and Shear Force Pumps" Aerospace Research Laboratories, ARL 65-118, June 1965.

76. Cunningham, E.R., "Pumps Without Seals," Plant Engineering (4 Aug. 1977).

77. Glollenberg, J.W. and Potter, J.H., "An Investigation of Regenerative Blowers and Pumps," ASME Paper 78 WA/PID-2, 1978.

78. Ludske, P.R., "Performance Characteristics of a Liquid Helium Pump," National Bureau of Standards NBSIR75-816, July 1975.

79. Colyer, D.B., "Miniature Cryogenic Refrigerator Turboalternator," Advances in Cryogenic Engineering, Vol. 14 (1969), pp. 405-415.

80. Aerojet Liquid Rocket Company, "Low-Thrust Chemical Rocket Engine Study," 5th Monthly Report 21940-M5, NASA Contract NAS 3-21940, January 1980.

81. Binder, R.C., Fluid Mechanics, Prentice-Hall, Inc., 1956.

82. Freeman, F.G., "Micro Pumps and Motors," 3rd International Fluid Power Symposium, Paper G2, May 1973.

83. Anonymous, "Designing for Zero-Wear or a predictable Minimum," Product Engineering, Vol. 37, No. 17 (15 Aug. 1966).

84. Gill, W. and Shouman, A.R., "State of the Art Review of Sliding Vane Machinery," ASME 76-DET-90, 1977.

85. Cunningham, R.G., "Jet Pump Theory and Performance with Fluids of High Viscosity," ASME Paper 56-A-58, 1958.

86. Gosline, James E. and O'Brien, Morrough P., "The Water Jet Pump," University of California Publications in Engineering, Vol. 3, No. 3 (1934), pp. 167-190.

87. Flugel, Gustav, "The Design of Jet Pumps," NCA Tech. Memorandum No. 982, July 1941.

88. Sidhom, M. and Hansen, A.G., "A Study of the Performance of Staged-Jet Pumps," ASME Paper 66-WA/FE-4, 1966.

89. Sanger, N.L., "An Experimental Investigation of Several Low-Area Ratio Water Jet Pumps," Transactions of the American Society of Mechanical Engineers, Journal of Basic Engineering (March 1970), pp. 11-20.

90. Arnberg, B.T., "Operating Characteristics of Jet Pumps Using Gaseous Primary and Secondary Streams," University of Colorado, Boulder, Colorado, Contract N123 (60530) 4188A, Naval Ordnance Test Station, China Lake, California, April 1958.

93. Aerojet-General Corp., "Analytical and Experimental Investigation of A Novel Liquid Propellant Pumping Concept," Final Report No. 7409-01F, Contract AF04(611)-7409, 1 June 1961-30 June 1962.

94. NASA SP-8100, "Liquid Rocket Engine Turbopump Gears," March 1974.

95. Buckinham, E., Analytical Mechanics of Gears, 1963.

96. Dudley, D.W., Practical Gear Design, 1954.

97. Hise, E.C., "Design Development and Operation of Metal-Diaphram Reactor-Service Pumps," ORNL-2841, 10 May 1960.

98. Karassik et al., Pump Handbook, 1976.

99. Wilson, W.E., "Analysis of Turbine Pumps," Product Engineering (Oct. 1947).

100. Wilson, W.A. et al., "A Theory of Fluid-Dynamic Mechanism of Regenerative Pumps," Transactions of the American Society of Mechanical Engineers, Vol. 77 (Nov. 1955).

101. Thomas, G.M. and Henke, R.W., "Pumps for Fluid Power - Part I ," Mechanical Engineering (September 1968).

102. Ting, L.L. and Maver, J.E., "Piston Ring Lubrication and Cylinder Bore Wear Analysis, Part I-Theory."

103. "High-Torque Low-Speed Hydraulic Motors," Hagglunds, Bird-Johnson Co., Walpole, Massachusetts.

104. Richter, E., "Power Density Considerations for Permanent Magnet Machines," Report No. 78CRD203, General Electric Co., October 1978.

105. NASA CR-113925, November 1971, "Conceptual Design Study of a Nuclear Brayton Turboalternator-Compressor," General Electric Co. Report.

106. Bailey, L.J. and Richter, E., "Development Report on a High-Speed Permanent Magnet Generator of the 200 KVA Rating Class Utilizing Rare Earth Cobalt Magnets," Report 8026, General Electric Co.

107. Lafuze, David L. et al., "150 KVA Samarium Cobalt USCF Starter/ Generator Electrical System," Final Technical Report, AFAPL-TR-78-104, December 1978.

108. Aerojet Liquid Rocket Co., "Low-Thrust Chemical Propulsion Pump Technology," Report 21960-M4, NASA Contract 3-21960, February 1980.

109. Glusek, F., Mokadam, To. I.H., Stanitz, J.D., and Wollschlager, J., "Liquid Oxygen/Liquid Hydrogen Boost/Vane Pump for the Advanced Orbit Transfer Vehicle Auxiliary Propulsion System," Contract No. NAS 3-20401, Technical Report prepared for NASA by Sundstrand Corporation, September 1979.

110. Goddard, Robert H., Rocket Development, Prentice-Hall Inc., 1948.

111. Balski, M.F., and Owens, S.L., "Electrical Power Generation: Subsystem for Space Shuttle Orbiter," United Technologies, Inc., Power Systems Division, August 1974.

112. NASA Space Vehicle Design Criteria, "Liquid Rocket Engine Turbines," NASA SP-8110, January 1974.

113. Csomor, A., "Small High-Pressure Liquid Oxygen Turbopump," NASA CR-159509, February 1979.

114. Csomor, A. and Sutton, R., "Small, High-Pressure Liquid Hydrogen Turbopump," NASA CR-135186, May 1977.

115. Baljé, O.E., "A Study on Design Criteria and Matching of Turbomachines, Part A: Similarity Relations and Design Criteria of Turbines," Transactions of the American Society of Mechanical Engineers, Journal of Engineering for Power, Vol 84 (Jan. 1962).

116. Deacon, W.K. and Wood, H.J., "Chemical Power Systems for Missiles and Space Vehicles," SAE Paper 469A, January 1969.

DISTRIBUTION LIST FOR FINAL REPORT - CR-165219
NAS 3-21960

Name	No. of Copies
National Aeronautics & Space Administration Lewis Research Center 21000 Brookpark Road Cleveland, Ohio 44135	
Attn: Contracting Officer, MS 501-11	1
E. A. Bourke, MS 501-5	5
Technical Utilization Office, MS 3-16	1
Technical Report Control Office, MS 5-5	1
AFSC Liaison Office, MS 501-3	2
Library, MS 60-3	2
Office of Reliability & Quality Assurance, MS 500-211	1
R. E. Connelly, MS 501-6	12
Patent Counsel, MS 500-318	1
National Aeronautics & Space Administration Headquarters Washington, D.C. 20546	
Attn: Office of Aeronautics & Space Technology	1
Director, Study, Analysis & Planning/RX	1
Director, Space Propulsion & Power/RP	1
F. W. Stephenson/RTP-6	1
Office of Space Flight	1
Director, Advanced Programs/MT	1
Director, Advanced Studies/MTE	1
Office of Industry Affairs & Technology Utilization	1
Director, Technology Utilization/KT	1
National Aeronautics & Space Administration Ames Research Center Moffett Field, CA 94035	
Attn: Library	1
National Aeronautics & Space Administration Flight Research Center P.O. Box 273 Edwards, CA 93523	
Attn: Library	1
National Aeronautics & Space Administration George C. Marshall Space Flight Center Huntsville, Alabama 35812	
Attn: Library	1
J. L. Sanders/PD13	1
R. Richmond/EP24	1
J. A. Lombardo/EP21	1
O. K. Goetz/EP21	1
F. J. Dolan/EH14	1
National Aeronautics & Space Administration Goddard Space Flight Center Greenbelt, Maryland 20771	
Attn: Library	1
National Aeronautics & Space Administration John F. Kennedy Space Center Cape Canaveral, Florida 32931	
Attn: Library	1
National Aeronautics & Space Administration Lyndon B. Johnson Space Center Houston, Texas 77001	
Attn: Library	1
H. O. Pohl/EP	1
National Aeronautics & Space Administration Langley Research Center Langley Station Hampton, Virginia 23365	
Attn: Library	2

Name	No of Copies
NASA Scientific & Technical Information Facility P.O. Box 33 College Park, Maryland 20740	
Attn: NASA Representative	10
Office of the Director of Defense Research & Engineering Washington, D.C. 20301	
Attn: Office of Asst. Director (Chemical Technology)	1
Jet Propulsion Laboratory 4800 Oak Grove Drive Pasadena, CA 91103	
Attn: Library	1
D. Dipprey	1
Defense Documentation Center Cameron Station Building 5 5010 Duke Street Alexandria, Virginia 22314	
Attn: TISIA	1
Advanced Research Projects Agency Washington, D.C. 20525	
Attn: Library	1
Aeronautical System Division Air Force Systems Command Wright-Patterson Air Force Base Dayton, Ohio	
Attn: Library	1
Air Force Missile Test Center Patrick Air Force Base, Florida	
Attn: Library	1
Air Force Systems Command Andrews Air Force Base Washington, D.C. 20332	
Attn: Library	1
Air Force Rocket Propulsion Laboratory Edwards, CA 93523	
Attn: Library	1
AFRPL/LK Col. B. A. Loving Edwards AFB, CA 93523	1
Air Force Office of Scientific Research Bldg. 410 Bolling Air Force Base Washington, D.C. 20332	
Attn: Library	1
U.S. Air Force Washington, D.C.	
Attn: Library	1
Air Force Aero Propulsion Laboratory Research & Technology Division Air Force Systems Command U.S. Air Force Wright-Patterson AFB, Ohio 45433	
Attn: Library	1
Arnold Engineering Development Center Air Force Systems Command Tullahoma, Tennessee	
Attn: Library	1

Name	No. of Copies
Space & Missile Systems Organization Worldway Postal Center P.O. Box 92960 Los Angeles, CA 90009 Attn: Library (Technical Data Center) Lt. Cold J. Graetch	 1 1
Office of Research Analyses (OAR) Holloman Air Force Base New Mexico 88330 Attn: Library (RRRD)	 1
RTD (RTNP) Bolling Air Force Base Washington, D.C. 20332	 1
Bureau of Naval Weapons Department of the Navy Washington, D.C. Attn: Library	 1
Naval Research Branch Office 1030 E. Green Street Pasadena, CA 91101 Attn: Library	 1
Picatinny Arsenal Dover, New Jersey 07801 Attn: Library	 1
U.S. Naval Research Laboratory Washington, D.C. 20390 Attn: Library	 1
U.S. Army Research Office (Durham) Box CM, Duke Station Durham, North Carolina 27706 Attn: Library	 1
U.S. Army Missile Command Redstone Scientific Information Center Redstone Arsenal, Alabama 35808 Attn: Document Section	 1
U.S. Naval Missile Center Point Mugu, CA 93041 Attn: Technical Library	 1
U.S. Naval Weapons Center China Lake, CA 93557 Attn: Library	 1
Rocketdyne Division of Rockwell International 6633 Canoga Avenue Canoga Park, CA 91304 Attn: Library H. G. Diem A. Csomor F. Kirby	 1 1 1 1
Aerospace Corporation 2350 E. El Segundo Blvd. Los Angeles, CA 90045 Attn: Library R. L. Doobler I. Madison	 1 1 1
AiResearch Mfg. Co. of California A Division of the Garrett Corp. 2525 W. 190th St. Torrence, CA 90509 Attn: Library	 1
AiResearch Mfg. Co. of Arizona A Div. of the Garrett Corp. 402 South 36th St. Phoenix, Arizona 85034 Attn: Library	 1
Atlantic Research Corp. 5390 Cherokee Ave. Alexandria, Virginia 22314 Attn: Library	 1
Battelle Memorial Institute 505 King Avenue Columbus, Ohio 43201 Attn: Library	 1
Bell Aerospace Company Box 1 Buffalo, New York 14240 Attn: Library	 1
Boeing Company Space Division P.O. Box 868 Seattle, Washington 98124 Attn: Library	 1
John Hopkins University John Hopkins Road Laurel, Maryland 20810	 1
Chrysler Corp. Defense-Space Group P.O. Box 757 Detroit, Michigan 48231 Attn: Library	 1
Curtiss-Wright Corporation One Rotary Drive Woodridge, New Jersey 07075 Attn: Library	 1
Deposits & Composites Incorporated 318 Victory Drive Herndon Industrial Park Herndon, Virginia 22070 Attn: J. C. Withers	 1
Fairchild Republic Company Fairchild Industries Farmingdale, L.I., NY 11735 Attn: Library	 1
General Dynamics/Convair P.O. Box 1128 San Diego, CA 92112 Attn: Library	 1
General Electric Company Valley Forge Space Technology Center P.O. Box 8555 Philadelphia, PA 19101 Attn: Library	 1
Grumman Aerospace Corporation Bethpage, L. I., NY 11714 Attn: Library	 1
Hamilton Standard Corporation Windsor Locks, Connecticut 06096 Attn: Library	 1

Name	No. of Copies
Hughes Aircraft Company Space & Communications Group P.O. Box 92919 Los Angeles, CA 90009 Attn: Library	1
IIT Research Institute Technology Center Chicago, Illinois 60616 Attn: Library	1
Walter Kidde & Company Belleville Division 675 Main St. Belleville, New Jersey 07109 Attn: Library	1
Lockheed Missiles & Space Company P.O. Box 504 Sunnyvale, CA 94087 Attn: Library	1
Marquardt Corporation 16555 Saticoy Street Box 2013 South Annex Van Nuys, CA 94109 Attn: Library	1
Martin-Marietta Corporation P.O. Box 179 Denver, Colorado 80201 Attn: Library	1
McDonnell Douglas Astronautics 5301 Bosa Avenue Huntington Beach, CA 92647 Attn: Library	1
Northrop Corporation 1800 Century Park East Century City, CA 90067 Attn: Library	1
Pratt & Whitney Aircraft Group United Technologies Corporation 400 Main Street East Hartford, CN 06108 Attn: Library	1
Pratt & Whitney Aircraft Group Government Products Division P.O. Box 2691 West Palm Beach, FL 33402 Attn: Library J. Brown	1 1
Space Division A Division of Rockwell International 12214 Lakewood Blvd. Downey, CA 90241 Attn: Library	1
Rocket Research Corporation Willow Road at 116th Street Redmond, Washington 98052 Attn: Library	1
Sundstrand Aviation Mechanical 2421 Eleventh Street Rockford, Illinois 61101 Attn: Library	1
Thiokol Corporation P.O. Box 1000 Newton, PA 18940 Attn: Library	1

Name	No. of Copies
TRW Systems Group 1 Space Park Redondo Beach, CA 90278 Attn: Library	1
Sundstrand Corporation Advanced Technology Group 1005A Courtney Drive Dayton, OH 45431 Attn: W. K. Thorson	1
TRW 23555 Euclid Avenue Cleveland, Ohio 44117 Attn: Library	1
Vought Corporation P.O. Box 5907 Dallas, Texas 75222	1
J. P. Layton 60 Penn Lyle Road Princeton Jct. New Jersey 08550	1
R. J. Salkeld 5921 Floris Heights Road Malibu, CA 90265	1
Dr. Lloyd Barrett University of Virginia Department of Mechanical & Aerospace Engineering Charlottesville, VA 22801	1
Dr. Dara W. Childs Texas A&M University Mechanical Engineering Dept. College Station, TX 77843	1
Professor M. C. Ek California State University Department of Mechanical Engineering Northridge, CA 91324	1